PROBABILISTIC SITE CHARACTERIZATION AND RELIABILITY ANALYSIS OF SHALLOW FOUNDATIONS AND SLOPES

A Thesis

Submitted for the Degree of

Doctor of Philosophy

in the Faculty of Engineering

By

Satyanarayana Murthy Dasaka

DEPARTMENT OF CIVIL ENGINEERING

INDIAN INSTITUTE OF SCIENCE

BANGALORE - 560012, INDIA

DECEMBER 2005

Abstract of Ph.D. thesis

Uncertainty is pervasive in almost every field of engineering, and geotechnical engineering is no exception. Natural soils are heterogeneous and anisotropic in physical properties due to their composition and complex depositional processes. The uncertainty in geotechnical engineering is mainly attributed to inherent or spatial variability, limited number of samples, testing and measurement errors, and the analytical models which relate the laboratory or in-situ properties with response characteristics in terms of stability and deformation behaviour of soil.

Professional practice has realized that due to economic constraints, the risk can not be reduced to zero level, and the foundations of infrastructure projects need to be designed considering that the risk is "as low as reasonably practicable", which the society can perceive. Unless all the sources of uncertainty are clearly brought out and included in the designs appropriately, it is not possible to explicitly assess the risk involved with respect to imposed loads on geotechnical systems.

A blanket factor of safety which is generally used in conventional design procedures to include implicitly all the sources of uncertainty arising in geotechnical property evaluation does not in any way truly account for involved risk. Owing to the random nature of soil media, it is essential to extensively study, characterize and evaluate the various sources of uncertainty in geotechnical parameter evaluation.

The present work aims at characterization of these sites using probabilistic techniques, and the total uncertainty attributed to design parameters is evaluated from the individual sources. It also highlights the importance of quantification of variability of engineering parameters in geotechnical engineering by extending the application of

probabilistic approaches to some studies on stability of shallow foundations and slopes.

For the present study, geotechnical data from four sites are considered. The data from first three sites are used for reliability analysis of shallow foundations. The data from fourth site are used to evaluate the stability of soil slopes. The first site consists of predominantly of cohesionless soil within the significant zone of influence. The second and third sites contain saturated cohesive soils, and the fourth site pertains to an unsaturated soil. The CPT cone tip resistance data in cohesionless soil is collected from the Texas A & M Riverside sand site, USA. The first set of CPT data on cohesive soil pertains to Keswick clay of Adelaide University campus, Australia. The second set of CPT data on cohesive soil was collected from a power plant site, on the East coast in Indian state of Andhra Pradesh. Both these clayey soil deposits were observed saturated with degrees of saturation greater than 95%, and the water table is located relatively at deeper depths compared to depth of significant zone. For the slope problem, the data was obtained from Powari landslide area of the Himalayan region, Himachal Pradesh, India.

A set of closely spaced cone tip resistance (q_c) profiles obtained from these sites are used in the analysis. Random field theory is used to analyse the influence of variability of vertical as well as horizontal cone tip resistance of supporting stratum on the allowable pressure of foundation. The test data have been checked for statistical homogeneity, which is recognized as a prerequisite for any statistical analysis using random field theory. Some of the non-parametric and parametric tests available till date to identify the statistical homogeneous layers have been used. The stationary residual component is used to evaluate the experimental autocorrelation

functions. Correlation distance, and subsequently the scale of fluctuation are calculated by using method of moments. The variance reduction function is evaluated from the computed autocorrelation distance and spatial averaging distance, and used to reduce the variance of the data within the statistically homogeneous layers.

The computed statistical parameters for the first three sites, viz., mean, variance, and autocorrelation characteristics for the cohesionless site of Texas A & M University Riverside sand site (NGES), cohesive sites of the Adelaide University, and the Power plant site, are used to evaluate the allowable pressure of shallow foundations. These assessments are made using the First-order reliability methods for predefined target reliability levels to be achieved in the design. Apart from this, the effect of anisotropy of correlation structure is studied in a 2-D space. The effect of using either isotropic scales of fluctuation or perfect correlation on the bearing capacity of shallow foundations is studied.

It is observed that the transformation model plays a major role on the total uncertainty associated with the design parameter. In the absence of appropriate scales of fluctuation in either direction for a particular site, it may be suggested to use an upper bound value of the range of observed values from the records of past experience within the similar sites, which obviously produce conservative estimates of bearing capacity. The study shows that the scale of fluctuation and averaging distance play a prominent role in prediction of inherent spatial variability of soil properties.

To ease the design engineers from dealing a huge amount of geotechnical data, and using rigorous and time consuming processes, resistances factor are developed through calibration process on a regional basis. The resistance factors are developed through calibration with both working stress design approach as well as reliability

based design approach, which when used with appropriate judgment, can serve and meet the purpose in routine geotechnical designs.

In the case of surficial stability analysis of unsaturated slopes, the soil-water characteristic curves were obtained from Agricultural University records for the nearby sites. These soil-water characteristic data are analysed and fitted to obtain hydraulic properties for the unsaturated soils using van Genuchten model. A finite difference code is used to evaluate the suction characteristics at different depths for various elapsed time periods after the cessation of a single rainfall record, taking into consideration the boundary and initial conditions evaluated from the above model. Due to lack of sufficient data on soil properties, a range of variability for the soil and suction properties reported in the published literature is considered in the analysis. Sensitivity analysis is carried out on all the input parameters to recognize the importance of variability associated with each parameter, and identify which parameters need to be considered as random variables. The performance of the infinite slopes in terms of stability is evaluated using both conventional deterministic approach as well as probabilistic approach. The effect of saturated hydraulic conductivity is also studied.

Seismic stability analysis of soil slopes is also carried out rigorously using probabilistic approach. Work has been focused to evaluate the optimum slope angle taking into consideration the effect of variations in soil properties, cross correlation, and socio-economic factors, such as importance and sensitivity of the project, initial cost and consequences of failure, etc. A pseudo-static approach is used in this work. It is demonstrated that evaluation of optimum slope angles under both static and seismic conditions could be obtained considering the variability in the material property.

The results obtained from the present study clearly demonstrate that the probabilistic analysis of the soil profile provides a format for quantifying the information about the subsurface condition of the site and it also provides the basis for predicting the reliability of the foundations.

TABLE OF CONTENTS

CHAPTER 8 RELIABILITY ANALYSIS OF SOIL SLOPES

CHAPTER 9 GENERAL CONCLUSIONS

LIST OF TABLES

LIST OF FIGURES

LIST OF SYMBOLS

Property	Description	Units
A	Amplification factor	-
a_h	Peak horizontal acceleration coefficient	-
B	Width of footing	m
b	Spatial averaging width	m
BC	Relative fluctuation of mean cone tip resistance at any depth	kPa
B_{crit}	Critical Bartlett statistic	-
B_{max}	Maximum Bartlett statistic	-
B_{stat}	Bartlett test statistic	-
B_{WSD}	Width of foundation obtained using working stress design	m
c	Cohesion of soil	kPa
$c(k)$	Autocovariance function for the entire population at lag k	
C	Cost of failure	Rs.
C^*	Normalized cost of failure	-
C_1	Embedment factor	-
C_2	Creep factor	-
CoV	Coefficient of variation	-
CoV_e	Coefficient of variation of measurement uncertainty	-
CoV_{qc}	Coefficient of inherent variability	-
CoV_w	Coefficient of variation of inherent variability	-
CoV_ε	Coefficient of variation of transformation model uncertainty	-
$CoV_{\xi d}$	CoV of design parameter	-
$CoV_{\xi a}$	CoV of spatial average	-
c_u	Undrained cohesion	kPa
D	Maximum depth of shear failure zone below footing base	m
D/L	Ratio of dead load to live load	-
d_c	Depth factors for cohesion component	-
D_f	Depth of foundation	m
D_K	cone bearing factor	-
d_q	Depth factor for overburden pressure component	-
d_γ	Depth factor for self weight of soil component	-
e	Measurement uncertainty	-
E	Elastic modulus of soil	kPa
E()	Expected cost	Rs.
E^*	Normalized expected cost	-
E[·]	Expected operator	-
f	Frequency of fatalities	-
FS	Factor of safety	-
g	acceleration due to gravity	m/s^2
g()	Performance function	-
h	Spatial averaging height	m
H	Height of slope	m

I	Initial cost	Rs.
I^*	Normalized initial cost	-
I_1	Normalized sampling length	-
I_2	Normalized segment length	-
I_o	Cost of construction of 1:1 slope	Rs.
I_z	Strain influence factor	-
k	Number of data points in one scale of fluctuation	-
k	Vector of separation distance	-
k	Saturated conductivity	m/s
L_{sh}	Length of shear failure zone	m
LSP	length of slip path	m
m	Number of data points in each window	-
N	Total number of data points	-
N_c	Bearing capacity factor for cohesion component	-
N_q	Bearing capacity factor for overburden pressure	-
N_γ	Bearing capacity factor for self weight of soil	-
p_a	Atmospheric pressure	kPa
P_{all}	Allowable pressure of footing	kPa
pdf	Probability density function	-
p_f	Probability of failure	-
p_{fcom}	Component probability of failure	-
p_{fsys}	System probability of failure	-
P_{shear}	Allowable bearing pressure	kPa
q	Applied pressure intensity of the footing	kPa
q_b	Applied pressure at footing base level	kPa
q_c	Cone tip resistance	kPa
q_T	Corrected cone tip resistance	kPa
Q_u, q_u	Ultimate bearing pressure	kPa
q_{unet}	Net ultimate bearing pressure	kPa
r	Number of runs in statistical run test	-
R	Resistance parameter	kPa
R^2	Determination coefficient	-
R_N	Nominal resistance	-
S	Load parameter	kPa
s	Allowable settlement of the footing	m
S_c	Shape factors for cohesion component	-
SD	Standard deviation	
SD_w	Standard deviation of residuals off the trend	
SD_{wa}	Standard deviation of spatial average	
S_N	Nominal load	
SPT 'N'	SPT blow count	-
S_q	Shape factor for overburden pressure component	-
S_u	Undrained shear strength	kPa
S_γ	Shape factor self weight of soil component	-
t	Non-stationary trend component	-
T	Spatial averaging length	m
t	Rain duration	Hour
T( )	Transformation model	-
t_R	reference time	Year
u_a	Pore air pressure	kPa

u_a-u_w	Matric suction	kPa
u_w	Pore water pressure	kPa
V	Volume of soil mass within the significant zone of influence	m^3
V_R	Coefficient of variation of resistance	-
V_S	Coefficient of variation of load	-
w	Stationary fluctuating component	-
W	Wind load	kPa
Z_i	In-situ soil property at location i	-
z_i^*	Reduced variate corresponding to the design point	-
B_{LSD}	Width of foundation obtained using limit state design method	m
β	Reliability index	-
ξ_m	Measured property of soil parameter	-
ξ_d	Soil Design parameter	-
σ'_{vo}	Effective overburden pressure	kPa
$\Gamma^2(\ )$	Variance reduction factor	-
Γ_v^2	Variance reduction factor in the vertical direction	-
Γ_h^2	Variance reduction factor in the horizontal direction	-
ϕ'	Effective friction	(˚)
σ	Total stress	kPa
ϕ^b	angle indicating the rate of increasing shear strength relative to the matric suction	(˚)
$\bar{\phi}_{TC}$	Triaxial compression effective stress friction angle	(˚)
$\sigma'_{v\|d}$	Effective vertical pressure at the foundation base level	kPa
$m_{\xi d}$	Mean design parameter	
σ_{vm}	Total overburden stress averaged over a length of L	kPa
Θ	Effective saturation	-
θ	volumetric water content	m^3/m^3
α_i	Direction cosine	-
θ_r	residual volumetric water content	m^3/m^3
θ_s	saturated volumetric water content	m^3/m^3
Δp	Net applied pressure of the footing	kPa
Δ_z	Thickness of sublayer	m
Φ	Resistance factor	-
Φ(·)	Cumulative normal probability function	-
α	Load factor	-
α_D	Dead load factor	-
α_L	Live load factor	-
β_{com}	Component reliability index	-
βsys	System reliability index	-
δ	Scale of fluctuation	m
ε	Transformation model uncertainty	-
ϕ	Friction angle	(˚)
γ	Unit weight of soil	kN/m^3
γ(T)	Variance reduction function	-

μ	Mean of the property	
θ	Slope of failure wedge	(˚)
$\rho(\Delta z)$	Autocorrelation function	-
$\rho_{c,\phi}$	correlation coefficient between cohesion and friction angle	-
ρ_k	Autocorrelation function for the entire population at lag k	-
σ	Standard deviation of the property	
σ'	Vertical effective overburden pressure	kPa
σ_n	Normal stress on slip path	kPa
τ	Kendall's test statistic	-
ψ	Slope angle	(˚)

Chapter 1

INTRODUCTION

1.1 Preamble

Founders and leaders of geotechnical profession contributed extensively on the importance of recognizing uncertainties and considering them appropriately in the design decisions. Terzaghi, who is respected as the father of the soil mechanics, recognized the importance of uncertainty in the measured soil property and cautioned the fellow engineers on the consequences of its negligence way back in 1930s. Casagrande's well known Terzaghi Lecture (1965) was on "calculated risk" by which he meant very careful consideration of risk in geotechnical studies is quite necessary. Probabilistic methods are now playing an important role in a number of engineering problems and there will be increasing spillover into problems now engineered by traditional methods.

Whitman (1984) presents the various areas in which the probabilistic considerations enable better designs in geotechnical engineering in his Terzaghi lecture. Morgenstern (1997) focused on some of the failures in geotechnical engineering and attributed the failures to the poor site characterization. Lacasse (2001) demonstrated the importance of soil variability studies using a case study on shallow foundations. A geotechnical structure with a higher factor of safety can have a higher risk of failure than a similar structure with a lower factor of safety, depending on the accuracy of the model used for analysis and the uncertainties of the input parameters (Lacasse 2001; Li and Lam 2001). The importance of research in this area is reflected in the increased number of important lectures, like Terzaghi lectures, and dedicated special issues in international journals as well as specialty journals devoted towards the study of risk and reliability

issues in civil/geotechnical engineering. Christian et al. (1994) and Whitman (2000) indicated that the continued challenge is to recognize problems in which probabilistic thinking can contribute effectively to the engineering solutions and reliability analysis is especially useful in establishing design values for factor of safety representing consistent risk for different types of failures. The most effective applications of probabilistic methods are those involving relative probabilities of failure or illuminating the effects of uncertainties in the parameters.

1.2 Uncertainty in Geotechnical Engineering

Significant and varying degrees of uncertainty are inherently involved in the design process and allowances must be made for these uncertainties. The sources of uncertainties in the geotechnical design can be grouped into four main categories:

1. Uncertainties in estimating the loads
2. Uncertainties associated with the variability of the ground conditions at the site
3. Uncertainties in estimating material properties
4. Uncertainties associated with the degree to which the analytical model represents the actual behaviour of the structure and the ground that supports the structure.

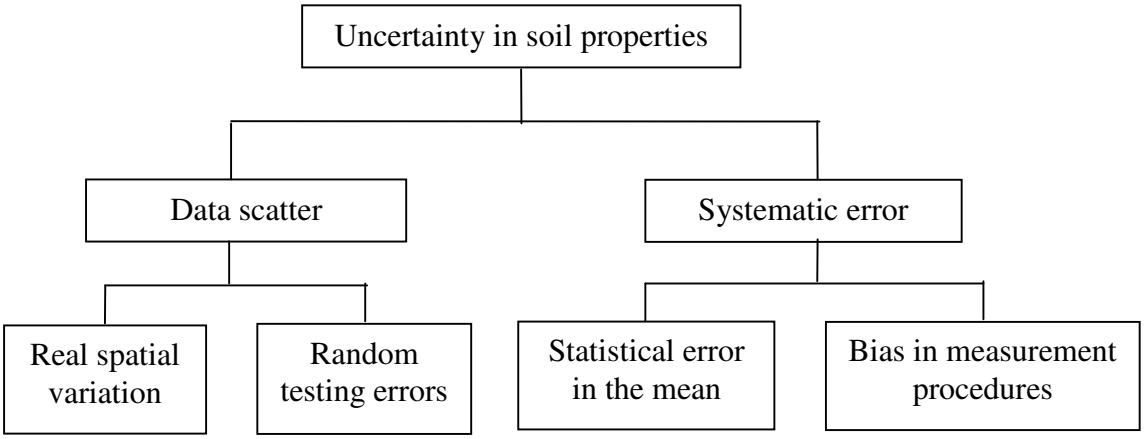

Figure 1.1 Categories of sources uncertainty in soil properties (Whitman 2000)

For assessment of reliability, Morgenstern (1997) classifies the uncertainties into three categories, viz., i) parameter uncertainty; ii) model uncertainty; and iii) human uncertainty. In engineering design, the influence and significance of the first two modes of uncertainty are important, while the third mode of uncertainty falls within the domain of regulatory agencies. While parameter uncertainty is easier to handle, the model uncertainty can be handled if the mechanism of failure is known.

1.3 Reliability Concepts in Geotechnical Engineering

Applications of reliability concepts in geotechnical engineering have been reported by Ang and Tang (1975), Vanmarcke (1977a & b), Whitman (1984), Li and Lumb (1987), Oka and Wu (1990), Mostyn and Li (1993), Tang (1993), Christian et al. (1994) and Chowdhury and Xu (1995), Morgenstern (1997), Phoon and Kulhawy (1999a & b), Duncan (2000), Lacasse (2001), Phoon et al. (2003b), Christian (2004), etc. Geotechnical engineers face uncertainties at all phases of a project. Some concerns expressed by the geotechnical engineers, reported by Whitman (1984) are

1. Is proposed field investigation adequate for characterizing the materials at a site?
2. What values should be assigned to soil parameters (strength, stiffness etc.) required for analysis?
3. How accurate is an analysis leading to an important derived quantity (e.g., safety factor)?
4. How confident are we that a proposed design is safe and adequate in other ways?
5. What about the uncertainties during implementation during actual construction?

Attempts towards site characterization using probabilistic considerations to consider in-homogeneity, spatial variations and importance of proper soil sampling have been made in literature, see for example, Lumb (1967), Vanmarcke (1977a & b, 1978,

1983), Tang (1984), Soulie et al. (1990), Cherubini et al. (1993), De Groot and Baecher (1993), Lacasse and Nadim (1996), Jaksa et al. (1997, 99), Kulathilake and Ghosh (1988), Fenton (1999a & b), Phoon and Kulhawy (1999a & b), Jaksa (2000), Cafaro and Cherubini (2002), Kulathilake and Um (2003), Phoon et al. (2003a, 2004), Vanmarcke and Fenton (2003), Uzielli et al. (2005).

In the area of slopes and embankments research on soil deformation and stability by Cornell (1971), Yucemen et al. (1973), Alonso (1976), Vanmarcke (1977a), A-Grivas and Harr (1979), Chowdhury and A-Grivas (1982), A-Grivas and Asaoka (1982), Chowdhury (1984, 1996), Nguyen (1985), Li and Lumb (1987), Christian et al. (1992, 1994), Wolff (1996), Juang et al. (1998), Tang et al. (1999), Dodagoudar and Venkatachalam (2000), Gui et al. (2000), El-Ramly et al. (2002), Griffiths and Fenton (2004), Sivakumar Babu and Mukesh (2004) were reported.

In the area of bearing capacity of foundations research focussed on both shallow and deep foundations and covered topics such as bearing capacity, settlement of foundations, foundation safety, offshore foundations. These subjects were addressed by Wu and Kraft (1967), Kay and Krizek (1971), Diaz and Vanmarcke (1974), Meyerhof (1976), Krizek et al. (1977), Nguyen (1985), Phoon et al. (1990), Li et al. (1993), Brzakala et al. (1995), Pula and Wyjadlowski (1999), Bauer and Pula (2000), Cherubini (2000), Fenton and Griffiths (2000, 2003), Honjo et al. (2000), Griffiths and Fenton (2001), Lacasse (2001), Nobahar and Popescu (2001, 2002), Elakateb et al. (2002), Griffiths et al. (2002), Zekkos et al. (2004), Fenton and Griffiths (2005) and work by many other research workers.

The above list of references is not exhaustive as there are number of reported applications of reliability methods in geotechnical engineering.

1.4 Objective of the study

The objective of the present study is to highlight the importance of quantification of variability of engineering parameters in geotechnical engineering by the application of probabilistic methods to evaluate the stability of shallow foundations and slopes.

1.5 Organization of the thesis

A brief description of the work carried out under various chapters is discussed below.

Chapter 2 briefs the conventional procedures adopted for the evaluation of bearing capacity and settlement of shallow foundations, and stability of unsaturated soil slopes. The procedures for probabilistic characterization and evaluation of various sources of uncertainty associated with the prediction of mean design parameters, viz., inherent variability, measurement uncertainty, and transformation model variability are discussed in this chapter. The development and application of risk and reliability concepts in civil engineering, in particular, geotechnical engineering for solving the strength and deformation characteristics are discussed. Load resistance factored design approach for the foundation code calibration is also presented and the scope of the investigation is clearly brought out.

Chapter 3 deals with probabilistic site characterization of three soil sites, viz., a cohesionless soil deposit belonging to Texas A & M Riverside Sand site, USA, a cohesive soil deposit of Keswick Clay, Adelaide City, Australia, and a cohesive soil deposit at a power plant site in Indian state of Andhra Pradesh. In-situ cone tip resistance (q_c) is used for the characterization of above three sites. The soil deposit within significant zones of influence is verified for statistical homogeneity using both

parametric and non-parametric tests. The statistical parameters of inherent variability of cone tip resistance are evaluated for these sites.

Chapter 4 deals with the allowable pressure of shallow foundations resting on cohesionless soil deposit of Texas A & M Riverside Sand site. The allowable pressure is based on two criteria of design, viz., the shear failure criterion and settlement criterion. Effect of all the possible sources of uncertainty on the design parameters are appropriately considered in the analysis. The effect of variance reduction due to spatial correlation and spatial averaging on the reliability index is also studied in this chapter using 1-D random field theory.

Chapter 5 highlights the probabilistic analysis of bearing capacity of shallow strip footing resting on the surface of clayey deposits using the results obtained in chapter 3. The transformation model uncertainty relating the in-situ cone tip resistance (q_c) and the undrained shear strength (S_u) obtained from unconsolidated undrained triaxial compression test conducted on the undisturbed soil samples is evaluated. The effect of total design variability and the variability of spatial average on the performance of foundations against complete shear failure is also narrated.

Chapter 6 describes the effect of anisotropy of autocorrelation characteristics in 2-D random field on the bearing capacity of shallow strip foundation resting on cohesionless soil deposit using the statistical parameters evaluated in chapter 3.

Chapter 7 describes the evaluation of resistance factors for the bearing capacity of shallow foundations against shear failure criterion. These resistance factors are developed for the code calibration process on a regional basis, taking into consideration appropriate values for various sources of uncertainty applicable to the region under consideration.

Chapter 8 describes the stability analysis of soil slopes in a probabilistic framework. The parameters affecting the performance of the slope are identified through a sensitive analysis. A lumped coefficient of variability is assigned to each of the uncertain parameters. The temporal variation of matric suction throughout the depth of interest is modeled using a 1-D numerical code, which solves coupled partial differential equations of moisture and heat transport. The chapter demonstrates a procedure for the evaluation of an optimum soil slope, considering the initial cost, failure consequences, and the probability of failure.

Chapter 9 describes summary and conclusions of the present study.

Chapter 2

LITERATURE REVIEW

2.1 Introduction

The objective of present study is to suggest rational methodologies for development of reliability based designs for shallow foundations and slopes. Hence, in this chapter, literature review pertaining to these topics is addressed in a systematic manner. The systematic approach in designs based on probabilistic methods makes risk explicit, formally describing them and making them easier to manage. A guide to suitable safety factors in foundation engineering has to include many additional factors, such as the variability and uncertainty of the loading and soil resistance and the seriousness of a failure (Meyerhof 1970). The need for incorporation of results of site investigation in the design of foundations and slopes in a rational manner using conventional and probabilistic approaches is addressed, and the scope of the investigation is brought out.

Numerous studies have been made in the recent past on the importance of implementation of risk and reliability concepts and extending its potential benefits in the field of geotechnical engineering. The Construction Industry Research and Information Association (CIRIA 2001) defines the risk as “the probability (or likelihood) of an unwanted uncertain event, and its unwanted consequences for objectives”. These factors when used cautiously, guarantee to a reasonable degree of confidence in the safety and serviceability of foundation system.

The success or failure of the site investigation and the structure depends on the approach to risk (CIRIA 2001). Risk management is not new. Traditionally it has

been in use with risk remaining implicit accounting for various sources and levels of uncertainty in footing loads and soil resistance and engineering design methods and processes have historically managed by experience and subjective judgment (Paikowsky 2002). This aspect has been highlighted by the engineers and academicians of geotechnical engineering at the highest level and has been the topic of Rankine and Terzaghi lectures of De Mello (1977), Whitman (1984), Lacasse (2001) and Christian (2004). In view of the increased awareness of these techniques and the impact of increased natural and man-made hazards and associated failure consequences, research work is being conducted in many countries and in India, a few attempts have been made in this direction. In this chapter, a brief review of literature is presented and pertinent literature is highlighted in the appropriate sections.

Terzaghi (1936) observed that no geotechnical site is truly homogeneous in engineering properties. However, in general, to simplify the analysis, analytical and transformation models are used to interpret results of site investigation using simplified assumptions and approximations. But, in reality due to the complexity in soil formation and depositional processes, soil behaviour is seldom homogenous. In addition, assessment of stability is based on the deterministic approaches using values based on judgement or average/low/high values of soil properties, which may conceal the realistic picture of degree of performance of a structure. Terzaghi (1936) aptly cautioned the geotechnical community not to reckon on oversimplified site models, its properties, or its response. Cornell (1969) indicated that the design of engineering systems subjected to an unpredictable natural environment is not easy when the system performance is predicted through imperfect mathematical theories using materials with variable properties. Geologic anomalies, inherent spatial variability of soil properties, scarcity of representative data, changing environmental conditions,

unexpected failure mechanisms, simplifications and approximations adopted in geotechnical models, and human mistakes in design and construction are all factors contributing to uncertainty. The evaluation of the role of uncertainty necessarily requires the implementation of probability concepts and methods (El-Ramly et al. 2002). Unless all the sources of uncertainty are clearly brought out and included in the designs, it is not possible to explicitly assess the amount of risk involved. A blanket factor that is generally used in conventional foundation designs to include implicitly all the sources of uncertainty arising in geotechnical property evaluation does not in any way truly account for involved risk.

2.2 Need for site characterization

The first and foremost phase in the formulation of probabilistic techniques in geotechnical engineering is that of having the information with regard to the subsoil conditions and its variations, at least within the zone of interest, in terms of stratigraphy, geotechnical properties, ground water table, suction characteristics in case if the soil is unsaturated, etc. Variations are expressed in terms of mean or average values and the coefficients of variation defined in terms of the ratio of standard deviation and mean value expressed as percentage.

A successful geotechnical design depends largely on how best the designer selects the basic soil parameters of the site under consideration from in-situ and/or laboratory test results. These values are subjective, and depend on the individual decisions based on personal experience and judgement of the engineer in-charge. Surprisingly, the higher variability with which the predictions have been done against the measured performance of foundations and embankments reveals that there is little consensus

among the designers on the values of soil parameters considered in the analysis (Kay 1993).

Probabilistic methods in geotechnical engineering have received considerable attention in the recent years and the incorporation of soil variability in geotechnical designs has become important. Guidelines have also been developed in this context (USACE 1997; JCSS 2000). Soil has high variability compared to manufactured materials like steel or cement, where variability in material properties is less, as they are produced under high quality control.

2.3 Characterization of variability of design parameters

It is generally agreed that the variability associated with geotechnical properties should be divided in to three main sources, viz., inherent variability, measurement uncertainty, and transformation uncertainty (Vanmarcke 1977a; Baecher 1982; Tang 1984; Phoon and Kulhawy 1999a).

2.3.1 Inherent variability

The inherent variability of a soil parameter is attributed to the natural geological processes, which are responsible for depositional behaviour and stress history of soil under consideration. The fluctuations of soil property about the mean can be modelled using a zero-mean stationary random field (Vanmarcke 1977a; Phoon et al. 2003a). A detailed list of the fluctuations in terms of coefficients of variation for some of the laboratory and in-situ soil parameters, along with the respective scales of fluctuation in horizontal and vertical directions are presented by Kulhawy (1992), Lacasse and Nadim (1996), Duncan (2000).

2.3.2 Measurement uncertainty

Measurement uncertainty is described in terms of accuracy and is affected by bias (systematic error) and precision (random error). It arises mainly from three sources, viz., equipment errors, procedural-operator errors, and random testing effects, and can be evaluated from data provided by the manufacturer, operator responsible for laboratory tests and/or scaled tests. Nonetheless the recommendations from regulatory authorities regarding the quality of produced data, the measuring equipment and other devices responsible for the measurement of in-situ or laboratory soil properties often show variations in its geometry, however small it may be. There may be many limitations in the formulation of guidelines for testing, and the understanding and implementation of these guidelines vary from operator to operator and contribute to procedural-operator errors in the measurement. The third factor, which contributes to the measurement uncertainty, random testing error, refers to the remaining scatter in the test results that is not assignable to specific testing parameters and is not caused by inherent soil variability (Jaksa et al. 1997; Phoon and Kulhawy 1999a).

2.3.3 Transformation uncertainty

Computation models, especially in the geotechnical field contain considerable uncertainties due to various reasons, e.g. simplification of the equilibrium or deformation analysis, ignoring 3-D effects etc. (JCSS 2000; Phoon and Kulhawy 2003, Zhang et al. 2004). Expected mean values and standard deviations of these factors may be assessed on the basis of empirical or experimental data, on comparison with more advanced computation models. Many design parameters used in geotechnical engineering are obtained from in-situ and laboratory test results. To

account for this uncertainty, the model or transformation uncertainty parameter is used.

2.3.4 Evaluation design parameter uncertainty

The total uncertainty of design parameter from the above three sources of uncertainty is combined in a consistent and logical manner using a simple second-moment probabilistic method (Phoon and Kulhawy 1999b). The design parameter may be represented as

$$\xi_d = T(\xi_m, \varepsilon) \tag{2.1}$$

where ξ_m is the measured property of soil parameter obtained from either a laboratory or in-situ test. The measured property can be represented in terms of algebraic sum of non-stationary trend, t, stationary fluctuating component, w, and measurement uncertainty, e. ε is the transformation uncertainty, which arises due to the uncertainty in transforming the in-situ or laboratory measured soil property to the design parameter using a transformation equation of the form shown in Equation 2.1. Hence, the design property can be represented by Equation 2.2.

$$\xi_d = T(t + w + e, \varepsilon) \tag{2.2}$$

Phoon and Kulhawy (1999b) expressed the above equation in terms of Taylor series. Linearizing the Taylor series after terminating the higher order terms at mean values of soil parameters leads to the Equation 2.3 for soil design property, subsequently the mean and variance of design property are expressed as given in Equations 2.4 and 2.5.

$$\xi_d \approx T(t,0) + w\left.\frac{\partial T}{\partial w}\right|_{(t,0)} + e\left.\frac{\partial T}{\partial e}\right|_{(t,0)} + \varepsilon\left.\frac{\partial T}{\partial \varepsilon}\right|_{(t,0)} \tag{2.3}$$

$$m_{\xi d} \approx T(t,0) \tag{2.4}$$

$$SD_{\xi d}^2 = \left(\frac{\partial T}{\partial w}\right)^2 SD_w^2 + \left(\frac{\partial T}{\partial e}\right)^2 SD_e^2 + \left(\frac{\partial T}{\partial \varepsilon}\right)^2 SD_\varepsilon^2 \quad (2.5)$$

The resulting variance of design parameter after incorporating the spatial average is given by Equation 2.6.

$$SD_{\xi a}^2 = \left(\frac{\partial T}{\partial w}\right)^2 \Gamma^2(L) SD_w^2 + \left(\frac{\partial T}{\partial e}\right)^2 SD_e^2 + \left(\frac{\partial T}{\partial \varepsilon}\right)^2 SD_\varepsilon^2 \quad (2.6)$$

Of the above, the treatment and evaluation of inherent soil variability assumes considerable importance as the uncertainties from measurements and transformation process can be handled if proper testing methods are adopted and transformation errors are quantified. Approaches for evaluation of inherent soil variability are developed based on random fields and a brief description of the theory and its relevance to characterisation of soil spatial variability is described in the following sections.

2.4 Random field Theory

Soil properties exhibit an inherent spatial variation, i.e., its value changes from point to point. Vanmarcke (1977a; 1983) provided a major contribution to the study of spatial variability of geotechnical materials using random field theory. In order to describe a soil property stochastically, Vanmarcke (1977a) stated that three parameters are needed to be described: (i) the mean (ii) the standard deviation (or the variance, or the coefficient of variation); and (iii) the scale of fluctuation. He introduced the new parameter, scale of fluctuation, which accounts for the distance within which the soil property shows relatively strong correlation from point-to-point.

Figure 2.1(a) shows a typical spatially variable soil profile showing the trend, fluctuating component, and vertical scale of fluctuation. Small values of scale of

fluctuation imply rapid fluctuations about the mean, whereas large values suggest a slowly varying property, with respect to the average.

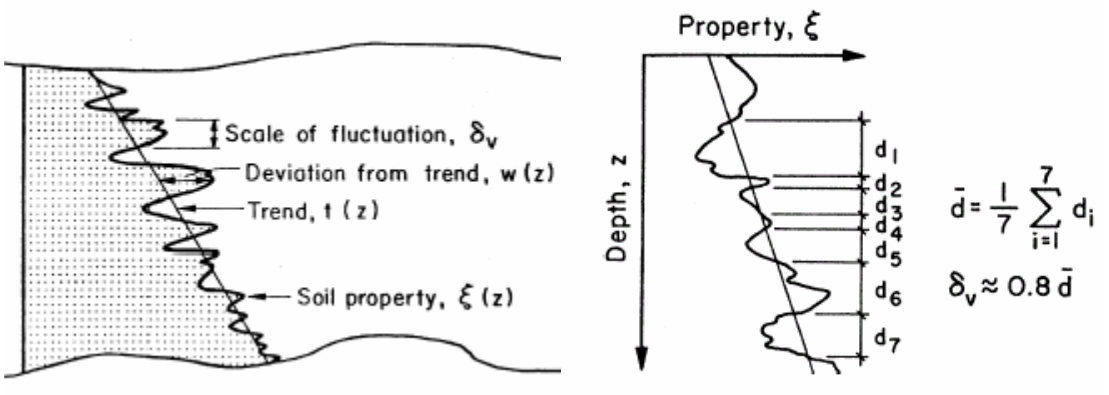

(a) (b)

Figure 2.1(a). Definition of various statistical parameters of a soil property (Phoon and Kulhawy 1999a); (b) approximate definition of the scale of fluctuation (Vanmarcke 1977a)

Vanmarcke (1977a) demonstrated a simple procedure to evaluate an approximate value of the vertical scale of fluctuation, as shown in Figure 2.1(b), which shows that the scale of fluctuation is related to the average distance between intersections, or crossings, of the soil property and the mean.

A random field is a conceivable model to characterize continuous spatial fluctuations of a soil property within a soil unit. In this concept, the actual value of a soil property at each location within the unit is assumed to be a realization of a random variable. Usually, parameters of the random field model have to be determined from only one realization. Therefore the random field model should satisfy certain ergodicity conditions at least locally. If a time average does not give complete representation of full ensemble, system is non-ergodic. The random field is fully described by the autocovariance function, which can be estimated by fitting empirical autocovariance data using a simple one-parameter theoretical model. This function is commonly

normalized by the variance to form the autocorrelation function. Conventionally, the trend function is approximately removed by least square regression analysis (e.g., Brockwell and Davis 1987; Kulhawy et al. 1992, Jaksa et al. 1999).The remaining fluctuating component, x(z), is then assumed to be a zero-mean stationary random field. When the spacing between two sample points exceeds the scale of fluctuation, it can be assumed that little correlation exists between the fluctuations in the measurements. Fenton (1999a & b) observed that the scale of fluctuation often appears to increase with sampling domain.

2.4.1 Statistical homogeneity

Statistical homogeneity in a strict sense means that the entire joint probability density function (joint pdf) of soil property values at an arbitrary number of locations within the soil unit is invariable under an arbitrary common translation of the locations. A more relaxed criterion is that expected mean value and variance of the soil property is constant throughout the soil unit and that the covariance of the soil property values at two locations is a function of the separation distance. Random fields satisfying only the relaxed criteria are called stationary in a weak sense.

Statistical homogeneity (or stationarity) of a data set is an important prerequisite for statistical treatment of geotechnical data and subsequent analysis and design of foundations. In physical sense, stationarity arises in soils, which are formed with similar material type and under similar geological processes. Improper qualification of a soil profile in terms of the statistical homogeneity leads to biased estimate of variance of the mean observation in the soil data. The entire soil profile within the zone of influence is divided into number of statistically homogeneous or stationary sections, and the data within each layer has to be analysed separately for further

statistical analysis. Hence, the partition of the soil profile into stationary sections plays a crucial role in the evaluation of soil statistical parameters such as variance.

2.4.2 Tests for statistical homogeneity

The methods available for statistical homogeneity are broadly categorised as parametric tests and non-parametric tests. The parametric tests require assumptions about the underlying population distribution. These tests give a precise picture about the stationarity (Phoon et al. 2003a).

In geostatistical literature, many classical tests for verification of stationarity have been developed, such as Kendall's τ test, Statistical run test (Phoon et al. 2003a). Invariably, all these classical tests are based on the important assumption that the data are independent (Cressie 1993). When these tests are used to verify the spatially correlated data, a large amount of bias appears in the evaluation of statistical parameters, and misleads the results of the analysis. To overcome this deficiency, Kulathilake and Ghosh (1988), Kulathilake and Um (2003), and Phoon et al. (2003a) proposed advanced methods to evaluate the statistical homogeneous layers in a given soil profile. The method proposed by Kulathilake and Ghosh (1988), Kulathilake and Um (2003) is semi-empirical window based method, and the method proposed by Phoon et al. (2003a) is an extension of the Bartlett test.

2.4.2.1 Kendall's τ test

The Kendall $\hat{\tau}$ statistic is frequently used to test whether a data set follows a trend (Jaksa et al. 1999). Kendall's $\hat{\tau}$ is based on the ranks of observations. The test statistic, which is also the measure of association in the sample, is given by

$$\hat{\tau} = \frac{S}{n(n-1)/2} \tag{2.7}$$

where n is the number of (X,Y) observations. To obtain S, and consequently $\hat{\tau}$, the following procedure is followed (Daniel 1990).

1. Arrange the observations (X_i, Y_i) in a column according to the magnitude of the X's, with the smallest X first, the second smallest second, and so on. Then the X's are said to be in natural order.
2. Compare each Y value, one at a time, with each Y value appearing below it. In making these comparisons, it is said that a pair of Y values (a Y being compared and the Y below it) is in natural order if the Y below is larger than the Y above. Conversely, a pair or Y values is in reverse natural order if the Y below is smaller than the Y above.
3. Let P be the number of pairs in natural order and Q the number of pairs in reverse natural order.
4. S is equal to the difference between P and Q;

A total of $\binom{n}{2} = \frac{n(n-1)}{2}$ possible comparisons of Y values can be made in this manner. If all the Y pairs are in natural order, then $P = \frac{n(n-1)}{2}$, Q=0, $S = \frac{n(n-1)}{2} - 0 = \frac{n(n-1)}{2}$, and hence $\tau = \frac{n(n-1)/2}{n(n-1)/2} = 1$, indicating perfect direct correlation between the observations of X and Y. On the other hand, if all the Y pairs are in reverse natural order, we have $P=0, Q = \frac{n(n-1)}{2}$, $S = 0 - \frac{n(n-1)}{2} = \frac{-n(n-1)}{2}$, and $\tau = \frac{-n(n-1)/2}{n(n-1)/2} = -1$, indicating a perfect inverse correlation between the X and Y observations.

Hence $\hat{\tau}$ cannot be greater than +1 or smaller than -1, thus, $\hat{\tau}$ can be taken as a relative measure of the extent of the disagreement between the observed orders of the Y. The strength of the correlation is indicated by the magnitude of the absolute value of $\hat{\tau}$.

2.4.2.2 Statistical run test

In this procedure, a run is defined as a sequence of identical observations that is followed and preceded by a different observation or no observation at all. The number of runs that occur in a sequence of observations gives an indication as to whether or not results are independent random observations of the same random variable. In this the hypothesis of statistical homogeneity, i.e., trend-free data, is tested at any desired level of significance, α, by comparing the observed runs to the interval between $r_{n;1-\alpha/2}$ *and* $r_{n;\alpha/2}$. Here, n=N/2, N being the total number of data points within a soil record. If the observed number of runs falls outside the interval, the hypothesis would be rejected at the α level of significance. Otherwise, the hypothesis would be accepted (Bendat and Piersol 1986).

Alonso and Krizek (1975) used the statistical run test to verify the stationarity of the soil data. For testing a soil record with run test, the soil record is first divided into number of sections, and variance of the data in each section is computed separately. The computed variance in each section is compared with the median of the variances in all sections, and the number of runs (r) is obtained. The record is said to be stationary or statistically homogeneous at significance level of α, if the condition given in Equation 2.9 is satisfied.

$$r_{n;\ 1-\alpha/2} < r \leq r_{n;\ \alpha/2} \tag{2.8}$$

2.4.2.3 Bartlett's approach

The classical Bartlett test is one of the important tests, which examines the equality of two or multiple variances of independent data sets (Kanji 1993, Phoon et al. 2003a). The following steps are involved in the Bartlett's test.

The sampling window is divided into two equal segments and sample variance (s_1^2 *or* s_2^2) is calculated from the data within each segment separately. For the case of two sample variances, s_1^2 *and* s_2^2 , the Bartlett test statistic is calculated as

$$B_{stat} = \frac{2.30259(m-1)}{C}\left[2\log s^2 - \left(\log s_1^2 + \log s_2^2\right)\right] \tag{2.9}$$

where m=number of data points used to evaluate s_1^2 *or* s_2^2 . The total variance, s^2, is defined as

$$s^2 = \frac{s_1^2 + s_2^2}{2} \tag{2.10}$$

The constant C is given by

$$C = 1 + \frac{1}{2(m-1)} \tag{2.11}$$

While choosing the segment length, it should be remembered that m≥10 (Lacasse and Nadim 1996). In this technique, the Bartlett statistic profile for the whole data within the zone of influence is generated by moving sampling window over the soil profile under consideration. In the continuous Bartlett statistic profile, the sections between the significant peaks are treated as statistically homogeneous or stationary layers, and each layer is treated separately for further analysis.

2.4.2.4 Modified Bartlett technique

Phoon et al. (2003a, 2004) developed the Modified Bartlett technique to test the condition of null hypothesis of stationarity of variance for correlated profiles suggested by conventional statistical tests such as Bartlett test, Kendall's test etc, and to decide whether to accept or reject the null hypothesis of stationarity for the correlated case. The modified Bartlett test statistic can also be used advantageously to identify the potentially stationary layers within a soil profile. This procedure was formulated using a set of numerically simulated correlated soil profiles covering all the possible ranges of autocorrelation functions applicable to soil. In this procedure, the test statistic to reject the null hypothesis of stationarity is taken as the peak value of Bartlett statistic profile. The critical value of modified Bartlett statistic is chosen at 5% significance level, which is calculated from simulated soil profiles using multiple regression approach, following five different autocorrelation functions, viz., single exponential, double exponential, triangular, cosine exponential, and second-order Markov.

The data within each layer between the peaks in the Bartlett statistic profile are checked for existence of trend. A particular trend is decided comparing the correlation length obtained by fitting a theoretical function to sample autocorrelation data. If the correlation lengths of two trends of consecutive order are identical, it is not required to go for higher order detrending process. However, it is suggested that no more than quadratic trend is generally required to be removed to transform a non-stationary data set to stationary data set (Jaksa et al. 1999).

The following dimensionless factors are obtained from the data within each layer.

Number of data points in one scale of fluctuation, $k = \dfrac{\delta}{\Delta z}$ (2.12)

Normalized sampling length, $I_1 = \frac{T}{\delta} = \frac{n\Delta z}{k\Delta z} = \frac{n}{k}$ (2.13)

Normalized segment length, $I_2 = \frac{W}{\delta} = \frac{m\Delta z}{k\Delta z} = \frac{m}{k}$ (2.14)

where δ is the scale of fluctuation evaluated, and 'n' is the total of data points in a soil record of T. The Bartlett statistic profile is computed from the sample variances computed in two contiguous windows. Hence, the total soil record length, T, should be greater than 2W. To ensure that $m \geq 10$, the normalized segment length should be chosen as $I_2=1$ for $k \geq 10$ and $I_2=2$ for $5 \leq k < 10$ (Phoon et al. 2003a).

Equations 2.15 and 2.16 show the typical results obtained from regression analysis for I_2 equals to 1 and 2 respectively for the single exponential simulated profiles. Similar formulations have also been developed for other commonly encountered autocorrelation functions and reported in Phoon et al. (2003a).

$B_{crit}=(0.23k+0.71)\ln(I_1)+0.91k+0.23$ for $I_2=1$ (2.15)

$B_{crit}=(0.36k+0.66)\ln(I_1)+1.31k-1.77$ for $I_2=2$ (2.16)

A comparison is made between the peaks of the Bartlett statistic within each layer with B_{crit} obtained from the respective layer. If $B_{max}<B_{crit}$, the layer can be treated as statistically homogeneous and hence, accept the null hypothesis of stationarity. Otherwise, if $B_{max}>B_{crit}$, reject the null hypothesis of stationarity, and treat the sections on either side of the peaks in the Bartlett statistic profile as stationary and repeat the above steps and evaluate whether these sections satisfy the null hypothesis of stationarity. However, while dividing the sections on either side of the peaks in the Bartlett statistic profile, it should be checked for $m \geq 10$, where 'm' is the number of data points in a segment.

2.4.2.5 Dual-window based method

Kulathilake and Ghosh (1988) and Kulathilake and Um (2003) proposed a simple window based method to verify the statistical homogeneity of the soil profile using cone tip resistance data. In this method, a continuous profile of 'BC' distance is generated by moving two contiguous sub-windows throughout the cone tip resistance profile. The distance 'BC', whose units are same as q_c, is the difference of the means at the interface between two contiguous windows. In this method it is verified whether the mean of the soil property is constant with depth, which is a prerequisite to satisfy the weak stationarity. At first, the elevation of the window is taken at a level that coincides with the level of first data point in the q_c profile. After evaluating the BC distance, the whole window is moved down at a shift each time. The computed distance 'BC' is noted each time at the elevation coinciding the centre of the window (i.e., the intersection of two contiguous sub-windows). This length of sub-window is selected based on the premise that at least 10 data points are available within the sub-window.

The data within the two sub-windows is treated separately, and checked for linear trend in the data of 10 points. The reason behind verifying the data with only linear trend is that within 0.2 m profile, higher-order trends are rarely encountered. In addition, in normally consolidated soils, the overburden stress follows a linear trend with depth. Kulathilake and Um (2003) suggested that the demarcation between existence and non-existence of a linear trend in the data be assumed at a determination coefficient (R^2) of 0.9. It means that if the R^2 value of theoretical linear fit is greater than 0.9, then the data set is said to be having a linearly trend in it, if not the mean value is said to be constant throughout the sub-window. Hence, within a window

length (i.e., two contiguous windows) there exist four sets of possibility of trend in the mean values. They are

1. Constant trend in both the contiguous sub-windows
2. Constant trend in upper sub-window and a linear trend in the lower sub-window
3. Linear trend in the upper sub-window and constant trend in the lower sub-window, and
4. Linear trend in both the contiguous sub-windows.

The above four sets possibilities of trend within the contiguous windows are shown in Figure 2.2. As the distance 'BC' increases, the heterogeneity of the q_c at the intersection between two sub-sections increases.

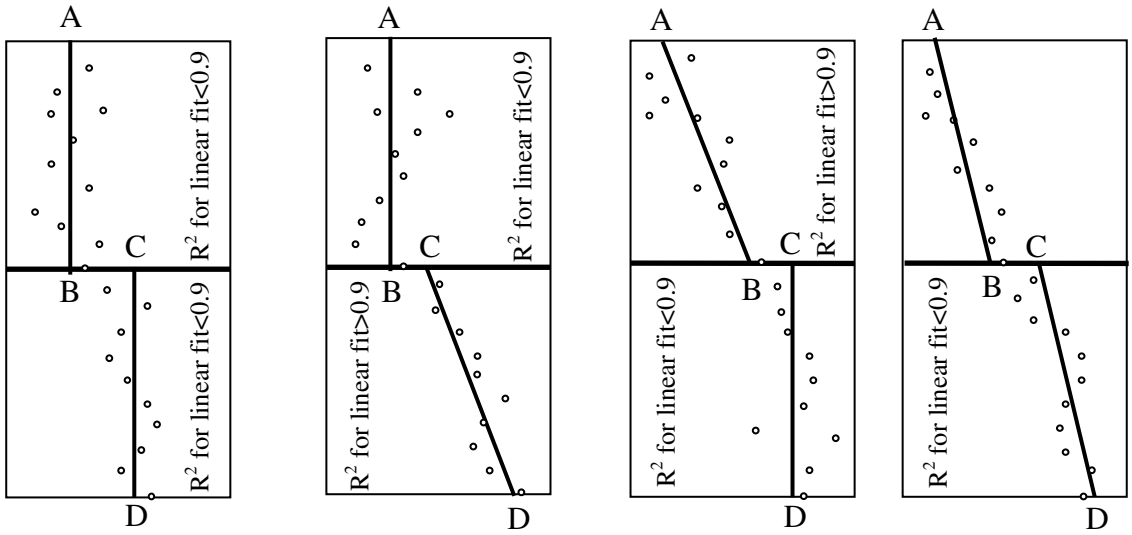

Figure 2.2. Evaluation of 'BC' distance in various possible combinations

2.4.3 Trend removal

Once the statistically homogeneous layers are identified within a soil profile, the individual statistical layers are checked for the existence of trend, and the same is removed before evaluating the variance and autocorrelation characteristics of the data

(Kulathilake and Um 2003). In general, all soil properties exhibit a trend with depth. The deterministic trend in the vertical soil profile may be attributed to overburden stress, confining pressure and stress history of soil under study. Generally, a smooth curve can be fitted using the Ordinary Least Square (OLS) method, except in special cases such as varved clays, where periodic trends are clearly visible (Phoon et al. 2003a). In most of the studies, the trend line is simply estimated by regression analysis using either linear or polynomial curve fittings (Alonso and Krizek 1975; Campanella et al. 1987; Kulhawy et al. 1992).

Other methods have also been applied, such as normalization with respect to some important physical variables (Hegazy et al. 1996), differencing technique (Bowerman and O'Connell 1983), which is routinely used by statisticians for transforming a non-stationary time series to a stationary one. The normalization method of trend removal with respect to a physical quantity accounts for systematic physical effects on the soil profiles. In general, the detrending process is not unique. Different trend removal procedures will in most cases result in different values of the random fluctuating components and different shapes of the autocorrelation function.

Baecher (1987) commented that the selection of a particular trend function is a decision on how much of the spatial variability in the measurements is treated as a deterministic function of space (i.e., trend) and how much is treated statistically and modelled as random processes. However, the detrending process cannot be entirely arbitrary. After all, the fluctuating components remaining in the detrended soil records must be stationary for meaningful statistical analyses to be undertaken on limited data points. Clearly, the chosen trend function should be reasonable in view of this stationary constraint. The scale of fluctuation or autocorrelation distance evaluated from the non-stationary data is always higher than the corresponding stationary data.

In other words, the trend removal invariably reduces the scale of fluctuation of the soil properties. One of the simplest methods to evaluate whether a linear or 2nd order polynomial trend is sufficient to be removed from the experimental data is to calculate the scale of fluctuation for the above both detrended data. If the evaluated scales of fluctuation are closer to each other, a detrending process using the lesser degree polynomial is chosen. In the limit, the scale of fluctuation is zero when the entire profile is treated as a ‘‘trend’’ with zero ‘‘random’’ variation (Phoon et al. 2003a).

If a trend is evident in the measurements, it should be decided whether or not it should be removed before statistical analysis of a set of raw data. An observed trend that has no physical or geological basis or is not predictable must not be removed prior to statistical analysis, since it is a part of the uncertainty to be characterized (Fenton 1999b). After selecting a proper trend function for the data, the residuals off the trend are calculated. Phoon et al. (2004) pointed out that trend removal is a complex problem, and there is at present no fully satisfactory solution to it. The identified trend in the data is removed by employing any of the following three widely used detrending methods.

2.4.3.1 Decomposition technique

In this method the data set is divided into stationary random field and nonstationary trend, by using the results obtained from either a non-parametric test or a parametric test discussed in the last section. Initially a linear trend is selected and removed from the original data. The linearly detrended data is tested for the weak stationarity. If the residuals off the linear trend do not satisfy the stationarity hypothesis, the above procedure is repeated by choosing a higher order polynomial. However, it is suggested that no more than quadratic trend is normally sufficient to transform a non-

stationary data set to stationary data set (Jaksa et al. 1999), and keep them fairly stationary, as complete removal of the trend in the data is rarely achieved.

2.4.3.2 Normalization technique

Normalisation of the data set with respect to a dominant parameter, such as cone tip resistance, q_c, effective overburden pressure, σ'_{vo}, is also used in geotechnical engineering to make the data trend free (Uzielli 2004; Uzielli et al. 2005).

2.4.3.3 Differencing technique

In this method, a nonstationary data set is made stationary by using first, second or higher order differencing technique. This method of testing a time series is suggested by Bowerman and O'Connell (1983), which is suitable for data containing no seasonal variations. According to Bowerman and O'Connell (1983) if the sample autocorrelation function for experimental data dies down fairly quickly, the original data set can be treated as stationary. However, if the sample autocorrelation function dies down extremely slow, then the original data set can be transformed to a stationary set by taking first or second difference of original data set. However, the term "fairly quickly" is rather subjective and extensive judgment is involved in it. Moreover, it is observed that if no seasonal variations exist in the data, no more than second difference is rarely needed to transform a nonstationary data to stationary data (Jaksa et al. 1999).

2.4.4 Estimation of autocorrelation

Available methods for estimating the sample autocorrelation functions differ in their statistical properties such as the degree of bias, sampling variability, ease of use, computational requirements, etc. (Akkaya and Vanmarcke 2003). The methods that

are commonly used for this purpose are method of moments, Bartlett's approach, method based on maximum likelihood principle, Geostatistics, etc. However, the method of moments is the most common used to estimate sample correlation function of soil properties.

2.4.4.1 Method of moments

A classical way of describing random functions is through the autocorrelation function, $\rho(\Delta z)$. It is the coefficient of correlation between values of a random function at separation of k. The spatial correlation of a soil property can be modelled as the sum of a trend component and a residual term (Vanmarcke 1977a), as shown in Equation 2.17.

$$x=z+e \tag{2.17}$$

where x is the measurement at a given location, z is the trend component, and e is the residual (deviation about the trend). The residuals off the trend tend to exhibit spatial correlation. The degree of spatial correlation among the residuals can be expressed through an auto-covariance function.

$$c(k) = E\left[P(Z_i) - t(Z_i)\right]\left[P(Z_j) - t(Z_j)\right] \tag{2.18}$$

where k is the vector of separation distance between point i and j, E[.] is the expectation operator, $P(Z_i)$ is the data taken at location i, and $t(Z_i)$ is the value of the trend at location i. The normalized form of the autocovariance function given in Equation 2.19 is known as the autocorrelation function.

$$\rho(k)= c[k]/c[0] \tag{2.19}$$

where c[0] is the autocovariance function at zero separation distance, which is nothing but variance data.

It is not possible to evaluate 'c_k' nor 'ρ_k' with any certainty, but only to estimate them from samples obtained from a population. As a result, the sample autocovariance at lag k, c_k^*, and sample autocorrelation at lag k, r_k, are generally evaluated. The sample autocorrelation function (ACF) is the graph of r_k for lags k=0,1,2, …h, where 'h' is the maximum number of lags allowable. Generally, 'h' is taken as a quarter of total number of data points in time series analysis of geotechnical data (Box and Jenkins 1970; Lumb 1975a). Beyond this number, the number of pairs contributing to the autocorrelation function diminishes and produces unreliable results. The sample ACF at lag k, r_k, is generally evaluated using

$$r_k = \frac{\frac{1}{(N-k-1)}\sum_{i=1}^{N-k}\left(X_i - \overline{X}\right)\left(X_{i+k} - \overline{X}\right)}{\frac{1}{(N-1)}\sum_{i=1}^{N}\left(X_i - \overline{X}\right)^2} \tag{2.20}$$

If no measurement error or noise is present, r becomes equal to 1 at a lag distance of zero. Statistically homogeneous data are used to evaluate the sample autocorrelation functions. The autocorrelation characteristics of soil properties can be characterized either by autocorrelation distance, or scale of fluctuation, which is theoretically equal to the area under the correlation function. The scale of fluctuation (or correlation radius) for one dimensional real field is defined as shown in Equation 2.21 (Vanmarcke 1977a).

$$\delta = 2\int_0^\infty \rho(\tau)\, d\tau \tag{2.21}$$

More generally, the scale of fluctuation δ is defined as the radius of an equivalent "unit step" correlation function, i.e., $\rho(\tau)=1$ for $\tau \le \delta$ and $=0$ for $\tau > \delta$, τ being the Euclidian lag (JCSS 2000). The autocorrelation distance (or scale of fluctuation) is

evaluated from the sample autocorrelation function using method of fitting or based on Bartlett limits, which are described in the following sections.

2.4.4.1.1 Method of fitting

Analytical expressions are fitted to the sample autocorrelation functions using regression analysis based on least square error approach. The least square error is generally characterised by the determination coefficient of the fit. Frequently used single-parameter theoretical auto-correlation functions are exponential, squared exponential, though models such as triangular, second order auto-regressive, spherical, etc. are also not uncommon to fit the sample autocorrelation data in geotechnical engineering. Some of these models are given in Table 2.1.

Table 2.1. Theoretical autocorrelation functions used to determine the autocorrelation distance and scale of fluctuation, δ (Jaksa et al. 1999)

Model No.	Theoretical autocorrelation function	Autocorrelation function	Auto-correlation distance, ρ	Scale of fluctuation, δ
1	Triangular	$\rho_{\Delta z} = \begin{cases} 1 - \dfrac{\lvert\Delta z\rvert}{a} & for\ \lvert\Delta z\rvert \le a \\ 0 & for\ \lvert\Delta z\rvert \ge a \end{cases}$	a	a
2	Single exponential	$\rho_{\Delta z} = \exp\left(-\lvert\Delta z\rvert / b\right)$	b	2b
3	Double exponential	$\rho_{\Delta z} = \exp\left(-\left(\lvert\Delta z\rvert / c\right)^2\right)$	c	$\sqrt{\pi}\, c$
4	Second-order Markov	$\rho_{\Delta z} = \exp\left(-\lvert\Delta z\rvert / d\right)\left(1 + \dfrac{\lvert\Delta z\rvert}{d}\right)$	d	4d
5	Cosine exponential	$\rho_{\Delta z} = \exp\left(-\lvert\Delta z\rvert / e\right)\cos\left(\dfrac{\Delta z}{e}\right)$	e	e

Table 2.1 shows the autocorrelation distance and corresponding scale of fluctuation for theoretical autocorrelation functions. A small scale of fluctuation (δ) implies rapid fluctuations about the mean and vice versa. and a large reduction in variance over any failure plane; this results in a small "spread" of the performance function. Conversely

a large δ means much longer variations about the mean and results in smaller reduction in variance over a failure plane (Mostyn and Soo 1992).

2.4.4.1. 2 Bartlett limits

In the field of time series analysis, the most commonly used method to compute the autocorrelation distance is by Bartlett's approximation. In this method the computed scale of fluctuation corresponds to two standard errors of the estimate, i.e., the lag distance at which the positive Bartlett's limits given by Equation 2.21, superimposed on the autocorrelation plot crosses the autocorrelation function (Jaksa et al. 1999).

$$|r_h| = \pm \frac{1.96}{\sqrt{N}} \tag{2.22}$$

The scale of fluctuation of cone tip resistance varies from site to site. Moreover, it also varies with type of soil, as Jaksa et al. (2004) reports smaller scales of fluctuation in sands than clays due to their nature of formation. Further, Fenton and Vanmarcke (1998) argue that the scale of fluctuation depends largely on the geological processes of transport of raw materials, layer deposition, and common weathering rather than on the actual property studied. Nonetheless, DeGroot and Baecher (1993) observed that the scale of fluctuation is also function of sampling interval on in-situ measured property.

2.4.5 Effect of anisotropy in correlation scales

Most soils in nature are usually anisotropic due to their mode of sedimentation and consolidation that cause preferred particle orientations. There are generally two types of anisotropy. Inherent or initial anisotropy manifests itself in the soil deposits as a result of applied stresses at the time of formulation in the form of first-structure on a macroscopic scale or as a fabric orientation on the microscopic scale. Stress or

induced anisotropy arises from changes in the effective stress state produced by subsequent loading history. This anisotropy can cause the elastic, strength and compressibility parameters of the soil deposits to vary with direction, and hence cannot be ignored.

The soil properties exhibit large variations and their directional behaviour is observed by many researchers (Vanmarcke 1983; Jaksa et al. 1999; Phoon and Kulhawy 1999a; Griffiths and Fenton 2000; Nobahar and Popescu 2002; Fenton and Griffiths 2003; Jaksa et al. 2004; Sivakumar Babu and Mukesh 2004; and Uzielli et al. 2005; Wei et al. 2005). The autocorrelation distances in vertical and horizontal directions are never the same, but in general, differ by an order of magnitude, with horizontal scale of fluctuation being higher than that in the vertical (Uzielli et al. 2005). Attempts have been made in the literature to formulate autocorrelation models for 1, 2, and 3-dimensional soil space (Vanmarcke 1977a; and Kulathilake and Miller 1987). The effect of anisotropy of soil properties on the bearing capacity in a probabilistic framework has not been studied extensively in the literature. Many times, due to economic feasibility, speed of exploration, availability of equipment and time constraints vertical cone penetration data alone is obtained and used in the evaluation of strength properties (Wei et al. 2005).

The autocovariance structure is called isotropic if the normalized autocovariance depends on the Euclidian distances between field points only, instead of the axis directional distance components, components, i.e.,

$$\rho(\Delta x, \Delta y, \Delta z) = \rho\left(\sqrt{\Delta x^2 + \Delta y^2 + \Delta z^2}\right) \tag{2.23}$$

Isotropy implies that the autocorrelation function is invariant to orthonormal transformation of the field coordinates. Also the autocorrelation structure may be partly isotropic, for example with respect to horizontal field directions:

$$\rho(\Delta x, \Delta y, \Delta z) = \rho\left(\sqrt{\Delta x^2 + \Delta y^2}, \Delta z\right) \tag{2.24}$$

For complete anisotropy, the exponential correlation function in 3-D space is

$$\rho(\Delta x, \Delta y, \Delta z) = \exp\left(-\frac{|\Delta x|}{D_x} - \frac{|\Delta y|}{D_y} - \frac{|\Delta z|}{D_z}\right) \tag{2.25}$$

If an isotropy in the horizontal direction is assumed, then the exponential correlation function shown in Equation 2.25 is reduced to

$$\rho(\Delta x, \Delta y, \Delta z) = \exp\left(-\frac{\sqrt{\Delta x^2 + \Delta y^2}}{D_h} - \frac{|\Delta z|}{D_z}\right) \tag{2.26}$$

Similar theoretical autocorrelation functions in 3-D field for other distributions can also be formulated on the similar lines shown above.

2.4.6 Spatial averaging

Parameters in geotechnical analyses usually refer to averages of a soil property over a sliding surface or a rupture zone in an ultimate failure analysis or significantly strained volumes in a deformation analysis. If the dimensions of such surfaces or volumes exceed the scales of fluctuation of the soil property, spatial averaging of fluctuations is substantial. This implies that the variance of an averaged soil property over a sliding surface or affected volume is likely to be substantially less than the field variance, which is mainly based on small sample tests (e.g. triaxial tests) or small affected volumes in insitu tests (JCSS 2002).

Because of the spatial variability of soil properties, encountering a sufficiently low strength to induce failure in localized areas is more likely than such an encounter over the entire zone of influence. Both the conventional analyses based on the factor of safety and the simplified probabilistic analyses fail to address this issue of scale of failure. Over the depth interval ΔZ the spatial average soil property is given as

$$u(\Delta Z) = \frac{1}{\Delta Z}\int_{\Delta Z} u(\Delta Z)dz \tag{2.27}$$

The spatial average of the soil property u(x,y,z) over a volume V is given in the same way as

$$u_v = \frac{1}{V}\iiint_V u(x,y,z)dxdydz \tag{2.28}$$

Averaging distance depends on the nature of the problem in hand. For design of shallow foundations in shear criterion, this distance is equal to the extent of shear failure zone within the soil mass (Cherubini 2000). This distance for shallow foundations in cohesionless soil subjected to vertical loading is approximately taken as 2B below the base of footing in the vertical direction and 3.5B from the centre of footing in the horizontal direction, where B is the width of the footing.

2.4.7 Evaluation of variance reduction function

The combined effect of spatial correlation and spatial averaging of soil properties over the failure domain are beneficially utilized to reduce the variance of the measured data within the zone of interest. The derivation of the variance reduction functions in terms of spatial correlation and spatial average is described in the following section. JCSS (2002) presents the evaluation of variance reduction function by both exact approach and simplified approach.

2.4.7.1 Variance reduction for data in 1-D space

The variability of soil property u_i from point to point is measured by standard deviation σ_i and the standard deviation of the spatial average property $u_{\Delta Z}$ is by $\sigma_{\Delta Z}$. The larger the length (or the volume) over which the property is averaged, higher is the fluctuation of u_i that tends to cancel out in the process of spatial averaging. This causes reduction in standard deviation as the size of the averaging length or volume increases, which is given by

$$\Gamma_u(\Delta Z) = \frac{\sigma_{\Delta z}}{\sigma_i} \tag{2.29}$$

A simple relationship of the variance reduction function in terms of scale of fluctuation and averaging distance is given in Equation 2.30 (Vanmarcke 1977a).

$$\left.\begin{array}{ll} \Gamma^2(\Delta Z) = \dfrac{\delta}{\Delta Z} & \dfrac{L}{\delta} > 1.0 \\ \Gamma^2(\Delta Z) = 1.0 & \dfrac{L}{\delta} \le 1.0 \end{array}\right\} \tag{2.30}$$

The Equation 2.30 indicates that with decrease in scale of fluctuation and increase in averaging distance, the value of variance reduction function reduces, which in turn reduces standard deviation of the spatially averaged soil property. In other words, the more erratic the variation (i.e., less correlated the soil property) of the soil property with distance and larger the soil domain considered, larger will be the reduction in variability of the average property. This phenomenon is a result of the increasing likelihood that unusually high property values at some point will be balanced by low values at other point (Vanmarcke 1977a). However, Vanmarcke (1983) emphasized that the variance reduction function $\gamma(T)$ is related to the autocorrelation function $\rho(\tau)$ as given in Equations 2.31 and 2.32.

$$\gamma(T) = \frac{1}{T^2}\int_0^T\int_0^T \rho(t_1 - t_2)dt_1 dt_2 \tag{2.31}$$

which reduces to

$$\gamma(T) = \frac{2}{T}\int_0^T \left(1 - \frac{\tau}{T}\right)\rho(\tau)d\tau \tag{2.32}$$

From Equation 2.32, the variance reduction functions for triangular, exponential, and squared exponential autocorrelation functions can be worked out as given in Equations 2.33 to 2.35, respectively.

$$\gamma(T) = \begin{cases} 1 - \dfrac{T}{3a} & for\ T \le a \\ \left(\dfrac{a}{T}\right)\left(1 - \dfrac{a}{3T}\right) & for\ T \ge a \end{cases} \tag{2.33}$$

$$\gamma(T) = 2\left(\frac{b}{T}\right)^2\left(\frac{T}{b} - 1 + \exp(-T/b)\right) \tag{2.34}$$

$$\gamma(T) = \left(\frac{d}{T}\right)^2\left(\sqrt{\pi}\,\frac{T}{d}E\left(\frac{T}{d}\right) + \exp\left(-\left(\frac{T}{d}\right)^2\right) - 1\right) \tag{2.35}$$

where a, b, d are referred to as the autocorrelation distances, T is the averaging length, the distance over which the geotechnical properties are averaged over a failure surface, and E(·) is the error function, which increases from 0 to 1 as its argument increases from 0 to ∞. In terms of standard Gaussian cumulative distribution function $E(u)=2[F_U(u)-0.5]$.

As the averaging length, $T\rightarrow\infty$ the variance reduction function, $\gamma(T) \rightarrow 0$. In other words, the chances associated with failure of huge volume of soil are very rare. In addition, $\gamma(T)$ is inversely proportional to T at very large values of T.

2.4.7.2 Variance reduction for data in 2-D and 3-D space

2.4.7.2.1 Exact approach

If a problem is solved in 2-D random field, such as, strip footing, where plane strain conditions prevail, the soil properties should be averaged over a vertical plane surface (x, z-plane) with height h and width b (JCSS 2002).

$$I_{bh}(p) = \frac{1}{bh}\int_0^b\int_0^h p(\underline{x})dxdz = \frac{1}{bh}\int_0^b\int_0^h \left(m_p + f_p(\underline{x})\right)dxdz \tag{2.36}$$

The expected value of $I_{bh}(p)$ is equal to m_p; and variance of $I_{bh}(p)$ is given by Equation 2.37.

$$\mathrm{var}\left(I_{bh}(p)\right) = \sigma^2\Gamma^2(b,h) \tag{2.37}$$

where $\Gamma^2(b,h)$ is referred to as variance reduction factor.

If the correlation function is one of the separable type, then Equation 2.37 can be written as

$$\mathrm{var}\left(I_{bh}(p)\right) = \sigma^2\Gamma^2(b)\Gamma^2(h) \tag{2.38}$$

where $\Gamma^2(b)\ and\ \Gamma^2(h)$ are variance reduction factors in horizontal and vertical directions respectively, defined as

$$\Gamma^2(b) = \frac{2}{b}\int_0^b\left(1-\frac{\tau}{b}\right)\rho(\tau)d\tau \tag{2.39}$$

$$\Gamma^2(h) = \frac{2}{b}\int_0^h\left(1-\frac{\tau}{h}\right)\rho(\tau)d\tau \tag{2.40}$$

Which for large values of b compared to the correlation radius α_l tend to

$$\Gamma^2(b) = \frac{\alpha_1}{b} \tag{2.41}$$

Similar expression holds good even for $\Gamma^2(h)$.

Realistic estimates of b/D_h for sliding surfaces in dike or road embankments range in the order of 0.5 to 2, so variance reduction due to averaging in a horizontal direction may range between 0.95 and 0.4. Realistic estimates of h/D_v for potential sliding modes in dike or road embankments on soft soil range from 5 and more (JCSS 2002).

2.4.7.2.2 A simplified approach

The variance reduction factor for averaging in one, 2 or 3-D random field may be approximated as given in Equations 2.42, 2.43, and 2.44 (JCSS 2002).

$$\begin{aligned} \Gamma^2(L_1 \ldots L_n) &= 1 \qquad for\,(L_1 \ldots L_n) \le \alpha_n \\ &= \frac{\alpha_n}{(L_1 \ldots L_n)} \qquad for\,(L_1 \ldots L_n) \ge \alpha_n \end{aligned} \tag{2.42}$$

where n=1, 2, 3, and L_1, L_2 and L_3 are the lengths over which averaging takes place and α_1, α_2, α_3 are the correlation radii. In case of "separable" autocorrelation functions, i.e. which can be written as a multiplication of factors for each of the dimensions of a 2- or 3-D surface or volume, the total variance reduction factor can, for the 3-D case be written as:

$$\Gamma^2(L_1 L_2 L_3) = \Gamma^2(L_1)\Gamma^2(L_2)\Gamma^2(L_3) \tag{2.43}$$

Similar to the above, Vanmarcke (1977a) also proposed an approximate and simplified resultant variance reduction factor in 2-D space as the product of individual variance reduction factors in vertical and horizontal directions in terms of scale of fluctuation (δ) and spatial averaging distance (L) in the respective directions as shown in Equation (2.44).

$$\Gamma_A^2 = \Gamma_v^2 \times \Gamma_h^2 \tag{2.44}$$

2.5 Parameter distribution

Many statistical test procedures and reliability approaches .are based on specific distributional assumptions. The assumption of normality is particularly common in classical statistical tests. Log-normal, beta, exponential, and Weibull distributions are also widely used in modelling the variability in engineering parameters.

2.5.1 Normal distribution

The normal or Gaussian distribution is the most common type of probability distribution function and the distributions of many random variables conform to this distribution. It is generally used for probabilistic studies in geotechnical engineering unless there are good reasons for selecting a different distribution. Typically, variables which arise as a sum of a number of random effects, none of which dominate the total, are normally distributed.

The probability density function for a normal distribution is defined by:

$$f_X(x) = \frac{1}{\sqrt{2\pi}\sigma} \exp\left[-\frac{1}{2}\left(\frac{x-\mu}{\sigma} \right)^2 \right] for -\infty \le x \le \infty \tag{2.45}$$

In order to overcome the problem of $-\infty \le x \le \infty$ the normal distribution is sometimes truncated so that only values falling within a specified range are considered valid.

2.5.2 Lognormal distributions

The multiplicative mechanisms tend to result in variables which are lognormally distributed as opposed to the normally distributed variables resulting from additive

mechanisms. In the reliability approach, the load, S, and resistance, R, are modelled as random variables. Since neither the load nor the resistance attains a negative value, it is more practical and refined to assume a log-normal distribution for both R and S, rather a simple normal distribution, in case of limited data.

2.5.3 Other distributions

In addition to the commonly used normal and lognormal distributions there are a number of other distributions which are used in probability analyses, such as, beta distribution, exponential distribution, Weibull distribution. A number of treatises on these distributions are available in geotechnical literature (Ang and Tang 1984; Harr 1987; Baecher 1987).

2.6 Reliability analysis

The performance a structure to the external loads is assessed in terms of safety, serviceability, and economy. The engineering design should be such that the structure is capable of resisting all the loads acting on it and serve the purpose for which it is designed during its design life time keeping in mind the above three constraints.

The first step in evaluating the reliability or probability of failure of a structure is to identify the various possible limit states in which the structure may fail to perform its intended function. There may be innumerous number of possible limit states in a structure. However, depending on the importance of the structure and other constraints within the particular region, the designer based on his experience chooses the limit states in which the performance of the structure may be critical. For each specific performance criterion, the relevant load and resistance parameters, called the basic variables X_i and the functional relationship among them are identified. Each limit state is evaluated for its performance in terms of a dimensionless parameter

called reliability index, and the subsequent probability of failure is also evaluated. The performance of a system as a whole depends not on the performance of individual limit states alone, but depends on the combined performance of all the individual limit states involved in the problem. In geotechnical engineering, in most of the cases, all the structures are checked for performance in two limit states, viz., limit state of collapse, and limit state of serviceability, though there are many other limit states, which are generally insignificant. It is recognised and practiced that both the above limit states are connected in series, in that the failure of any one performance function leads to total collapse of the system. Mathematically, the performance function can be described as shown in Equation 2.62.

$$Z = R(X) - S(X) = g(X_1, X_2, X_3, ..., X_n) \tag{2.46}$$

Where R(X) and S(X) are resistance and load, and X is the collection of random input parameters. The failure surface or limit state of interest can be defined as Z=0. This is the boundary between the stable and unstable states in the design parameter space and represents the state beyond which a structure can no longer fulfil the function for which it was designed. The failure surface and safe and unsafe regions are shown in Figure 2.3 for two basic random variables R (resistance) and S (load). A limit state can be an explicit or implicit function of basic random variables.

From Equation 2.46 failure occurs when Z<0. Therefore, the probability of failure p_f is given by the integral shown by Equation 2.47.

$$p_f = \int .....\int_{g0} f_X(x_1, x_2, x_3 .....x_n) dx_1 dx_2 .....dx_n) \tag{2.47}$$

where $f_X(x_1, x_2 ... x_n)$ is the joint probability density function for the basic random variables $X_1, X_2, \ldots\ldots X_n$, and integration is performed over the failure region, that is,

g( )<0. If the random variables are statistically independent, then the product of the individual probability density functions in the integral can replace the joint probability density function.

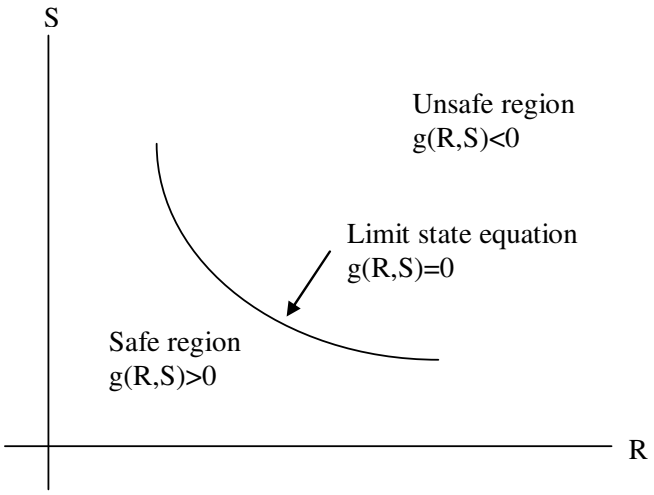

Figure 2.3. A typical limit state showing failure surface, safe and unsafe regions

However, Equation 2.47 can be evaluated easily, without performing the integration, for some special cases. For a performance function defined as given in Equation 2.48, if the load (S) and resistance (R) are statistically independent and follow normal distribution, the variable Z will also follow a normal distribution. For this case, the probability of failure is defined as given in Equations 2.49, 2.50, and 2.51.

$$Z = R - S \tag{2.48}$$

$$p_f = P(Z < 0) \tag{2.49}$$

$$\text{or, } p_f = \Phi\left(\frac{0-(\mu_R - \mu_S)}{\sqrt{\sigma_R^2 + \sigma_S^2}}\right) \tag{2.50}$$

$$\text{or, } p_f = 1-\Phi\left(\frac{(\mu_R - \mu_S)}{\sqrt{\sigma_R^2 + \sigma_S^2}}\right) \tag{2.51}$$

So the probability of failure depends on the ratio of the mean value and standard deviation of the variable Z. This ratio is known as the reliability index (β).

$$\beta = \left(\frac{(\mu_R - \mu_S)}{\sqrt{\sigma_R^2 + \sigma_S^2}} \right) \tag{2.52}$$

The probability of failure in terms of reliability index (β) is defined as

$$p_f = P(Z \le 0) = \Phi(-\beta_c) = 1 - \Phi(\beta_c) \tag{2.53}$$

where $\Phi(\cdot)$ is the cumulative normal probability function.

On the other hand, if R and S are statistically independent lognormal variables, considering the physical aspect of the problem an another random variable is defined as

$$Y = \frac{R}{S} \tag{2.54}$$

$$\text{or, } Z = \ln Y = \ln R - \ln S \tag{2.55}$$

In this case, the failure event can be defined as Y<1 or Z<0. Since R and S are lognormal, lnR and lnS follow a normal distribution, and subsequently lnY or Z follows a normal distribution. Hence, the probability of failure and reliability index (β) can be defined as shown in Equations 2.56 and 2.57.

$$p_f = 1 - \Phi\left[\frac{\ln\left\{ \left(\frac{\mu_R}{\mu_S} \right) \sqrt{\frac{(1 + CoV_S^2)}{(1 + CoV_R^2)}} \right\}}{\sqrt{\ln(1 + CoV_R^2)(1 + CoV_S^2)}} \right] \tag{2.56}$$

$$\beta = \Phi^{-1}(1-p_f) = \left[\frac{\ln\left[\left(\frac{\mu_R}{\mu_S}\right)\sqrt{\frac{(1+CoV_S^2)}{(1+CoV_R^2)}}\right]}{\sqrt{\ln(1+CoV_R^2)(1+CoV_S^2)}} \right] \tag{2.57}$$

where μ_R, μ_S, CoV_R, and CoV_S are the mean resistance, mean load, coefficient of variation of resistance and coefficient of variation of load parameters, respectively.

2.6.1 Reliability analysis using analytical methods

These methods are based on the several approximations on the limit state given in Equation 2.46. In general, obtaining joint probability density function of random variables is almost impossible and evaluation of the multiple integral given in Equation 2.47 is extremely complicated and highly involved. Therefore, a simple approach to deal such problems is to use analytical approximation of the integral shown in Equation 2.47. These methods can be broadly grouped into First-order reliability method (FORM) and Second-order reliability method (SORM).

The limit state of interest can be linear or non-linear functions of the basic random variables. When the limit state function is a linear function of uncorrelated normal variables or when the non-linear limit state function is represented by a first order or linear approximation with equivalent normal variables, FORM can be used advantageously. If the underlying equation is nonlinear, SORM produce satisfying results of safety indices. A detailed discussion of these issues for application to geotechnical problems is presented by many authors (Ang and Tang 1975; Harr 1987; Kottegoda and Rosso 1998; Haldar and Mahadevan 2000; Baecher and Christian 2003). However, the first-order reliability method of analysis is discussed in the following section.

2.6.1.1 First-order reliability methods (FORM)

The first order reliability methods can be classified into first-order second moment (FOSM) and advanced first order second moment (AFOSM) methods.

2.6.1.1.1 First-order second moment method (FOSM)

This method is also referred to as mean value first-order second moment (MVFOSM) method, and it is based on the first order Taylor series approximation of the performance function linearized at the mean values of the random variables. It uses only second-moment statistics (mean and variance) of the random variables. Originally, Cornell (1969) used the simple two variable approaches. On the basic assumption that the resulting probability of Z is a normal distribution, by some relevant virtue of the central limit theorem, Cornell (1969) defined the reliability index as the ratio of the expected value of Z over its standard deviation. The Cornell reliability index (β_c) is the absolute value of the ordinate of the point corresponding to Z=0 on the standardized normal probability plot as given in Figure 2.4 and Equation 2.58.

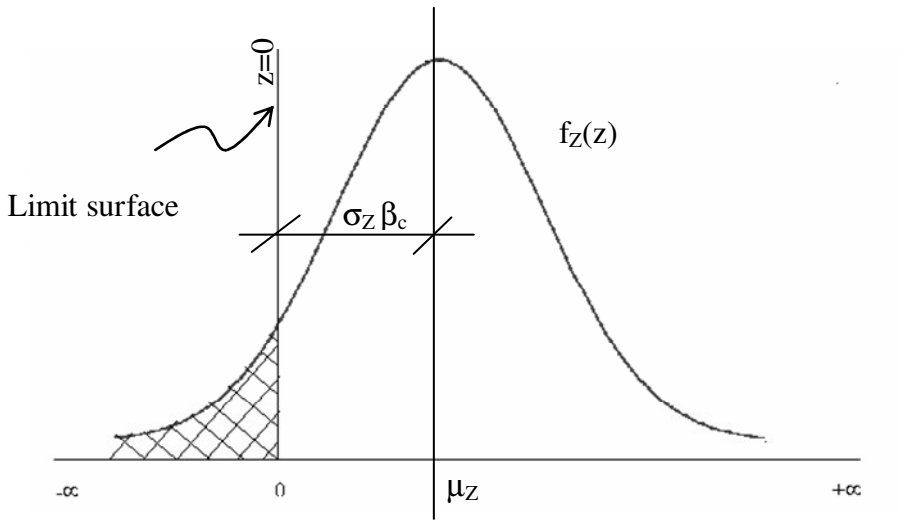

Figure 2.4. Definition of limit state and reliability index

$$\beta_c = \frac{\mu_z}{\sigma_z} = \frac{\mu_R - \mu_S}{\sqrt{\sigma_R^2 + \sigma_S^2}} \tag{2.58}$$

On the other hand, if the joint probability density function $f_X(x)$ is known for the multi variable case, then the probability of failure p_f is given by

$$p_f = \int_L f_X(x)\, dX \tag{2.59}$$

where L is the domain of X where g(X)<0.

In general, the above integral cannot be solved analytically, and an approximation is obtained by the FORM approach. In this approach, the general case is approximated to an ideal situation where X is a vector of independent Gaussian variables with zero mean and unit standard deviation, and where g(X) is a linear function. The probability of failure p_f is then:

$$p_f = P(g(X) < 0) = P(\sum_{i=1}^{n} \alpha_i X_i - \beta < 0) = \Phi(-\beta) \tag{2.60}$$

where α_i is the direction cosine of random variable X_i, β is the distance between the origin and the hyperplane g(X)=0, n is the number of basic random variables X, and Φ is the standard normal distribution function. The Equation 2.60 is the fundamental equation of reliability analysis, and various methods are developed in the literature to solve for the probability of failure.

The above formulations can be generalized for many random variables denoted by the vector X. Let the performance function is in the form given as

$$Z = g(X) = g(X_1, X_2 \ldots X_n) \tag{2.61}$$

A Taylor series expansion of the performance function about the mean value is given by Equation 2.62.

$$Z = g(\mu_X) + \sum_{i=1}^{n} \frac{\partial g}{\partial X_i}(X_i - \mu_{X_i}) + \frac{1}{2}\sum_{i=1}^{n}\sum_{j=1}^{n} \frac{\partial^2 g}{\partial X_i \partial X_j}(X_i - \mu_{X_i})(X_j - \mu_{X_j}) + ... \quad (2.62)$$

where derivatives are evaluated at the mean values of the random variables (X_1, X_2… X_n) and μ_{X_i} is the mean value of X_i. Truncating the series in linear terms, the first order mean and variance of Z can be obtained as

$$\mu_Z \approx g(\mu_{X_1}, \mu_{X_2}, ...\mu_{X_n}) \quad (2.63)$$

$$\text{and, } \sigma_Z^2 \approx \sum_{i=1}^{n}\sum_{j=1}^{n} \frac{\partial g}{\partial X_i}\frac{\partial g}{\partial X_j} \text{var}(X_i, X_j) \quad (2.64)$$

where var(X_i, X_j) is the covariance of X_i and X_j. If the variances are uncorrelated, then the variance for z is given as

$$\sigma_Z^2 \approx \sum_{i=1}^{n} \left(\frac{\partial g}{\partial X_i} \right)^2 \text{var}(X_i) \quad (2.65)$$

The reliability index can be calculated by taking the ratio of mean (μ_Z) and standard deviation of Z (σ_z) as in Equation 2.66.

$$\beta = \frac{\mu_z}{\sigma_z} \quad (2.66)$$

The method discussed above has some limitations and deficiencies. It does not use the distribution information about the variable and function g( ) is linearized at the mean values of the X_i variables. If g( ) is non-linear, neglecting of higher order term in Taylor series expansion introduces significant error in the calculation of reliability index. The more important observation is that the Equations 2.58 and 2.64 do not give constant value of reliability index for mechanically equivalent formulations of the same performance function. For example, safety margin R-S<0 and R/S <1 are mechanically equivalent yet these safety margins will not lead to same value of

probability of failure. Moreover, MVFOSM approach does not use the distribution information about the variables when it is available.

2.6.1.1.2 Advanced first-order second moment method (AFOSM)

It is essential that irrespective of method of evaluation of reliability of a limit state, all the mechanically equivalent performance functions must produce same safety indices. However the MVFOSM method fails to satisfy the above condition in some cases, such as in case of correlated variables and nonlinear limit state formulations. Hence, a new approach, called Hasofer-Lind reliability index (Hasofer and Lind 1974) was developed to tackle the problem of variant reliability indices produced using Cornell index. In this method the reduced variables are defined as given in Equation 2.67.

$$X_i^{'} = \frac{X_i - \mu_{X_i}}{\sigma_{X_i}}, \text{ i=1, 2 …n} \tag{2.67}$$

where $X_i^{'}$ is a random variable with zero mean and unit standard deviation. The above equation is used to transform the original limit state g(X) =0 to reduced limit state g'(X) =0. X is referred to as the original co-ordinate system and X′ reduced co-ordinate system. Note that if X_i is normal in original co-ordinate system it will be standard normal in reduced co-ordinate system.

The Hasofer-Lind reliability index (β_{HL}) can be defined as the minimum distance from the origin of the axes in the reduced co-ordinate system to the limit state surface. The minimum distance point on the limit state surface is called the design point or checking point. Considering the limit state function in two variables as given in Equation 2.68, wherein R and S should be normal variables, the reduced variables can be written as given in Equations 2.69 and 2.70.

$$Z = R - S = 0 \tag{2.68}$$

$$R' = \frac{R - \mu_R}{\sigma_R} \tag{2.69}$$

$$S' = \frac{S - \mu_S}{\sigma_S} \tag{2.70}$$

Substituting values of R' and S' in the above equation, the limit state equation in the reduced co-ordinate system can be written as

$$g() = \sigma_R R' - \sigma_S S' + \mu_R - \mu_S = 0 \tag{2.71}$$

The position of the limit state surface relative to the origin in the reduced coordinate system is a measure of the reliability of the system. By simple trigonometry, the distance of the limit state line from the origin can be calculated and it will give the reliability index value.

$$\beta_{HL} = \frac{\mu_R - \mu_S}{\sqrt{\sigma_R^2 + \sigma_S^2}} \tag{2.72}$$

This is same as the reliability index defined by the MVFOSM method, if both R and S are normal. In this definition the reliability index is invariant, because regardless of the form in which the limit state equation is written, its geometric shape and the distance from the origin remains constant.

To be specific, β is the First-order second moment reliability index, defined as the minimum distance from the origin of the standard, independent normal variable space to the failure surface as discussed in detail by Hasofer and Lind (1974). Figure 2.5 shows the plot depicting the functional relationship between probability of failure (p_f) and reliability index (β), and classifies the performance of designs based on these two values. As seen from the figure, the performance is high if the reliability index is equal to 5, which corresponds to a probability of failure of approximately 3×10^{-7}.

2.6.1.2 Other methods

Unlike in the FORM methods, in SORM the limit state function is approximated using a second order polynomial. Other methods, such as numerical approaches using on finite difference scheme, random field finite element method, Monte Carlo simulation technique, response surface methods are also gaining acceptance in geotechnical applications. However, they are out of scope of this study.

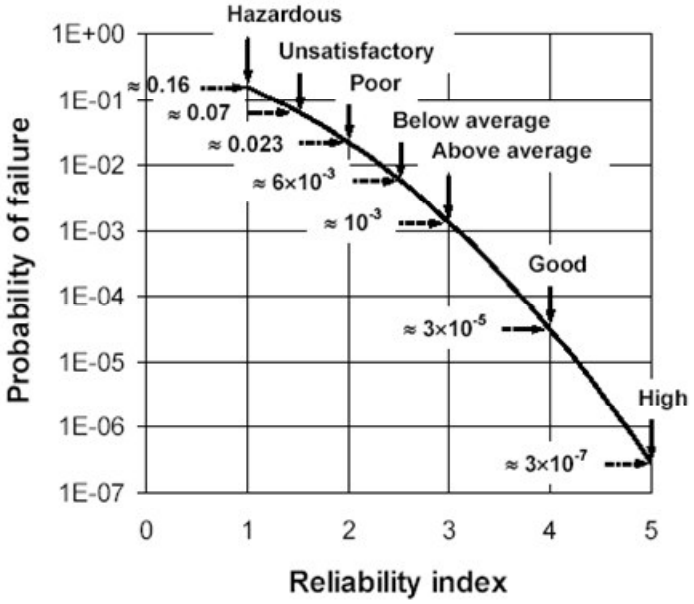

Figure 2.5. Relationship between reliability index (β) and probability of failure (p_f) (Phoon 2002) (adapted from USACE 1997)

2.7 Guidelines and codal provisions

2.7.1 Tolerable risk criteria

In a simple form, quantitative risk analysis of slope stability problems involves identification of hazards, which have potential for failure and damages leading to undesirable consequences. It is recognized that in many cases, the idea of annual probability of failure, depending on f-N relationships (frequency of fatalities (f), and number of fatalities (N)) is a useful basis (Fell and Hartford 1997; Christian and Urzua 1998) on which assessment of existing stability in terms of reliability and

stabilization of slopes can be taken up. Figure 2.6 shows a typical f-N diagram adopted by Hong Kong Planning Department (Hong Kong Government Planning Department 1994). Some guidelines on tolerable risk criteria are formulated by a number of researchers and engineers involved in risk assessment (Morgenstern 1997; Fell and Hartford 1997). They indicated that the incremental risk from a slope instability hazard should not be significant compared to other risks and that the risks should be reduced to "As Low As Reasonably Practicable" (ALARP).

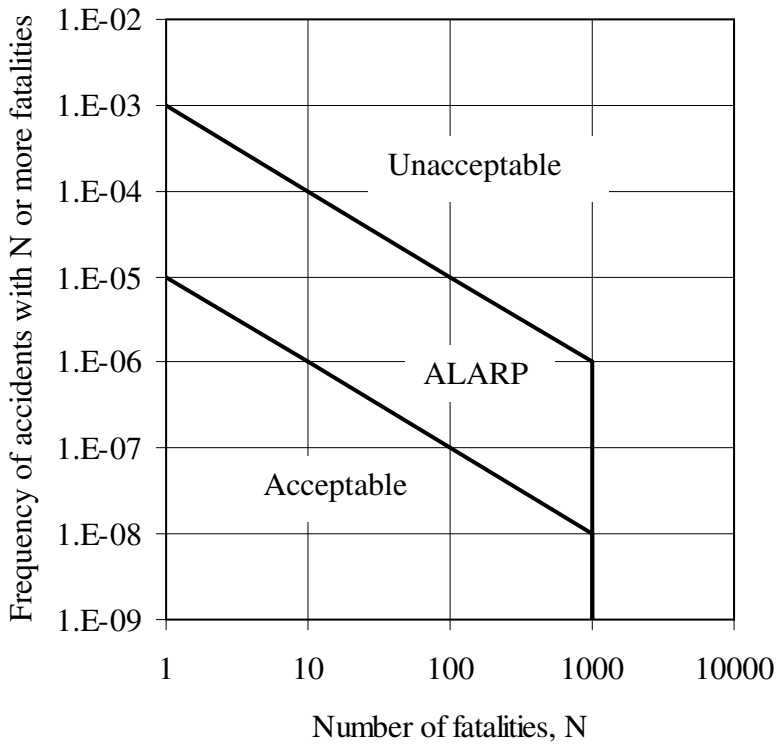

Figure 2.6. f–N diagram adopted by Hong Kong Planning Department for planning purposes (reproduced from Christian 2004)

In UK, risk criteria for land use planning made based on f-N curves on annual basis suggest lower and upper limits of 10^{-4} and 10^{-6} per annum for probability of failure or risk. Risk assessment in the case of dams is reasonably well developed and practiced in many countries such as USA, Canada and Hong Kong. The guidelines present the recommendations in terms of probability of failure p_f, or reliability index (β).

Whitman (1984) based on the collected data pertaining to performance of different engineering systems categorized these systems in terms of annual probability of failure and their associated failure consequences, as given in Figure 2.7.

Christian and Urzua (1998) proposed that it is necessary to study the extent of risk posed by earthquake as additional hazard in slope stability problems and presented a simple approach to estimate the probability of failure in seismic conditions. The annual probability of failure corresponds to an expected factor of safety E(F), which is variable and the variability is expressed in terms of standard deviation of factor of safety σ_F. If factor of safety is assumed to be normally distributed, reliability index (β) is expressed by

$$\beta = \frac{(E(F) - 1.0)}{\sigma_F} \tag{2.73}$$

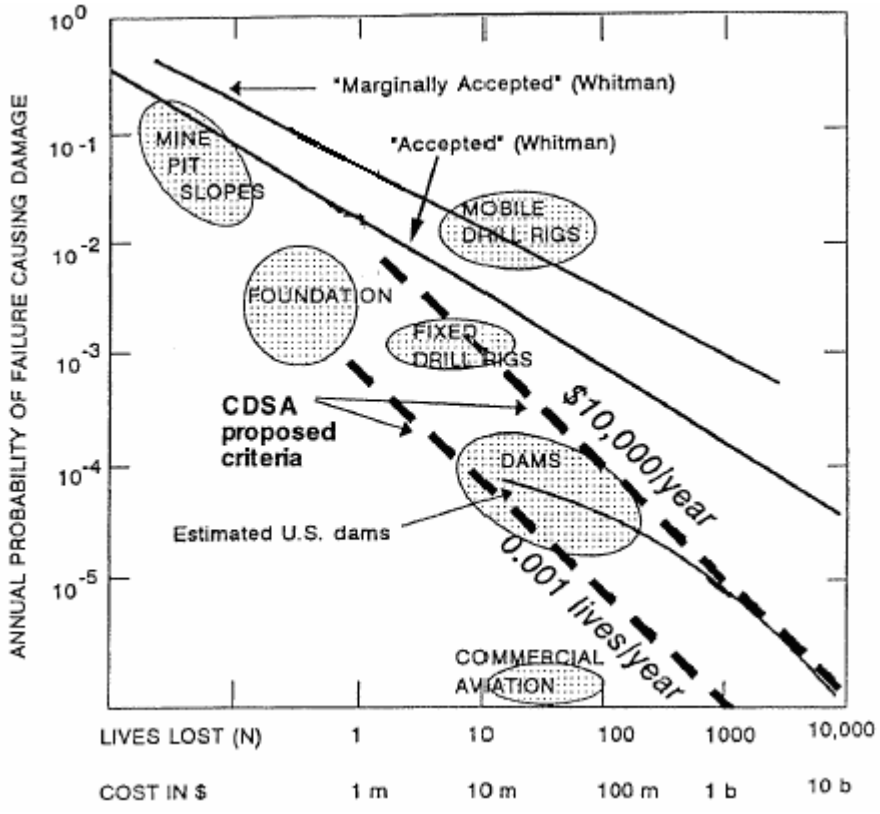

Figure 2.7. Annual probabilities of failure and consequence of failure for various engineering projects (Whitman 1984)

2.7.2 Role of consequence cost

The role of consequence costs is realized in recent times and has been receiving considerable attention in the geotechnical profession. Recently, Joint Committee on Structural Safety (JCSS 2000) presented relationships between reliability index (β), importance of structure and consequences of failure. The committee divided consequences into 3 classes based on risk to life and/or economic loss, and they are presented in Tables 2.2 and 2.3 respectively. From these tables, it can be inferred that if the failure of a structure is of minor consequence (i.e., $C^* \leq 2$, where C^* is the normalized consequence cost (normalized with respect to initial cost)), then a lower reliability index may be chosen. On the other hand, if the consequence costs are higher (i.e., $C^* = 5$ to 10) and if the relative cost of safety measures is small, higher reliability index values can be chosen. It can also be noted from the tables that reliability index in the range of 3 to 5 can be considered as acceptable in design practice.

Table 2.2. Relationship between reliability index (β), importance of structure and consequences (JCSS 2000)

Relative cost of safety measure	Minor consequence of failure	Moderate consequence of failure	Large consequence of failure
Large	β = 3.1	β = 3.3	β = 3.7
Normal	β = 3.7	β = 4.2	β = 4.4
Small	β = 4.2	β = 4.4	β = 4.7

Table 2.3. Classification of consequences (JCSS 2000)

Class	Consequences	C^*	Risk to life and/or economic consequences
1	Minor	≤ 2	Small to negligible
2	Moderate	$2 < C^* \leq 5$	Medium or considerable
3	Large	$5 < C^* \leq 10$	High or significant

The relative cost of safety measure and the consequences of failure of the structure are also considered and related to probability of failure (p_f) and reliability index (β) and are given in Table 2.2 and 2.3. From Tables 2.3 and 2.4, the following aspect points are clear.

i. The targeted reliability indices vary from 3 to 5, depending on the expected level of performance.

ii. Consequence costs should also be considered in the analysis. If the consequence costs are not significant compared to initial costs ($C^* \leq 2$) (for example slope design in a remote area), lower reliability index can be allowed, whereas higher reliability index is required where the consequence costs are high (for example slope in an urban locality).

2.8 Levels of reliability methods

Madsen et al. (1986) and Becker (1996a) explained the levels of reliability analysis, which can be used in any design methodology depending on the importance of the structure. The term 'level' is characterized by the extent of information about the problem that is used and provided. The methods of safety analysis proposed currently for the attainment of a given limit state can be grouped under four basic “levels” (namely levels IV, III, II, and I) depending upon the degree of sophistication applied to the treatment of the various problems.

Level IV methods are appropriate for structures that are of major economic importance, involve the principles of engineering economic analysis under uncertainty, and consider costs and benefits of construction, maintenance, repair, consequences of failure, and interest on capital, etc. Foundations for sensitive projects

like nuclear power projects, transmission towers, highway bridges, are suitable objects of level IV design.

Level III methods encompass complete analysis of the problem and also involve integration of the multidimensional joint probability density function of the random variables extended over the safety domain.

Reliability methods, which employ two values of each uncertain parameter (i.e., mean and variance), supplemented with a measure of the correlation between parameters, are classified as level II methods. Random variables are characterized by their known or assumed distribution functions. Reliability is expressed in terms of suitable safety indices, viz., reliability index, β, through "operational" failure probabilities, in contrast to "real" ones that can be deduced on the basis of level III methods. Generally it is possible to determine only the upper and lower bounds of failure probability.

In level I methods, the probabilistic aspect of the problem is taken into account by introducing into the safety analysis suitable "characteristic values" of the random variables, conceived as fractiles of a predefined order of the statistical distributions concerned. These characteristic values are associated with partial safety factors that should be deduced from probabilistic considerations so as to ensure appropriate levels of reliability in the design. In this method, the reliability of the design deviate from the target value, and the objective is to minimize such an error. Load and Resistance Factor Design (LRFD) methods come under this category.

2.9 Evolution of code calibration

Traditionally foundations are designed such that the resistance of the foundation system is some multiple of service load expected to act on the structure during its design period, such as shown in Equation 2.74.

$$R_N \geq FS \times \sum S_N \tag{2.74}$$

where R_N is the nominal resistance calculated using characteristic soil parameters, S_N are the nominal loads, dead load, live load, etc., calculated from respective characteristic loads, and FS is the overall factor of safety.

However, neither the service loads nor the resistance of the soil-foundation system is constant, rather random phenomena. Efforts are being made over past few decades to evolve new methodologies, which suitably account for the aforementioned uncertainties in the design calculations and codes, and simultaneously replace the existing WSD approach (Boden 1981; Meyerhof 1982, 1995; Becker 1996a & b; Baikie 1998; Day 1998; Honjo et al. 2003; Scott et al. 2003). New approaches, such as limit state designs and reliability based design methods have been evolved. However, the latter method requires a huge amount of test data for the analysis. This often creates difficulties to the concerned design engineer of the project.

Obtaining sufficient and reliable data for individual projects is of major concern to engineering design offices, and particularly in the geotechnical engineering arena, due to the complicated nature of underlying soil and the limited financial resources allotted for the subsurface exploration. Hence the appraisal of exact analysis of safety involved in the project is seldom possible.

2.9.1 Methods of analysis

The past several decades have witnessed an evolution of new and innovative methods in design philosophy – from the traditional 'working stress method', through the 'ultimate load method', to the modern 'limit states method' of design.

2.9.1.1 Working stress method

This traditional method of design is based on the premise that the material properties responsible for resistance, are in a linear elastic state throughout the design period of the structure. The various sources of uncertainty in loads and resistance are implicitly accounted for by introducing a reduction factor (or a factor of safety) on the ultimate resistance of the system under consideration. The designs are simple to perform and by designing the supporting system in the elastic state, the effect of complicated stress-strain behaviour of the material at higher strain levels can be purposefully ignored. This method of design works normally well and obviously produces uneconomical designs, since strength of the materials is not fully utilized. The traditional factor of safety of three on ultimate bearing capacity developed from experience generally limits the deformations to acceptable levels (Becker 1996a).

2.9.1.2 Ultimate stress method

This method also referred to as the load factor method or the ultimate strength method. The stress condition at the state of impending collapse of the structure is analysed, and the non-linear stress-strain behaviour of materials is made use of. The safety measure in the design is introduced by an appropriate choice of the load factor, defined as the ratio of the ultimate load to the working load. However, the satisfactory "strength" performance at the ultimate loads does not guarantee satisfactory "serviceability" performance at the normal service loads.

Moreover, the use of the nonlinear stress-strain behaviour for the design of sections becomes truly meaningful only if appropriate nonlinear limit analysis is performed on the structure. However, such an analysis is generally not performed. This is significantly an error, because significant redistribution of stress resultants takes place, as the loading is increased from service loads to ultimate loads.

2.9.1.3 Limit state method

The "limit state" conceived as that state beyond which a structure, or part of it, can no longer fulfill the functions or satisfy the conditions for which it is designed. In this manner, all the possible states of behaviour of a structure are taken into consideration. In case of design of shallow foundations, the possible limit states are loss of overall stability, bearing resistance failure, punching failure, squeezing, failure by sliding, combined failure in the ground and in the structure, structural failure due to foundation movement, excessive settlements, excessive heave due to swelling, frost and other causes, and unacceptable vibrations. Most modern codes adopt the limit states operational method and divide the above limit states into two main groups, viz., ultimate limit states corresponding to the maximum load-carrying capacity and service limit states related to the criteria governing normal use and durability.

The Limit State Design (LSD) methods developed so far produce a compromising solution between WSD and designs based on reliability theory, and are based on experience, reliability theory and direct calibration between WSD and LSD methods where there is a lack of reliable statistical data (Becker 1996a; Baikie 1998).

The LSD method attempts to separate to some extent the various sources of uncertainty. The load factors take into account the variability of the loads and their distribution and frequency of occurrence, whereas the resistance or performance

factors account for the uncertainties related to the soil profile, soil properties, testing and sampling effects, and method of analysis (Baikie 1998).

2.9.1.3.1 Factored strength design approach (LSFD)

This method is based on Brinch Hansen (1953) approach of using separate partial factors for soil parameters, such as c, ϕ, etc.

2.9.1.3.2 Factored resistance design approach (LRFD)

Unlike in factored strength approach, partial factors are used on the resistance parameter. However, in both these design approaches, the load is always factored.

The general LRFD equation is:

$$\gamma \sum \beta_i Q_i \le \varphi R_n \tag{2.75}$$

where $\gamma, Q_i, \beta_i, \varphi, R_n$ are load factor for load combination, service load, load factor for particular load, resistance factor, and nominal resistance, respectively. The emphasis in LRFD is primarily on the re-distribution of the original global factor of safety in WSD into separate load and resistance factors. Figure 2.8 shows the Limit state design format for LRFD approach.

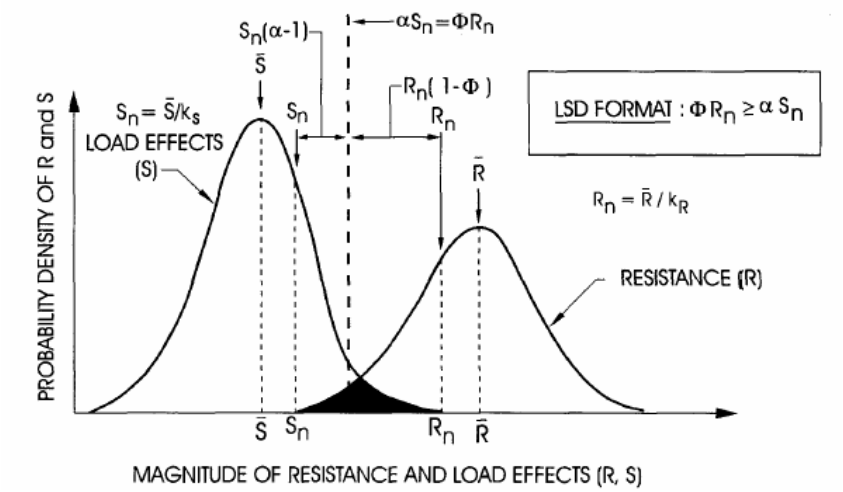

Figure 2.8. Load and resistance factored design format (Becker 1996a)

The development of load and resistance factors in foundation design is not new, but dated back, when Taylor (1948) introduced partial factors of safety for the cohesive and frictional component of the shear strength of the soil for the stability analysis of slopes. Subsequently, Brinch Hansen (1953) introduced partial factors to loads and strength in his book on "Earth pressure calculation".

Though many countries already realized the importance of such studies and revising their foundation codes, efforts to re-evaluate the national codes in geotechnical engineering and for redrafting the present codes incorporating the uncertainty issues and harmonizing with the various international codes have not been significant in Indian context. The new European codes of practice (EN 1997-1:2004) are based on limit state design concept with use of partial safety factors. It introduces three geotechnical categories, referred to as Geotechnical Categories 1, 2 and 3 with different partial factors to take account of the different levels of complexity in a design. This code is rational and comprehensive code for geotechnical design.

2.9.2 Characteristic values

The characteristic value of a geotechnical parameter is defined in Eurocode 7 (EN 1997-1:2004) as a cautious estimate of the value affecting the occurrence of the limit state. More precisely, the characteristic value should be derived such that the calculated probability of a worse value governing the occurrence of a limit state is not greater than 5%. The characteristic value of a geotechnical parameter needs to be selected with reference to the particular limit state being analysed, taking account of the volume of ground involved, the extent of field and laboratory investigations, the type and number of samples, the extent of zone of ground governing the behaviour of geotechnical structure at the limit state being considered, the ability of geotechnical

structures to transfer the loads from weak to strong zones in the ground, etc. Hence, the characteristic value of a particular parameter, e.g. angle of internal friction, in any one stratum may have different values for different combinations of the above influencing parameters.

Conversely, in the structural design, characteristic value of a strength parameter is defined as the value having a prescribed probability of not being attained in a hypothetical unlimited test series. This corresponds to a specified fractile of the assumed statistical distribution of the property. IS 456:2000 and ENV 1997-1:2004 define the characteristic value as the 5% fractile for strength parameters.

2.9.3 Target probability of failure

The probability that the safety margin is less than the unity, which is referred to as the risk or probability of failure is evaluated for each limit state being considered, and the inherent probability of failure should be less than the target probability of failure, which is defined on a project basis, keeping in mind the importance of the project, and the imposed socio-economical constraints on the project.

A suitable criterion for selecting rational values for the failure probability has been identified by introducing the concept of "generalized cost", conceived as the initial cost of the structure to which is added the product of the probability of failure and the direct and indirect losses that the occurrence of such failure would entail. In order to optimize a design, the expected generalized cost should be minimized. However, Lacasse and Nadim (1998) pointed out that establishing the basis for acceptable risk level is difficult and controversial. Since structural collapse is generally perceived as an unavoidable risk, a probability of failure for majority of the structures is of the order of 5×10^{-5} per year (MacGregor 1976). However, based on a survey of

numerous failures of foundations in conjunction with semi-probabilistic methods and considerable judgment, a life time probability of failure is considered as 10^{-4} per year (Meyerhof 1970).

2.9.4 Methods of calibration of resistance factors

The resistance factors can be calibrated by fitting with working stress design approach and the reliability based approach. The method of evaluation of these factors is discussed in detail by Becker (1996a).

The load and resistance factors corresponding to any particular limit state are calculated for a predefined safety level to be achieved by the system. The target level of predefined safety could be expressed in terms of threshold minimum probability of failure (p_f) or in terms of an equivalent index, called reliability index (β).

2.10 Design of shallow foundations

In the following sections, design aspects of shallow foundations are presented along with the conventional methods of estimation of allowable bearing pressure. Studies on reliability analysis of shallow foundations are reviewed and the need for developing/integrating the uncertainties in soil variability in foundation design is brought out.

In general, the design of foundations must satisfy two primary requirements: (1) An adequate safety against shear failure; and (2) the total and differential settlements of the foundation must be within limits that can be tolerated by the superstructure (Meyerhof 1951). In routine geotechnical engineering, the failure of shallow foundations is treated as a two-component series system: bearing capacity and excessive settlement (Zekkos et al. 2004). These two aspects of the design are

normally treated separately, in the sense that they are treated as strength and deformation problems respectively. The allowable pressure of a shallow foundation is defined as the lesser of the pressures satisfying the following criteria (a) and (b).

(a). The pressure that will result in a shear failure divided by a suitable factor of safety

(b). The pressure that results in a specified limiting amount of vertical or differential settlement of the foundations to meet serviceability requirements.

Plasticity parameters, such as cohesion and friction angle along with unit weight of foundation soil are used in the strength analysis while theory of elasticity is usually employed in the deformation analysis. In the computation of bearing capacity, solutions using limit analysis, slip-line, limit equilibrium, and finite element methods have been developed. However, large discrepancies are observed in the solutions obtained from the above approaches. The concept of perfect plasticity is mostly assumed in these methods and this assumption was proven to be conservative (Yamaguchi et al. 1977).

2.10.1 Method of evaluation

2.10.1.1 Direct methods

In the direct methods, the measured cone tip resistance is directly substituted in the well established empirical formulae to provide estimates of foundation capacity and settlement, e.g., ultimate bearing pressure of shallow foundations can be correlated with cone tip resistance in both cohesionless as well as cohesive soils (Awkati 1970; USACE 1992).

2.10.1.2 Indirect methods

Use of theoretical models for bearing capacity/deformation response, such as bearing capacity and settlement of shallow foundations on granular soils (Schmertmann 1970; Schmertmann et al. 1978; Zekkos et al. 2004), bearing capacity of shallow foundations on clays forms indirect methods. Measured in-situ data (ex. cone tip resistance) are used to estimate soil properties such as angle of internal friction (ϕ), undrained shear strength of cohesive soil (s_u) and deformation modulus (E_d). General procedures for interpreting engineering parameters for foundation analysis from in-situ data are given by Kulhawy & Mayne (1990). Schmertmann et al. (1978) and Berardi et al. (1991) outline settlement analysis procedures for spread footings on sand from CPT data.

2.10.2 Bearing capacity analysis

The footing load is resisted by shear force developed along the slip path or failure surface. If τ_s ($=c+\sigma_n\tan\phi$) is the soil shear strength, then the force resisting shear is τ_s times the length of slip path (LSP). The force resisting shear in a purely cohesive soil is $c_u \times$LSP, where, c_u is undrained shear strength (or cohesion) of the soil. On the other hand, in purely frictional soil τ_s is equal to $\sigma_n\tan\phi \times$ LSP, where, σ_n is normal stress on slip path, ϕ is angle of internal friction of soil in degrees. Shear failure usually occurs on only one side because soils are not homogeneous in their engineering properties (USACE 1992). Bearing capacity analysis of foundations is frequently limited by the geotechnical engineer's ability to accurately determine material properties as opposed to inadequacies in the theory used to develop the bearing capacity equations. Clearly, the uncertainties in the material properties control the uncertainty of a bearing capacity computation to a large extent.

In the conventional analysis, minimum factors of safety for shallow foundations against bearing capacity failure are in the range of 2.5 to 3.5. This factor of safety is selected through a combination of applied theory and experience. As such, the uncertainty in both the magnitude of the loads and the available soil bearing strength are combined into this single factor of safety.

There are two ways in which the bearing capacity of footings can be evaluated from cone tip resistance data. In the first method, the correlations developed for similar sites between cone tip resistance and bearing capacity are made use of in the evaluation of bearing capacity of the foundation in hand. The bearing capacity has been correlated with the cone tip resistance q_c for shallow foundations (Awkati 1970; Schmertmann 2005, private communication). Figure 2.9 shows the chart for evaluating the ultimate bearing pressure of shallow footings resting on both cohesionless and cohesive soils. These charts are valid for a footing with embedment depth, D_f (in feet), defined as

$$D_f \geq 1.5^{'} + \frac{B^{'}}{2} \tag{2.76}$$

$$D_f \geq 4^{'} \tag{2.77}$$

Equations (2.76) and (2.77) are valid when B, the minimum width of the footing is less than or equal to 3 feet, and greater than 3 feet, respectively.

The average cone point bearing capacity data obtained from the mechanical cone within a depth of 1.5B below the footing was used in the regression model. The bearing capacity of cohesionless soils is given by

Strip footing: $Q_u=28-0.0052(300-q_c)^{1.5}$ (2.78)

Square footing: $Q_u=48-0.0090(300-q_c)^{1.5}$ (2.79)

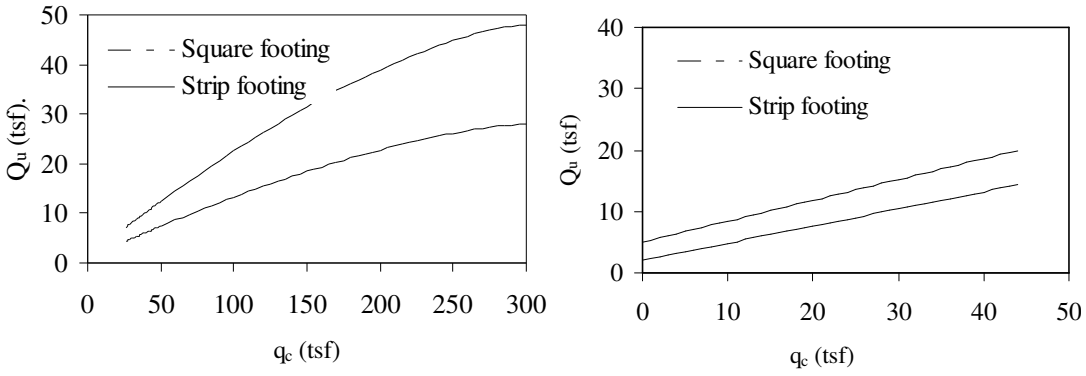

Figure 2.9. Chart for estimating the ultimate bearing pressure of shallow footings on sand and clay (friction ratio, R_f>4%) from static cone tip resistance (Reproduced from Awkati 1970, Schmertmann 2005 private communication)

The bearing capacity of cohesive soils is given by

Strip footing: $Q_u=2+0.28q_c$ (2.80)

Square footing: $Q_u=5+0.34q_c$ (2.81)

where Q_u, ultimate bearing pressure and q_c, cone penetration resistance are in units of tsf or kg/cm^2. In the case footings resting on cohesive soils, the bearing capacity of foundations according to Prandtl's solution is given by Equation 2.82. Here 'c_u' is undrained shear strength (or cohesion).

$$q_u = 5.14\,c_u \tag{2.82}$$

In the second method, the cone tip resistance data is used to evaluate the equivalent friction angle of the soil using well developed transformation models, such as shown in Equation 2.83. The data of computed friction angle are then used to compute the bearing capacity through conventional bearing capacity formulae. Kulhawy and Mayne (1990) presented an equation for transforming cone tip resistance to drained angle of internal friction in case of cohesionless soils.

$$\phi = \tan^{-1}\left[0.1+0.38\log\left(\frac{q_c}{\sigma'}\right)\right] \tag{2.83}$$

where ϕ is peak friction angle, q_c is cone tip resistance, σ' is vertical effective overburden pressure. Apart from the above equation, many other equations have also been developed correlating the triaxial compression effective friction angle $\bar{\phi}(TC)$ and the cone tip resistance (q_c), such as shown in Equation 2.84.

$$\phi = 17.6 + 11.0 \log_{10}\left(\frac{q_c / p_a}{\sqrt{\sigma_{vo} / p_a}}\right) \tag{2.84}$$

where p_a is the atmospheric pressure ($1p_a$=101.325 kPa). The bearing capacity is evaluated from the above obtained friction angles using the Equation 2.85.

$$q_{ult} = cN_c S_c d_c + \gamma D_f N_q S_q d_q + 0.5\gamma B N_\gamma S_\gamma d_\gamma \tag{2.85}$$

Net bearing pressure, $q_{net} = q_{ult} - \gamma D_f$ (2.86)

where N_c, N_q, and N_γ are the bearing capacity factors, S_c, S_q, and S_γ are shape factors, d_c, d_q, and d_γ are depth factors. Das (1995) presented these factors as a function of angle of internal friction, depth of foundation (D_f), and width of foundation (B).

2.10.2.1 Zone of influence - shear failure criterion

The failure zone or zone of influence (the volume of soil which is enveloped within the shear failure zones) under an axially loaded rough rigid footing in cohesionless soil with an average friction angle of 30° extends approximately to a depth of 2B from the base of footing and in the transverse direction it extends to 3.5B on either side from center of the footing, where B is the width of the footing (USACE 1992). However, USACE (1992) approximated the depth of shear zone 'D' by assuming that the maximum depth of shear failure occurs beneath the edge of the foundation. The depth of shear zone is given by Equation 2.111.

$$D = B\tan\left(45 + \frac{\phi'}{2}\right) \tag{2.87}$$

The depth of shear zone (D) approaches a value of 2B if the effective angle of internal frction (ϕ') is 38°. In the case of purely cohesive soils, since $\phi' = 0$, the depth of shear zone (D) equals to width of foundation (B). In the similar way, the length of shear failure zone, L_{sh}, extends from the foundation perimeter at the foundation depth to a distance given by the Equation 2.88.

$$L_{sh} = \left(D + D_f\right)\tan\left(45 + \frac{\phi'}{2}\right) \tag{2.88}$$

where D_f is the depth of foundation.

2.10.3 Settlement analysis

Total settlement of a shallow foundation will result from one, or more likely, a combination of immediate compression, primary consolidation, and secondary settlement. Initial compression accounts for the major portion of consolidation in granular soils. Primary compression accounts for the major portion of consolidation in cohesive soils. Primary and secondary compression both contribute significantly to consolidation settlement in organic soils. Schmertmann (1970) and Schmertmann et al. (1978) presented a method to evaluate the settlement of foundations resting on cohesionless soils based on in-situ cone tip resistance data (q_c).

2.10.3.1 Zone of influence - settlement criterion

The primary factors affecting the settlement of foundations are width of foundation (B), net applied pressure (Δp), the soil compressibility within the depth of influence. The other factors which influence to a lesser degree are depth of ground water table,

footing embedment ratio (D_f/B), footing geometry (L/B ratio), and the thickness of soil layer beneath the foundation (Shahin et al. 2002).

For settlement criterion, the zone of influence (the depth till the strains in the soil due to applied load are significant) under a loaded footing resting on cohesionless soil is generally taken to extend till 0.1q bulb for spread footings and 0.15q for strip footing. By using Boussinesq theory elastic stress distribution, the pressure contour 0.1q extends downward a distance of about 2B below the bottom of the square footing. Similarly for strip footing, the pressure contour of 0.15q extends downward a distance of about 4B below the bottom of the footing. The difference occurs since the pressure under a spread footing can be dispersed laterally in all four directions, while under a strip footing the pressure can be dispersed only in two directions. It thus takes roughly twice as much depth to dissipate the soil pressure under a strip footing as it does under a spread footing (French 1999).

Within the usual limits of accuracy in soils, the influence of the building load outside the 10% pressure contour is minimal and can be ignored. In general, the ground conditions at a depth greater than about four times the lesser plan dimension of a continuous spread footing will be affected by less than about ten percent of the stresses induced under the footing (2 times the lesser plan dimension for square or nearly square footings) (Kimmerling 2002). However, Shahin et al. (2002) observed that there is no unanimous agreement in the literature for the definition of depth of zone of influence of a foundation.

For a given foundation the depth of influence is not unique, but depends on the variation of stiffness with depth (Burland and Burbidge 1985). This value depends on the dimensions and shape of the footing, the way the soil modulus varies with depth. However, in case of footings on cohesionless soils, Burland and Burbidge (1985)

proposed some guidelines on the depth of zone of influence. The recommended value of zone of influence is 2B below the base of the footing, if the SPT 'N' decreases with the depth. On the other hand, if the SPT 'N' is constant or increases with depth, the zone of influence is taken equal to $B^{0.75}$. AASHTO guidelines distinguish a strip footing as one whose length (L_f) exceeds five times the footing width (B_f). USACE (1990) suggest that the significant depth is the depth at which the increase in stresses from foundation loads decrease to about 10% (cohesionless soil) to 20% (cohesive soil) of the effective vertical overburden pressure. It is observed that errors in settlement contributed by nonlinear, heterogeneous soil below this depth are not significant.

Some of the significant contributions in the area of probabilistic analysis of bearing capacity and settlement of shallow foundations are briefly mentioned below.

Wu and Kraft (1967) evaluated the probability of foundation safety in a qualitative manner using uncertain load and soil strength parameters. The effect of spatial correlation is ignored. Unconfined compression test for clays is used for the evaluation of bearing capacity in clays and the standard penetration test results were used for settlements in cohesionless soils. In the case of bearing capacity limit state the conventional factors of safety of 2 or 3 produce very low values of probability of failure. The results dictate that the number of borings (m) rather than number of specimens tested from each boring (n) governs the safety of foundations. It is observed that Increasing 'm' from 3 to 6 greatly improves the safety, while increasing 'n' from 10 to 20 does not contribute as much.

Krizek et al. (1977) used the probabilistic concepts to develop models for predicting the total settlement, based on either consolidation test data or the results of standard

penetration tests, and the time rate of settlement for a compressible clay layer extending about 15 m below the base of the structure in terms of uncertain values for soil compressibility and applied loads. The total settlement and time rate of settlement in one dimensional consolidation are well approximated by lognormal distributions.

Cherubini (1990) developed a closed form solution for probability density function of ultimate bearing capacity from that of effective friction angle for a shallow strip footing resting on cohesionless deposit. The mean values of effective friction angle are assumed in the range of 20˚ to 30˚, and coefficients of variation of effective friction angle are assumed in the range of 10%-30%. Simple transformation function proposed by Krizek (1965) to compute the ultimate bearing capacity from effective friction angle was used in the analysis. It is observed from the results that the conventional factor of safety of 3 on ultimate bearing pressure produces higher probabilities of failure than that is admissible 10^{-4} (reliability index, $\beta \approx 3.72$).

Easa (1992) proposed an exact probabilistic solution for bearing capacity for shallow strip foundation resting on cohesionless soil. The two random variables are effective friction angle and soil unit weight. It is observed that the uncertainty of soil unit weight was found to have a considerable effect on the probability of failure.

Cherubini (2000) studied the reliability analysis of bearing capacity of shallow foundations resting on a c-ϕ soil. Parametric studies have been carried out considering vertical autocorrelation characteristics of cohesion and friction angles and cross-correlation coefficients between the shear strength parameters. The spatial averaging length is approximated as D_f+B, i.e., the summation of depth and width of foundation. The results show that higher reliability indexes are found when correlations between *c*' and ϕ' are negative and when the fluctuation scale has a minimum value.

Fenton and Griffiths (2000) used Monte Carlo Simulation technique to evaluate the bearing capacity of smooth rigid strip footing in plane strain with spatially random shear strength represented using c and ϕ, by combining nonlinear elasto-plastic finite element analysis with random field theory. Soil cohesion is assumed lognormally distributed and a bounded distribution is selected for friction angle. It is observed from the results that for vanishing coefficients of variation (CoV) in the soil shear strength, the expected value of the bearing capacity tends to the Prandtl solution, N_c. However, for increasing values of CoV, the expected value of the bearing capacity is observed reducing quite rapidly. The magnitude of decrease of the mean bearing capacity is greatest for small correlation lengths. Increasing the spatial correlation length consistently increases the CoV of the bearing capacity. It was observed that a FS of 4 and greater may be required to reduce the probability of failure for soils to a negligible amount. It is also observed that the influence of the correlation length on the probabilistic interpretation of the bearing capacity problem was seen to be not greatly significant, within the range of lengths considered. However, the CoV is identified as a major factor influencing the probability of failure.

Honjo et al. (2000) analysed the bearing capacity of shallow foundations subjected to earthquake-induced loading. The variable design earthquake load is based on peak ground acceleration of recurring period of 100 years. The soil resistance is characterized by SPT 'N' value, which is taken as an uncertainty parameter. The authors demonstrated that in the case of foundations more uncertainty is associated with resistance parameters than the load parameters. It is observed from the results that when CoV of SPT 'N' is high, the uncertainty involved in the soil resistance dominates the reliability, whereas if it is small, the uncertainty in earthquake loading dominates.

Griffiths and Fenton (2001) studied the bearing capacity of spatially random clay soil under undrained conditions by merging elasto-plastic finite element analysis with random field theory. A minimum mean bearing capacity was observed for correlation lengths of approximately one half of the footing width. For still smaller correlation lengths, a modest increase in the mean bearing capacity was detected. In the extreme condition of no spatial correlation, there are no preferred paths of weaker material to attract the mechanism, and the material response is 'homogeneous', yielding an essentially deterministic system mechanism at failure. It is also observed that the coefficient of variation increases with coefficient of variation of the soil strength and its spatial correlation length. The influence of correlation length on the probabilistic interpretations of the bearing capacity problem was shown to be significant, especially for soils with higher values of CoV of undrained shear strength.

Nobahar and Popescu (2001) observed that the inherent spatial variability of soil strength was shown to affect soil behaviour, by modifying the failure mechanism. It is observed that in many cases, the rotations resulting from spatial variability of soil, may control the design.

Elkateb et al. (2002) studied the behaviour of strip footing resting on a spatially variable sand medium, where friction angle and elastic modulus, were treated as random variables. The numerical simulation is carried out using FLAC software. The results state that the probability of failure of shallow foundation was insensitive to probability distribution type and the correlation structure model. However it is observed that the CoV of sand friction angle had a considerable influence on p_f. A target probability of failure is assumed as 1%. It is observed that FS of 3 on ultimate bearing pressure produces over conservative designs. Factor of safety of 2.5 is suggested as a reasonable value.

Griffiths et al. (2002) demonstrated that the mean bearing capacity of a footing on a soil with spatially varying shear strength is always lower than the deterministic bearing capacity based on the mean value. It is due to the linking up of weak elements beneath the footing, and shows that weak element rather than strong elements tend to dominate the expected bearing capacity of a footing on spatially random soil. Due to greater volume of soil involved in the failure mechanism beneath a rough footing, the bearing capacities were marginally higher and hence the probabilities of design failure marginally lower than in the smooth case.

Nobahar and Popescu (2002) concluded that the scale of fluctuation in vertical direction has significantly less influence on the bearing capacity than the one in horizontal direction. Larger horizontal correlation distances tend to diminish the local averaging effect of the BC mechanism, and therefore induce larger variability of the results in terms of both ultimate bearing capacity and differential settlements. They concluded that probability distributions of soil strength in shallow layers are skewed to the right, indicating a stronger influence of a lower bound.

Popescu et al. (2002) studied the effect of soil heterogeneity on the bearing capacity and differential settlement of shallow strip foundations resting on overconsolidated clay layer under undrained conditions using a Monte Carlo simulation method including digital generation of two dimensional non-Gaussian random fields and nonlinear finite element analyses with stochastic input. The foundation is placed on a "stochastically homogeneous" soil layer, with average shear strength assumed constant with depth. A correlation structure based on the exponentially decaying model is assumed, with a range of scales of fluctuations: θ_H/B=1 to 4, and θ_V/B=0.25. The results are presented in terms of fragility curves that express the probability of exceeding a certain limit state. The degree of variability and the shape of the left tail

of the probability distribution of soil strength are found to have the strongest effects on bearing capacity. The soil failure mechanism is strongly influenced by presence of loose zones in the soil mass. The failure mechanism is changed by the presence of looser and denser zones in the soil mass, and the displacement is no longer symmetrical.

Zekkos et al. (2004) studied the reliability of shallow foundation design in shear criterion using the SPT results. All the sources of uncertainty are properly accounted for in the analysis. The results of the reliability analyses show that the factor of safety approach can provide an imprecise degree of conservatism. They also observed that in some cases the foundations with smaller factors of safety have smaller probabilities of failure than foundations with higher factors of safety.

2.11 Stability of soil slopes

2.11.1 Unsaturated soil slopes

In many countries frequent slope failures of mountains and man made slopes in rainy seasons cause various problems like damage to infrastructure projects, loss of lives and properties. Slope failures and landslides are influenced by geologic, topographic and climatic factors. In tropical regions, where residual soils are abundant, most of the slope failure occurs during severe rainfall, and ground water table does not exist at finite depth from top of ground surface. Most of the rainfall-induced landslides in residual soils consist of relatively shallow slip surface above the ground water table, the thickness of the failed zone is generally observed to be less than 3 m (Lumb 1975b; Rao et al. 1995, Lin and Kung 2000; Deutscher et al. 2000). In-situ pore water pressure in these residual soils is often negative with respect to the atmospheric conditions. This negative pore water pressure is called matric suction. There has been

increasing evidence that matric suction contributes towards the stability of natural slopes in residual slopes. Rain water infiltrates into the slope and reduces the soil matric suction. This in turn reduces the shear strength to a point where equilibrium can no longer sustain in the slope (Krahn et al. 1989; Fredlund and Rahardjo 1993; Yagi et al. 2000; Shao and Wang 2000; Tsaparas et al. 2002, Zhang et al. 2005). The negative effect of the infiltration on the pore-water pressures in the soil and subsequently on the stability of the slope is dependent on several parameters, such as the behaviour of the soil material under unsaturated conditions, the precipitation rate, the vegetation and the groundwater conditions within the slope at the time of the rainfall. The upper layers of residual soils are always partly saturated, and have a relatively higher permeability to infiltrating rainwater. Bishop (1967) hypothesized the shear strength of a partly saturated soil as a function of an effective stress defined as

$$\sigma' = (\sigma - u_a) + \chi(u_a - u_w) \tag{2.89}$$

Where σ' and σ are the effective and total stresses respectively, u_a and u_w are the pore air pressure and the pore water pressure, respectively. χ is a function that depends on the saturation with a value of 1 at 100% saturation and 0 for completely dry soil. Fredlund and Morgenstern (1977) showed from a stress analysis that any two combinations of the three possible stress variables $(\sigma - u_a), (\sigma - u_w)$, and $(u_a - u_w)$ can be used to define unsaturated soil. The equation for unsaturated shear strength, τ is written in terms of the stress state variables for an unsaturated soil, as given in Equation 2.90, which is an extension of the form of equation used for saturated soils.

$$\tau = c' + (\sigma - u_a)\tan\phi' + (u_a - u_w)\tan\phi^b \tag{2.90}$$

where c' and ϕ' are the effective cohesion and effective angle of internal friction, σ is the total stress, u_a *and* u_w are the pore air pressure and pore water pressure, $(u_a - u_w)$ is the matric suction, and ϕ^b is the gradient with respect to changes in $(u_a - u_w)$ when $(\sigma - u_a)$ is held constant.

In the assessment of stability of a natural slope, or in cut slope design, the controlling factor is the distribution of pore pressure (both positive and negative) along the potential failure surface (Brand 1982).

Lumb (1975b), Brand (1982, 1984), and Anderson and Howes (1985) provided some insights on the phenomenon of rain-induced landslides of Hong Kong residual soil. Fredlund (1987), Reddy and Wu (1991), Fell et al. (1991), Chong et al. (2000), and Tung and Chan (2003) also studied the effect of suction on the rainfall induced landslides. Anderson and Howes (1985) studied the impact of soil suction on the stability of infinite slope failures in probabilistic approach using one-dimensional soil water infiltration scheme taking into consideration the variability associated with the determination of various parameters.

In light of the above discussions, to understand the failure mechanism of the residual soil slopes, two processes need to be examined. One is the change of pore water pressure in the soil mass due to infiltration of rainwater. The other process is the change in shear strength of the soil due to the increase in pore-water pressure and hence its effect on the stability against slope failure.

2.11.1.1 Infiltration behaviour

When rainwater infiltrates into the soil, the redistribution of soil moisture will result in three different zones of soil mass: (1) infiltration zone, (2) transition zone, and (3)

non-infiltration zone. Lumb (1975b) simplified these three zones into a wetting front and a non-wetting front. The depth of the wetting front can be expressed as

$$h = (Dt)^{0.5} + \frac{kt}{n(s_f - s_i)} \tag{2.91}$$

where parameter t is the rain duration, D is the diffusivity parameter, n is the soil porosity, k is the saturated conductivity, s_f represents the degree of saturation in the wetting front, and s_i is the degree of saturation before rainfall. If diffusion is assumed negligible at the end of an intensive rainfall, the Equation (2.91) can be reduced to Equation (2.92).

$$h = \frac{kt}{n(s_f - s_i)} \tag{2.92}$$

2.11.1.2 Analytical method

Fredlund et al. (1981) proposed the general limit equilibrium method (i.e. GLE method) which could consider the suction effects on the soil shear strength. This approach considers the suction term as part of the apparent cohesion (c). They indicate that often the matric suction governs the shear strength in an unsaturated soil. Therefore, the effective cohesion of the soil (c') used in the traditional analysis could be added with the matric suction term, given as

$$c = c' + (u_a - u_w)\tan\phi^b \tag{2.93}$$

where c and c' are apparent cohesion of the soil and effective cohesion, $(u_a - u_w)$ is matric suction, ϕ^b is the angle indicating the rate of increasing shear strength relative to the matric suction. Fredlund (1987) and Satija (1978) conducted comprehensive experimental studies on unsaturated soils which indicate that ϕ^b values are in the

range of 15˚ to 22˚ for different types of soils with higher values attributed to soils with less clay content.

Soil suction has an important bearing on the water entry, structural stability, stiffness, shear strength and volume change. Soil matric suction and water content variation with time are often the most important variables in unsaturated soil engineering design. Shao and Wang (2000) showed with two numerical examples how the stability in terms of factors of safety of sand and glacial till slopes varies with rise of ground water table.

When the pore water is in hydrostatic equilibrium, matric suction at a point of the soil can be determined by the height of the point over the ground water table. When the pore water is in movement, which is most common in nature, matric suction may be determined by investigating water content (or degree of saturation) and soil water characteristics of the soil. Once the suction characteristics within a soil profile are determined, its effect on the stability of unsaturated slopes is evaluated using the model for predicting the shear strength of the unsaturated soils (Fredlund and Rahardjo 1993). Based on the theory of unsaturated soils, seepage analysis, shear strength and volumetric deformation of unsaturated soil are related to matric suction (Fredlund and Rahardjo 1993). There are many methods available to measure the suction in soil. Wang et al. (2000) based on critical study of measurement of matric suction in slopes of unsaturated soil suggested that the suction measurement using tensiometers gave direct and accurate results. On the other hand, thermal conductivity has the advantage of rapid response, but when the condition of calibration equation is not consistent with in-situ observations, the accuracy is low. The filter paper method has the advantage of simplicity of equipment, but greater care must be taken in

weighing the filter paper, in order to get better accuracy. The above calculation models do not consider the uncertainties/variability associated with the parameters.

Geotechnical engineers have recognized the role of uncertainties in slope stability quite a few years back (Wu and Kraft 1970; Alonso 1976; Vanmarcke 1977b; Chowdhury et al. 1987; Li and Lumb 1987; Chowdhury 1996; Tang et al. 1999) but have been slow on implementing them in analysis and design and to assess the probability of success (satisfactory performance) or failure (unsatisfactory performance) of a structure. Christian et al. (1992) suggest that the effective applications of probability and reliability principles lie in identifying the relative probabilities of failure or in which the effects of uncertainties on design are clearly brought out. The impact of uncertainty on the reliability of slope design and performance assessment is often significant. The evaluation of the role of uncertainty necessitates the implementation of probability concepts and reliability based design methods. Recognizing the aspects of safety, uncertainty and consequence costs, efforts are being made to formulate guidelines and codes.

Shear strength parameters, suction pressures and hydraulic properties in a slope regime are highly variable, and expressing stability in terms of a single factor of safety is questionable (Alonso 1976). Conventional methods of analyzing an unsaturated slope neglecting the shear strength contribution may not provide economical designs (Fredlund and Rahardjo 1993). Cho and Lee (2002) evaluated the surficial stability of homogenous unsaturated soil slopes using an infinite slope model considering infiltration characteristics. They showed that distribution of suction within the slope has a major influence on the performance of slopes and is variable. Many studies have been reported in the literature on the simulation of seepage conditions within a slope under unsaturated conditions using either a finite element or

finite difference codes (Döll 1996; Tsaparas et al. 2002). Bergado and Anderson (1985), Li and Lumb (1987), Gui et al. (2000) considered the influence of uncertainties associated with pore pressures on slope reliability. Tsaparas et al. (2002) observed that the ratio between the saturated coefficient of permeability with respect to water and the rainfall patterns can significantly influence the seepage pattern within an unsaturated soil slope.

Yong et al. (1977) examined the problem of the prediction of stability of natural clay slopes in view of the random intrinsic nature of both soil properties and external actions. Using the method of slices, the different sources of uncertainty were incorporated into a first-order probability analysis of the simplified Bishop model. Field and laboratory data from an instrumented test valley slope in the Ottawa region were considered to arrive at an instability risk prediction of the test slope. A relatively high value of probability of failure is obtained for this experimental filed test slope, as evidenced by several scars and land slides of various sizes occurred in the surrounding regions. It is concluded that the surprising findings of instability can only be revealed using the risk analysis, which would not be evident with the usage of a deterministic analysis with FS=1.46.

Chowdhury (1996) observed that considerable changes occur over time and observed performance, which needs the reassessment of risk and updating of the estimated failure probabilities. Bayesian approach is used for updating the risk associated with systematic uncertainty to study the survival case of an open cut mining slope. The results show that there is a significant improvement in the estimate of the achieved reliability as a result of single updating.

Tang et al. (1999) used a back analysis approach to evaluate the soil shear strength parameters from the failed slopes. A methodology is presented based on the

information on 39 landslides in the Orinda Formation in the San Francisco Bay area, which allows the implied level of reliability associated with soil shear strength parameters back calculated from slope failures to be estimated. A reliability approach is also used to estimate the probability of failure for a given limit equilibrium slope stability method based on Bishop's slip circle approach, design factor of safety, and combination of back calculated Mohr-Coulomb shear strength parameters, c' and ϕ'.

Gui et al. (2000) investigated the effect of stochastic hydraulic conductivity on the slope stability of an earth slope that is undergoing internal water flow using a combination of two-dimensional random field simulation. The hydraulic conductivity distribution is treated as a spatially stationary random field following a lognormal distribution. The FOSM reliability index β was employed to characterize the influence of the variability of K_s, and hence, pore-water pressures, on the stability of the downstream slope. Simulation results show that neither standard deviation nor coefficient of variation of the factor of safety is constant when only the variability of hydraulic conductivity is considered. A linear relationship between standard deviation of hydraulic conductivity σ_{lnKs} and that of factor of safety σ_F was obtained. A relationship between β and σ_{lnKs}, in which every 0.1 σ_{lnKs} increment results in a decrease of 1.0 in β, is deduced based on the simulation results. It is concluded that uncertainty of soil hydraulic conductivity K_s does not significantly affect the mean factor of safety in variable K_s soils, but has a very significant effect on the standard deviation of the factor of safety, and hence, on the reliability index. It is also observed that the reliability index is very sensitive to the uncertainty of K_s, indicating that β provides more information than the deterministic factor of safety.

El-Ramly et al. (2002) developed a simple spreadsheet approach for probabilistic slope stability analysis based on Monte Carlo simulation technique. The methodology is illustrated by a probabilistic slope analysis of the dykes of the James Bay hydroelectric project. The approach is flexible in handling real slope problems. The sensitivity analyses undertaken in this study showed that the uncertainty of Bjerrum's vane correction factor is substantial and could have a large impact on the reliability of the design. It is also recognized that simplified probabilistic analyses, neglecting spatial variability of soil properties and assuming perfect autocorrelations, can be erroneous, misleading, and significantly overestimate the probability of unsatisfactory performance.

2.11.2 Stability of slopes against earthquake-induced loading

Landslides are exceedingly wide spread geologically and frequent in occurrence. They pose serious threats to the safety of highways, railway and residential areas on mountainous terrain. Hence, the evaluation of performance of soil slopes subjected to perturbations, such as induced by rainfall and earthquakes are some of the challenging tasks to the geotechnical engineers for many years. By reviewing historical investigations and engineering judgment it was found that the annual probability of slides in limestone of the Motes de Caneja near San Juan, Puerto Rico is approximately 10% under static loading (Christian and Urzua 1998). The traditional way to assess whether a slope is safe or not relies mainly on the use of factor of safety by applying a limit equilibrium of the soil or rock mass. Christian and Urzua (1998) extended the conventional analytical formulation of factor of safety in static loading to include the simplified parameters of earthquake loading, viz., the peak horizontal ground acceleration coefficient, the amplification factor, etc. They also presented a simple procedure for assessing the risk associated with the evaluation of mean factor

of safety. A triangular failure wedge mechanism was adopted in the analysis. It was also demonstrated that for a reasonable range of parameters, the increase in probability of slope failure due to earthquake loading is about 0.1 to 0.2 times the preexisting probability of failure under static conditions.

A-Grivas and Asaoka (1982) presented a procedure to evaluate the stability of natural and man-made slopes under static and earthquake-induced loading in probabilistic framework. Limiting equilibrium was expressed as a function of random soil strength parameters, obtained during strength tests under drained conditions. The earthquake-induced loading was introduced in terms of the maximum horizontal ground acceleration expected to occur at the site of the slope. The Bayesian technique was used in order to provide an improved measure for the predicted probability of failure under earthquake-induced loading from the observations made on the safety of the slope under static conditions, prior to the occurrence of an earthquake. The developed procedure was illustrated with an example involving the safety of a slope located in the seismic environment of New York state. It is observed that the simple method of slices always provided larger values for the probability of failure than the modified Bishop method. Conversely, based on the results of conventional deterministic procedures the former approach overestimates the factor of safety.

Earthquake induced slope failures occur in seismically active zones and lead to loss of lives and economic losses. The slope design in these situations needs to address the issues of uncertainty, safety and consequence costs in a rational manner. Conventional slope design based on the factor of safety cannot explicitly address uncertainty (Alonso 1976).

2.12 Scope of the present study

The extensive work quoted in the above sections and the importance of reliability based analysis in geotechnical engineering is the motivation for the present study. Figure 2.10 shows a general format of presentation of various phases of the analyses carried out in the present study.

It is felt that there is dire need to conduct comprehensive studies in this area to bridge the gap between the theoretical aspects and geotechnical engineering practice and apply these concepts to the most common problems in geotechnical engineering, viz., the bearing capacity, settlement of shallow foundations, stability of slopes in saturated and unsaturated states subjected to both static and seismic loading. Attempts have also been made on the examination of effect of anisotropy in the correlation structure on the bearing capacity, and some codal provisions have been formulated for resistance factors to be used in routine geotechnical designs for shallow foundations.

The objectives of the study are:

1. To evaluate the statistical parameters of in-situ cone tip resistance data, viz., mean and variance, and the autocorrelation characteristics for the three sites, one for the cohesionless site, and two for cohesive soil sites.
2. To evaluate the uncertainty of design parameters considering all the three sources of uncertainty, viz., inherent variability, measurement uncertainty, and transformation or model uncertainty.
3. To assess the risk associated with the evaluation of bearing capacity of shallow foundations resting on all the three sites and settlement of shallow foundations resting on cohesionless soil deposit.

4. To evaluate the effect of anisotropic behaviour spatial correlation structure on the bearing capacity of shallow foundations resting on cohesionless soil deposit.
5. To evaluate the resistance factors for shallow foundations in ultimate limit state.
6. To conduct the sensitivity analysis and identify the significant parameters that influence the stability of unsaturated soil slopes, and conduct the reliability analysis of slopes prone to landslides.
7. To evaluate an economical design of soil slopes subjected to static and earthquake induced loading, considering the essential factors, such as initial cost, consequence costs, and probability of failure.

It is intended that the results from the above study provide insights into the design of shallow foundations and slopes, and focus on the need for early implementation of probabilistic methods in geotechnical engineering.

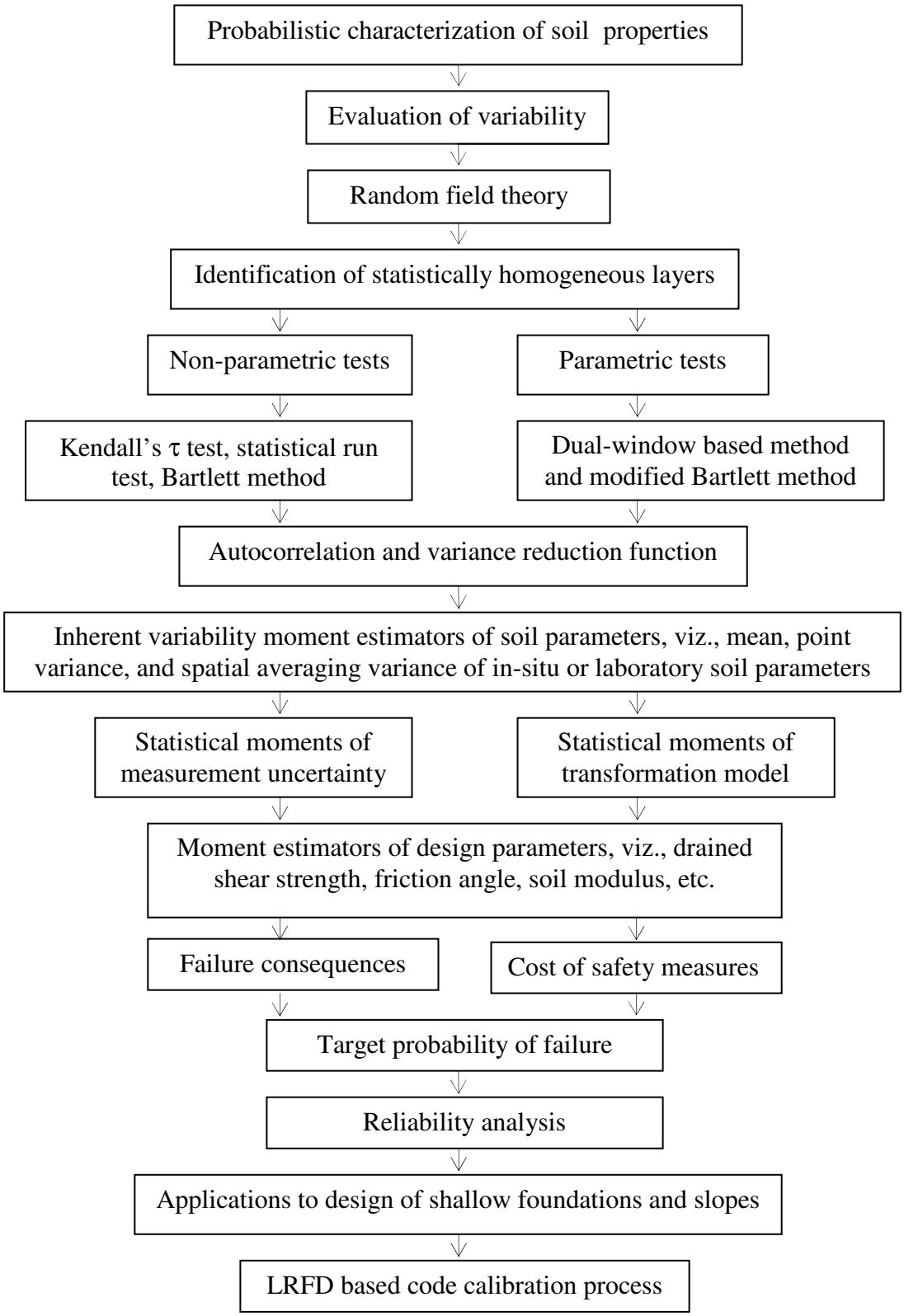

Figure 2.10. General layout of various phases of the analyses carried out in the work

Chapter 3

PROBABILISTIC SITE CHARACTERIZATION

3.1 Introduction

In this chapter the in-situ cone tip resistance profiles obtained from three well established sites, one for cohesionless soil and other two for cohesive soils are analysed for the statistical properties of strength and deformation characteristics based on the procedures outlined in Chapter 2. The mean and standard deviation are evaluated from the in-situ measured cone tip resistance data. Statistical homogeneous layers are identified and the scales of fluctuation of cone tip resistance within significant zones of influence are evaluated.

3.2 Data analysis and soil profiles considered

The following cone tip resistance (q_c) profiles have been considered in the analysis.

8 CPT 'q_c' profiles (CPT21, CPT23, CPT24, CPT25, CPT26, CPT27, CPT28 and CPT29) pertaining to cohesionless soils, obtained from Texas A & M Riverside Sand Site, National Geotechnical Experimentation Site (NGES).

1 CPT 'q_c' profile (C8) pertaining to Keswick clay, Adelaide city obtained from Jaksa (1995).

1 CPT 'q_c' profile (SCPT-04) pertaining to a power plant site in Indian state of Andhra Pradesh.

It is stressed at this stage that both non-parametric and parametric tests have been developed over a period of time to examine the statistical homogeneity of data and the difficulties associated with some of these tests when applied to soil profiles have been

brought out in this chapter. It is also brought out that this area is developing towards better quantification procedures for identification of statistical homogeneity.

Figure 3.1 shows the flowchart of various phases of analysis to be considered to evaluate the statistical parameters of the in-situ measured data.

All the cone tip resistance profiles corresponding to cohesionless soils (NGES Texas A & M Sand Sites), and cohesive soils (Keswick clay of the Adelaide city and clayey deposit of power plant site) are first checked for statistical homogeneity using both non-parametric and parametric tests. The Kendall's τ test and statistical run test under non-parametric category and Modified Bartlett test and dual-window technique under parametric tests are used in this study. Once the statistical homogeneity of cone tip resistance within the significant zone of influence is satisfied, the data are used for evaluation of the autocorrelation characteristics of the cone tip resistance.

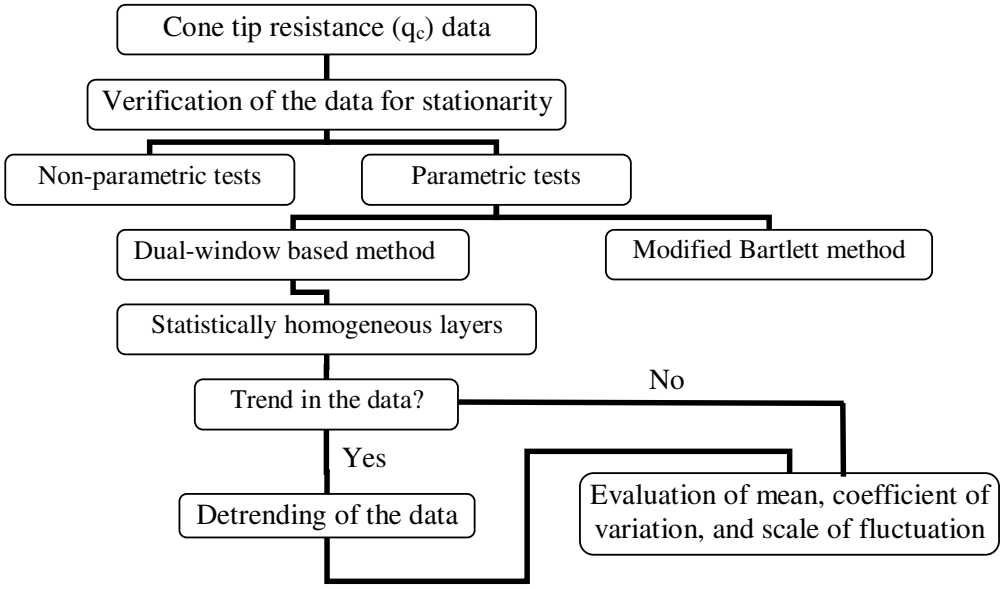

Figure 3.1. Flow chart of various phases of analysis in this chapter

Using the statistical parameters thus obtained, shallow foundations resting on both cohesionless and cohesive profiles are designed in probabilistic approach. The entire foundation analyses reported in this thesis pertain to a smooth strip footing of width

1 m placed on a level ground and subjected to only vertical loading. From the observations made from available literature presented in Chapter 2, significant depths of influence below the loaded footing for shear criterion are taken as 2 m and 1 m for cohesionless soil and cohesive soil respectively. On the other hand, a significant depth of influence of 4 m below the loaded footing is considered for settlement analysis in cohesionless soils.

3.3 Cohesionless soil - shear failure criterion

Figure 3.2 to 3.9 show the experimental, linear detrended and quadratic detrended cone tip resistance within 2 m below the ground surface for CPT21, CPT22-CPT soundings. The linear and quadratic trends are evaluated using method of Ordinary Least Squares (OLS) based on regression analysis. The mean values of experimental q_c, linear and quadratic trends for q_c of cohesionless soils in NGES sites within 2 m depth of zone of influence (shear failure planes extend to a depth approximately equal to 2B below the footing base) for CPT21, CPT23, CPT24, CPT25, CPT26, CPT27, CPT28, CPT29 soundings are given in Table 3.1.

3.3.1 Identification of statistically homogeneous layers

3.3.1.1 Kendall's τ test

Table 3.2 shows the summary of results of the Kendall's τ test for cone tip resistance for experimental, linear, and 2^{nd} order polynomial detrended data for all the cohesionless soil profiles. The Kendall's hypothesis test of statistical homogeneity is that the τ value close to zero represents a statistically homogeneous layer.

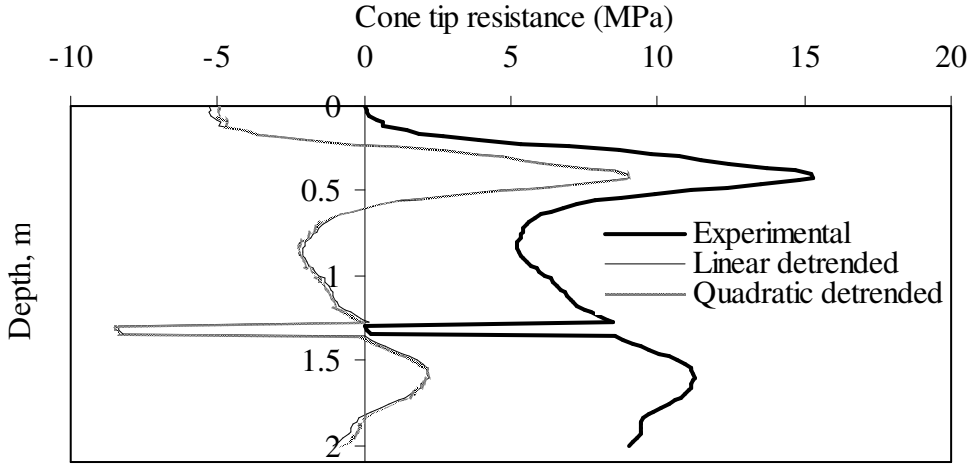

Figure 3.2. Cone tip resistance profile of CPT21 for shear criterion

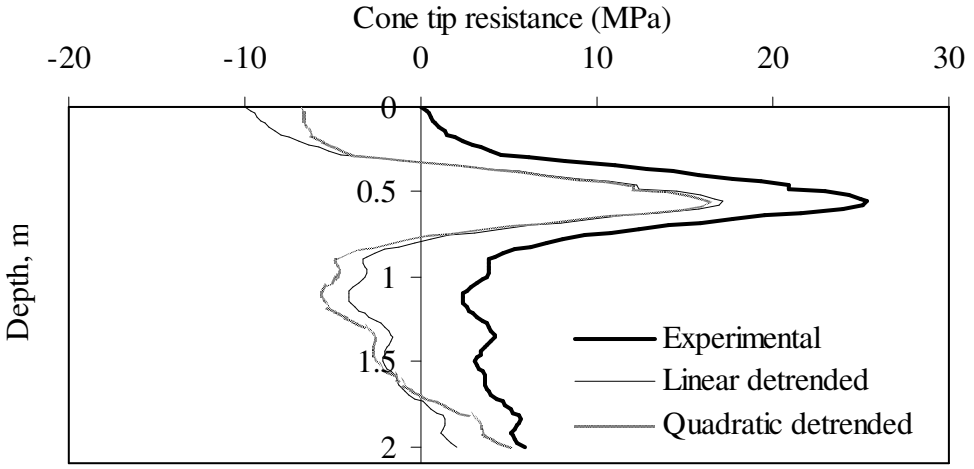

Figure 3.3. Cone tip resistance profile of CPT23 for shear criterion

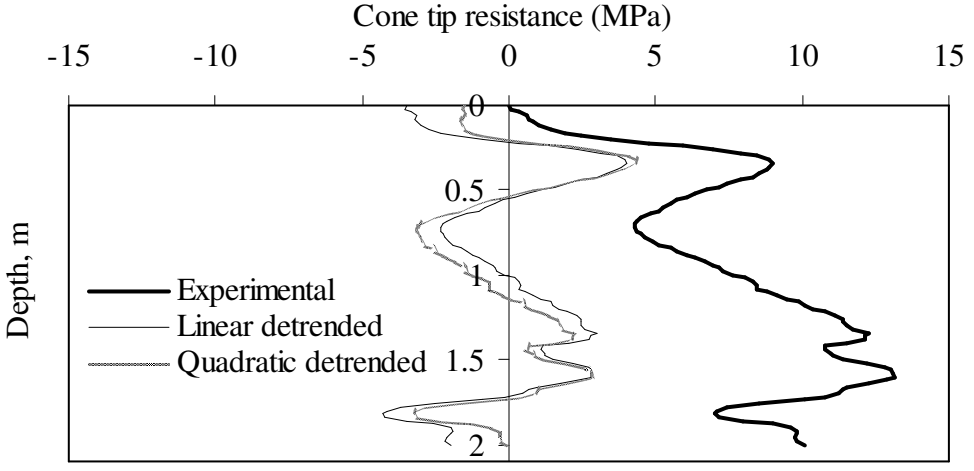

Figure 3.4. Cone tip resistance profile of CPT24 for shear criterion

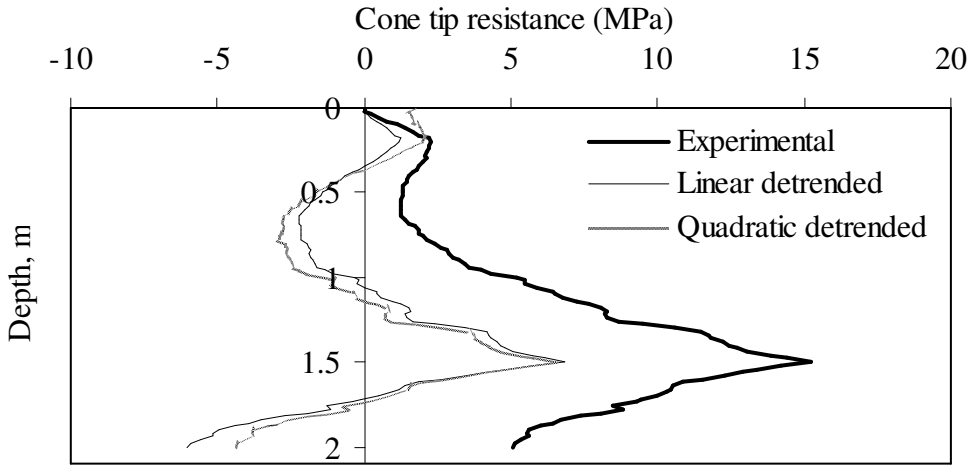

Figure 3.5. Cone tip resistance profile of CPT25 for shear criterion

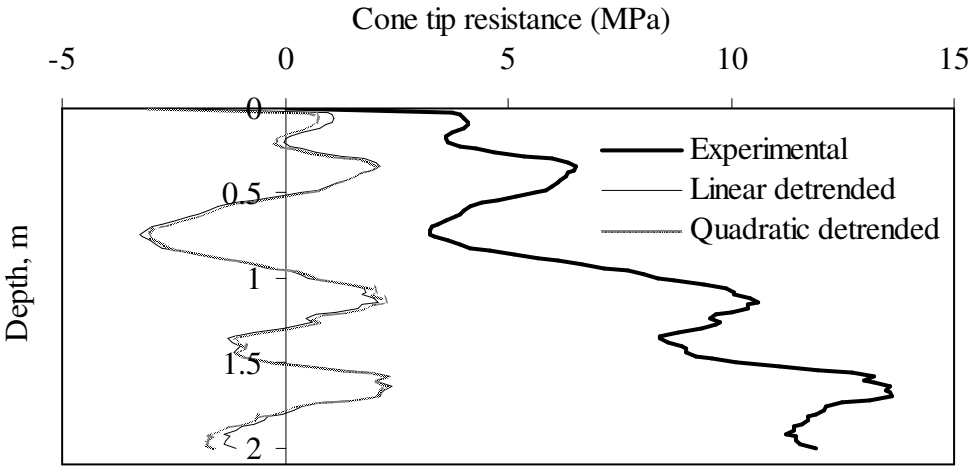

Figure 3.6. Cone tip resistance profile of CPT26 for shear criterion

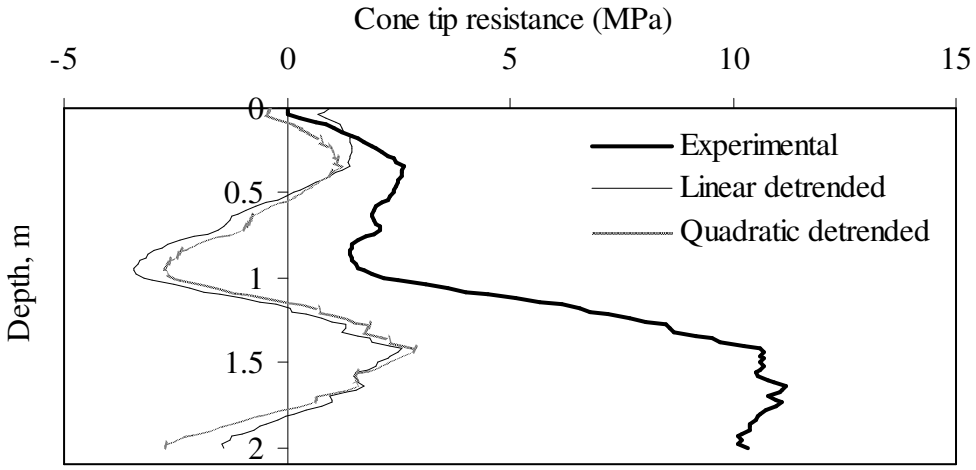

Figure 3.7. Cone tip resistance profile of CPT27 for shear criterion

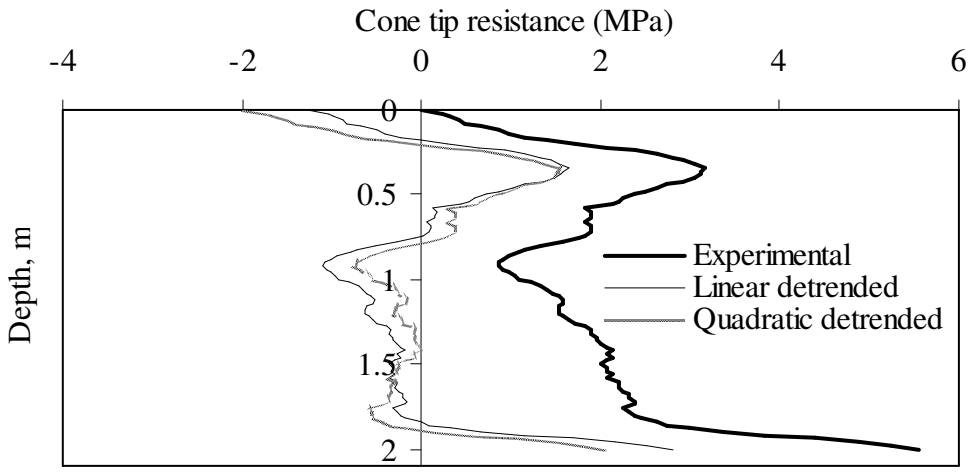

Figure 3.8. Cone tip resistance profile of CPT28 for shear criterion

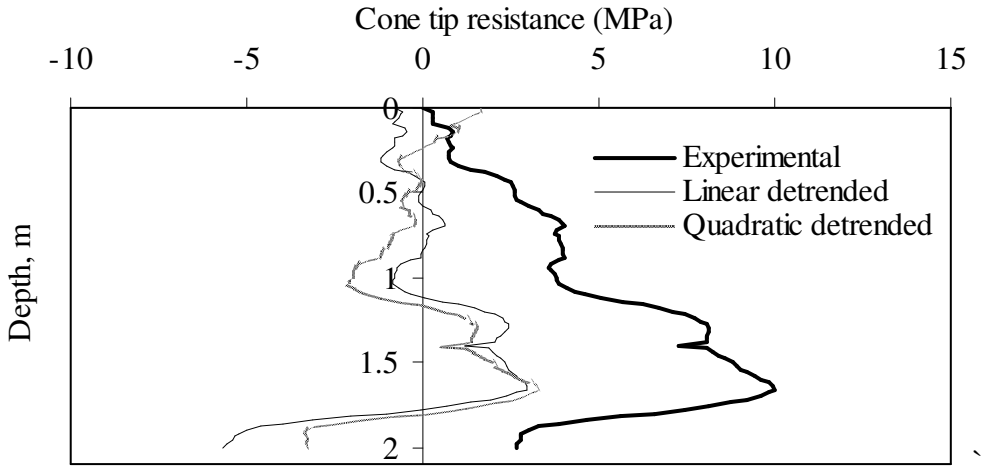

Figure 3.9. Cone tip resistance profile of CPT29 for shear criterion

The sample calculations of τ for cone tip resistance of CPT27 sounding are presented below. For the experimental cone tip resistance within 0-2 m below the ground surface, the Kendall's τ is computed from Equation 2.7, as given below. For this data the number of pairs in natural and reverse natural order are 4084 and 900 respectively. Since, the cone tip resistance is obtained at a vertical spacing of 0.02 m, the total number of data points for 2 m depth is 101 (i.e., 1+2/0.02=101).

Table 3.1. Mean and point standard deviation of cone tip resistance of cohesionless soil within the significant zone of influence for shear failure criterion (0-2 m)

	Mean (kPa)			Standard deviation (kPa) (point coefficient of variation (%))		
Sounding	Experi-mental q_c	Linear trend	Quadratic trend	Experi-mental q_c	Residuals off linear trend	Residuals off quadratic trend
CPT21	7676	7677	7677	3700 (48%)	3421 (45%)	3418 (45%)
CPT23	6892	6891	6891	6610 (96%)	6351 (92%)	6188 (90%)
CPT24	7789	7789	7789	3381 (43%)	2268 (29%)	2066 (27%)
CPT25	5535	5535	5535	4265 (77%)	2728 (49%)	2619 (47%)
CPT26	7826	7826	7826	3417 (44%)	1557 (20%)	1544 (20%)
CPT27	5390	5390	5390	4080 (76%)	1685 (31%)	1567 (29%)
CPT28	2011	2011	2011	952 (47%)	846 (42%)	778 (39%)
CPT29	4569	4569	4569	2985 (65%)	1998 (44%)	1672 (37%)

Table 3.2. Summary of results of the Kendall's test for cohesionless data in shear criterion

Data set	Kendall's τ corresponding to shear criterion (0-2 m) for the data		
	Experimental	Linear detrended	Quadratic detrended
CPT 21	0.32	0.15	0.16
CPT 23	0.04	0.25	0.26
CPT 24	0.53	0.06	0.06
CPT 25	0.59	0.01	-0.06
CPT 26	0.63	-0.03	-0.02
CPT 27	0.63	-0.05	-0.03
CPT 28	0.34	0.06	-0.09
CPT 29	0.66	0.24	-0.03

$$\tau = \frac{S}{n(n-1)/2} = \frac{P-Q}{n(n-1)/2} = \frac{(4084-900)}{101(101-1)/2} = 0.63$$

From the Kendall's test hypothesis, the high magnitude of τ for experimental data (0.63) suggests that the data is highly non-stationary. Hence, a detrending process is applied on the experimental data, and the residuals off the trend are verified again for Kendall's τ. The linear detrended data results in a τ value of 0.1.

$$\tau = \frac{S}{n(n-1)/2} = \frac{P-Q}{n(n-1)/2} = \frac{(2775-2275)}{101(101-1)/2} = 0.1$$

Further detrending is tried by removing the 2nd order polynomial (or quadratic) trend from the experimental data, and a τ value of -0.05 has been obtained.

$$\tau = \frac{S}{n(n-1)/2} = \frac{P-Q}{n(n-1)/2} = \frac{(2399-2651)}{101(101-1)/2} = -0.05$$

Further detrending using higher order polynomial trend is not done, as removal of trend no higher than a quadratic is generally sufficient to transform a non-stationary geotechnical data set to a stationary set using random field theory by method of ordinary least squares (Jaksa et al. 1999). This value of -0.05 obtained from the 2nd order polynomial detrended data is very close to zero, and hence, can be regarded as second-order (or weak) stationary data. The Kendall's τ values computed for other q_c profiles are also presented in Table 3.2. From the results, it is seen that except for cone tip resistance data of CPT23 sounding, the test produced lower τ values for linear detrended data. From the results of the Kendall's hypothesis test of stationarity presented in Table 3.2, it may be seen that the quadratic detrending do not produce τ values close to zero. However, in case of cone tip resistance of CPT23 sounding, the experimental, linear detrended and quadratic detrended data results in t values of 0.04, 0.25 and 0.26, respectively. Unlike other soundings, the τ value of experimental data for this sounding is very close to zero, and from the Kendall's hypothesis, the experimental data are fairly stationary and no detrending is necessary to be performed

on this data set. However, for this sounding, the τ value is increased for linear and quadratic detrended data. In case of CPT29 sounding, the τ value for linear detrended data is not reduced significantly, but the quadratic detrending produced fairly stationary data.

3.3.1.2 Statistical run test

Statistical run test has been carried out on all the profiles considered using the approach given in section 2.5.2.1.2. The results for cone tip resistance data of CPT27 are discussed here. The whole profile is analysed in terms of number of sections of 2 'q_c' points, 5 'q_c' points, 6 'q_c' points, and 11 'q_c' points, which correspond to 0.02 m, 0.08 m, 0.1 m, and 0.2 m depth. The variance in each of these sections is evaluated, and compared with the median of all the variances. The total number of runs is computed and compared with the interval given Equation 2.8, for a 5% level of significance, which is generally considered as a customary level in statistical analysis. The interval is a function of the total number of data points in the record being verified for statistical homogeneity, and the level of significance. The entire length CPT27 'q_c' profile of 15.24 m, containing 763 data points is used to verify the statistical homogeneity. For example, in the case of 0.2 m length of window, number of sections within 15.24 m record are 69 as given in Table 3.3. For 5% significance level, and n=N/2, where N is the total number of sections, the lower ($r_{n;\ 0.975}$) and upper ($r_{n;\ 0.025}$) values of interval are 27 and 44, respectively. For this length of window, the median of variance of cone tip resistance data computed within individual sections is obtained as 271827 kPa^2. The number of runs (r) counted from the variance record is 15. For this section length the number of runs (r=15) is not bounded within the intervals computed above (27-44). Hence, according to the statistical run test hypothesis, the cone tip resistance record of length 15.24 m can be

treated as a statistically non-homogeneous layer. Like the above sections length, the total runs (r) is not bounded within the corresponding limit even for section of length 0.08 m. Hence, the statistical run test hypothesis of stationarity for cone tip resistance data (CPT27) is rejected at 5% significance level with section lengths of 0.08 m and 0.2 m.

Table 3.3. Summary of statistical run test for cone tip resistance of CPT27

Length of section	Median of variance of all sections (kPa^2)	Runs (r)	n=N/2	$r_{n;\,0.975}$	$r_{n;\,0.025}$	Hypothesis of Stationarity at 5% significance level
0.02 m	16200	105	381/2	86	115	Accept
0.08 m	69694	36	152/2	63	88	Reject
0.1 m	16200	36	127/2	54	77	Accept
0.2 m	271827	15	69/2	27	44	Reject

The results given in Table 3.3 reveal that the stationarity by statistical run test hypothesis is accepted for sections with lengths 0.02 m and 0.1 m. The results obtained from the statistical run test hypothesis for verifying the statistical homogeneity are sensitive to the length of section considered, i.e., the results are departed with different length of sections. Hence, a proper value for length of the section is selected to get a realistic picture of statistical homogeneity of soil profile by statistical run test hypothesis. To the author's knowledge, there are no guidelines available to tackle the problem of variant results obtained above. In this method it is verified whether the data satisfy the second condition of weak stationarity, i.e., the variance is constant throughout the depth. For the stationary data, the variance is constant throughout all the sections.

3.3.1.3 Bartlett approach

The Bartlett approach, another non-parametric test, described in section 2.4.2.3 is used to analyse the cone tip resistance profiles of CPT21, and CPT22-CPT29 obtained from NGES Texas A & M Riverside sand site for statistical homogeneity. The Bartlett profile is obtained for each of the soil profiles. The Bartlett test hypothesis of stationarity is that the portions between the peaks in Bartlett profile are statistically homogeneous.

Since the spacing between 'q_c' values in the case of cohesionless data set of NGES test site is 0.02 m, a total of 11 sample data points are taken in each segment (or 21 data points in a sampling window) for evaluating the sample variance for generating continuous Bartlett statistic profile for experimental data. The above selected number of data points corresponds to segment and window lengths of 0.2 m and 0.4 m respectively.

Figure 3.10 shows the Bartlett statistic profile for experimental, linear detrended, and quadratic detrended 'q_c' data of CPT27 sounding computed using Equations 2.9-2.11. Once the continuous Bartlett profile is ready, the statistically homogeneous regions are identified as sections of the Bartlett profile between highest peaks. However, it is suggested to disregard the 'q_c' spikes produced by thin partings of sand or silt in clay (Phoon et al. 2003). Figures 3.11 to 3.18 show the Bartlett statistic profiles for the complete experimental 'q_c' data sets of CPT21, and CPT23-CPT29.

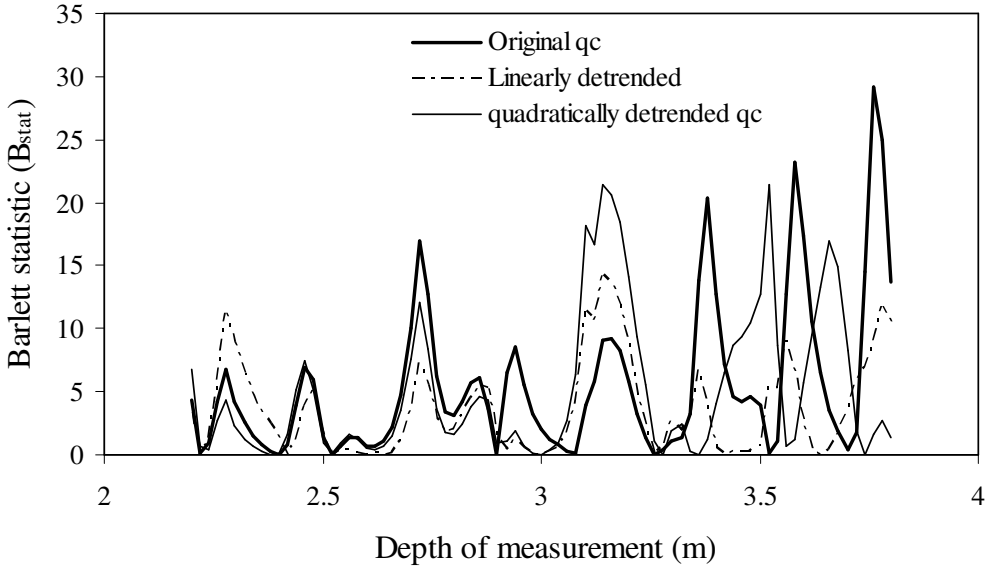

Figure 3.10. Bartlett statistic profile for original, linearly detrended and quadratic detrended cone tip resistance of CPT27

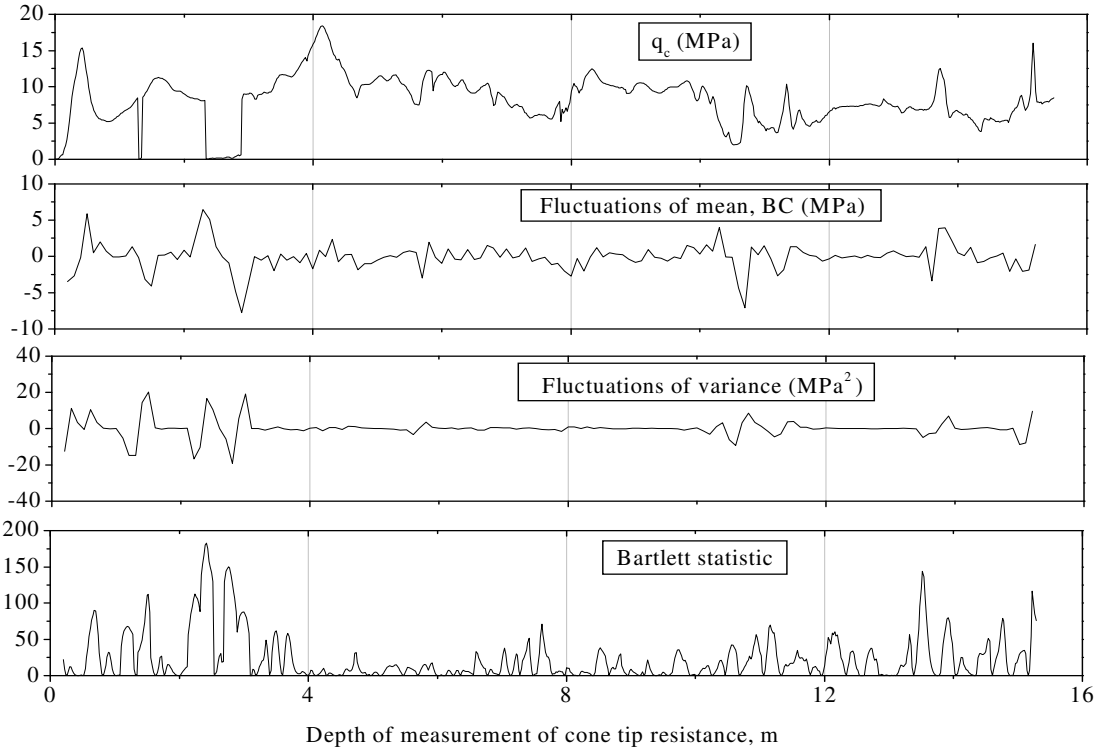

Figure 3.11. Comparison of the Bartlett statistic and BC (MPa) profiles for CPT21

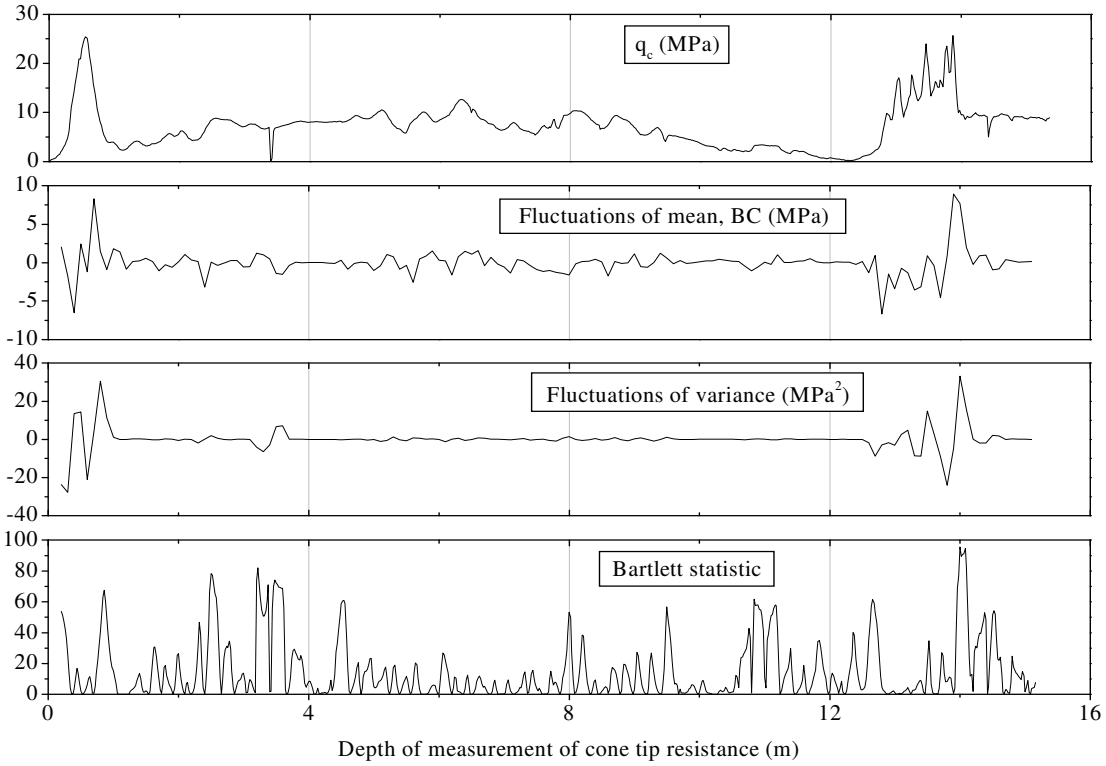

Figure 3.12. Comparison of the Bartlett statistic and BC (MPa) profiles for CPT23

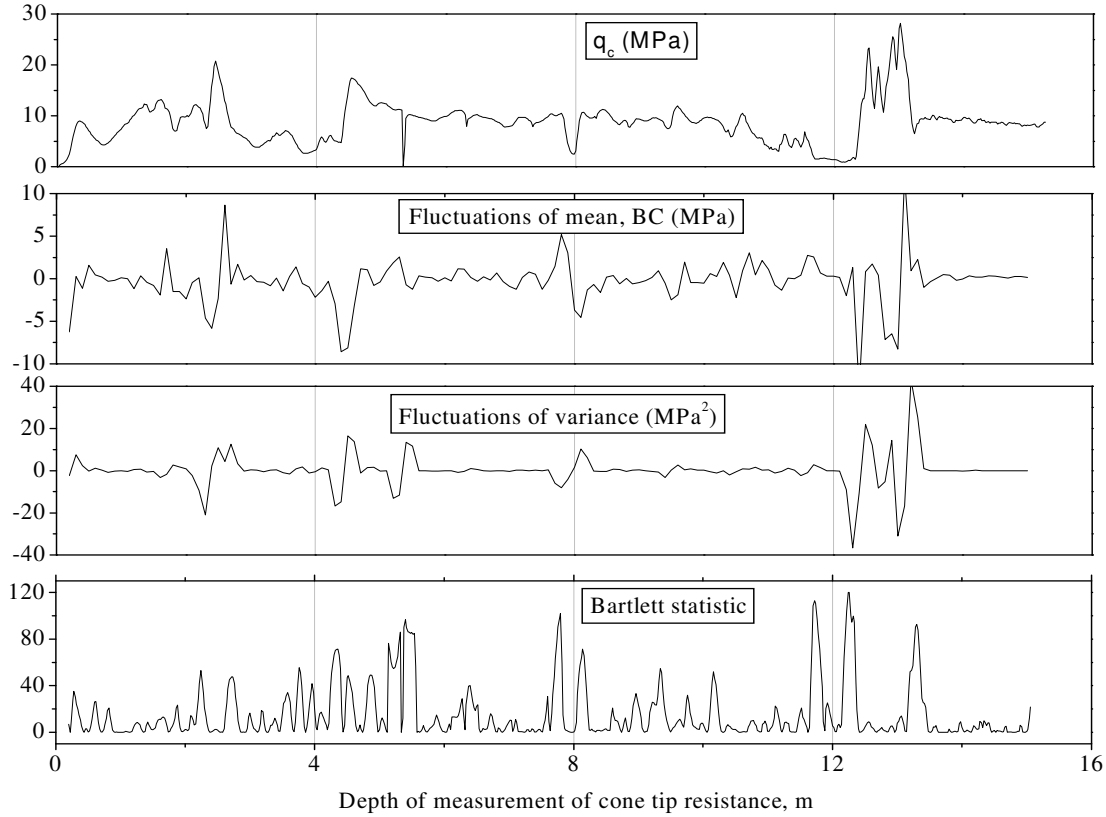

Figure 3.13. Comparison of the Bartlett Statistic and BC (MPa) profiles for CPT24

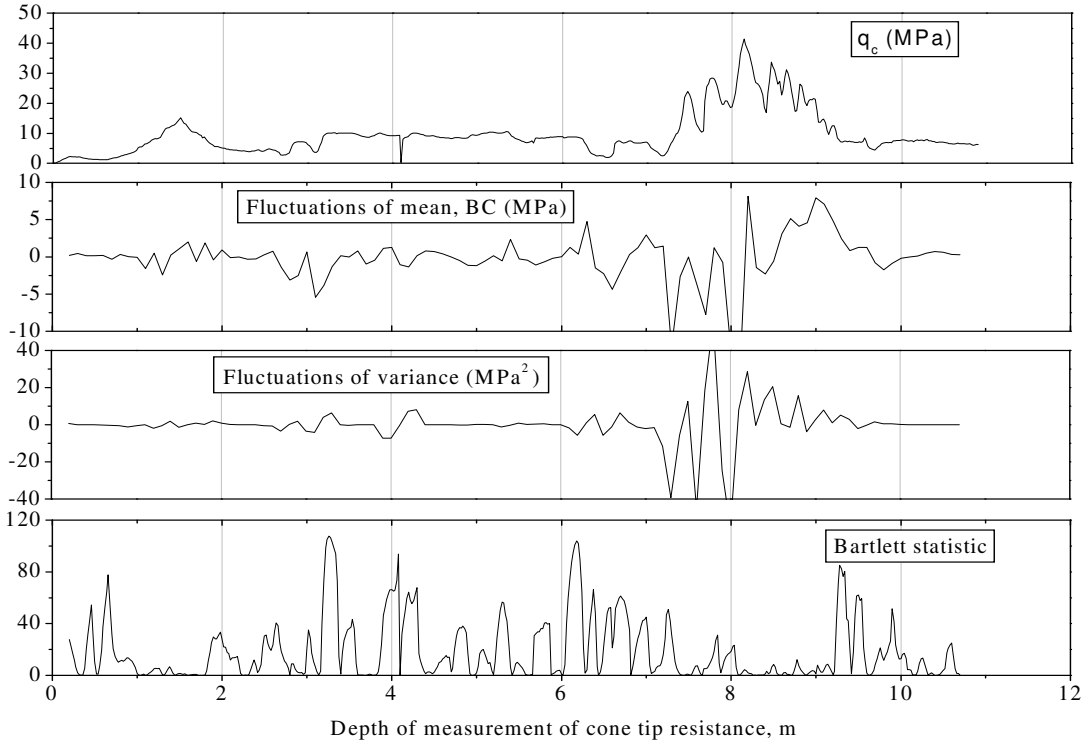

Figure 3.14. Comparison of the Bartlett Statistic and BC (MPa) profiles for CPT25

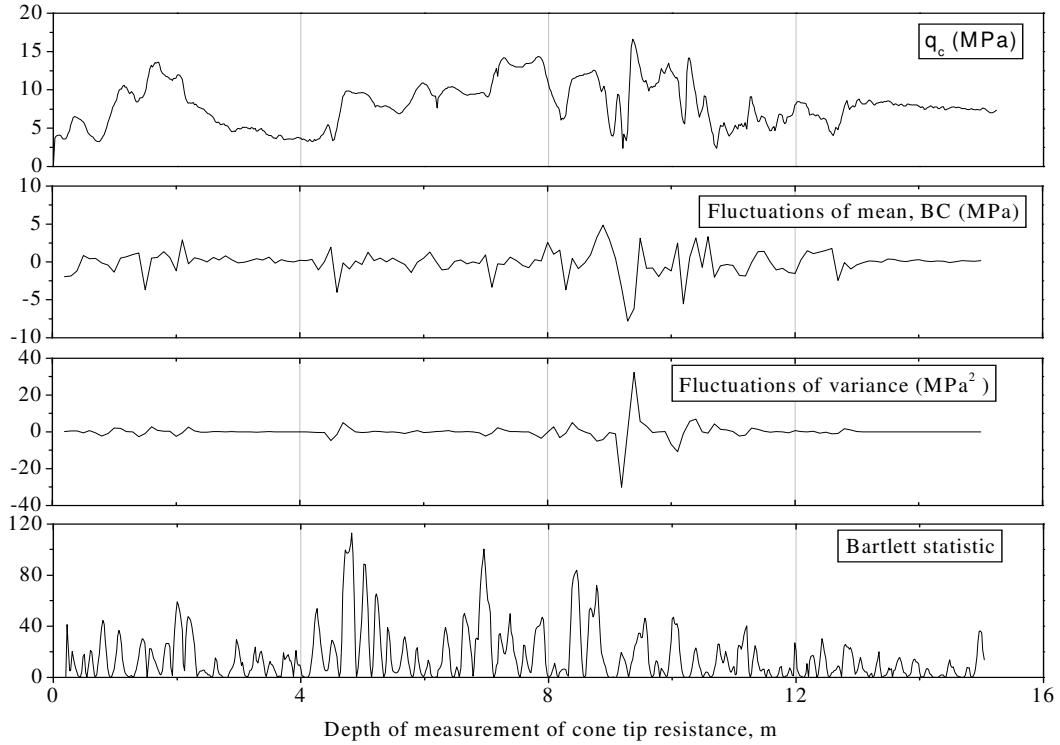

Figure 3.15. Comparison of the Bartlett Statistic and BC (MPa) profiles for CPT26

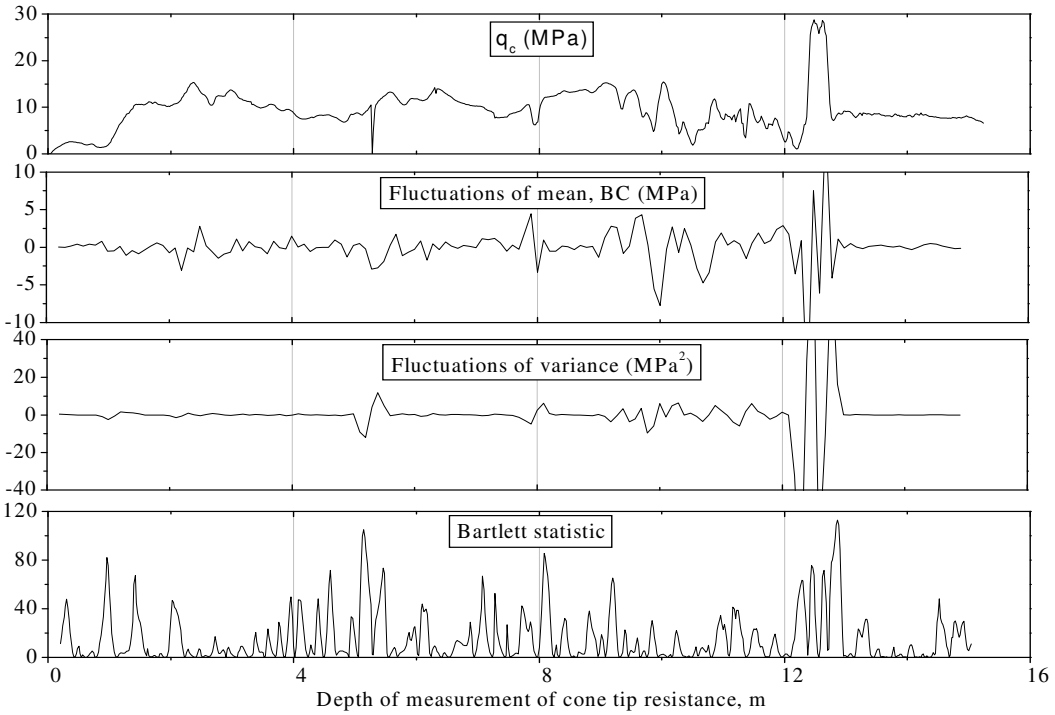

Figure 3.16. Comparison of the Bartlett Statistic and BC (MPa) profiles for CPT27

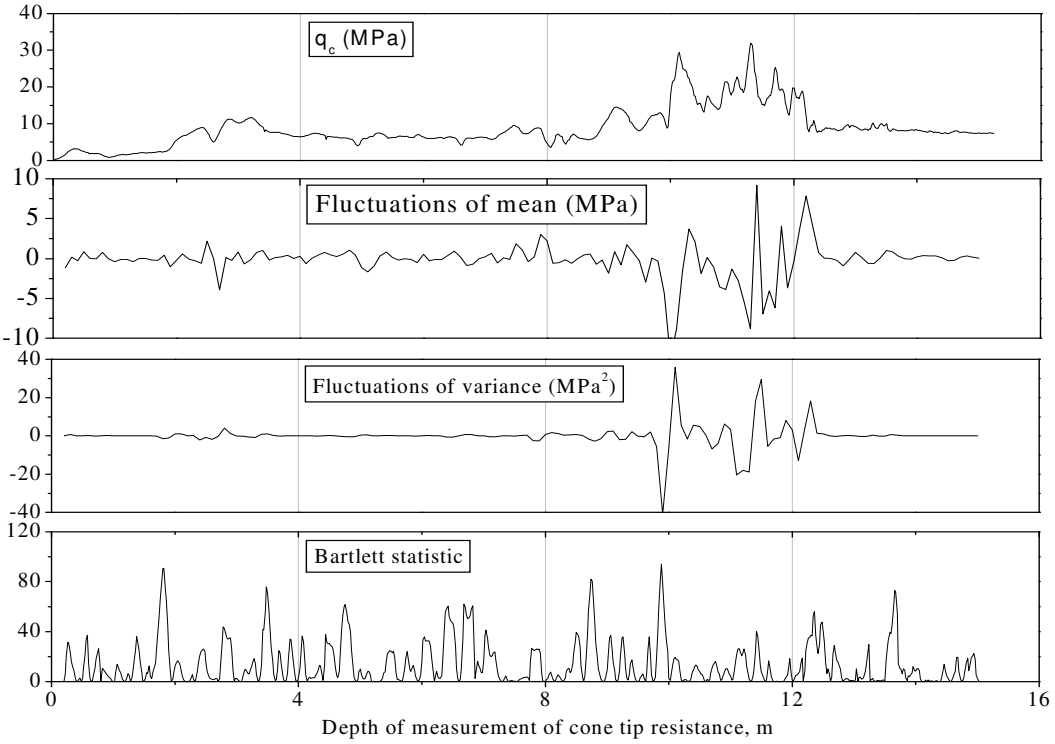

Figure 3.17. Comparison of the Bartlett Statistic and BC (MPa) profiles for CPT28

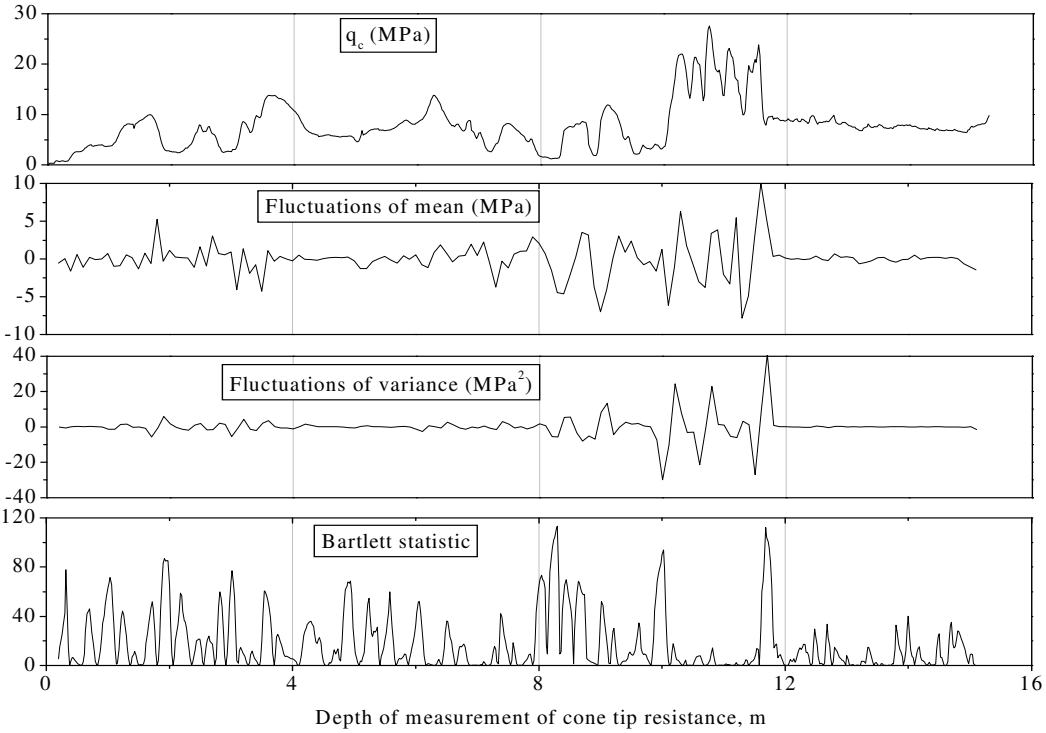

Figure 3.18. Comparison of the Bartlett Statistic and BC (MPa) profiles for CPT29

However, the above non-parametric tests, viz., Kendall's τ test, statistical run test, and the Bartlett test, do not consider the effect of spatial correlation as well as distributional characteristics of the data set (Phoon et al. 2003a). With the advent and application of better parametric methods for statistical stationarity of the geotechnical data set, and availability of large amount of experimental data from routine in-situ tests facilitate the distributional as well as spatial characteristics of in-situ soil properties.

3.3.1.4 Modified Bartlett hypothesis

After identifying the statistically homogeneous layers from the Bartlett statistic profile, the null hypothesis of stationarity of each layer is checked using the modified Bartlett statistic technique.

In Bartlett procedure of verifying the statistical homogeneity, the hypothesis is that the sections between the peaks of Bartlett statistic are statistically homogeneous. However, since the Bartlett statistic does not consider the spatial correlation characteristics of soil parameter, the modified Bartlett statistic is used to check the validity of the results obtained from the Bartlett statistic for correlated case. So, a null hypothesis of stationarity would be, "the Bartlett test is no more effective than modified Bartlett test". If the probability of the observed results under the null hypothesis is sufficiently low, the alternative hypothesis that Bartlett test statistic is indeed more effective is valid.

For each layer, critical Bartlett Statistic (B_{crit}) is evaluated from the empirical equations presented by Phoon et al. (2003a) using multiple regression analysis of the maximum Bartlett Statistic (B_{max}) of the simulated profiles corresponding to a 5% level of significance, which is described as the customary level used in most hypothesis testing.

The autocorrelation distance and hence the scale of fluctuation is computed for the data within each statistically homogeneous layer using method of moments using Equation 2.20 and Table 2.1, for experimental, linear detrended, and quadratic detrended data.. While doing so, it is suggested to see that the difference in scales of fluctuation obtained from two consecutive data sets, (either experimental and linear detrended data, or linear detrended and quadratic detrended data) should be significantly small. However, a trend higher than quadratic is generally not employed for detrending the geotechnical data. The critical Bartlett test statistic also depends on the spacing of data points (Δz), the number of data points in the statistically homogeneous layer obtained from the Bartlett test (n), and the number of points in one segment length (m). The critical Bartlett Statistic (B_{Stat}) is developed in terms of

three critical parameters, viz., number of data points in one scale of fluctuation, k, normalized sampling length, I_1, and normalized segment length, I_2, as shown by Equations 2.12-2.14, respectively. The computed critical Bartlett Statistic (B_{crit}) is also a function of the type of the theoretical fit selected for sample autocorrelation function. Phoon et al. (2003a) developed B_{crit} for five types of autocorrelation models taking I_2=1, and also presented B_{crit} corresponding to single exponential model and I_2=2. I_2 is a user defined parameter and should be selected keeping in mind a minimum number of data points for proper evaluation of the sample variance and maximum data points for a reasonable moving profile to be generated. If the value of maximum values B_{stat} profile obtained for a statistically homogeneous layer exceeds B_{crit} evaluated for this layer, the null hypothesis of stationarity is rejected at a level of significance used in the computation of B_{crit}. Conversely, if the B_{Stat} is less than the B_{crit} throughout the statistically homogeneous layer, the null hypothesis of stationarity portrayed from the Bartlett statistic profiling cannot be rejected at the prescribed level of significance.

The procedure involved for verifying the statistical homogeneous layers within the significant zone of influence is described for the 'q_c' profile of CPT27. From the Bartlett statistic profile shown in Figure 3.16 for CPT27 profile, it is observed that from 2 m to 4 m there are no significant peaks in the Bartlett statistic. Hence, from the Bartlett test hypothesis, this data could be taken to represent the statistically homogeneous layer for subsequent statistical analysis. The statistically homogeneous data within 2 m to 4 m is then verified for any possible trend. Based on the determination coefficient (R^2) obtained from regression analysis, a triangular fit is chosen to fit the detrended sample autocorrelation data. Correspondingly the correlation distances corresponding to original, linearly detrended and quadratically

detrended data within this homogeneous layer evaluated by fitting theoretical correlation functions to sample autocorrelation data are 0.5 m, 0.2 m and 0.2 m respectively. Since the correlation distances for linearly detrended and quadratically detrended data do not differ much at the first decimal level, it is assumed that linear detrending is sufficient to remove the trend in the data and keep the residual off the trend fairly stationary. For evaluating the critical modified Bartlett statistic for this stationary layer, the following three parameters are obtained, viz., the number of 'q_c' points in one scale of fluctuation, $k=\delta/\Delta z=0.2/0.02=10$, Normalized sampling length, $I_1=T/\delta=2/0.2=10$, and the normalized segment length, $I_2=W/\delta=0.2/0.2=1$. Hence, the critical modified Bartlett test statistic described by Phoon et al. (2003a) corresponding to 5% significance level is computed from the Equation 3.1, developed for $I_2=1$, and triangular autocorrelation function.

$$B_{crit} = (0.3k + 0.29)\ln(I_1) + 1.15k - 0.52 \tag{3.1}$$

From the above equation, critical Bartlett statistic (B_{crit}) is obtained as 18.5. From the Figure 3.10 it is observed that the maximum Bartlett statistic (B_{stat}) for the linearly detrended profile is 14.2, which is less than the B_{crit} ($B_{max}<B_{crit}$, $14.2<18.5$). Hence, the Bartlett hypothesis of stationarity is accepted at 5% significance level for the cone tip resistance data of CPT27 between 2 m to 4 m. Hence, the cone tip resistance data within 2 m-4 m can be considered as statistically homogeneous.

It is observed that the modified Bartlett statistic is sensitive to many parameters, like the number of data points used to evaluate the variances, m, the scale of fluctuation of the cone tip resistance, δ, and the chosen theoretical fit to sample autocorrelation function. The outcome of the computed critical Bartlett statistic may vary depending

on the values of the parameters mentioned above, which are not unique but matter of subjective judgement and expertise of the individuals.

3.3.1.5 Dual-window based method

Statistical homogeneity of the cone tip resistance profiles belonging to the Riverside sand site is examined using dual-window based method described in section 2.4.2.5. Figures 3.11 to 3.18 also present the 'BC' distance profile for the 'q_c' profiles of CPT21, CPT23-CPT29 respectively. The hypothesis of dual-window based method is that the significantly higher fluctuations of mean indicates that there is an interface of two different materials at the crossing, and depict that either a loose material is following a dense one, or a soft material following a stiff material, and vice versa (Kulathilake and Um 2003). Hence, it may be beneficial to use the results obtained from dual window technique for depicting the interface of two significantly different materials.

Though the dual-window method suggested by Kulathilake and Um (2003) identifies the statistically homogeneous layers within a soil profile using the fluctuations of mean cone tip resistance in qualitative terms, it does not provide any quantitative measure for the scatter of mean fluctuations to identify the statistically homogeneous layers, which may lead to bias in the results. Hence, a more meaningful measure, which supplements the results obtained from dual-window based method, is proposed in this study to identify the statistical homogeneous layers. The proposed measure is evaluated from the first two moments (i.e., mean and standard deviation) of 'BC' distance profile. The boundaries are identified quantitatively at locations where the 'BC' distance crosses the mean±1.65×standard deviation of 'BC' distance fluctuations within the same profile. The hypothesis of the proposed methodology is that the

profile is not statistically homogeneous if the 'BC' distance (fluctuations of mean) crosses the limits described above. Hegazy et al. (1996) proposed a similar measure for identification of significant boundaries within a soil profile using intraclass correlation coefficient (RI). Figure 3.19 shows the 'BC' distance profile along with the proposed measures to identify the statistically homogeneous sections with a soil profile. The mean and standard deviation of the 'BC' distance profile obtained from total 'q_c' record of 15.18 m length are -0.02 MPa and 2.79 MPa respectively, and the above limits are computed as -4.63 MPa and 4.59 MPa. From the figure, it may be seen that the cone tip resistance data up to 10 m depth is bounded within the above described limits, and can be treated as a statistically homogeneous layer.

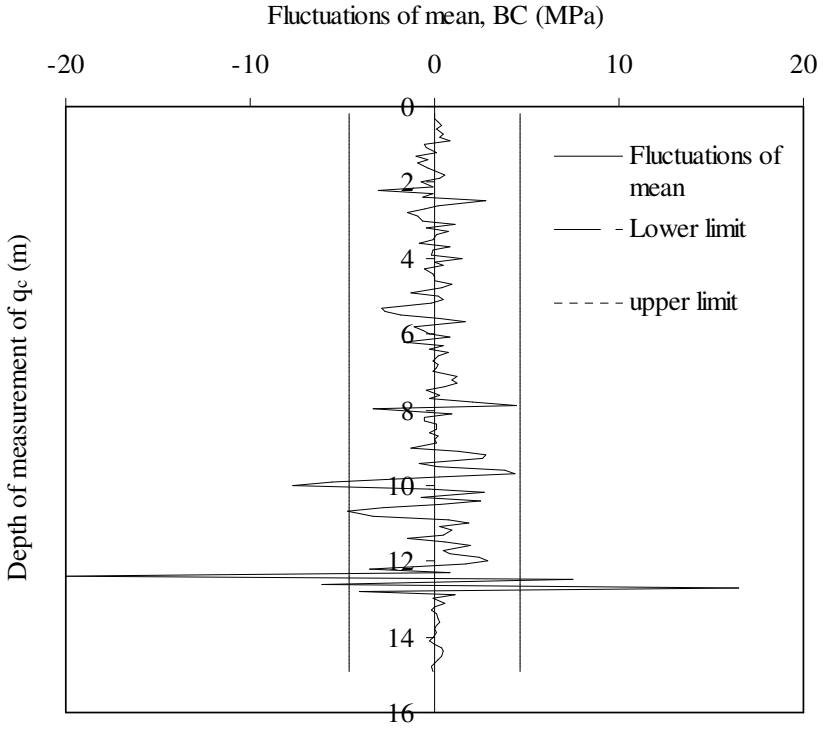

Figure 3.19. Proposed quantitative measures on fluctuations of mean profile to supplement the 'BC' distance method to identify the statistically homogeneous layers

The advantage of using the proposed quantitative measure to supplement the 'BC' distance profile is that the modified procedure of identification of statistically homogeneous layers is invariant to the individual's decisions.

Similar to dual-window based method of identification of statistically homogeneous layers in terms of mean fluctuations of cone tip resistance, the fluctuations of variance throughout the depth are also evaluated, and shown in Figures 3.11 to 3.18. The same quantitative measure discussed above is applied to the data of fluctuations of variance, and the results are shown in Figure 3.20 for cone tip resistance profile of CPT 27. The mean and standard deviation of the variance fluctuations within the entire cone tip resistance profile of length 15.18 m are 0 and 15.7 MPa^2, and the proposed lower and upper limits are 25.9 MPa^2. From Figures 3.19 and 3.20, it may be noted that the cone tip resistance profile is statistically homogeneous up to a depth of 10 m below ground level.

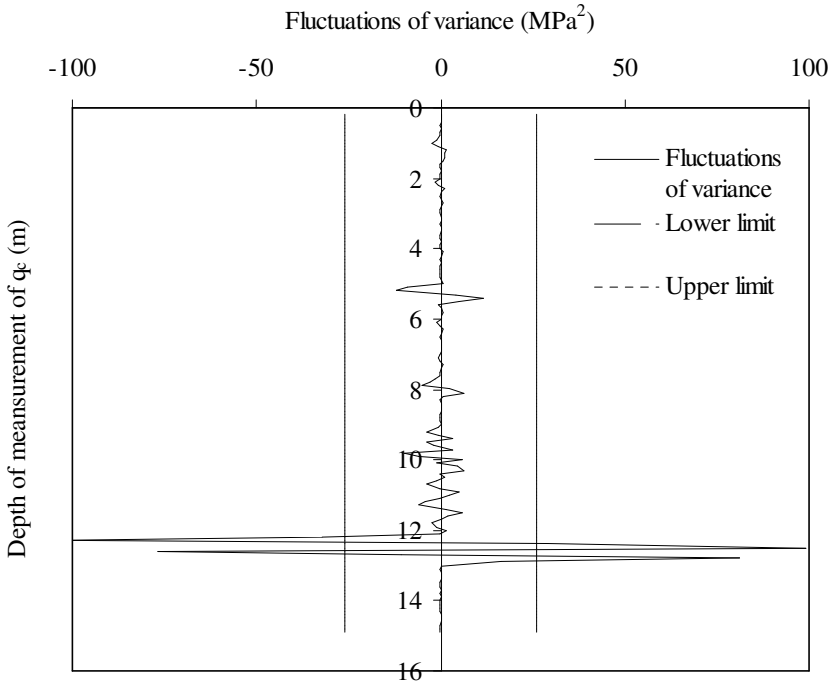

Figure 3.20. Proposed quantitative measures on fluctuations of variance profile to identify the statistically homogeneous layers

3.4 Cohesionless soil - settlement criterion

A similar procedure that is adopted in the above section is used to analyse the data within the significant zone of influence of 4 m below the ground surface for

settlement criterion. The experimental cone tip resistance profiles along with the linear and quadratic trends for all soundings are given in Figures 3.21-3.28. The mean, standard deviation and coefficients of variation of experimental, linear detrended, and quadratic detrended cone tip resistance (q_c) of cohesionless soils in NGES sites within 4 m depth of zone of influence for all the soundings are shown in Table 3.4.

The results obtained from the Bartlett test and dual-window based methods for this data are already presented in Figures 3.11-3.18. Hence, the results from the Kendall's test and statistical run test alone are presented here.

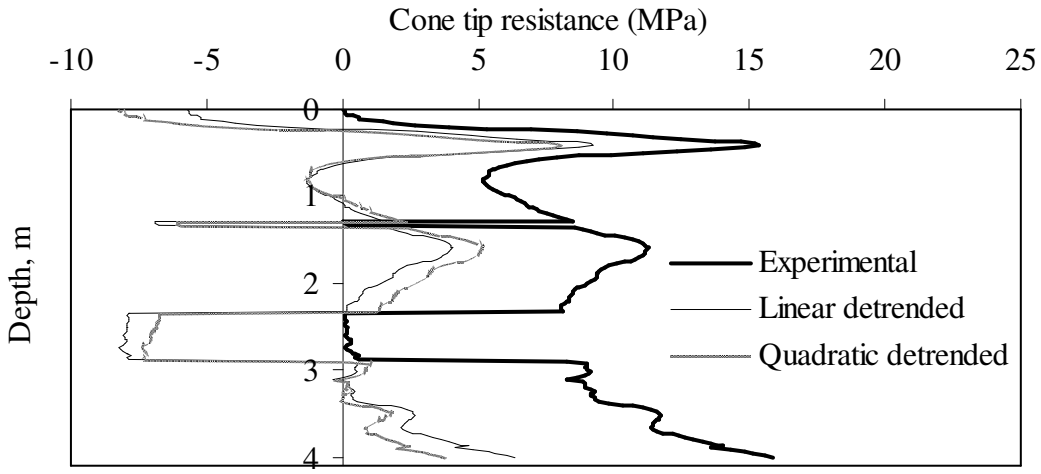

Figure 3.21. Cone tip resistance profile of CPT21 for settlement criterion

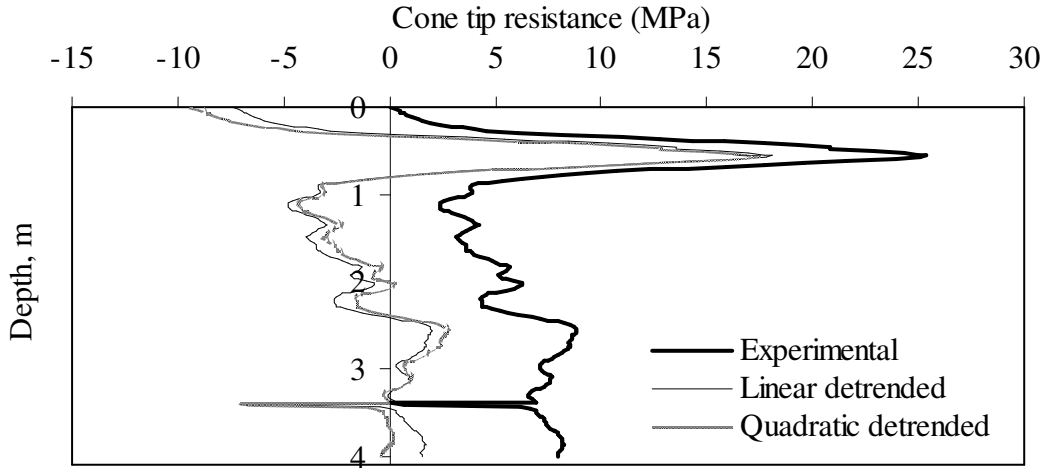

Figure 3.22. Cone tip resistance profile of CPT23 for settlement criterion

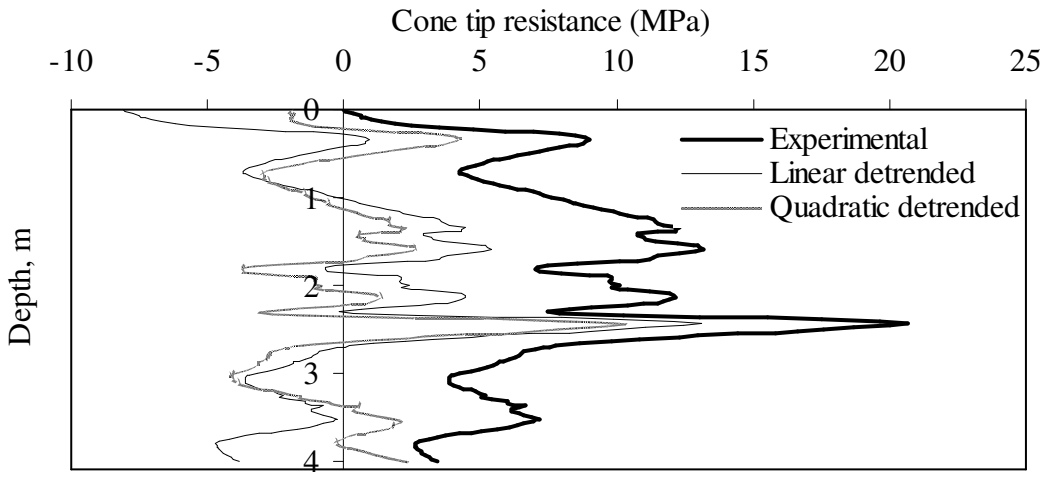

Figure 3.23. Cone tip resistance profile of CPT24 for settlement criterion

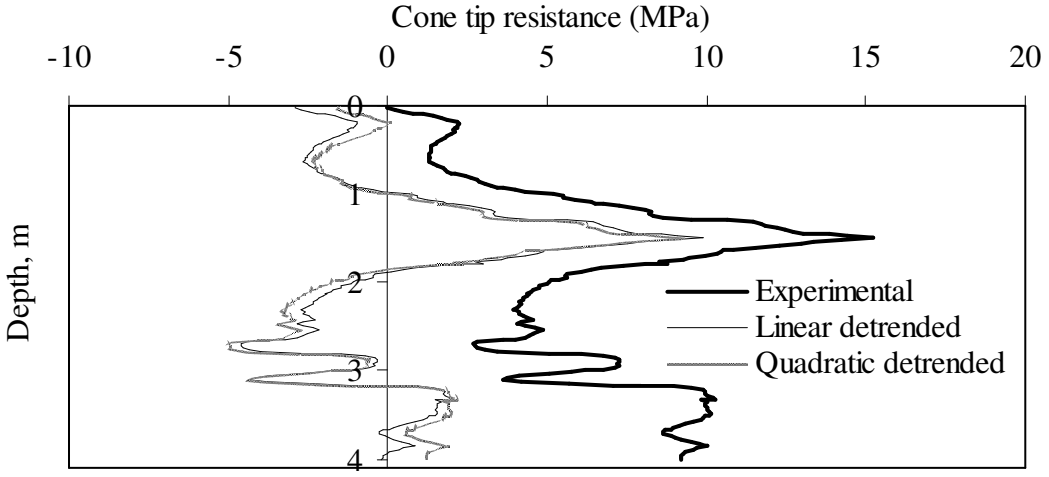

Figure 3.24. Cone tip resistance profile of CPT25 for settlement criterion

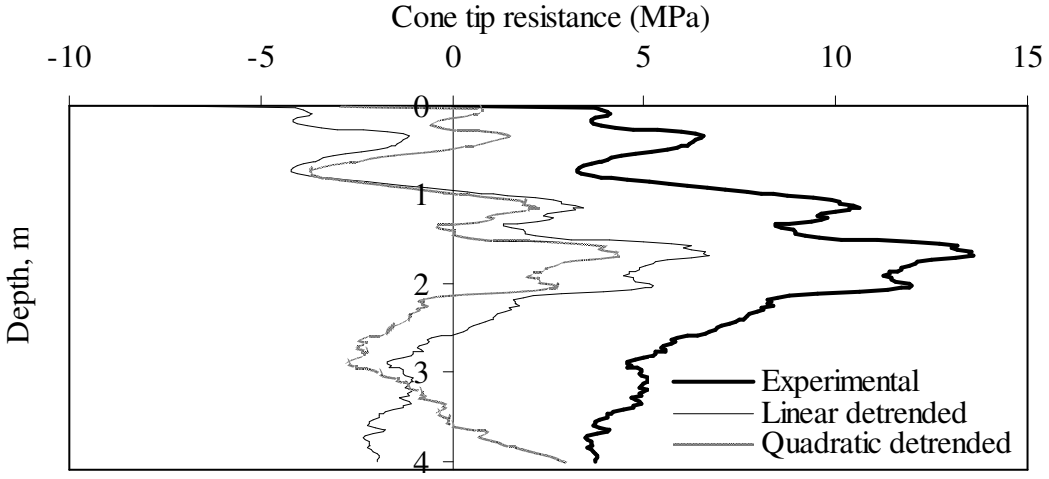

Figure 3.25. Cone tip resistance profile of CPT26 for settlement criterion

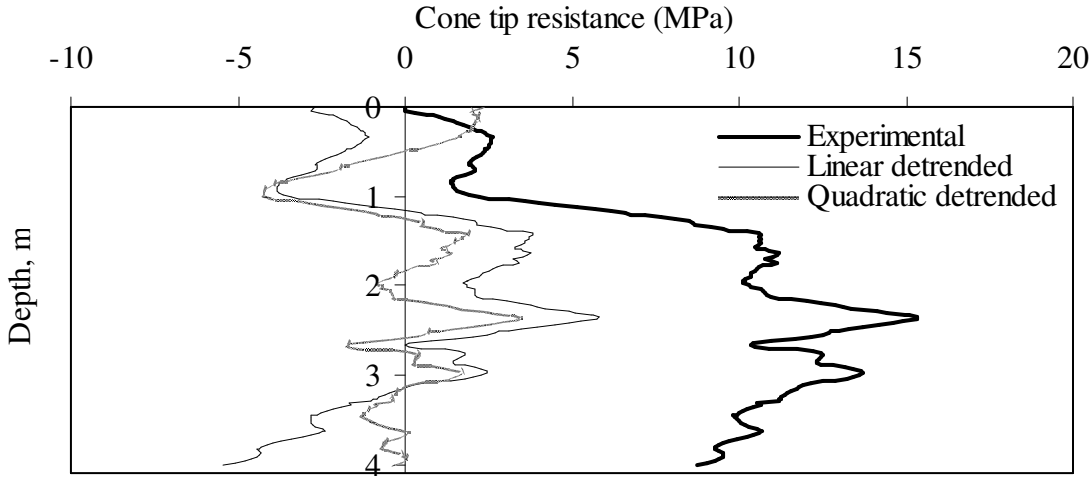

Figure 3.26. Cone tip resistance profile of CPT27 for settlement criterion

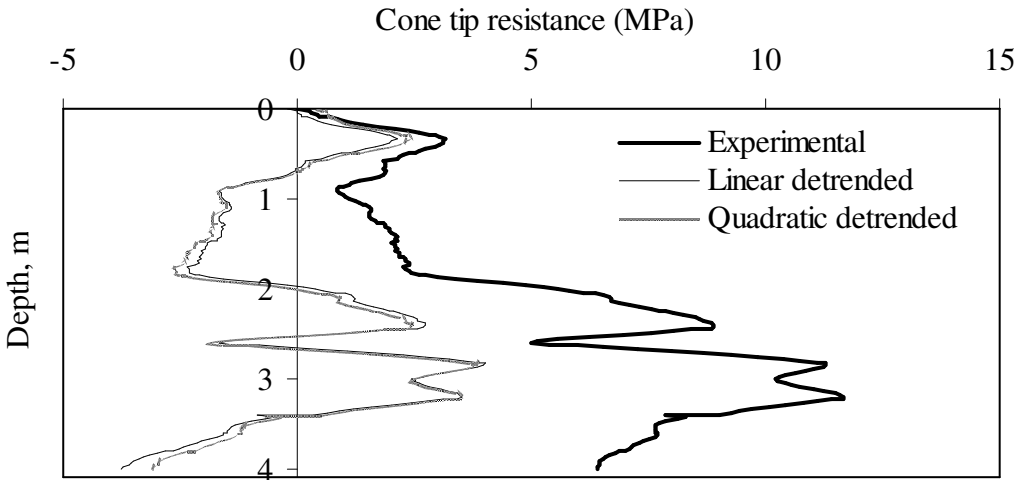

Figure 3.27. Cone tip resistance profile of CPT28 for settlement criterion

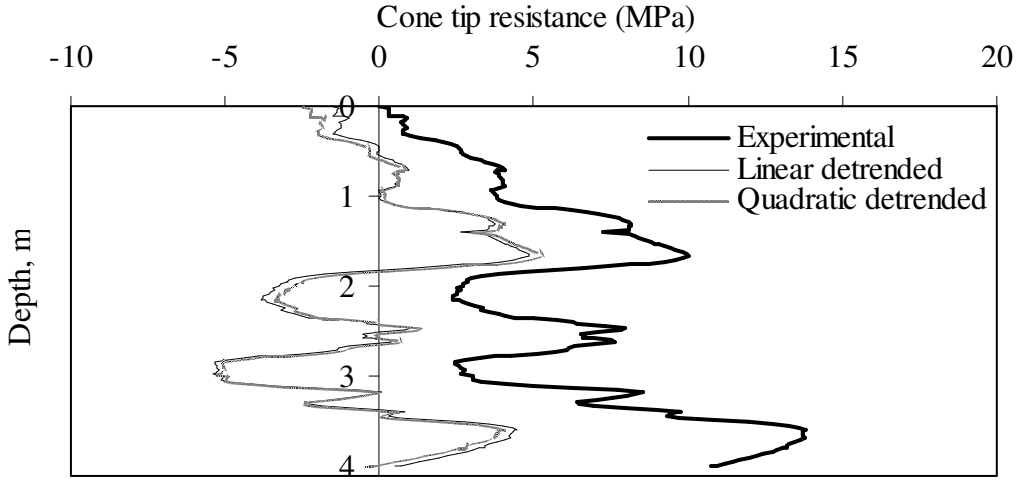

Figure 3.28. Cone tip resistance profile of CPT29 for settlement criterion

Table 3.4. Statistical parameters of cone tip resistance of cohesionless soil within the depth of zone of influence for settlement criterion (0-4 m)

	Mean (kPa)			Point standard deviation (kPa) (and point coefficient of variation (%))		
Sounding	Experi-mental q_c	Linear trend	Quadratic trend	Experi-mental q_c	Residuals off linear trend	Residuals off quadratic trend
CPT21	7610	7610	7610	5046 (66)	4602 (60)	3860 (51)
CPT23	6968	6968	6968	2505 (36)	1607 (23)	1578 (23)
CPT24	7689	7689	7689	4635 (60)	4334 (56)	3206 (42)
CPT25	6146	6146	6146	2810 (46)	1906 (31)	2359 (38)
CPT26	6745	6745	6745	2081 (31)	1579 (23)	1486 (22)
CPT27	8456	8456	8455	2045 (24)	2844 (34)	1650 (20)
CPT28	5189	5189	5189	2000 (39)	2311 (45)	2108 (41)
CPT29	5919	5919	5919	3980 (67)	2980 (50)	2702 (46)

3.4.1 Identification of statistically homogeneous layers

3.4.1.1 The Kendall's τ method

The results of the Kendall's τ for the cone tip resistance within significant zone of influence for settlement criterion are presented in Table 3.5.

Table 3.5. Results of the Kendall's τ for cohesionless data in settlement criterion

Data set	Kendall's τ corresponding to shear criterion (0-4 m) for the data		
	Experimental	Linear detrended	Quadratic detrended
CPT 21	0.28	0.09	0
CPT 23	0.28	0.31	0.24
CPT 24	-0.09	-0.05	0
CPT 25	0.39	0.05	0
CPT 26	-0.23	-0.09	0.01
CPT 27	0.41	-0.07	-0.11
CPT 28	0.58	-0.05	-0.05
CPT 29	0.49	0.05	0.04

3.4.1.2 Statistical run test

This hypothesis of statistical run test is checked for the CPT27 q_c profile, within 0 to 4 m, and the results are presented in Table 3.6. Similar to the results obtained from analysis of full q_c record, even in this case the 0.1 m section satisfies the stationarity hypothesis at 5% significance level.

Table 3.6. Statistical run test for cone tip resistance data of CPT27 (length of record=4m)

Length of section	Median of the sample (kPa)	Runs (r)	n	$r_{n;\,0.975}$	$r_{n;\,0.025}$	Hypothesis of Stationarity at 5% significance level
0.02 m	7200	36	100/2	42	61	Reject
0.08 m	45288.7	12	40/2	14	27	Reject
0.1 m	66404.17	15	33/2	11	22	Accept
0.2 m	207126.8	7	18/2	5	14	Accept

3.5 Analysis of autocorrelation characteristics for statistically homogeneous layers – cohesionless soil data

3.5.1 Detrending process

Though five methods are described and used in the above section to verify the statistical homogeneity of the data within the significant zones of influence for shear and settlement criteria, only the results obtained from the dual-window based method (Kulathilake and Um 2003) are used for further analysis. The data which show statistical homogeneity from the dual-window based method of hypothesis is verified for any trend in the data, and the same is removed before attempting to evaluate the autocorrelation characteristics. The cone tip resistance data within significant zone of influence for settlement criterion from CPT27 sounding is selected to show in detail the various calculations performed in the analysis.

3.5.2 Evaluation of autocorrelation distance

The autocorrelation function for the experimental cone tip resistance data of CPT27 sounding is obtained using the method of moments. The scale of fluctuation of cone tip resistance is computed from the sample autocorrelation function using the method of fitting. Based on the regression analysis, a theoretical triangular function is chosen to best fit the sample autocorrelation data for experimental cone tip resistance. The scale of fluctuation of cone tip resistance obtained from the above procedure is 1.37 m. To verify whether the data follows a trend, a linear detrending process followed by a quadratic detrending is applied on the experimental cone tip resistance data. A detrending process is restricted to a quadratic, as no more than a quadratic trend is generally used for geotechnical applications. The scales of fluctuation computed for linear detrended and quadratic detrended data using decomposition technique are 0.83 m and 0.39 m, respectively. Tables 3.7 and 3.8 present the scales of fluctuation obtained for the cone tip resistance data within significant depths of influence.

Table 3.7. Vertical scale of fluctuation of cone tip resistance of cohesionless soil from fitting method and Bartlett's limits within the significant zone of influence for shear failure criterion (0-2 m)

	Scale of fluctuation, δ_v (m) based on					
	Fitting method			Bartlett's limits		
Sounding	Experi-mental q_c	Residuals off linear trend	Residuals off quadratic trend	Experi-mental q_c	Residuals off linear trend	Residuals off quadratic trend
CPT21	0.20	0.20	0.20	0.16	0.16	0.16
CPT23	0.36	0.32	0.33	0.24	0.22	0.22
CPT24	0.36	0.24	0.25	0.41	0.18	0.18
CPT25	0.74	0.35	0.38	0.50	0.26	0.24
CPT26	0.90	0.23	0.23	0.68	0.16	0.16
CPT27	0.82	0.43	0.36	0.56	0.28	0.24
CPT28	0.22	0.24	0.19	0.18	0.2	0.16
CPT29	0.58	0.23	0.23	0.5	0.2	0.2

Table 3.8. Vertical scale of fluctuation of cone tip resistance of cohesionless soil from fitting method and Bartlett's limits within the significant zone of influence for settlement criterion (0-4 m)

	Scale of fluctuation, δ_v (m) based on					
	Fitting method			Bartlett's limits		
Sounding	Experi-mental q_c	Residuals off linear trend	Residuals off quadratic trend	Experi-mental q_c	Residuals off linear trend	Residuals off quadratic trend
CPT21	0.40	0.40	0.33	0.32	0.32	0.28
CPT23	0.35	0.35	0.32	0.26	0.26	0.24
CPT24	0.56	0.56	0.23	0.54	0.54	0.20
CPT25	0.68	0.64	0.63	0.50	0.46	0.46
CPT26	0.95	0.90	0.50	0.78	0.74	0.42
CPT27	1.37	0.83	0.39	1.02	0.74	0.28
CPT28	1.63	0.54	0.53	1.12	0.48	0.48
CPT29	0.58	0.48	0.48	0.46	0.36	0.36

The results show that the scales of fluctuation obtained from quadratic detrended data differs much from that produced by experimental and linear detrended data. Hence, a quadratic detrended data is considered as fairly trend-free, and the scale of fluctuation of 0.39 m is considered to represent the correlation characteristics of cone tip resistance data in settlement criterion. The autocorrelation characteristics are also evaluated using the differencing technique, which is another widely accepted detrending technique used in the data analysis (Bowerman and O'Connell (1983). Accordingly, the autocorrelation function is first computed using the first differenced data. It is seen from the results of differencing technique that the autocorrelation function dies down rapidly, and at lag 13 the autocorrelation coefficient attains a negative value. Figure 3.29 shows the experimental, quadratic detrended, and first differenced cone tip resistance data within the significant zone of influence for settlement criterion.

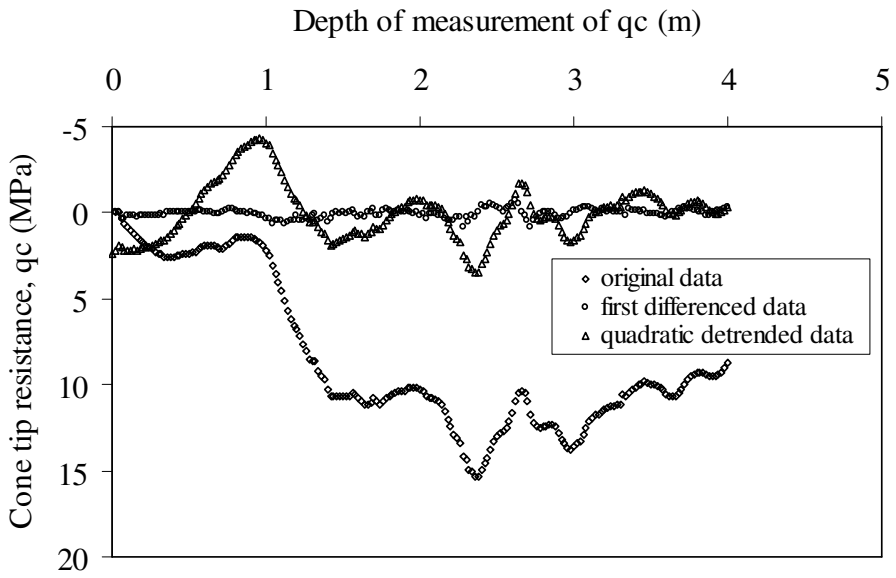

Figure 3.29. Comparison of experimental, quadratic detrended, and first differenced cone tip resistance data of CPT27 within 4 m zone of influence

Figure 3.30 shows the autocorrelation functions for the above data sets, along with theoretical exponential fit to first differenced data. The scales of fluctuation for the experimental and first differenced data are obtained as 1.2 m and 0.1 m. The autocorrelation distance for the experimental data set is 12 orders of magnitude higher than that produced by first differenced data. Hence, according to Bowerman and O'Connell (1983), this data set is fairly trend free after first differencing, and further differencing is not needed to apply on this data set. Intuitively the trend obtained from the above first differencing technique is compared with that obtained by conventional decomposition technique of trend removal, and observed that the detrending by first differencing corresponds to removal of a higher degree polynomial (>8) from the experimental data. The scales of fluctuation are evaluated using both the methods of detrending and the results are reported in Table 3.9.

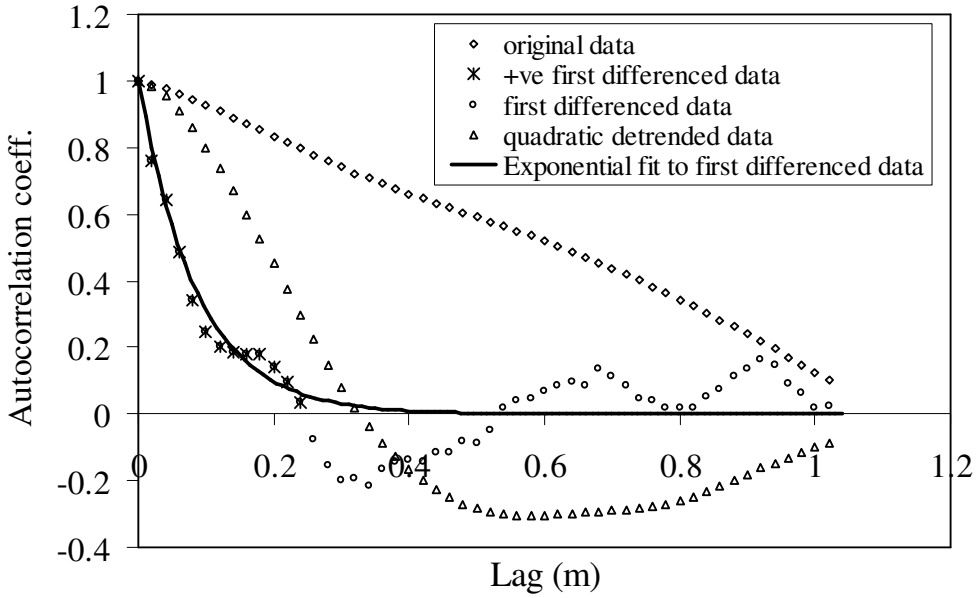

Figure 3.30. Comparison of autocorrelation coefficient for experimental, quadratic detrended, and first differenced cone tip resistance data of CPT27 within 4 m zone of influence

Table 3.9. Scale of fluctuation of cone tip resistance data (CPT27) by decomposition and first differencing techniques of trend removal

Method of trend removal	Type of data	Scale of fluctuation for data within significant zone of influence for shear criterion	Scale of fluctuation for data within significant zone of influence for settlement criterion
	Raw data	0.82 m (squared exponential fit)	1.37 m (triangular)
Decomposition technique	Linear detrended	0.43 m (squared exponential fit)	0.83 m (triangular)
	Quadratic detrended	0.36 m (squared exponential fit)	0.39 m (squared exponential fit)
First differencing technique		0.27 m (triangular)	0.1 m (exponential fit)

The scale of fluctuation is also evaluated based on the Bartlett's limits, given in Equation 2.22 superimposed on the sample autocorrelation function, and the results are presented in Tables 3.7 and 3.8 for experimental, linear detrended and quadratic detrended data for all the soundings (CPT21, CPT22-29) in both failure criteria. The method based on the Bartlett's limits produced satisfactory results and these results are close to those obtained from the fitting method. Jaksa et al. (1999) applied the

method based on the Bartlett's limits to evaluate the scales of fluctuation of cone tip resistance in Keswick clay, and observed that this method is simple and produces fairly good results and avoids the rigorous and time consuming fitting procedure.

3.6 Analysis of data on cohesive soil

Unlike in the case of cohesionless soils, the analysis is done for ultimate limit state alone, i.e., the data is analysed for allowable pressure considering shear failure criterion. The cone tip resistance data for C8 sounding is used in the present analysis. The results obtained from statistical analysis of cone tip resistance data of Keswick clay are presented in the following sections. Figures 3.31 shows the experimental, linear detrended, and quadratic detrended cone tip resistance for the data between 1.1 m-2.1 m. Table 3.10 presents the mean, point standard deviation, and coefficient of variation of experimental, linear detrended, and quadratic detrended cone tip resistance for two sets of data.

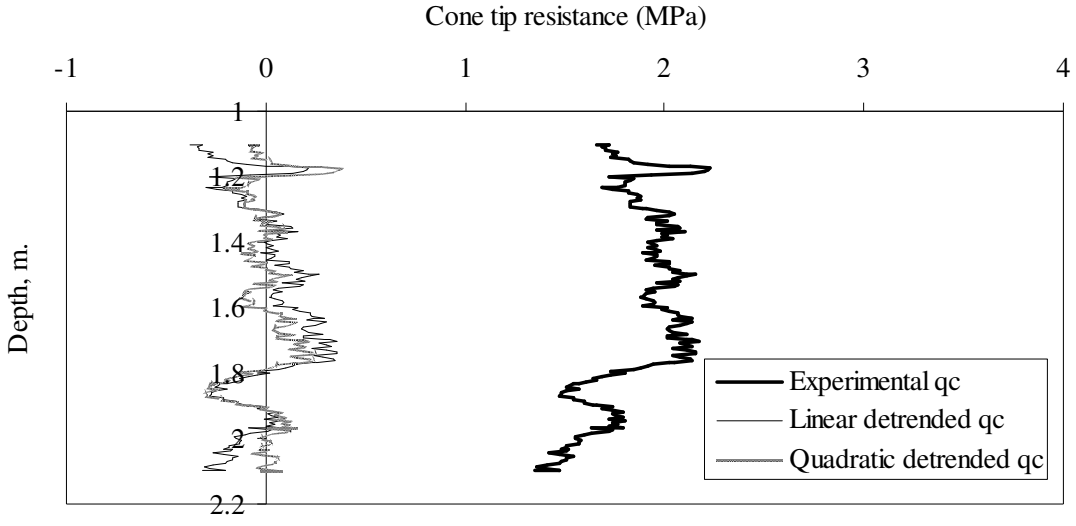

Figure 3.31. Experimental, linear detrended and quadratic detrended cone tip resistance profile of Keswick Clay (Profile C8 from 1.1 m to 2.1 m)

Table 3.10. Statistical parameters of cone tip resistance of cohesive soil (Keswick clay) within the depth of zone of influence for shear failure criterion

	Mean (kPa)			Point standard deviation (kPa) (and point coefficient of variation (%))		
Profile from	Experi-mental q_c	Linear trend	Quadratic trend	Experi-mental q_c	Residuals off linear trend	Residuals off quadratic trend
1.1-2.1 m	1853	1853	1853	213 (11)	183 (10)	125 (7)
1.1-5 m	1707	1707	1707	294 (17)	283 (17)	152 (9)

Jaksa (1995) observed that the Keswick clay at C8 sounding location is available at a depth of 1.1 m from ground surface, and the cone tip resistance (q_c) data are obtained up to a depth of 5 m at a vertical spacing of 5 mm. The analysis for this soil profile is focussed on the bearing capacity of foundation placed on the top surface of Keswick clay (depth of the foundation is 1.1 m). As mentioned above the significance depth of influence in shear failure criterion in clayey soils is 1B (or 1 m), where B is width of the strip footing. Hence, for evaluating the statistical parameters, the cone tip resistance within the depth of 1.1 m-2.1 m is analysed. However, from the previous experience it is noted that the number of pairs of data corresponding to each lag influences the evaluation of autocorrelation characteristics. Hence, two cone tip resistance data sets, one from 1.1 m to 2.1 m, which corresponds to significant depth of influence for shear criterion, and the other from 1.1 m to 5 m is used for the evaluation of autocorrelation characteristics for the Keswick clay. The objective of considering a large data base of cone tip resistance than that corresponds to significant zone of influence is to verify whether the autocorrelation characteristics show significant changes with the size of data set. The experimental, linear detrended and quadratic detrended cone tip resistance profiles within a depth range of 1.1 m to 5 m are shown in Figure 3.32.

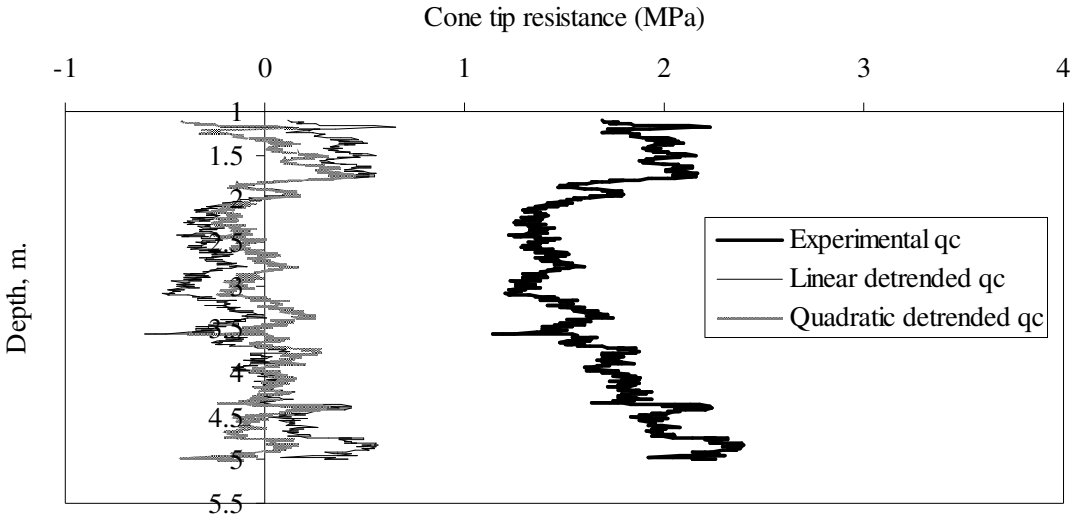

Figure 3.32. Experimental, linear detrended and quadratic detrended cone tip resistance profile of Keswick Clay (Profile C8 from 1.1 m to 5 m)

3.6.1 Verification of statistical homogeneity

3.6.1.1 Kendall's τ test

The cone tip resistance data within the Keswick clay is verified using the Kendall's test. The Kendall's τ for the experimental data of Keswick clay (data from 1.1-5 m) is obtained as 0.22. Since the Kendall's τ for experimental data is far from zero, a detrending process has been applied to make the data stationary. The τ values for linear detrended and quadratic detrended data are obtained as 0.1 and 0.03 respectively. Hence, from the Kendall's test hypothesis a quadratic detrending seems to produce a stationary data set for the data within 1.1 m-5 m. The same procedure is applied on the cone tip resistance data within 1.1-2.1 m data. The Kendall's τ for experimental, linear detrended, and quadratic detrended data are -0.24, 0.03, and 0.08 respectively.

3.6.1.2 Modified Bartlett's approach

To verify the statistical homogeneity of a soil profile using modified Bartlett test, the soil profile is first separated into statistically homogeneous and non-homogeneous

layers using the Bartlett test hypothesis. For preliminary statistically homogeneous layer demarcation, the Bartlett statistic profiles for cone tip resistance data of Keswick clay are evaluated with sampling segment widths of 0.1, 0.17 m, 0.35 m, and 0.5 m, as given in Figures 3.33 to 3.36, respectively. Since, the fluctuation of profiles differ quietly with segment lengths, and there are no proper guidelines on the selection of width of the segment for preliminary demarcation of statistically homogeneous layers, the entire Keswick clay profile (from 1.1 m to 5 m below ground level) is assumed as statistically homogeneous layer.

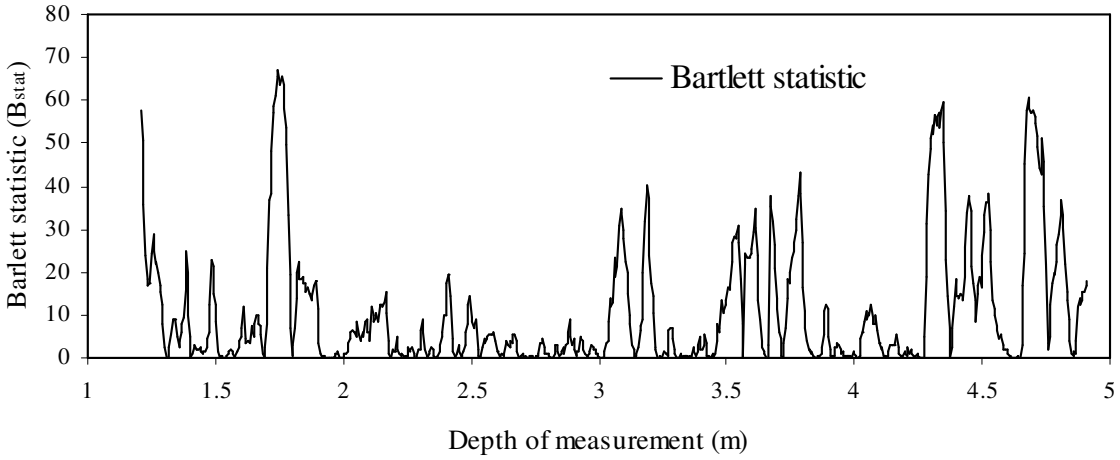

Figure 3.33. Bartlett statistic for cone tip resistance of Keswick clay with 21 data points in a segment (sampling segment size =0.1 m)

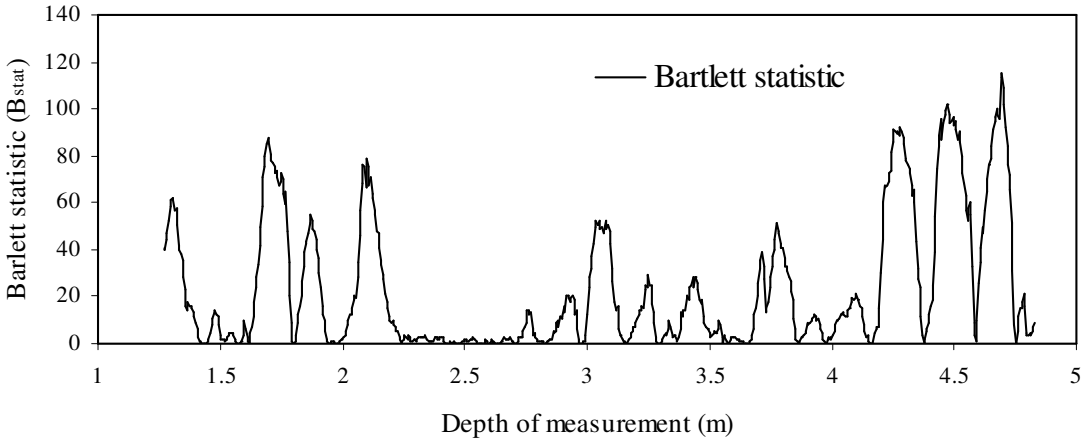

Figure 3.34. Bartlett statistic for cone tip resistance of Keswick clay with 35 data points in a segment (sampling segment size =0.17 m)

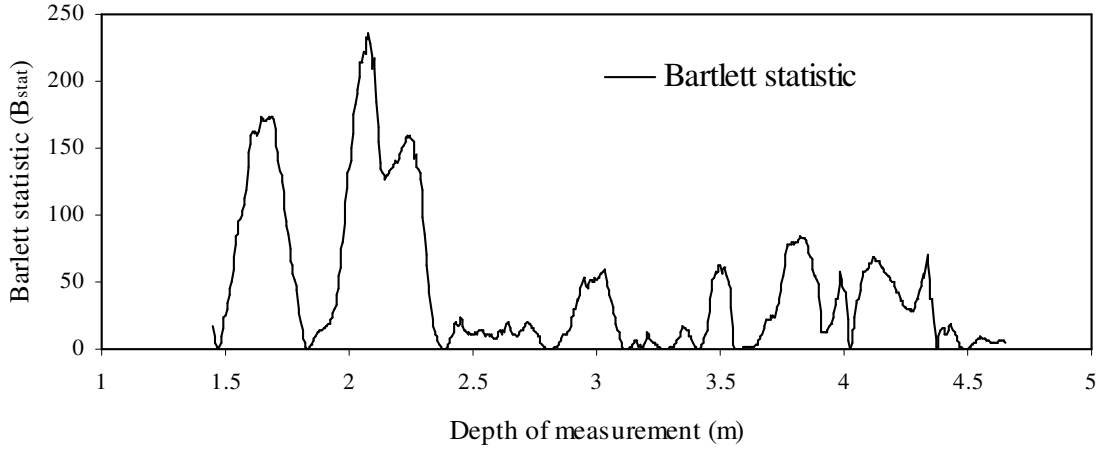

Figure 3.35. Bartlett statistic for cone tip resistance of Keswick clay with 71 data points in a segment (sampling segment size =0.35 m)

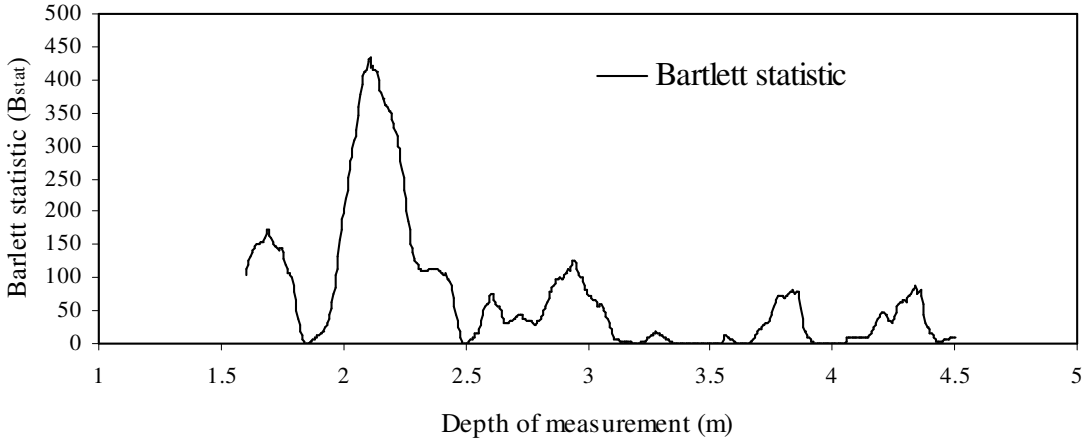

Figure 3.36. Bartlett statistic for cone tip resistance of Keswick clay with 101 data points in a segment (sampling segment size =0.50 m)

The autocorrelation functions using the experimental, linear detrended, and quadratic detrended cone tip resistance data of entire Keswick clay (1.1 m-5 m) are evaluated using method of moments. The corresponding scales of fluctuation are computed by using the fitting method. A triangular function is chosen to fit the experimental and linear detrended autocorrelation data, and a single exponential function for quadratic detrended data based on regression analysis. The scales of fluctuation for above data are 0.81 m, 0.72 m, and 0.17 m, respectively. It is clear from the results that the observed variations in scales of fluctuations are high among the experimental, linear detrended, and quadratic detrended cone tip resistance data. However, based on the

past observations that no higher than a quadratic detrending is generally used to remove the trend in the data (Jaksa et al. 1999), the scale of fluctuation obtained for the quadratic detrended data is chosen to represent the cone tip resistance of Keswick clay. Jaksa et al. (1999) also reported approximately the same value of scale of fluctuation (183 mm) for this data set. The non-dimensional factors described in section 2.4.2.4, viz., the number of points in one scale of fluctuation (k), normalised sampling length (I_1), and normalised segment length (I_2) are evaluated for the cone tip resistance data set of 1.1-5 m. The number of cone tip resistance data points in one scale of fluctuation (k) is 35. The sampling length (T) for this data set is 3.9 m. The normalised sampling length ($I_1=T/\delta=3.9/0.17$) is 22.94.

A precise Bartlett statistic profile is then evaluated. The length of the segment (half the sampling window) for evaluating sample variances is based on the recommended minimum number of data points of 10 in a segment. Phoon et al. (2003a) based on the results of many simulated soil profiles presented guidelines for selection of normalised segment length (I_2) to ensure the minimum number of data points in one segment suggested by Lacasse and Nadim (1996). Accordingly, if the number of data points in one scale of fluctuation (k) is equal to or more than 10, the normalised segment length (I_2) should be taken equal to 1. On the other hand, if the number of data points in one scale of fluctuation is between 5 and 10, I_2 should be taken equal to 2. For this data, as the value of k is more than 10, I_2 is taken equal to 1. Since, a theoretical exponential function better fits the quadratic detrended data, Equation 2.15 is used to compute the critical Bartlett statistic at 5% level of significance.

$$B_{crit}=(0.23\times34+0.71)\ln(22.94)+0.91\times34+0.23\approx58$$

The maximum Bartlett statistic (B_{stat}) given in Figures 3.33-3.36 for different segment lengths is higher than the B_{crit}, the Kendall's test hypothesis of statistical homogeneity is rejected at 5% significance level.

3.6.1.3 Dual-window based method

Figure 3.37 shows the results obtained from the dual-window technique for the cone tip resistance data of C8 profile from 1.1-5 m containing Keswick clay deposit. As per dual-window method of hypothesis, as the fluctuations in 'BC' distance profile are quite less and the whole profile can be treated as statistically homogeneous layer. Similar to the above procedure to evaluate the fluctuations in mean cone tip resistance, the same dual-window technique is used to compute the fluctuations of variance of cone tip resistance data with depth. The variance of cone tip resistance within each contiguous window is computed and the difference of the two variances at the interface between the upper and lower windows is evaluated, and the results are presented in Figure 3.37.

The results show that the fluctuations of variance are negligible, and the profile may be taken to consist of a single statistically homogeneous layer. Out of statistical run test, Bartlett test, and Dual-window based method (Kulathilake and Um 2003) discussed above to verify the statistical homogeneity of soil profiles, the first two methods test the fluctuations in variance of the data. However, the latter method verifies the fluctuations of mean. It is imperative for the data to satisfy both the above conditions, viz., the mean and variance should be constant with depth, for qualifying the condition of statistical homogeneity.

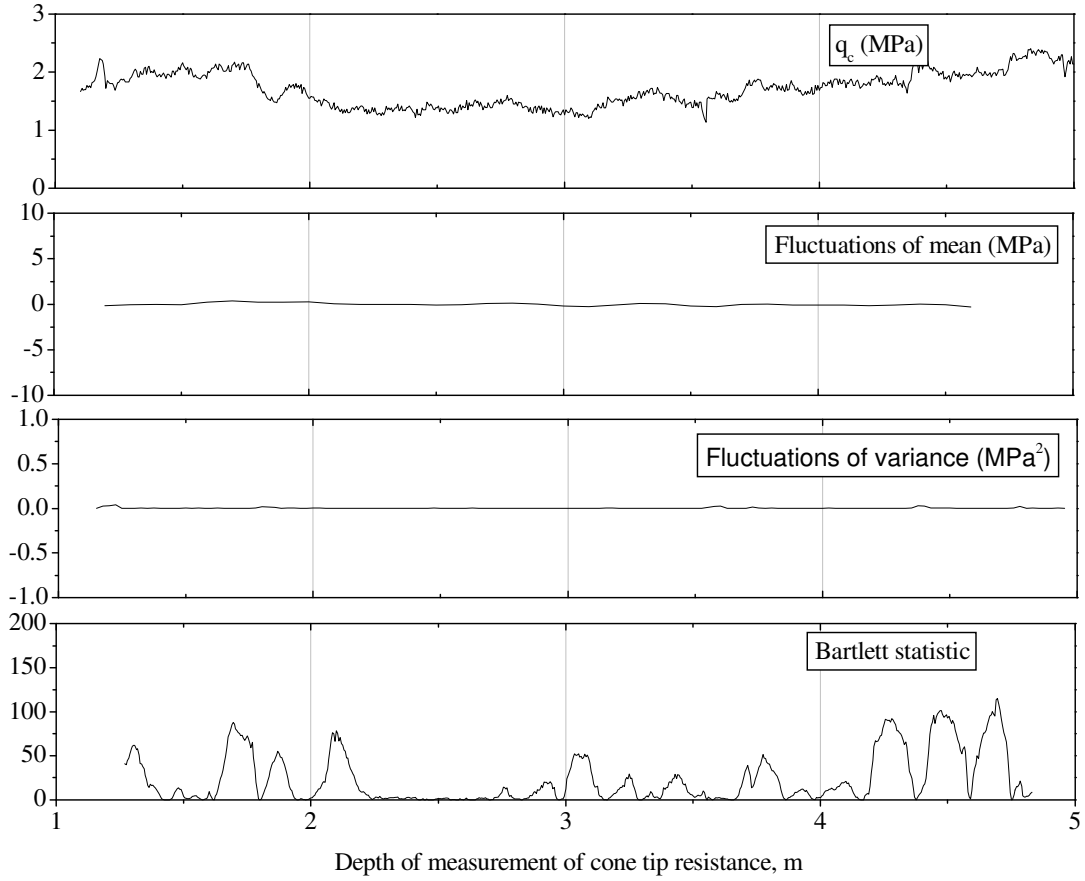

Figure 3.37. Cone tip resistance, Bartlett statistic (with segment length, W=0.17 m, 35 data points), fluctuations of mean and variance profiles for Keswick clay data (1.1 m-5 m)

3.6.2 Analysis of autocorrelation characteristics for statistically homogeneous layers-cohesive soil data

3.6.2.1 Detrending process

Once the statistical homogeneous layers are identified in a soil profile within the zone of influence, these cone tip resistance layers are checked for any deterministic trends within the data (Kulathilake and Um 2003). The trend in the data is generally estimated by regression analysis using either a linear or quadratic curve fitting (Phoon et al. 2003a), keeping in mind that the detrending process should produce a fairly stationary fluctuating component.

3.6.2.1.1 Method of fitting

Figure 3.38 shows the autocorrelation functions for experimental, linear detrended, and quadratic detrended cone tip resistance of Keswick clay from 1.1 m to 2.1 m. Based on regression analysis a theoretical exponential function is used to fit the sample autocorrelation functions for both experimental and linear detrended cone tip resistance data. However, a triangular function is chosen to fit the sample autocorrelation function obtained from quadratic detrended cone tip resistance. The computed scales of fluctuation are 0.24 m, 0.15 m, and 0.05 m respectively for experimental, linear detrended, and quadratic detrended cone tip resistance profiles.

The autocorrelation functions computed from method of moments for experimental, linear detrended, and quadratic detrended cone tip resistance data of complete Keswick clay profile, i.e., from 1.1 m to 5 m, are shown in Figure 3.39.

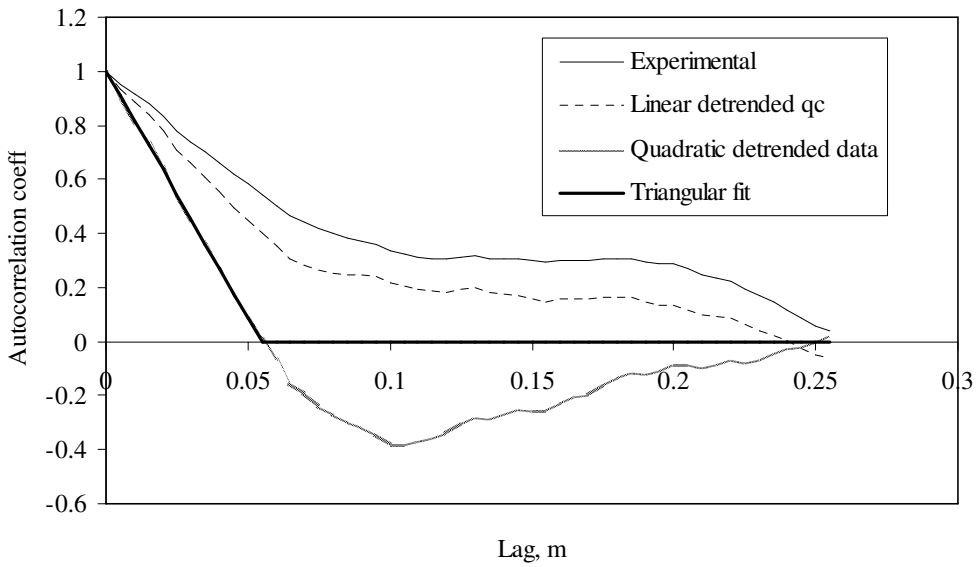

Figure 3.38. Autocorrelation function for experimental, linear detrended, and quadratic detrended cone tip resistance data for Keswick clay in C8 profile (1.1-2.1 m)

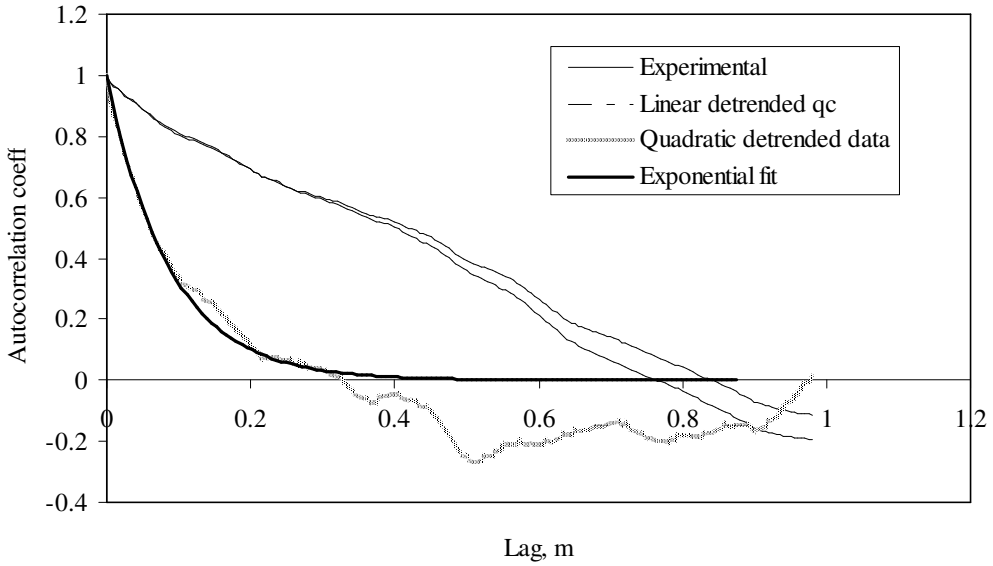

Figure 3.39. Autocorrelation function for experimental, linear detrended, and quadratic detrended cone tip resistance data for Keswick clay in C8 profile (1.1-5 m)

The computed scales of fluctuation are 0.81 m, 0.76 m, and 0.17 m for experimental, linear detrended, and quadratic detrended cone tip resistance data respectively. Figure 3.40 shows the autocorrelations functions evaluated for two sets of quadratic detrended cone tip resistance (1.1 m-2.1 m and 1.1 m-5 m) discussed above. The theoretical functions fitted to these sample autocorrelation functions are also shown in Figure 3.40. For the data set from 1.1 m-2.1 m, the theoretical best fit is triangular function and for the data set from 1.1 m-5 m, an exponential function best fits the positive values of sample autocorrelation data. The results are presented in Table 3.11. Comparing the scales of fluctuation evaluated for the quadratic detrended cone tip resistance for two different data sets, may reveal the fact that though both the data sets are statistically homogeneous, in the former case, the number of pairs of cone tip resistance data for the evaluation of autocorrelation characteristics are quite less at various lags than that for larger data set.

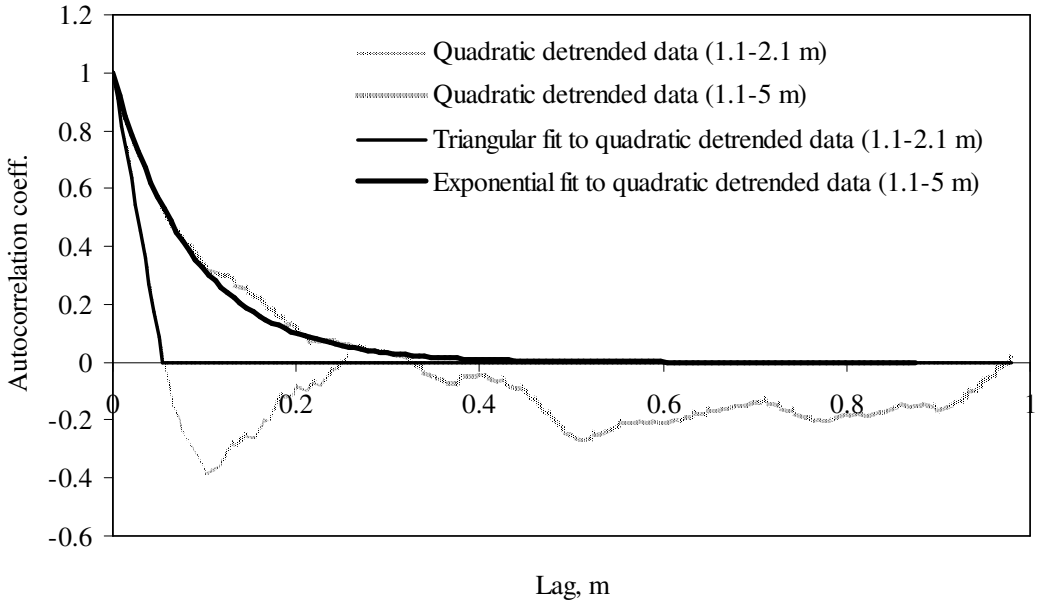

Figure 3.40. Autocorrelation functions for two sets of quadratic detrended cone tip resistance data (1.1 m-2.1 m and 1.1 m-5 m)

Table 3.11. Vertical scale of fluctuation and Bartlett's distance of cone tip resistance of cohesive soil (Keswick clay) within the depth of zone of influence for shear failure criterion

	Scale of fluctuation, δ_v (m)			Bartlett's distance, r_B (m)		
Profile from	Experi-mental q_c	Residuals off linear trend	Residuals off quadratic trend	Experi-mental q_c	Residuals off linear trend	Residuals off quadratic trend
1.1-2.1 m	0.24	0.15	0.05	0.24	0.20	0.05
1.1-5 m	0.81	0.72	0.17	0.77	0.68	0.21

3.6.2.1.2 Based on Bartlett limits

The data are also checked for autocorrelation characteristics using Bartlett's approximation. The Bartlett's limits given in Equation 2.22 are superimposed on the sample autocorrelation function computed for the detrended data, as shown in Figure 3.41. The Bartlett's distance (or scale of fluctuation) is the lag distance corresponding to the first intersection of Bartlett's limits and sample autocorrelation function. Hence, the Bartlett's distance for the two 'q_c' profiles, viz., 1.1 m-2.1 m and 1.1 m-5 m, are 0.05 m and 0.22 m, respectively. The evaluation of correlation characteristics based

on Bartlett's limits is easy to implement and avoids the rigorous exercise of fitting a theoretical function to sample autocorrelation data.

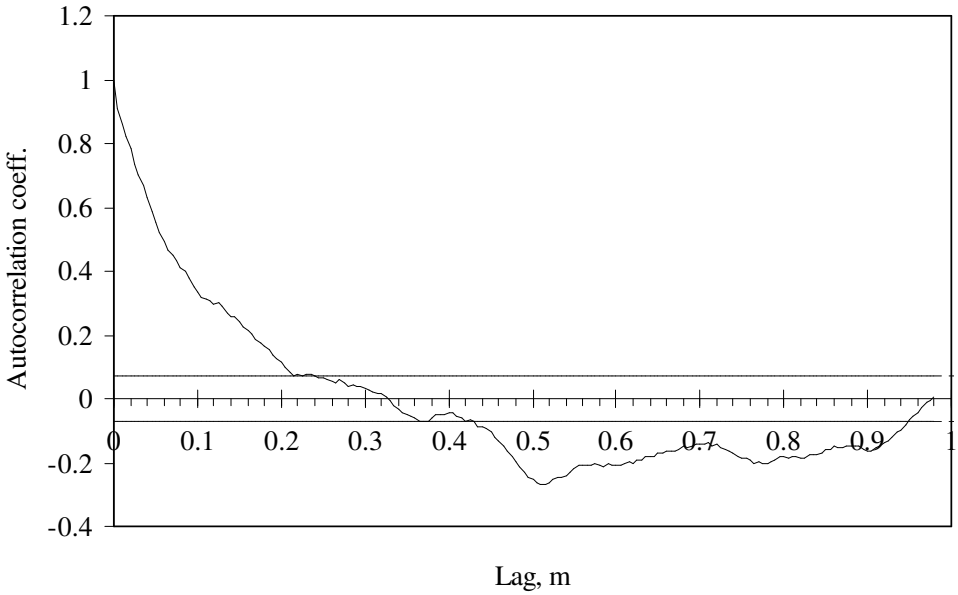

Figure 3.41. Bartlett's limits for evaluating the autocorrelation characteristics for Keswick clay in C8 profile (1.1-5 m)

3.7 Analysis of bearing capacity using CPT data of Indian origin

A representative cone tip resistance profile given in Figure 3.42 is used for probabilistic site characterization. The significant zone of influence for shear failure criterion for this case is taken equal to 1 m. However, the cone tip resistance data up to 3 m below ground level is analysed for verification of statistical homogeneous layers.

3.7.1 Identification of statistical homogeneous layers

The statistical homogeneity of the data set is verified using the Kendall's τ test as well as dual-window based method.

3.7.1.1 The Kendall's test

The Kendall's test on the experimental, linear detrended, and quadratic detrended 'q_c' data produces τ values of 1, -0.69, and -0.31 respectively. Based on the Kendall's test hypothesis the quadratic detrended cone tip resistance data can not be considered as statistically homogeneous, as it produces a τ value very much different from zero.

3.7.1.2 Dual-window based method

From the observations made in the previous sections, it is realized that the dual-window method of identification of statistical homogeneity is simple, and results obtained from this method may be more meaningful than the Kendall's method as the effect of spatial correlation characteristics are appropriately considered in the former method. Figure 3.42 also shows the results of the window-based method, wherein mean fluctuations of cone tip resistance and fluctuations of variance along the depth are verified.

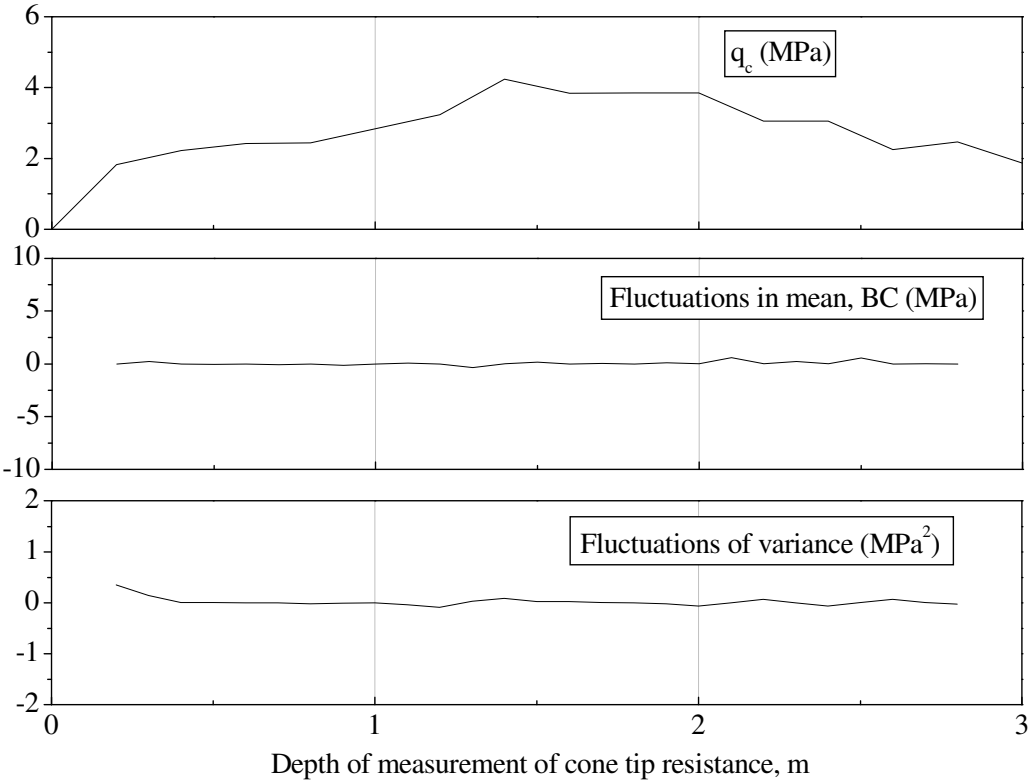

Figure 3.42. A typical cone tip resistance profile recorded at power plant site

The results clearly demonstrate that the data is fairly uniform in terms of mean cone tip resistance with negligible variations in the mean as well as variance of cone tip resistance. Hence, the data up to 3 m may be considered as a single statistically homogeneous layer. According to Kulathilake and Um (2003), once the statistical homogeneity is satisfied, the data are checked for the physically significant trend in the data within the statistical homogeneous layer of interest. The mean of the significant trend and coefficient of variation of fluctuations off the trend (CoV_w) within the significant depth of influence are evaluated.

The mean of the quadratic trend for the experimental cone tip resistance data within 1 m below base of the foundation resting on surface of the ground is obtained as 2 MPa. From the regression analysis, a quadratic detrending is found appropriate for this data. The coefficient of variation of quadratic detrended cone tip resistance (CoV_w) is obtained as 12.46%. By taking into consideration the observations made in section 3.6.2.1.1, the quadratic detrended data within the whole statistically homogeneous layer of 3 m length are used for the evaluation of autocorrelation characteristics, though the significant depth of influence is only 1 m. From the results obtained from the present study, it is recommended that when the depth of statistical homogeneous layer is more than the significant depth of influence, the autocorrelation characteristics should be evaluated using the entire data set within the statistical homogeneous layer. For example, as the statistically homogeneous layer for the cone tip resistance data at power plant site is found within 0 to 3 m from ground surface, though the significance depth is only 1 m below the ground surface, the entire cone tip resistance profile from 0 to 3 m is used for the evaluation of autocorrelation characteristics. This guarantees availability of sufficient number of pairs of data for the evaluation of correlation coefficient at every lag till N/4 lags, where N is number

of data points. Figure 3.43 shows the sample autocorrelation function evaluated from the quadratic detrended cone tip resistance data within 0-3 m. Based on the regression analysis, a theoretical squared exponential function shown in Table 2.1 is selected to fit the positive autocorrelation coefficient data, as shown in Figure 3.43.

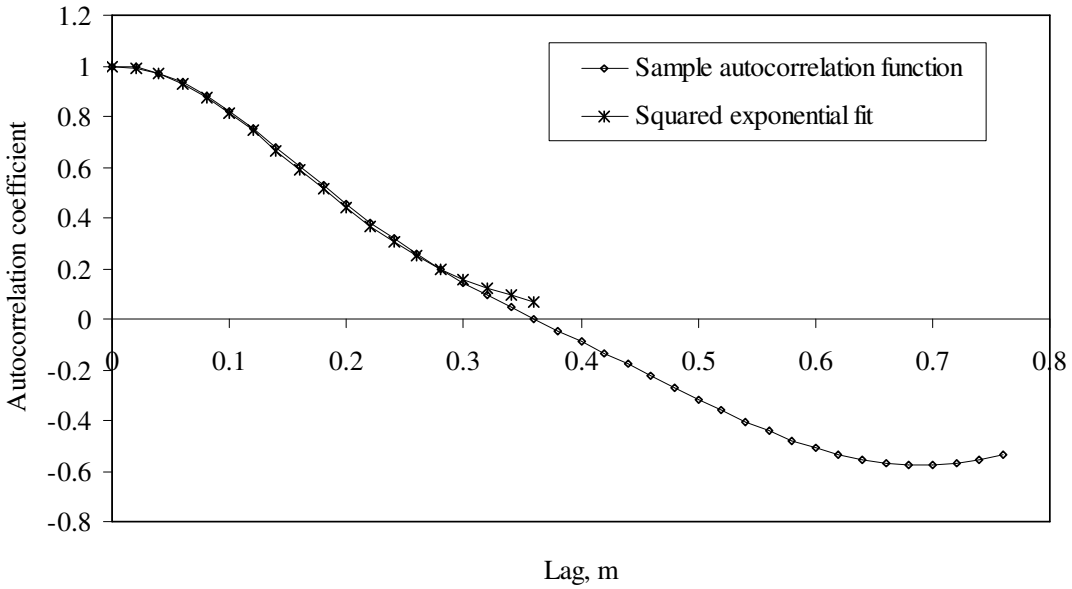

Figure 3.43. Theoretical fit to sample autocorrelation function of quadratic detrended cone tip resistance data at power plant site

The autocorrelation distance (c) and scale of fluctuation ($\delta = \sqrt{\pi}c$) for the quadratic detrended vertical cone tip resistance data of clayey soil of power plant site are obtained as 0.22 m and 0.39 m, respectively.

3.8 Conclusions

The following are the specific statistical properties for the three sites obtained using the methods and analysis described in this chapter.

The mean, coefficient of variation of inherent variability and scale of fluctuation of cone tip resistance of the CPT27 sounding at Texas A & M Riverside sand site are

8.46 MPa, 20%, and 0.36 m for shear failure criterion and 5.39 MPa, 29%, and 0.39 m for settlement criterion respectively.

The mean, coefficient of variation of inherent variability and scale of fluctuation of cone tip resistance for the Adelaide clay site are 1.86 MPa, 7%, and 0.17 m, respectively. These findings on scale of fluctuation are in agreement with Jaksa et al. (1999).

The mean, coefficient of variation of inherent variability and scale of fluctuation of cone tip resistance for the power plant site are computed approximately as 2 MPa, 12.5% and 0.4 m respectively. These computed scales of fluctuation fall within the observed range of vertical scales of fluctuation of cone tip resistance, viz., 0.1 m to 2.2 m (Phoon and Kulhawy 1999a).

The following are the general observations with regard to methods of analysis.

The mean value of soil property may be obtained as statistical mean of soil point property, which is same as the mean of the trend for the data, as described by Phoon and Kulhawy (1999a).

In the evaluation of autocovariance function, the sum of the product of residuals off the trend separated by a lag should be averaged over the number of pairs of data at the respective lags as suggested by Keaveny et al. (1989), Fenton (1999b), Kulathilake and Um (2003), and Phoon et al. (2003a), than that averaged over the total number of data points, as suggested by Jaksa et al. (1999).

The data of stationary and non-stationary layers should be dealt separately for the evaluation of point variance of the soil property.

The choice of trend function is still a subjective judgment of the engineer and care should be taken to choose the same for the data analysis.

The results obtained from the Kendall's τ statistic show that a second order detrending on the experimental data produces fairly stationary data.

In the case of statistical run test, the test statistic is highly sensitive to the length of the section, and hence in the present form it is not suitable to test the statistical homogeneous layers.

The demarcation of the total soil profile into stationary and non-stationary layers by the Bartlett statistic approach is useful. However, this method does not suggest any guidelines on the cut-off values of the Bartlett statistic, which helps in distinguishing stationary and non-stationary layers within a soil profile.

The modified Bartlett statistic produces satisfactory results. However, the test statistic is sensitive to many parameters, such as window length, scale of fluctuation, etc.

The dual-window based method is simple and straightforward for the identification of statistical homogeneous layers within a soil profile. However, there is no explicit limit on the peak value of 'BC' distance, the value above which a soil profile can be treated as statistically heterogeneous layer. In the present study, it is suggested that the boundaries may be identified quantitatively at locations where the 'BC' distance crosses the mean$\pm$1.65$\times$standard deviation of 'BC' distance fluctuations within the same profile.

Chapter 4

SHALLOW FOUNDATIONS RESTING ON COHESIONLESS SOIL

4.1 Introduction

The geotechnical community has recognized the importance of site characterization long back and many failures of the structures have been attributed to the inadequate geotechnical site characterization (Morgenstern 1997). From the compilation of many such failures it is noted that the causes of majority of the geotechnical failures are not because of erroneous analysis and design but attributed to poor site characterization. In this chapter the allowable pressure of shallow foundations resting on cohesionless soil deposit is analysed in probabilistic framework taking into consideration the complete probabilistic soil characteristics evaluated from the detailed investigation in Chapter 3.

4.2 Description of the present study

Reliability analysis of allowable pressure of strip footing of width 1 m resting on surface of cohesionless soil deposit and subjected to axial loading is studied in this chapter using vertical cone tip resistance (q_c) data, obtained from the Texas A & M University riverside campus sand site. These data were reported at regular intervals of 2 cm. Figure 4.1 shows a typical vertical soil profile of the site. The ground water table was observed at deeper depths, and its effect is assumed insignificant. In this study, the cone tip resistance alone is treated as variable parameter.

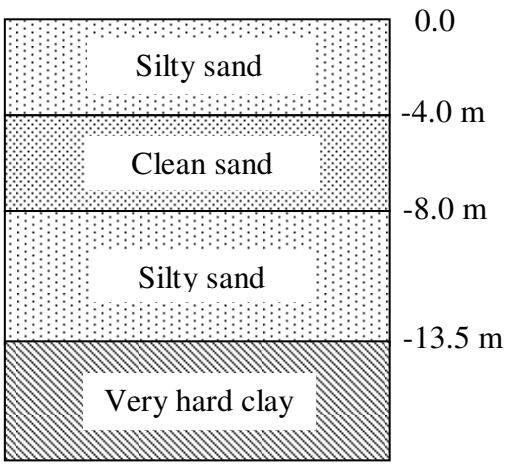

Figure 4.1. Soil profile at the Texas A & M Riverside sand site

Figure 4.2 shows the classification of cohesionless soils based on cone tip resistance (q_c). The variation of friction angle (ϕ) of soil with respect to the cone tip resistance is also shown in the same figure. The 'q_c' data of CPT27 is superimposed on the figure and it may be seen that the majority section of the profile is classified as medium, though intermittent lenses of dense material can also be seen.

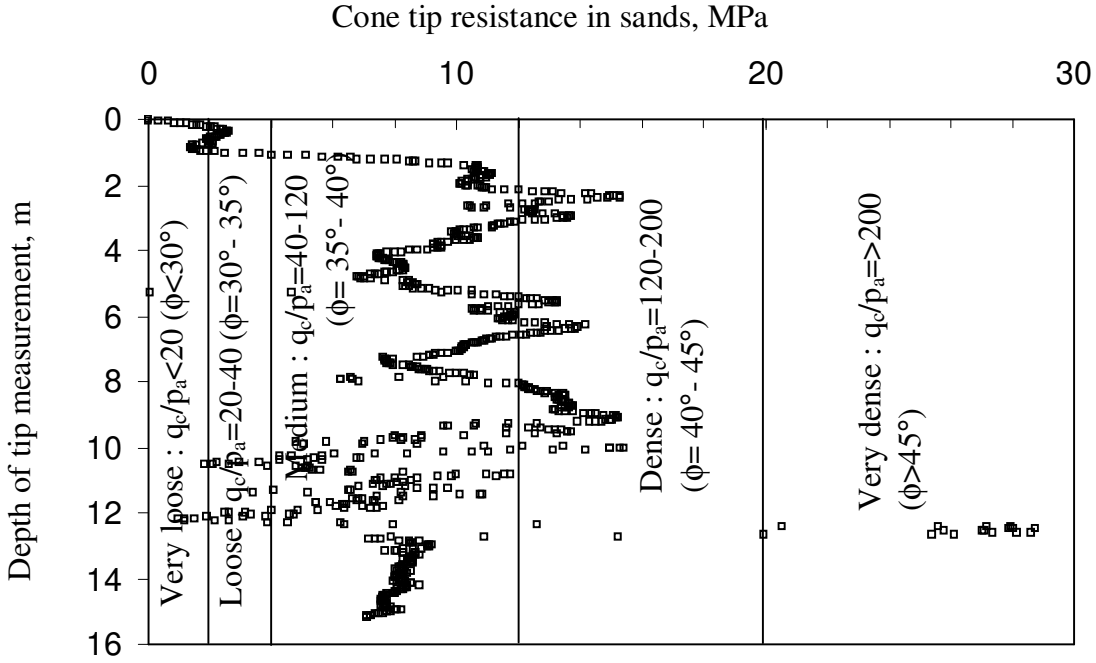

Figure 4.2. Classification of cohesionless soil based on cone tip resistance data

The zone of influence in shear criterion is taken as the depth at which failure surfaces form in the soil, represented by failure zones. This depth for a strip footing resting on cohesionless soil is taken as 2B (i.e., 2 m) below the base of footing. For settlement criterion for the strip footing resting on cohesionless soil, this significant zone of influence is taken as 4B below the base of the strip foundation, where the effect of applied pressure on the induced strains in insignificant.

The cone tip resistance record of CPT27 sounding is checked for statistical homogeneity with window based method (Kulathilake and Um 2003) in Chapter 3, and it is found from the results that the cone tip resistance data up to 10 m from the ground surface may be as statistically homogeneous. The results of the statistical analysis are presented in Tables 3.1 and 3.7 for cone tip resistance in shear criterion. From Table 3.1, the mean cone tip resistance of CPT27 sounding within the significant depth of influence for shear criterion is 5390 kPa. The standard deviation and coefficient of variation of quadratic detrended cone tip resistance data are 1567 kPa and 29% respectively. The autocorrelation distance and scale of fluctuation of cone tip resistance (Table 3.7) within the significant zone for shear failure criterion is evaluated as 0.20 m and 0.36 m respectively. Similarly, the statistical parameters of cone tip resistance used for settlement criterion, i.e., within 0-4 m, are presented in Tables 3.4 and 3.8. From 3.8, the scale of fluctuation of quadratic detrended cone tip resistance used in settlement analysis is 0.39 m.

In the present work, the analysis of allowable pressure of foundation is carried out in the following three ways.

1. Allowable pressure neglecting the uncertainty in the design parameters, generally referred to as deterministic approach.

2. Analysis incorporating the uncertainty in design parameters in terms of only first two moments (i.e., mean and standard deviation), neglecting the effect of spatial correlation and spatial averaging. This approach is hereafter referred to as simple probabilistic approach.

3. Analysis considering the effect of mean, standard deviation, correlation structure of the cone tip resistance, and the spatial averaging on the design parameters. This approach is referred to as advanced probabilistic method.

The effects of spatial variability and spatial averaging distance on the predicted allowable pressure of shallow strip footing based on both shear failure criterion and settlement criterion are studied in a rational approach using the 1-D random field theory.

In all the three approaches described above, the bearing capacity of shallow foundations is computed indirectly from the in-situ cone tip resistance data, in two phases. In the first phase of analysis, the in-situ cone tip resistance data within the significant zone of influence is used to evaluate the average effective friction angle of soil along the failure surface. A correlation model given by Equation 4.1 is used to transform the in-situ cone tip resistance to a representative mean effective friction angle (Kulhawy and Mayne 1990). The correlation model shown in Equation 4.1 was developed for 20 data sets, containing 633 data points obtained from laboratory calibration chamber tests on reconstituted sand in normally consolidated and overconsolidated states using triaxial compression effective stress friction angle $\left(\overline{\phi}_{TC}\right)$ and the normalized cone tip resistance $\left(\frac{q_c / p_a}{\sqrt{\overline{\sigma}_{vo} / p_a}}\right)$ parameters. Where q_c, p_a, and $\overline{\sigma}_{vo}$ are cone tip resistance, atmospheric pressure, and effective overburden pressure,

respectively. The coefficient of determination and standard deviation of this model were evaluated as 0.64 and 2.8˚, respectively (Kulhawy and Mayne 1990). It was observed that the mineralogy, particle shape, compressibility, and percent fines largely account for the range of $\bar{\phi}_{TC}$ at any normalized q_c value. The range of $\bar{\phi}_{TC}$ values used in this calibration model varies from 28˚ to 52˚.

$$\bar{\phi}_{TC} = 17.6 + 11.0 \log_{10}\left(\frac{q_c / p_a}{\sqrt{\bar{\sigma}_{vo} / p_a}}\right) \tag{4.1}$$

In the second phase, the bearing capacity factors, and hence the bearing capacity are evaluated from the mean effective friction angle computed in the first phase of analysis using the equations 4.2, 4.3, and 4.4 (Terzaghi 1943; Meyerhof 1951, 1963).

$$q_u = \gamma D_f N_q + 0.5\gamma B N_\gamma \tag{4.2}$$

$$N_q = \exp(\pi \tan\phi)\tan^2\left(45 + \frac{\phi}{2}\right) \tag{4.3}$$

$$N_\gamma = (N_q - 1)\tan(1.4\phi) \tag{4.4}$$

where γ, D_f, B, N_q, N_γ, and ϕ are the unit weight of soil, depth, width of foundation, bearing capacity factor for surcharge, bearing capacity factor for self weight of soil, and friction angle respectively. The friction angle (ϕ) used in Equations 4.3 and 4.4 are taken equal to the triaxial compression effective friction angle $\bar{\phi}_{TC}$, obtained in Equation 4.1.

Similar to the procedure used for bearing capacity analysis in shear criterion, the settlement of shallow foundations is also evaluated in two phases. In the first phase, the elastic modulus (E) is computed from the measured cone tip resistance (q_c), and in the second phase, the settlement of the footing is computed using the elastic modulus

obtained in the first phase along with other properties. Equation 4.5 is widely used for computing the settlement of shallow foundations resting on cohesionless soil deposit (Schmertmann 1970; Schmertmann et al. 1978; Lee and Salgado 2002). For settlement calculations using Equation 4.5, the entire zone of influence is divided into number of sublayers.

$$s = C_1 C_2 \left(q_b - \sigma_v^{'}|_d\right) \sum \left(\frac{I_{zi} \Delta z_i}{E_i} \right) \tag{4.5}$$

$$C_1 = 1 - 0.5 \left(\frac{\sigma_v^{'}|_d}{q_b - \sigma_v^{'}|_d} \right) \tag{4.6}$$

$$C_2 = 1 + 0.2 \log \left(\frac{t}{0.1 t_R} \right) \tag{4.7}$$

where δ, C_1, C_2, q_b, $\sigma_{v|d}^{'}$, I_{zi}, Δ_{zi}, E_i, t, and t_R are settlement of footing under applied pressure, embedment factor, creep factor, applied pressure at footing base level, effective vertical pressure at the foundation base level, average strain influence factor in each sublayer, thickness of sublayer, elastic modulus of soil within each sublayer, time period for which settlements are required to be computed, and reference time, usually one year, respectively.

Figure 4.3 shows an approximated strain influence factor diagram, developed from observed vertical strain variations below a loaded footing (Schmertmann 1970; Schmertmann et al. 1978). Lee and Salgado (2002) summarized the most commonly used correlations between the elastic modulus (E) and cone tip resistance (q_c) suggested by Schmertmann et al. (1978) and Robertson and Campanella (1989).

Equation 4.5 accounts for both immediate as well as long term creep effects. Although the settlements in cohesionless soils due to applied pressure are regarded as immediate, observations also show a long-term creep (Schmertmann 1970;

Schmertmann et al. 1978). The long term creep can be approximated by a factor, C_2, computed from Equation 4.7, which when multiplied with immediate settlements gives the total settlements at the end of design period of the foundation. Figure 4.4 shows the resulting variation of creep factor with elapsed time (Schmertmann 1970; Schmertmann et al. 1978).

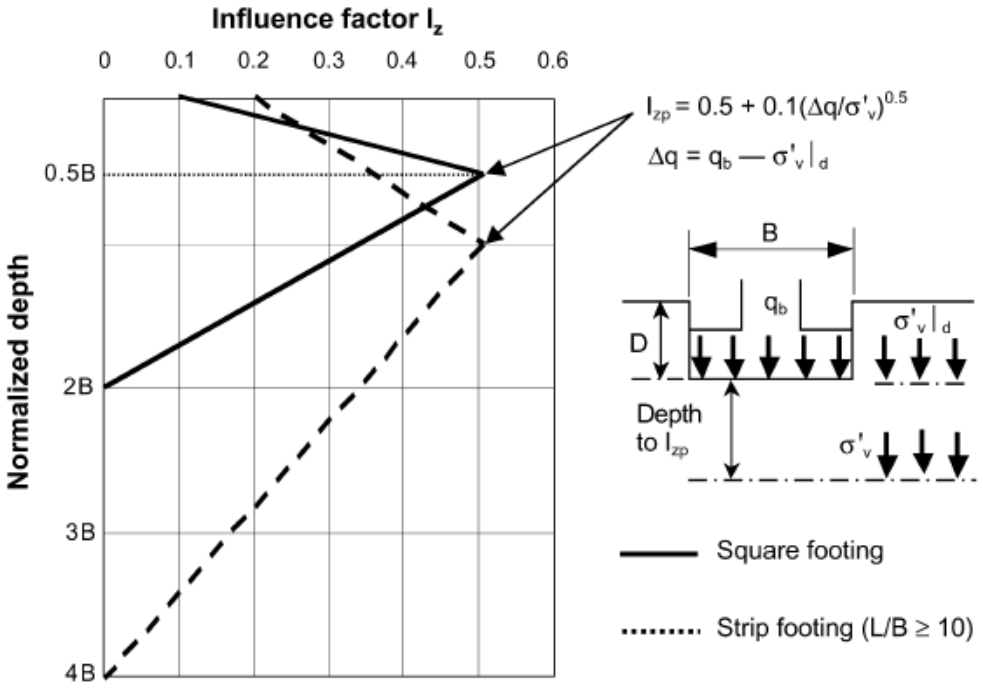

Figure 4.3. Variation of influence factor I_z with depth below base of foundation (Schmertmann et al. 1978; reproduced from Lee and Salgado 2002)

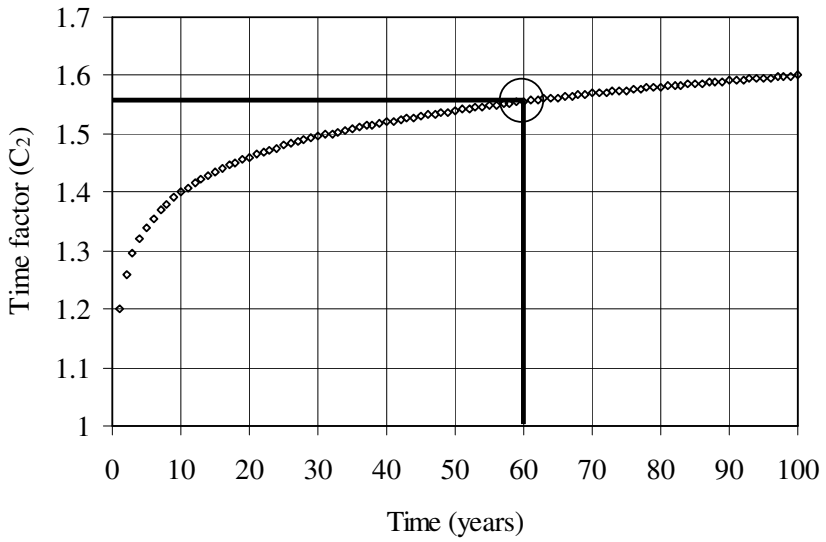

Figure 4.4. Variation of creep factor (C_2) with time used in the analysis (Schmertmann et al. 1978)

It is clear from Figure 4.3 that the peak influence factor occurs at 0.5B and 1B below base of foundation in case of square and strip footing respectively. In physical terms, stiffness of soil increases with depth due to higher overburden and confining pressures, and the intensity of stresses induced by the applied pressures reduce with the depth because of larger area for load dispersion. The above statement on accumulation of strain holds good except for the zone which is very close to the foundation base (Schmertmann 1970; Schmertmann et al. 1978; Lee and Salgado 2002).

4.3 Results of the analysis

4.3.1 Deterministic analysis of allowable pressure

4.3.1.1 Shear criterion

The mean effective friction angle $\left(\bar{\phi}\right)$ computed from Equations 4.1 using the mean cone tip resistance (q_c=5390 kPa) within the significant depth of influence for shear criterion is obtained as 40.7°. The ultimate bearing pressure, q_u, evaluated using Equations 4.2, 4.3, and 4.4 for surface footing based on mean friction angle is 967 kPa (density of sand=18 kN/m^3, N_q=70.8, N_γ=107.4). Factors of safety in the range of 2-3 are generally used on ultimate bearing pressure for design of onshore foundations to account for various sources uncertainty in the estimation of characteristic soil properties representative of in-situ conditions in a lumped manner (Meyerhof 1982; Cherubini 2000). An allowable bearing pressure (p_{shear}) of 322 kPa is obtained using a factor of safety of 3 on ultimate bearing pressure.

4.3.1.2 Settlement criterion

The entire zone of influence is divided into four number of layers. The cone tip resistance data averaged over depths of 0-1 m, 1 m-2 m, 2 m-3 m, and 3 m-4 m are 1764 kPa, 8955 kPa, 12560 kPa, and 10560 kPa respectively. The creep settlement calculations are performed over a period of 60 years, as all the general buildings and structures are designed for a life span of 50-60 years (SP 7(1):1983). From Equation 4.5, the back-calculated footing pressures (q_{b25}, q_{b40}, q_{b50}) to achieve a total settlement of 25 mm, 40 mm, and 50 mm are 142 kPa, 213 kPa, and 257 kPa respectively using the following transformation equation relating the cone tip resistance and elastic modulus of sands. The peak influence factors corresponding to above applied pressures are 0.78, 0.84, and 0.88 respectively.

$$E = 3.5q_c \tag{4.8}$$

4.3.1.3 Allowable pressure

The allowable pressure of the footing (P_{all}) based on above two performance criteria is taken as the lesser of P_{shear} and q_{b25} in case of 25 mm allowable settlement, P_{shear} and q_{b40} in case of 40 mm allowable settlement, and P_{shear} and q_{b50} in case of 50 mm allowable settlement. The results obtained from the deterministic analyses are shown in Table 4.1. The results show that at all the three settlement levels (25 mm, 40 mm, and 50 mm settlements), the allowable pressure in shear criterion is observed more than that in settlement criterion. Hence, the allowable pressures of the foundations from deterministic approach are 142 kPa, 213 kPa, and 257 kPa for 25 mm, 40 mm, and 50 mm allowable settlements respectively.

Table 4.1. Results obtained from deterministic analyses using mean values of q_c

Safe bearing pressure, kPa with FS=3 (Shear failure criterion)	Safe pressure (kPa) based on settlement criterion for footing settlement of			Allowable pressure of the footing based on both failure criteria (kPa)		
322 (=967/3)	25 mm	40 mm	50 mm	FS=3		
				25 mm	40 mm	50 mm
	142	213	257	142	213	257

The above results support the well recognized fact that the allowable pressure of footings in cohesionless soils is generally controlled by settlement criterion, except for very narrow footings.

4.3.2 Probabilistic analysis

4.3.2.1 Shear failure criterion

For the transformation equation shown in Equation 4.1, Phoon and Kulhawy (1999b) derived the mean, point standard deviation, point coefficient of variation, and coefficient of variation of spatial average, as given in Equations 4.9 to 4.12 respectively.

$$m_{\xi d} \approx 17.6 + 11.0 \log_{10}\left(\frac{t / p_a}{\sqrt{\overline{\sigma_{vo}} / p_a}}\right) \tag{4.9}$$

$$SD^2_{\xi d} \approx 22.8\left(CoV_w^2 + CoV_e^2\right) + SD_\varepsilon^2 \tag{4.10}$$

$$CoV^2_{\xi d} \approx \frac{22.8\left(CoV_w^2 + CoV_e^2\right) + SD_\varepsilon^2}{m^2_{\xi d}} \tag{4.11}$$

$$CoV^2_{\xi a} \approx \frac{22.8\left(\Gamma^2(L) CoV_w^2 + CoV_e^2\right) + SD_\varepsilon^2}{m^2_{\xi d}} \tag{4.12}$$

The spatial averaging distance, the distance within which the cone tip resistance data is averaged, is taken equal to 2 m, as the significant depth of influence in shear criterion is taken equal to 2B, where B is the width of the footing. The variance

reduction factor is computed from the autocorrelation and spatial averaging distances using Equation 2.35, as squared exponential function is chosen to best fit the sample autocorrelation data using regression analysis. The variance and standard deviation reduction factors obtained for the cone tip resistance data are 0.167 and 0.41 respectively. Table 4.2 shows the results of first phase of analysis for shear criterion. The effect of variance reduction due to spatial correlation and spatial averaging reduces the inherent CoV to 11%.

Table 4.2. Statistical parameters of cone tip resistance data for shear criterion (CPT27)

Parameter	Value
Mean of trend, t (kPa)	5390
Standard deviation of the residuals off the trend, SD_w (kPa)	1567
Coefficient of variation of inherent variability, CoV_{qc}	29%
Autocorrelation distance in vertical direction (fitting squared exponential function to quadratic detrended q_c), m	0.20
Scale of fluctuation in vertical direction, m	0.36
Spatial averaging length, L (m)	2.0
Variance reduction factor, Γ^2_L	0.167
Standard deviation of spatial average, SD_{wa} (kPa)	641
Coefficient of variation of spatial average, CoV_{qca}	12 %

From Equation 2.35, it is shown that the variance reduction factor is directly proportional to δ/L ratio and the effect of autocorrelation and spatial averaging reduces the inherent variability of cone tip resistance.

It is noted that the cone penetration tests at NGES sites were conduced with an electrical cone. Phoon and Kulhawy (1999a) documented the coefficients of variation attributed to equipment, procedural and random measurement errors for tip resistance measurement with an electrical cone as 3%, 5%, and 5% respectively. The total measurement uncertainty of cone tip resistance (CoV_e) is computed from the above

three sources using Equation 4.13 (Phoon and Kulhawy 1999a), which is obtained as 8%.

$$CoV_e = \sqrt{\left(CoV_{equipment}\right)^2 + \left(CoV_{procedural}\right)^2 + \left(CoV_{random}\right)^2} \tag{4.13}$$

The standard deviation of transformation uncertainty (SD_ε) of Equation 4.1 is reported as 2.8° (Kulhawy and Mayne 1990). The mean, coefficients of variation (CoV) of total effective friction angle $\left(\overline{\phi}_d\right)$ and spatial average effective friction angle $\left(\overline{\phi}_a\right)$ are derived by linearizing the transformation equation given in Equation 4.1 about the mean using a first-order Taylor series expansion and by applying second-moment probabilistic technique (Benjamin and Cornell 1970; Phoon and Kulhawy 1999b). Using Equation 4.9 and 4.11, the mean and point coefficient of variation of friction angle ($CoV_{\phi d}$) are 40.7˚ and 8% respectively. Taking into consideration the benefit of autocorrelation and spatial averaging, the coefficient of variation of spatial averaged friction angle ($CoV_{\phi a}$) from Equation 4.12 is 7%.

The observations from the above analysis is that though the individual element sources of uncertainty are higher (CoV_{wqc}=29%, CoV_{aqc}=11%, CoV_e=8%, and CoV_ε=2.8/40.7×100≈7%), the combined effect on the design parameter uncertainty is quite lower. Hence, it may be noted that the computed uncertainty of the dependent variable is strongly influenced by the transformation model used to correlate the independent and dependent variables.

In the second phase of analysis, the uncertainty in bearing capacity is evaluated from that of mean effective friction angle obtained in the first phase of analysis. The uncertainty involved in transformation models given in Equations 4.3 and 4.4 is neglected due to unavailability of empirical data for which these equations have been

developed. Hence, the coefficient of variation of predicted mean friction angle computed in the first phase is assumed equal to the coefficient of variation of bearing capacity. Using mean friction angle obtained in phase 1, the mean value of q_u is obtained as 967 kPa. Table 4.3 shows the results obtained from both the phases of analysis in shear criterion.

Table 4.3. Design property uncertainty in the analysis for shear criterion

Property	Property value
Mean friction angle, $m_{\xi dqc}$	40.7°
CoV of inherent variability of q_c, CoV_{wqc}	29%
CoV of spatial averaged q_c, CoV_{waqc}	12%
CoV of measurement error, CoV_{eqc}	5%-15%
SD of transformation uncertainty, $SD_{\varepsilon\phi}$	2.8°
CoV of point friction angle, $CoV_{\xi d\phi}$	8%
CoV of spatial averaged friction angle, $CoV_{\xi a\phi}$	7%
Mean ultimate bearing pressure, $m_{\xi dqu}$	967 kPa
CoV of point ultimate bearing capacity, $CoV_{\xi dqc}$	8%
CoV of spatial averaged bearing capacity, $CoV_{\xi aqc}$	7%

The limit state function for shear failure criterion can be defined as given in Equation 4.14 (Cherubini 2000; Zekkos et al. 2004).

$$Z_1 = R - S \tag{4.14}$$

where R is variable friction angle (ϕ) represented by mean friction angle of 40.7˚ and coefficients of variation of 8% and 7% for point and spatial average friction angles respectively. The friction angle (ϕ) is assumed to follow log-normal distribution. The load (S) is equal to the ultimate bearing pressure predicted deterministically by the Equation 4.2 divided by a suitable factor of safety. As it is generally done in practice, these loads are evaluated deterministically without accounting for the uncertainties in the friction angle and in the correlation of the friction angle to the ultimate bearing

pressure (Zekkos et al. 2004). Hence, S is taken as the allowable bearing pressure (322 kPa) obtained by using a factor of safety of 3 on deterministic ultimate bearing pressure of 967 kPa. The probability of failure (p_f) and reliability index (β) are calculated for the limit state function shown in Equation 4.14 using the Advanced First-order Second Moment reliability method (AFOSM) also known as Hasofer-Lind reliability approach, for the load and resistance parameters described above.

In the case of shear failure criterion, the reliability indices for the limit state shown in Equation 4.14 obtained using simple and advanced probabilistic approaches are 2.5 and 2.9 respectively. From the above results, one could observe a higher reliability index in advanced probabilistic approach, as it takes into consideration the beneficial effect of spatial variability in terms of autocorrelation distance and spatial averaging. For satisfying the stability of routine geotechnical structures Meyerhof (1982) and Cherubini (2000) suggest a reliability index of three, which corresponds to probability of failure, $p_f \approx 10^{-3}$ is sufficient. Hence, the maximum tolerable allowable pressures on the footing which can be allowed for satisfying the above requirement are back calculated, and presented for the above two approaches. The allowable pressures of the footing for a component reliability index of three using simple and advanced probabilistic approaches are 270 kPa and 310 kPa.

4.3.2.2 Settlement criterion

A similar procedure described above is applied for settlement criterion to evaluate the pressure that produce the stipulated settlement of foundation. The statistical parameters used in probabilistic settlement evaluation are calculated from cone tip resistance data and the results are shown in Tables 4.4 to 4.7.

Table 4.4. Statistical parameters of cone tip resistance data (CPT27) for settlement criterion Layer 1 (0-1 m)

Property	Property value
Mean cone tip resistance, t (kPa)	1764
SD of residuals off the trend of q_c, SD_{wqc} (kPa)	372
CoV of inherent variability of q_c, CoV_{wqc}	21%
SD reduction factor of q_c, Γ_{vqc}	0.31
SD of spatial average qc, SD_{waqc} (kPa)	116
CoV of spatial average q_c, CoV_{aqc}	7%

Table 4.5. Statistical parameters of cone tip resistance data (CPT27) for settlement criterion Layer 2 (1 m-2 m)

Property	Property value
Mean cone tip resistance, t (kPa)	8955
SD of residuals off the trend of q_c, SD_{wqc} (kPa)	317
CoV of inherent variability of q_c, CoV_{wqc}	4%
SD reduction factor of q_c, Γ_{vqc}	0.31
SD of spatial average qc, SD_{waqc} (kPa)	99
CoV of spatial average q_c, CoV_{aqc}	1%

Table 4.6. Statistical parameters of cone tip resistance data (CPT27) for settlement criterion Layer 3 (2 m-3 m)

Property	Property value
Mean cone tip resistance, t (kPa)	12560
SD of residuals off the trend of q_c, SD_{wqc} (kPa)	1412
CoV of inherent variability of q_c, CoV_{wqc}	12%
SD reduction factor of q_c, Γ_{vqc}	0.31
SD of spatial average qc, SD_{waqc} (kPa)	438
CoV of spatial average q_c, CoV_{aqc}	4%

Table 4.7. Statistical parameters of cone tip resistance data (CPT27) for settlement criterion Layer 4 (3 m-4 m)

Property	Property value
Mean cone tip resistance, t (kPa)	10560
SD of residuals off the trend of q_c, SD_{wqc} (kPa)	400
CoV of inherent variability of q_c, CoV_{wqc}	4%
SD reduction factor of q_c, Γ_{vqc}	0.31
SD of spatial average qc, SD_{waqc} (kPa)	124
CoV of spatial average q_c, CoV_{aqc}	2%

The cone tip resistance data within 4 m below the footing base is used to evaluate the autocorrelation characteristics. However, inherent variability of cone tip resistance alone is considered in the reliability of settlement evaluation. The limit state function for settlement failure criterion corresponding to 25 mm settlement can be written as

$$Z_2 = 0.025 - s_1 \tag{4.15}$$

where s_1 is random variable representing settlement of the footing computed using Equation 4.5, wherein the cone tip resistance (q_c) alone is considered as random variable following lognormal distribution. The corresponding limit state functions for 40 mm and 50 mm allowable settlements are

$$Z_3 = 0.025 - s_2 \tag{4.16}$$

$$Z_2 = 0.025 - s_3 \tag{4.17}$$

The autocorrelation distance and scale of fluctuation of cone tip resistance computed from data within 0-4 m below base of the footing are 0.22 m and 0.39 m respectively. The spatial averaging distance for settlement evaluation is taken as the depth of significant zone of influence below the loaded footing, which is equal to 4 m. A squared exponential function is chosen to best fit the sample autocorrelation data based on regression analysis. A standard deviation reduction factor of 0.31 is obtained using Equation 2.35. The variance reduction factor derived from the analysis of whole q_c data within the significant zone of influence is used to reduce the point variances computed in each sublayer. The first two moments of q_c (mean and standard deviation) in each sublayer are computed from the respective cone tip resistance data in each sublayer. For these sublayers, the point variances are reduced from 21% to 7%, 4% to 1%, 12% to 4%, and 4% to 2% for 1st, 2nd, 3rd and 4th sublayers

respectively. The summary of calculations of the data in these sublayers is shown in Tables 4.4 to 4.7.

Reliability calculations are performed for settlement criterion considering the limit state functions shown in Equations 4.15 to 4.17, and the allowable pressures corresponding to a reliability index of 3 are obtained. Table 4.9 presents the pressures corresponding to 25 mm, 40 mm, and 50 mm allowable settlements for a reliability index of 3. Using the simple probabilistic approach, the allowable pressures computed are 92 kPa, 139 kPa, and 169 kPa for 25 mm, 40 mm and 50 mm settlements respectively. However, using the advanced probabilistic approach the allowable pressures are 124 kPa, 187 kPa, and 226 kPa corresponding to 25 mm, 40 mm, and 50 mm settlements. It is may be seen from the results presented in Tables 4.1 and 4.8 that the allowable pressures obtained from probabilistic based technique are less than the corresponding pressures obtained using deterministic approach for both the individual limit states.

Table 4.8. Allowable pressure (kPa) of the footing for component reliability index of three

Shear criterion		Settlement criterion					
Without spatial variability	With spatial variability	Without spatial variability			With spatial variability		
		Allowable settlement (mm)			Allowable settlement (mm)		
		25	40	50	25	40	50
270	310	92	139	169	124	187	226

4.3.2.3 Allowable pressure

In the case of probabilistic stability calculations for foundations, both the significant failure criteria, viz., shear and settlement, are treated as individual entities connected in series, because failure of foundation occurs if any of the two components fails

(Zekkos et al. 2004). The system probability of failure (p_{fsys}) is evaluated from the component probabilities of failure of individual limit states (p_{fcom}), using Equation 4.18 (Haldar and Mahadevan 2000). The reliability index is evaluated from probability of failure using Equation 2.60. Table 4.9 presents the allowable pressures of the footing corresponding to target system reliability index of 3.

$$p_{fsys} = 1 - \Pi(1 - p_{fcom}) \tag{4.18}$$

Table 4.9. Allowable pressure of the footing corresponding to system reliability index of three

Without spatial variability			With spatial variability		
Allowable settlement (mm)			Allowable settlement (mm)		
25	40	50	25	40	50
92	139	169	124	187	226

It is obvious to note that the allowable pressure of the footing increases with increase in settlement level. Furthermore, it is lower in case the effect of spatial variability and spatial averaging are disregarded. When the failure probabilities of two individual limit states differ by an order of magnitude or more, the limit state having higher probability of failure governs the design (Zekkos et al. 2004). Accordingly for the data considered, the settlement limit state, which produces a lower allowable pressure for the same level of reliability, governs the footing design.

Table 4.11 shows the comparison of allowable pressures deemed to be appropriate from both deterministic as well as probabilistic approaches for all the three settlement levels considered in the analysis. The deterministic allowable pressures, q_{all}, presented in Table 4.1 are shown as numerator, and the allowable pressures corresponding to a system reliability index of 3 are shown as denominator. At all the three settlement levels considered in the analysis, the deterministic procedures give higher allowable

pressures than that obtained by probabilistic approaches, for a generally accepted system target reliability index of 3. From the above discussion, it may be said that deterministic approaches produce unconservative estimates of allowable pressure. However, the computed allowable pressure in probabilistic approach, q_{all} (probabilistic), is highly dependent on the uncertainty associated with determining the mean soil properties. As usual, keeping all other parameters same, the advanced probabilistic analysis taking into consideration the beneficial effect of autocorrelation structure and spatial averaging of cone tip resistance produce higher allowable pressures of footing due to reduced variability. Moreover, the ratio of q_{all} (deterministic)/q_{all} (probabilistic) in this case is reduced when compared to previous case based on simple probabilistic approach. However, the results obtained from the above study are site specific and needs further work in this direction.

Table 4.10. Comparison of allowable pressures from deterministic and probabilistic approaches

	Method of probabilistic analysis	
	Simple	Advanced
Ratio of allowable pressure obtained from deterministic approach (with FS=3 and 25 mm settlement) and probabilistic approach (with β_T =3)	1.54 (=142/92)	1.15 (=142/124)
Ratio of allowable pressure obtained from deterministic approach (with FS=3 and 40 mm settlement) and probabilistic approach (with β_T =3)	1.53 (=213/139)	1.14 (=213/187)
Ratio of allowable pressure obtained from deterministic approach (with FS=3 and 50 mm settlement) and probabilistic approach (with β_T =3)	1.52 (=257/169)	1.14 (=257/226)

4.4 Conclusions

The following conclusions may be drawn from the above study.

Scale of fluctuation, δ, and spatial averaging length, L, significantly influence the inherent variability of soil property, CoV_w. The combined effect of spatial variability and spatial averaging reduces the inherent variability.

The detrending process produces the reduced autocorrelation distances. These lower correlation distances increase the L/δ ratio and subsequently estimates lower standard deviation. Hence, directly using the experimental data without any detrending process overestimates the uncertainty in the designs. It is suggested that the in-situ data should be verified for physically admissible trend in the data in a comprehensive manner before taking up for rigorous statistical analysis.

A theoretical squared exponential function is best fitted to the sample autocorrelation data for the two data sets, viz., data for settlement calculations and bearing capacity calculations.

Transformation model has been identified as a crucial factor influencing the degree of variability of design parameter. Depending on the transformation model chosen the combined effect of all the three individual components of uncertainty (inherent variability, measurement and transformation uncertainty) may either be more or less than their individual values of uncertainty.

In both deterministic and probabilistic approaches, the settlement of the footing governs the allowable pressure of the foundation.

At all the three settlement levels considered in the analysis, the deterministic procedures give higher allowable pressures than that obtained by probabilistic approaches, for a generally accepted target reliability index of 3.

Chapter 5

SHALLOW FOUNDATIONS RESTING ON COHESIVE SOILS

5.1 Introduction

The bearing capacity of shallow foundations resting on cohesive soil deposits is evaluated in this chapter in a probabilistic framework. The cone tip resistance data pertaining to the Adelaide university site and a power plant site in India are used in this work.

5.2 Design of foundations resting on the Keswick clay

The CPT are conducted using an electric cone penetrometer, with standard cone of 60°, and 10 cm^2 base area. Jaksa (1995) studied the micro behaviour of Keswick Clay from the CPT tests conducted in a 50 m × 50 m area to a depth of 5 m below ground surface. From the continuous core samples collected near the CPT sounding location, it is observed that there exists sandy clay and clayey sand to a depth of 0.2 m, silty sandy clay of medium plasticity from 0.2 m to 0.9 m, and silty sandy clay of high plasticity from 0.9 to 1.1 m depth. Keswick clay deposit is available from 1.1 m to a depth of 5 m below the ground surface. A single CPT 'q_c' profile, denoted as C8 is used in the analysis. The bearing capacity analysis is carried out for a footing of width 1 m, and placed on the surface of Keswick clay deposit, i.e., at a depth of 1.1 m from the ground surface.

Figure 5.1 shows the classification of cohesive soils based on cone tip resistance (q_c). The unconfined shear strength (S_u) values are also shown in the same figure corresponding to different possible values of con tip resistance. The cone tip

resistance profile (C8) obtained from Adelaide site (Jaksa 1995) is superimposed on Figure 5.1, and it may be seen from the figure that majority of the qc profile used in the analysis is classified as soft to medium and stiff.

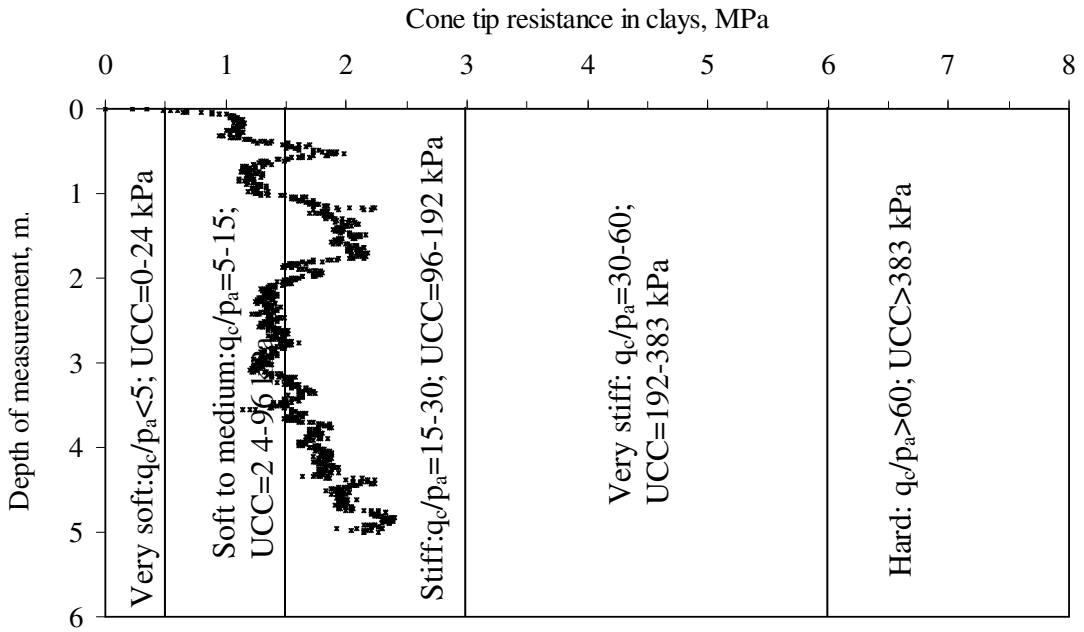

Figure 5.1. Classification of cohesive soil based on cone tip resistance data

The degree of saturation of the Keswick clay obtained from undisturbed core samples was observed to be very high, and hence treated saturated for further analysis. Since, the soil is saturated, and undrained condition are assumed to prevail due to application of foundation loads, ϕ=0 analysis is chosen appropriate to model the bearing capacity of shallow foundation resting on these soils. It is noted from the literature that the foundation is designed in such a way that an adequate factor of safety against a complete shear failure in the underlying soil is available. The possibility of a complete shear failure in clays is a very real one, and frequently in practice it is considered necessary, for economic reasons, to work with factors of safety against ultimate failure of not more than 3 (Skempton 1951).

5.2.1 Allowable bearing pressure

In the general case, the net ultimate bearing pressure of foundation (q_u) resting at a depth (D_f) below the surface may be expressed in the form of Equation 5.1.

$$q_u = \left[cN_c + p_o\left(N_q - 1\right) + \frac{\gamma B}{2} N_\gamma \right] \tag{5.1}$$

where c, p_o, γ, and B are the apparent cohesion of the soil, effective overburden pressure at foundation level, density of soil beneath the foundation, and breadth of foundation, respectively.

N_c, N_q, N_γ are the bearing capacity factors which are functions of the angle of shearing resistance (ϕ) of the soil, the aspect ratio, viz., ratio of length of the foundation (L) to width of the foundation (B), and depth ratio, viz., ratio of depth of foundation (D_f) to width of the foundation. However, in case of ϕ=0 analysis, N_q and N_γ are observed as 1 and 0 respectively, and N_c is expressed in terms of above mentioned factors. Hence, for ϕ=0 analysis the Equation 5.1 reduces to

$$q_u = \left[cN_c \right] \tag{5.2}$$

In this problem the strip footing of width 1 m is placed at a depth of 1.1 m below the ground surface, hence, the depth ratio (D_f/B) for this footing is 1.1. The following N_c values as a function of depth ratio have been evaluated for strip footings (Skempton 1951).

$$\begin{aligned} N_c &= 6.4 \; for \; \frac{D_f}{B} = 1 \\ N_c &= 6.8 \; for \; \frac{D_f}{B} = 1.5 \end{aligned} \tag{5.3}$$

By linear interpolation, N_c for D_f/B=1.1 is obtained as 6.48, and substituting this value in Equation 5.2 results in net ultimate bearing pressure given in Equation 5.4.

$$q_u = [6.48\, c_u] \tag{5.4}$$

where c_u is undrained cohesion of soil. The significant zone of influence till the shear failure planes extend below a loaded strip footing in cohesive soils is observed to be approximately 1B, where B is width of the foundation. Hence, the cone tip resistance (q_c) data of the Keswick clay from 1.1 m to 2.1 m below ground surface is analysed for bearing capacity.

5.2.2 Evaluation of variability of undrained shear strength

5.2.2.1 Inherent variability of cone tip resistance

The detailed analysis of the cone tip resistance data is presented in section 3.6 of chapter 3. The mean, standard deviation and coefficient of variation of inherent variability of quadratic detrended q_c within the significant depth of influence, i.e., 1.1-2.1 m below the ground surface, are 1853 kPa, 125 kPa, and 7% respectively. The autocorrelation distance and scale of fluctuation evaluated for the quadratic detrended data using an exponential fitting based on regression analysis are 0.09 m and 0.17 m respectively.

By way of approximation, the spatial averaging distance (L) of cone tip resistance is taken equal to the width of the foundation, i.e., 1 m. The variance reduction function for an exponential fit to sample autocorrelation is computed from Equation 2.34. The variance reduction factor computed from Equation 2.34 for an autocorrelation distance of 0.09 m and spatial averaging distance of 1 m is 0.164. The corresponding standard deviation reduction factor is 0.41. Hence, the coefficient of variation of spatial average cone tip resistance is equal to $7/100 \times 0.41 \approx 3\%$.

5.2.2.2 Measurement uncertainty of cone tip resistance

The uncertainty in measurement of cone tip resistance associated with electrical cones was compiled by Phoon and Kulhawy (1999a). The total coefficient of variation associated with measurement of cone tip resistance (q_c) obtained from electric cone penetrometer is approximately in the range of 8% (Phoon and Kulhawy 1999a).

5.2.2.3 Transformation uncertainty of S_u evaluated from q_c

Another important source of uncertainty is attributed to the transformation of in-situ soil property to design strength property, which is often neglected due to insufficient data. However, it is observed from the previous studies that the transformation uncertainty contributes significantly to the design uncertainty. The following transformation model is frequently used in geotechnical engineering to evaluate the undrained shear strength (S_u) of clayey soil from cone tip resistance (q_c) (Kulhawy and Mayne 1990).

$$S_u = D_K (q_c - \sigma_{V0}) \tag{5.5}$$

where q_c, D_K, S_u, σ_{vo} are the cone tip resistance, cone bearing factor representing the model slope, undrained shear strength of the soil, and the total overburden pressure. The application of classical plasticity theory to the bearing capacity problem suggests the value of D_K of the order of 1/9 for general shear model, and other theories produce different values of D_K (Jaksa 1995). It is more common to calibrate the D_K factors using back calculation from measured values of S_u. A wide range of D_K factors are reported in the literature ranging from 1/4.5 to 1/75. The above transformation model can also be expressed in a probabilistic terms as given in Equation 5.6 (Phoon and Kulhawy 1999b).

$$\frac{s_u}{\overline{\sigma}_{vo}} = D_K \frac{(q_T - \sigma_{vo})}{\overline{\sigma}_{vo}} = (m_{DK} + \varepsilon)\frac{(q_T - \sigma_{vo})}{\overline{\sigma}_{vo}} \tag{5.6}$$

where q_T is the measured cone tip resistance corrected for pore water pressure, $\overline{\sigma}_{vo}$ is the effective overburden pressure, D_K is uncertain model slope, m_{DK} is the mean of D_K, and ε is the zero-mean random variable representing transformation uncertainty. Since, no ground water table was observed within the 5 m depth at the Adelaide University site, q_T is taken equal to q_c, and effect of pore water pressure is neglected.

The cone factor, D_K is modeled as random field. The statistical parameters, m_{DK}, standard deviation of fluctuating component, σ_ε, and the coefficient of variation of measurement uncertainty, CoV_ε ($=SD_\varepsilon/m_{DK}$) are evaluated from the measured cone tip resistance (q_c) from in-situ tests, and undrained shear strength (S_u) computed from UU test results on the undisturbed core samples obtained from the site very close to locations where CPT soundings have been conducted. Phoon and Kulhawy (1999b) demonstrated that the transformation uncertainty is significant and independent source of uncertainty in geotechnical engineering. However, to evaluate the transformation uncertainty devoid of extraneous variability originating from inherent variability and measurement uncertainty, the following two conditions are suggested to be followed (Phoon and Kulhawy 1999b).

(a) Both the in-situ measured property (q_c) and design property (S_u) of soil should be evaluated on samples located at very close spacing to avoid the effect of inherent variability of soil.

(b) In the measurement of cone tip resistance the same cone type and method of obtaining should be used, and in case of undrained cohesion the same test is used to avoid the systematic measurement errors.

Kulhawy et al. (1992) evaluated the statistical parameters of D_k, viz., m_{DK} and CoV_ε from corrected cone tip resistance (q_T) and undrained shear strength (S_u) of clay obtained from consolidated isotropic undrained triaxial compression (CIUC) test and unconsolidated-undrained (UU) triaxial compression tests. The mean value of D_k (m_{DK}) obtained from CIUC and UU tests were 0.0789 and 0.0512 respectively. Similarly, the coefficients of variation of D_k (or CoV of transformation uncertainty, CoV_ε) were 35% and 29% respectively.

For evaluation of transformation model uncertainty for the Keswick clay deposit, 3 additional CPT tests and 6 unconsolidated undrained (UU) tests on undisturbed samples were conducted (Jaksa 1995). These UU test results are used with the measured values of cone tip resistance averaged over the length of triaxial specimen in the evaluation of statistical parameters of model slope (D_K) given in Equation 5.6. From the above results, the mean (m_{DK}), standard deviation (SD_ε), and coefficient of variation of model slope ($CoV_\varepsilon = SD_\varepsilon/m_{DK}$) for Keswick clay are computed as 0.0621, 0.0049, and 8% respectively. The location of C8 sounding is at a radial distance of approximately 14 m from the place where the empirical parameters of model slope have been evaluated. Since, the same Keswick clay is found to exist at the location under consideration, i.e., location of C8, the empirical model slope parameters evaluated above are assumed valid to even the Keswick clay at location C8.

5.2.2.4 Mean and total uncertainty of S_u

Phoon and kulhawy (1999b) conducted a pioneering study of various sources of uncertainty and formulated the total uncertainty of design property in terms of three individual sources of uncertainty, viz., inherent variability (CoV_w), measurement uncertainty (CoV_e), and transformation uncertainty (CoV_ε) using the second-moment

probabilistic techniques (Benjamin and Cornell 1970). The design property, S_u, is expressed in terms of Equation 5.7. The mean (m_{Su}) and coefficient of variation of design parameter (CoV_{su}) can be expressed using Equations 5.8 and 5.9.

$$S_u = (m_{DK} + \varepsilon)(t + w + e - \sigma_{vo}) \tag{5.7}$$

$$m_{Su} = m_{DK}(t - \sigma_{vo}) \tag{5.8}$$

$$COV_{\xi d}^2 = \frac{\left(COV_w^2 + COV_e^2\right)}{\left(1 - \frac{\sigma_{vo}}{t}\right)^2} + COV_\varepsilon^2 \tag{5.9}$$

where CoV_ε is SD_ε/m_{DK}, and t is the trend or mean value of q_T in clay. The CoV of design property due to spatial average ($CoV_{\xi a}$) is obtained as shown in Equation 5.10.

$$COV_{\xi a}^2 = \frac{[\Gamma^2(L)COV_w^2 + COV_e^2]}{\left(1 - \frac{\sigma_{Vm}}{t}\right)^2} + COV_\varepsilon^2 \tag{5.10}$$

where $\Gamma^2(L)$ and σ_{vm} are variance reduction function and the total overburden stress averaged over a length of L respectively. Terms $COV_{\xi d}$ and $COV_{\xi a}$ are the coefficients of variation of design property considering point estimates and spatial average respectively. In the present study, the above equations are used to obtain the statistical parameters (mean and variance) of undrained shear strength (S_u) with and without consideration of spatial variability of cone tip resistance in the vertical direction.

The mean cone tip resistance for the data within the significant zone of influence, i.e., from 1.1 m–2.1 m, is obtained as 1853 kPa, as reported in Table 3.10. From Equation 5.8, the mean undrained shear strength (m_{Su}) is computed as

$$m_{Su} = 0.0621 \times (1853 - (1.1 + 0.5) \times 19) = 113 \ kPa$$

The design coefficient of variation of S_u (CoV_{Sud}) is

$$CoV_{Sud} = \sqrt{\frac{(7\%)^2 + (8\%)^2}{\left(1 - \frac{(1.1+0.5)\times 19}{1853}\right)^2} + (8\%)^2} \approx 14\%$$

Similarly, the spatial average coefficient of variation of Su (CoV_{Sua})is

$$CoV_{Sua} = \sqrt{\frac{0.164\times(7\%)^2 + (8\%)^2}{\left(1 - \frac{(1.1+0.5)\times 19}{1853}\right)^2} + (8\%)^2} \approx 12\%$$

The allowable bearing pressure given by Equation 5.4 is a function of undrained cohesion (c_u). The undrained cohesion is obtained as half of the undrained shear strength, i.e., $c_u=S_u/2$, for a completely saturated soil tested under unconfined and undrained conditions. Since, the undrained cohesion is a linear function in S_u, the mean of c_u is obtained as half of that for S_u, and coefficient of variation of c_u is equal to that of S_u. Hence, mean undrained cohesion (m_{cu}), coefficient of variation of design undrained cohesion (CoV_{cud}), and spatial average undrained cohesion (CoV_{cua}) are 113/2≈56 kPa, 14%, and 12% respectively.

Similarly, the statistical parameters of net ultimate bearing pressure are evaluated from that of undrained cohesion. The mean net ultimate bearing pressure (m_{qu}) and coefficient of variation of design net ultimate bearing pressure (CoV_{qud}), and coefficient of variation of spatial average net ultimate bearing pressure (CoV_{qua}) are

$m_{qu} = 6.48\times m_{cu} = 6.48\times 113/2 = 366\ kPa$,

$CoV_{qud} = CoV_{cud} = 14\%$, and

$CoV_{qua} = CoV_{qud} = 12\%$

The above statistical parameters of net ultimate bearing pressure are used in section 5.6 to evaluate the reliability indices for net ultimate bearing pressure of shallow

foundations corresponding to the allowable bearing pressure obtained from deterministic procedures.

5.3 Design of foundations for power plant site

The risk associated with the computed allowable bearing pressure of a shallow foundation, resting on the surface of a spatially varying cohesive soil deposit in the site of a proposed 445 MW Konaseema EPS Oakwell gas-fired combined cycle power plant on the East coast in Indian state of Andhra Pradesh, is analysed using 1-D random field theory. Because of the importance of plant (estimated approximate project cost is Rs.1383 crores), extensive geotechnical in-situ tests, such as, Static cone penetration tests (CPT), Standard penetration tests (SPT), Plate load tests, Vane shear tests (VST), etc., followed by various laboratory tests for the evaluation of index as well as strength parameters, have been conducted by ECC division of Larsen & Toubro Limited, as part of detailed soil exploration programme.

Figure 3.42 shows a typical 'q_c' profile of the cohesive soil deposit up to 3 m depth below base of the foundation. From the observed CPT profile and visual observation of undisturbed core samples, the soil up to a depth of 3 m is termed as stiff with cone tip resistance varying upto 2.84 MPa. The CPT 'q_c' profile shown in Figure 3.42 is used for probabilistic site characterization, and the results are used for the evaluation of bearing capacity of shallow strip foundation of width 1 m, resting on the surface of cohesive soil deposit. The ground water table is observed at a depth 5 m below ground level, and the results of the index properties demonstrate that the soil is completely saturated, with observed degree of saturation close to 100%. Hence, no pore pressure correction on the measured cone tip resistance is applied.

5.3.1 Allowable bearing pressure

The ultimate bearing pressure of shallow foundations resting on cohesive soil is discussed in section 5.2.1. For surface footings under undrained conditions, the ultimate bearing pressure is given by Equation 5.16 (Skempton 1951).

$$q_u = 5.14\, c_u \tag{5.11}$$

where c_u is undrained cohesion.

5.3.2 Evaluation of variability of undrained shear strength

5.3.2.1 Inherent variability of cone tip resistance

The mean of the cone tip resistance within 1 m below base of the foundation resting on surface of the ground is obtained as 2 MPa. The coefficient of variation of the deviations about this quadratic trend (CoV_w) is 13%.

Figure 3.43 shows the sample autocorrelation function and a squared exponential fit to the portion of positive autocorrelation coefficient data. For the squared exponential correlation function of the type shown in Table 2.1, the variance reduction function is evaluated using Equation 2.35. The autocorrelation distance (c) and scale of fluctuation ($\delta = \sqrt{\pi} c$) are obtained as 0.22 m and 0.39 m, and with a spatial averaging distance of 1 m, the variance reduction factor evaluated using Equation 2.35 is 0.34. Hence, the coefficient of variation of inherent variability due to spatial averaging is reduced to $13\% \times \sqrt{0.34} \approx 8\%$.

5.3.2.2 Measurement uncertainty of cone tip resistance

A mechanical cone of weight 0.77 kg, and base are of 10 cm^2 is used in the entire CPT exploration programme. Phoon and Kulhawy (1999a) reported coefficients of

variation of equipment, procedural, and random error components of measurement uncertainty equal to 5%, 10% and 10% respectively. Using the Equation 4.13, the individual sources of measurement uncertainty are combined. The CoV of measurement uncertainty (CoV_e) of cone tip resistance obtained from the above individual sources is 15%.

5.3.2.3 Transformation uncertainty of S_u evaluated from q_c

Since, laboratory test data on the shear strength characteristics of undisturbed samples within the close vicinity of CPT test locations was not available, the transformation model slope parameters have been obtained from Kulhawy et al. (1992), as reported in Phoon and Kulhawy (1999b). The mean (m_{DK}) and coefficient of variation (CoV_ε) for transformation model uncertainty are obtained as 0.0512 and 29% respectively corresponding to UU test results.

5.3.2.4 Mean and total uncertainty of S_u

The mean and coefficients of variation of design and spatial average undrained shear strength (S_u) are evaluated using second-moment probabilistic techniques (Benjamin and Cornell 1970; Phoon and Kulhawy 1999b) using the mean cone tip resistance, coefficients of variation of inherent, measurement uncertainty of 'q_c', and transformation uncertainty, using Equations 5.8-5.10.

The mean undrained shear strength (m_{Su}) is evaluated through transformation model given in Equation 5.8 using the mean cone tip resistance (q_c) data. The mean undrained shear strength profile is shown in Figure 5.2. Since, the design parameter, i.e., undrained cohesion (c_u), is obtained from linear transformation of undrained shear strength (S_u), the mean undrained cohesion (m_{cu}) is half of the mean undrained shear strength (m_{su}), and the coefficient of variation of c_u is same as that of S_u.

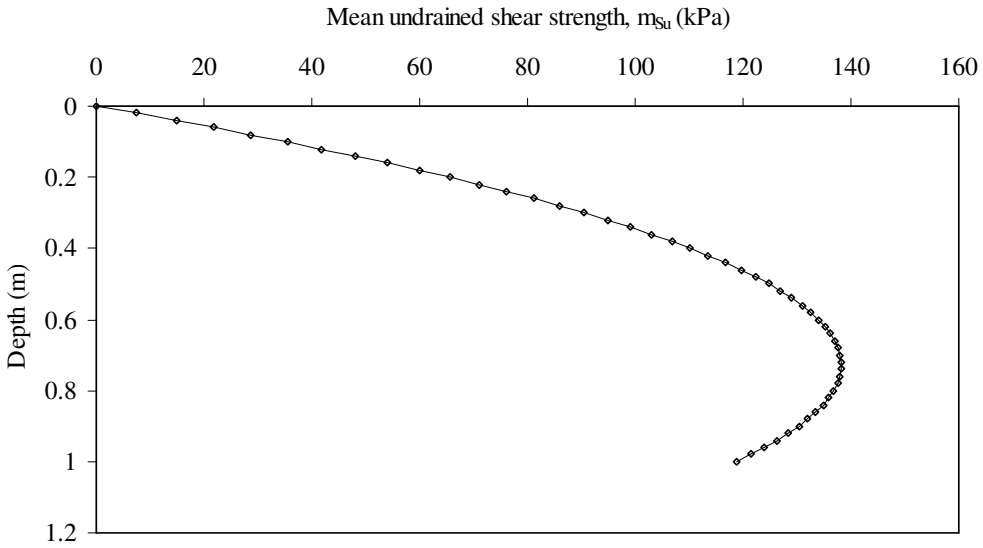

Figure 5.2. Typical profile of mean undrained shear strength (Power plant site)

The mean undrained shear strength within the depth of influence for shear criterion, i.e., 0-1 m, is

$$m_{\xi d} = m_{Su} \approx 0.0512 \times (2000 - 0.5 \times 19) \approx 102 \ kPa$$

The coefficient of variation of design undrained shear strength is

$$CoV_{\xi d} = CoV_{Sud} \approx \sqrt{\frac{(0.13)^2 + 0.15^2}{\left(1 - \frac{0.5 \times 19}{2000}\right)^2} + 0.29^2} \approx 0.36 = 36\%$$

The coefficient of spatial average undrained shear strength is

$$CoV_{\xi a} = CoV_{aSu} \approx \sqrt{\frac{(0.13)^2 \times 0.34 + 0.15^2}{\left(1 - \frac{0.5 \times 19}{2000}\right)^2} + 0.29^2} \approx 0.34 = 34\%$$

The mean undrained cohesion (m_{cu}), CoV of design undrained cohesion (CoV_{cud}), and spatial average undrained cohesion (CoV_{cua}) are

$$m_{cu} = \frac{m_{Su}}{2} = \frac{102}{2} = 51 \ kPa \ ,$$

$$CoV_{cu} = CoV_{Su} = 36\% \ , \text{ and}$$

$$CoV_{acu} = CoV_{aSu} = 34\%$$

The above computed statistical parameters of undrained cohesion (c_u) are used to evaluate the corresponding parameters of ultimate bearing pressure (q_u) of foundation, described by Equation 5.11. The mean ultimate bearing pressure (m_{qu}), CoV of design ultimate bearing pressure (CoV_{qud}), and CoV of spatial average ultimate bearing pressure (CoV_{qua}) q_u are obtained as

$m_{qu} = 5.14 \times m_{cu} = 5.14 \times 51 \approx 262\ kPa$,

$CoV_{qud} = CoV_{cud} = 36\%$, and

$CoV_{qua} = CoV_{cua} = 34\%$

5.4 Reliability Analysis

The reliability calculations are performed according to the procedures given in section 2.6 of chapter 2. It is assumed in the analysis that *R* (resistance) and *S* (applied pressure) are two basic parameters, and the performance function or limit state of interest is defined as given in Equation 2.48. For lognormally distributed R, the probability of failure (p_f) and reliability index (β) are given by Equations 2.56 and 2.57.

Mean of resistance is taken as the mean of net ultimate bearing pressure, which is obtained from Equation 5.1, and CoV of resistance is the same as CoV of net ultimate bearing pressure, which is same as CoV of undrained cohesion, as q_u is obtained as linear transformation of c_u. Applied pressure of the footing (S) is assumed as a deterministic parameter, which is obtained from Equation 5.1 with mean undrained cohesion and applying an appropriate factor of safety. The reliability that a foundation carries an applied pressure as determined from deterministic analysis with different factors of safety is evaluated in the following section.

5.5 Results and discussion

5.5.1 Foundations on the Keswick clay

The reliability indices are evaluated using Equation 2.57 for various values of deterministic allowable bearing pressures of the footing. The allowable bearing pressures are computed using different factors of safety on net ultimate bearing pressures given in Equation 5.2. All the three sources of uncertainty, viz., inherent variability of in-situ cone tip resistance, measurement uncertainty associated with cone tip resistance, and transformation model shown by Equation 5.5 to model undrained shear strength from cone tip resistance are considered appropriately in the analysis. The reliability indices are evaluated for design uncertainty and spatial average uncertainty. Figure 5.3 shows the variation of reliability index (β) with factors of safety (FS) when all the three sources of uncertainty are taken into consideration. It may be seen from the figure that when spatial average property of cone tip resistance is considered the total variance of the data is reduced, leading to higher values of reliability indices.

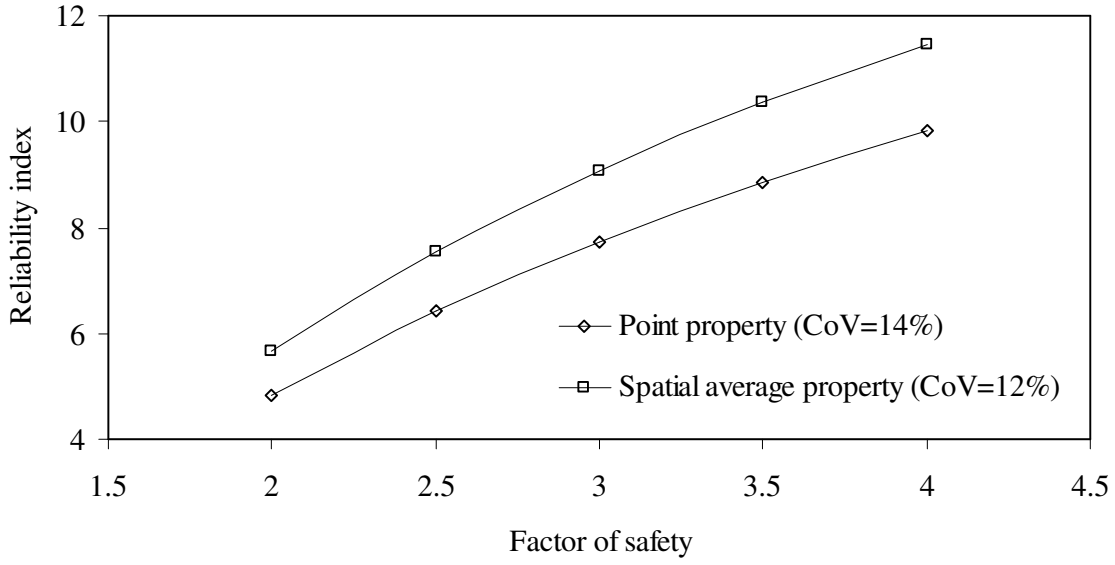

Figure 5.3. Variation of reliability index with factor of safety against complete shear failure when all the three sources of uncertainty are considered

Higher factors of safety on net ultimate bearing pressure lowers the applied pressures on the footing (S), which in turn result in higher reliability indices.

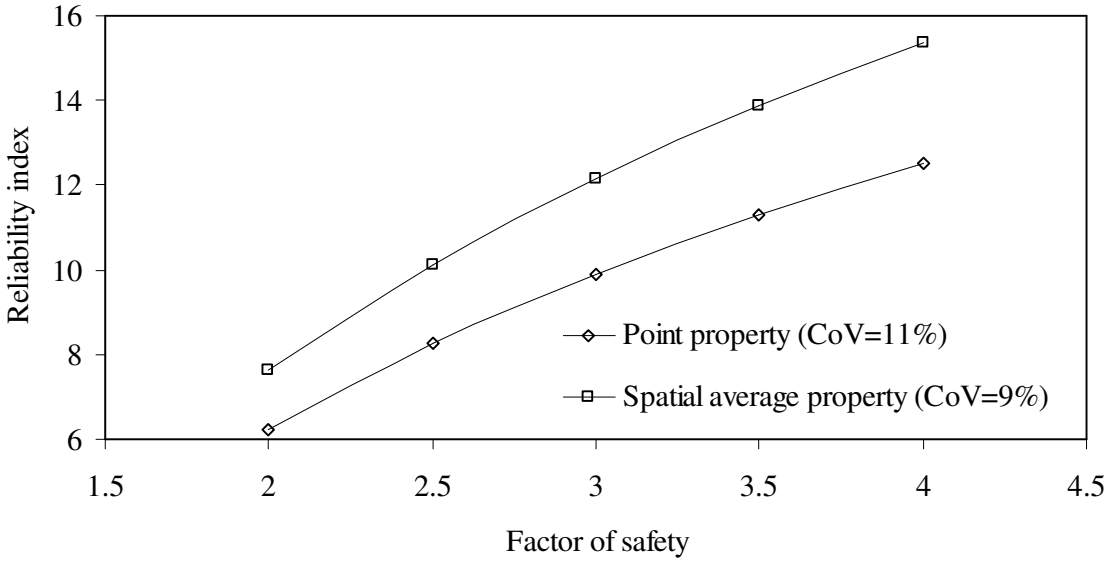

Figure 5.4. Variation of reliability index with factor of safety against complete shear failure when only inherent variability and measurement uncertainty are considered

Figure 5.4 shows the variation of reliability indices by neglecting the transformation uncertainty. The coefficients of variation of design property with respect to point and spatial average properties are 11% and 9% respectively. These low CoVs result in higher reliability indices.

Figure 5.5 shows the variation of reliability index when the effect of inherent and transformation uncertainty are considered, neglecting the measurement uncertainty. In this case, the coefficient of point and spatial average design variability are 11% and 9% respectively.

Figure 5.6 shows the variation of β with FS when inherent variability of cone tip resistance alone is considered. It may be seen that very high values of reliability indices could be achieved in this case, as the Keswick clay deposit is highly homogeneous, which is reflected in terms of very low coefficients of variation of

inherent variability of cone tip resistance, in the range of 8% and 3% for point and spatial average design property.

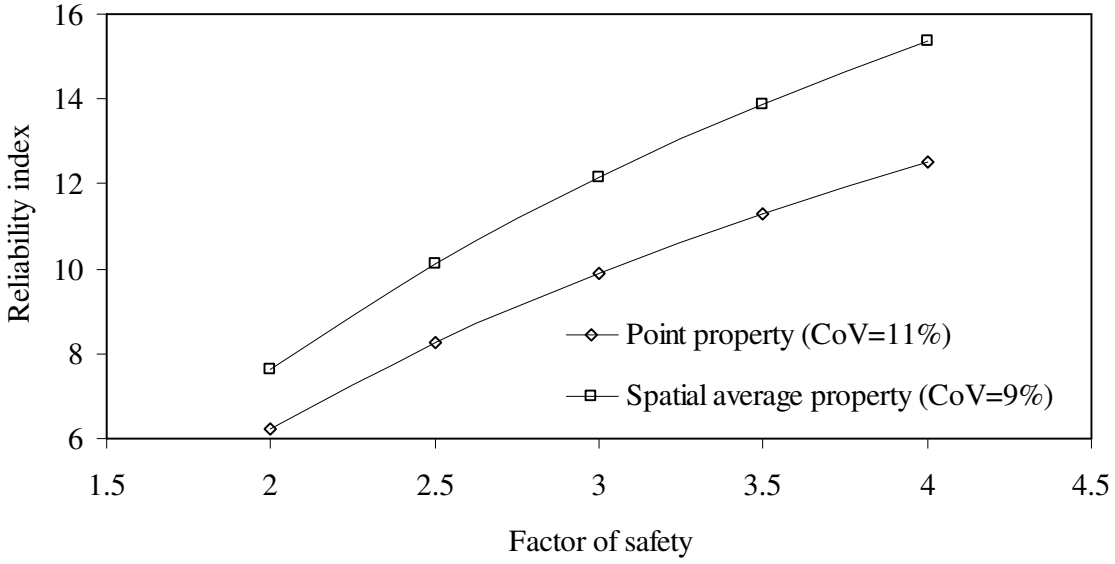

Figure 5.5. Variation of reliability index with factor of safety against complete shear failure when only inherent variability and transformation uncertainty are considered

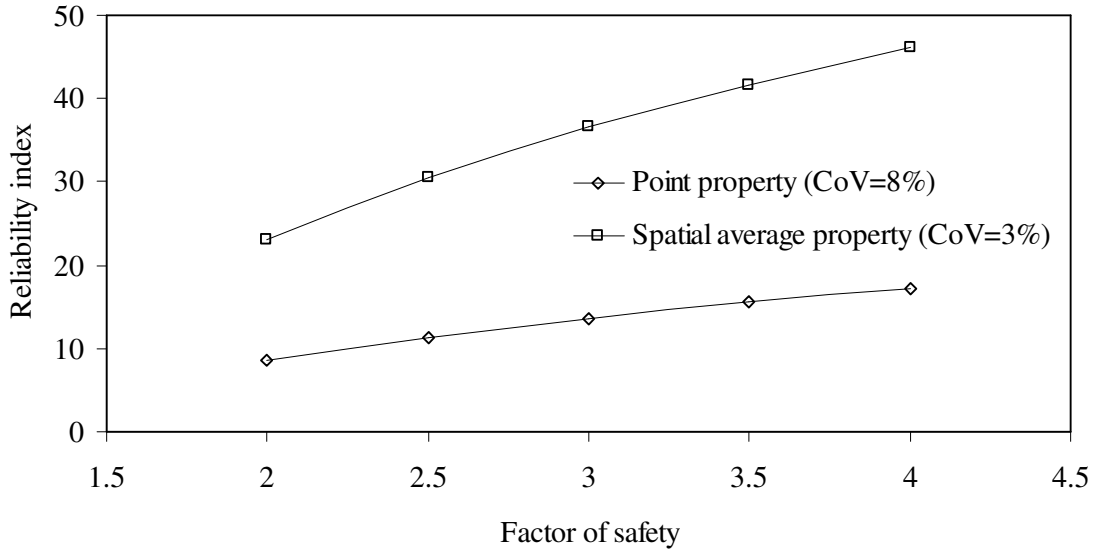

Figure 5.6. Variation of reliability index with factor of safety against complete shear failure when only inherent variability is considered

The reliability indices as high as 17 and 46 are achieved corresponding to a factor of safety of 4 on the net ultimate bearing pressure for point design property, where beneficial effect of spatial variability and averaging distance are neglected, and the spatial average property.

Tables 5.1 to 5.4 presents the summary of results showing the variation of factors of safety with respect to target reliability index for the four combinations of different sources of uncertainty as described in the above section. It may be seen from the tables that if the required target reliability index is low, the factor of safety associated with net ultimate bearing pressure could be low, that is higher pressures may be applied on the foundation. If the spatial average design property is considered the factor of safety could be reduced further, as higher applied pressures can be used to achieve a target reliability index corresponding to lower uncertainty of bearing capacity (CoV_{qua}). For example, as the target reliability index is varied from 2 to 5, the factors of safety increase from 1.28 to 1.82, in the case where all the three sources of uncertainty are considered appropriately. On the other hand, higher factors of safety than the above are needed if point design property are used instead of spatial average design property.

Table 5.1. Variation of factor of safety with reliability index considering all the three sources of variability (inherent, measurement, and transformation uncertainty) for Adelaide clay site

Reliability index (β)	Factor of safety (FS) corresponding to	
	Point property (CoV_{qud}=14%)	Spatial average property (CoV_{qua}=12%)
2	1.33	1.28
3	1.52	1.43
4	1.75	1.61
5	2.01	1.82

Table 5.2. Variation of factor of safety with reliability index considering inherent and measurement uncertainty for Adelaide clay site

Reliability index (β)	Factor of safety (FS) corresponding to	
	Point property (CoV_{qud}=11%)	Spatial average property (CoV_{qua}=9%)
2	1.25	1.20
3	1.39	1.31
4	1.55	1.43
5	1.73	1.57

Table 5.3. Variation of factor of safety with reliability index considering inherent and transformation uncertainty for Adelaide clay site

Reliability index (β)	Factor of safety (FS) corresponding to	
	Point property (CoV_{qud}=11%)	Spatial average property (CoV_{qua}=9%)
2	1.25	1.20
3	1.39	1.31
4	1.55	1.43
5	1.73	1.57

Table 5.4. Variation of factor of safety with reliability index considering inherent variability of cone tip resistance for Adelaide clay site

Reliability index (β)	Factor of safety (FS) corresponding to	
	Point property (CoV_{qud}=8%)	Spatial average property (CoV_{qua}=3%)
2	1.18	1.06
3	1.27	1.09
4	1.38	1.13
5	1.49	1.16

The coefficients of variation of design variability (CoV_{qud}) and spatial average (CoV_{qua}) from Equations 5.9 and 5.10 considering all the three sources of uncertainty are 14% and 12% respectively. The respective values considering only inherent variability and transformation uncertainty are 11% and 9% respectively. With inherent and transformation uncertainty the CoV_{qud} and CoV_{qua} are evaluated as 11% and 9%, and with inherent variability alone, CoV_{qud} and CoV_{qua} are 8% and 3%.

Hence, from the results, if designs are based on inherent uncertainty alone, the CoV_{qu} of spatial average is underestimated to one fourth of that corresponds to considering all the three sources of uncertainty. The contribution of measurement and transformation uncertainty on the CoV of bearing capacity is observed the same.

5.5.2 Foundations for power plant site

In the reliability analysis using Equation 2.57, the resistance (R) is taken as variable parameter represented by the ultimate bearing pressure given by Equation 5.11, and the load (S) is taken as conventional allowable pressure on the foundation used in the deterministic approach. The conventional allowable bearing pressure on the foundation, which is treated as deterministic parameter is obtained by using an appropriate factor of safety on the mean ultimate bearing pressure (m_{qu}) evaluated in section 5.3.2.4. These allowable bearing pressures corresponding to factors of safety of 2, 2.5, 3, 3.5, and 4 on net ultimate bearing pressure are obtained as 131 kPa, 104.8 kPa, 87.3 kPa, 74.9 kPa and 65.5 kPa, respectively.

Considering all the three sources of uncertainty, the coefficients of variation of design and spatial average bearing capacity are 36% and 34% respectively. The corresponding coefficients of variation neglecting the transformation uncertainty are 20% and 17% respectively. In the similar way, if the measurement uncertainty is disregarded, CoV_{qud} and CoV_{qua} are 32% and 30% respectively. For the case where only the transformation uncertainty is considered, the above values reduce to 13% and 8% respectively. Similar to the observations made in section 5.5.1 for Keswick clay deposit, the coefficient of spatial average q_u disregarding the measurement and transformation uncertainty is reduced to one fourth the value obtained considering all the three sources of uncertainty.

The risk associated with using these conventional allowable pressures is evaluated using Equation 2.57, and results are presented in Figures 5.7 to 5.10.

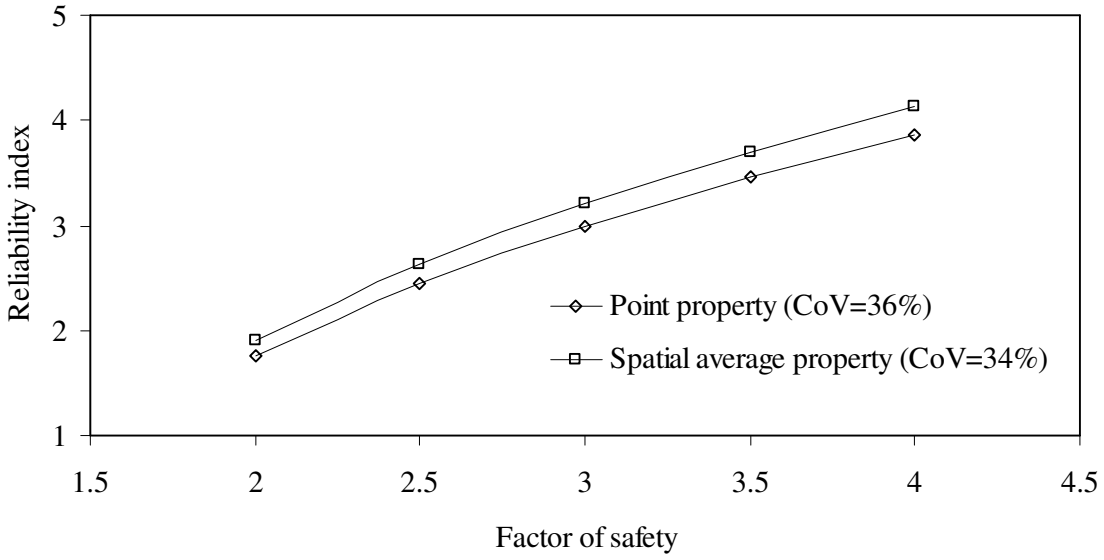

Figure 5.7. Variation of reliability index with factor of safety against complete shear failure when all the three sources of uncertainty are considered (Power plant site)

The Figure 5.7 shows the variation of reliability index with factor of safety for both design and spatial average variability of q_u, when the effect of all the three sources of uncertainty are accounted for appropriately. For this case, the effect of spatial averaging does not reduce the CoV of the bearing capacity significantly.

Figure 5.8 shows the results when effect of transformation uncertainty is neglected, and the design uncertainty is evaluated using CoV of inherent variability and measurement uncertainty. In this case, the CoV of point and spatial average properties are 20% and 17% respectively. Neglecting the transformation uncertainty leads to moderate increase in reliability indices.

Figure 5.9 shows the results obtained from reliability analysis taking into consideration the inherent variability as well as transformation uncertainty, completely neglecting the uncertainty associated with the measurement of cone tip

resistance. For this case, the point CoV and spatial average CoV differ by only 2%. Hence, the reliability indices evaluated for these two CoV do not vary significantly.

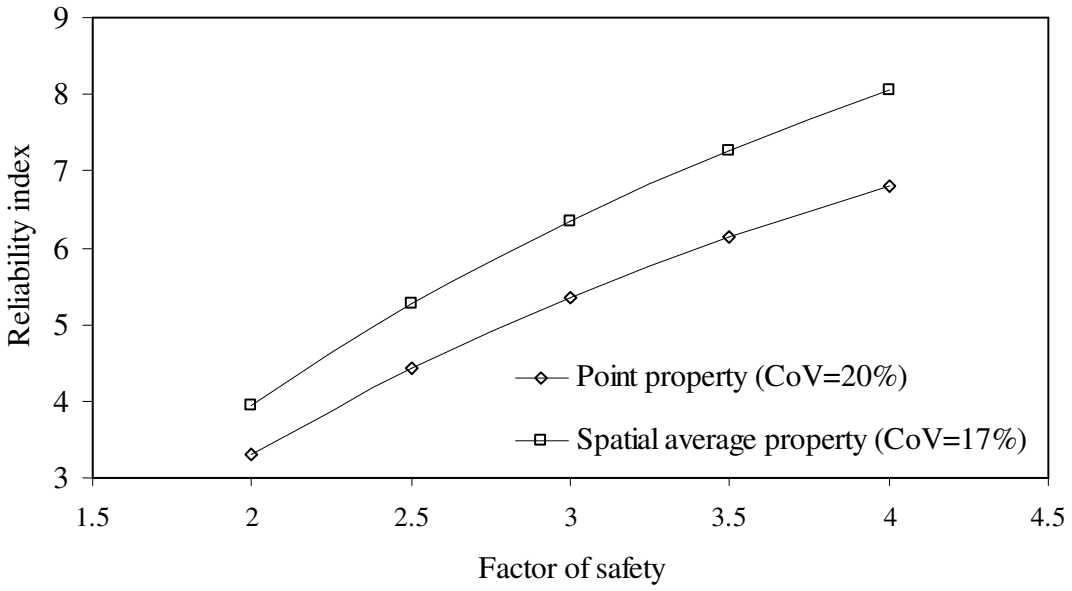

Figure 5.8. Variation of reliability index with factor of safety against complete shear failure when only inherent variability and measurement uncertainty are considered (Power plant site)

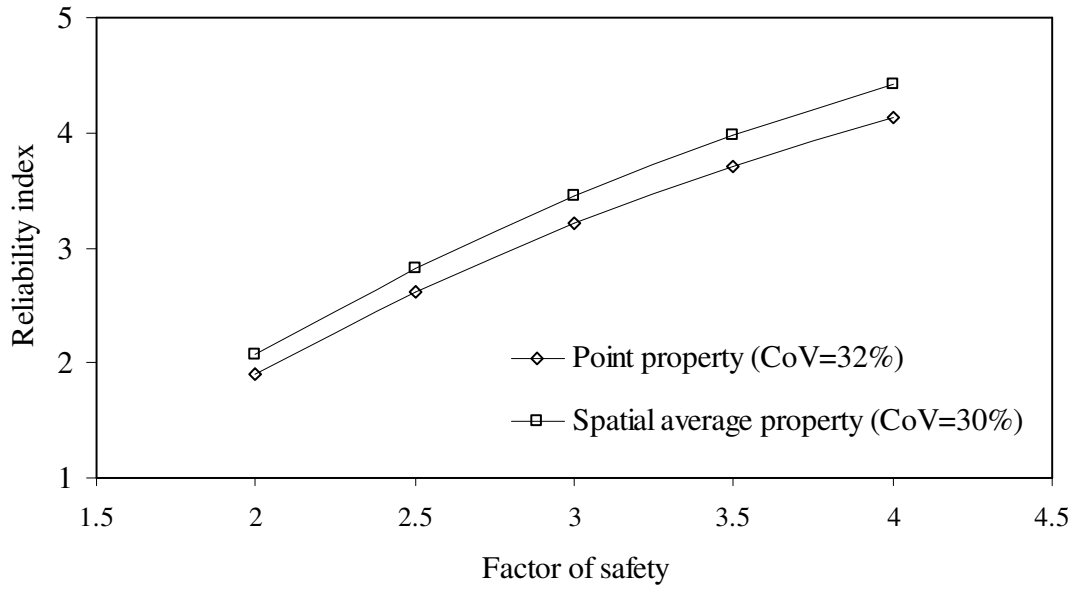

Figure 5.9. Variation of reliability index with factor of safety against complete shear failure when only inherent variability and transformation uncertainty are considered (Power plant site)

The results show that the spatial average CoV reduced by 50%, from 34% when all the three sources of uncertainty are considered, to 17.6% when the effect of transformation uncertainty on the uncertainty of design parameter is neglected, which strongly demonstrates that the transformation uncertainty in this case is quite influential and should be treated cautiously, and can not be overlooked in the design.

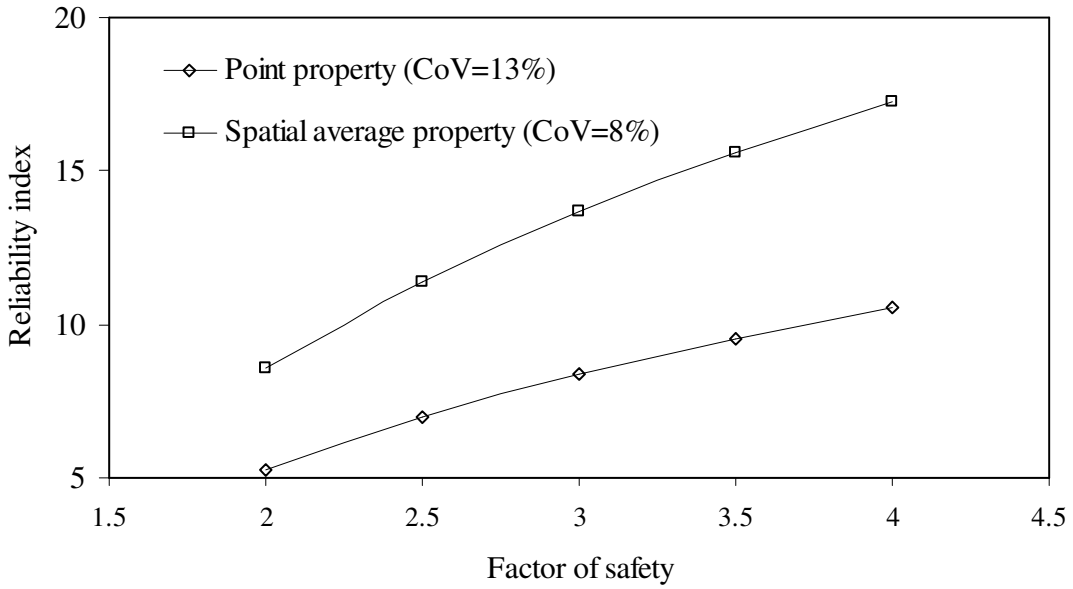

Figure 5.10. Variation of reliability index with factor of safety against complete shear failure when only inherent variability is considered (Power plant site)

Figure 5.10 shows the similar results when inherent variability of cone tip resistance alone is considered in the analysis. As can be seen, neglecting the measurement and transformation uncertainties reduce the level of uncertainty drastically and report very high values of reliability index. These higher values of reliability index produce highly unconservative designs and detrimental to the stability of foundations.

5.6 Conclusions

The relative values of autocorrelation distance and spatial average length rather than the absolute values decide on the scale of reduction applied to inherent variability.

It is observed from the results that all the three sources of uncertainty, viz., inherent variability, measurement uncertainty, and the transformation model uncertainty play a dominant role on the coefficients of variation of design and spatial average uncertainty.

For the Adelaide clay site, the coefficient of variation of inherent variability of cone tip resistance within the significant zone of influence is obtained as 7%, and the autocorrelation distance is 0.09 m. For a spatial averaging length of 1 m, the variance reduction factor is obtained as 0.164. The coefficient of variation of transformation model calibrated using UU test results and in-situ measured cone tip resistance for this site is evaluated as 8%. The CoV of design and spatial average bearing capacity are 14% and 12% respectively.

For the Adelaide clay site, considering all the sources of uncertainty effecting the design parameter and effect of spatial averaging, the net ultimate bearing pressure reduced by 1.43 produces a target reliability index of 3, which is generally acceptable in geotechnical engineering practice.

The transformation model parameters for Keswick clay are evaluated with limited data, hence these values are site specific and used with caution to correlate the q_c and S_u of other clayey profiles.

The CoV of design q_u and spatial average q_u obtained for power plant site are 36% and 34% respectively. The higher variability of q_u for design of footings in the power plant site is mainly attributed to higher values of assumed CoV for transformation model based on Kulhawy (1992). In this case, the net ultimate bearing pressure needs to be reduced using a factor of 2.7 to produces a target reliability index of 3.

The reduction factor used on net ultimate bearing pressure for satisfying the safety requirements in the case footings on power plant site (i.e., FS=2.7) is almost double the value that obtained for Adelaide university site (i.e., FS=1.43). This difference is attributed to higher CoV_{qua} in the former case.

It is observed that the mean and reduced standard deviations of spatial averaging soil property provide rational estimates of reliability of allowable bearing pressure of shallow foundations.

CHAPTER 6

EFFECT OF ANISOTROPIC STRUCTURE OF SPATIAL CORRELATION ON THE DESIGN OF SHALLOW FOUNDATIONS

6.1 Introduction

Directional variant autocorrelation structure is quite natural for soil properties due to the complex geological mechanisms involved in the formation and deposition of soil mass. This type of anisotropic structure of spatial variability is quite evident due to soil layering in sedimentary deposits (Vanmarcke 1977a; Soulie et al. 1990; Mostyn and Soo 1992; Przewlócki 2000; Nobahar and Popescu 2002; Fenton and Griffiths 2003). It is observed from the results presented in chapters 4 and 5 that the spatial correlation of soil properties plays a prominent role in the reduction of variance of the data. The results obtained from the studies by Catalan and Cornell (1976) and Alonso (1976) show that the variance reduction and hence the probability of failure reduces with reduction in autocorrelation distances. Mostyn and Soo (1992) and Li and White (1987) studied the performance of slopes incorporating the realistic autocorrelation structure in horizontal and vertical directions. The results show that the probabilities of failure were overestimated when the effect of correlation structure was neglected. Griffiths and Fenton (1997) found that the variance reduction factor consistently increases with the scale of fluctuation of coefficient of permeability. Fenton and Griffiths (2002) based on the analysis of settlement of shallow foundation state that taking autocorrelation distance as large is conservative and on the extreme side spatially constant soil property assumption leads to largest variability.

Section 2.4.7.1 presents a method to evaluate the variance reduction function for soil data in 1-D space. In addition, section 2.4.7.2.1 presents a method to compute variance reduction function using anisotropic autocorrelation structure of soil properties in 2-D and 3-D space. However, Vanmarcke (1977b) suggests an approach for dealing with anisotropic correlation characteristics by computing an equivalent autocorrelation distance, which is a function of horizontal and vertical autocorrelation distances. However, due to the complexity of the analysis and in practice there is often an insufficient number of measurements at suitable separation distances in 2-D and 3-D space to predict the necessary parameters for 2- or 3-dimensional models. Accordingly, the autocorrelation structure often is assumed isotropic in the horizontal plane, and the vertical and horizontal planes are treated separately (DeGroot 1996).

In this section, the effect of directional behaviour of soil property correlation structure on the bearing capacity of shallow strip footing resting on cohesionless soil deposit is analysed in 2-D random field.

6.2 Variance reduction of inherent variability in 2-D space

In this chapter two important issues are addressed. Firstly, parametric studies are conducted for the evaluation of simplified variance reduction function for data in 2-D random field using the corresponding functions developed for a 1-D field. The second part of the chapter presents the results of effect of autocorrelation distance on the reliability of shallow foundations. The significant contribution from all the three phases of uncertainty (inherent variability, measurement uncertainty, and transformation uncertainty) is considered appropriately in the analysis.

One of the following four alternative correlation structures are assumed to characterize the spatial variability of soil properties in a 2-D random field when no appropriate correlation structure either in horizontal, or vertical, or both directions is available.

I. Isotropic behaviour of correlation structure in horizontal and vertical directions (Alonso 1976; Griffiths and Fenton 1997; Fenton and Griffiths 2002, 2003, 2005).

II. Anisotropic behaviour of correlation structure in horizontal and vertical directions (Catalan and Cornell 1976; Mostyn and Soo 1992; Nobahar and Popescu 2001, 2002; Popescu et al. 2002)

III. Perfect correlation in horizontal direction

IV. Perfect correlation in both horizontal and vertical directions (D'Andrea and Sangrey 1982; Chowdhury 1987)

The effect of the above four cases on the variance reduction in 2-D space is illustrated using the cone tip resistance data pertaining to Texas A & M Riverside sand site. Analysis is done for shallow strip footing of width 1 m resting on the surface of cohesionless soil deposit in shear criterion. In general, for strip footings in cohesionless soils of loose to medium density subjected to a vertical load, it is safe to assume that the shear failure envelope extends to 2B from base of the footing in the vertical direction, and 3.5B from centre of the footing in the horizontal direction, where B is width the foundation (USACE 1992).

The spatial averaging distances in vertical and horizontal directions (L_v and L_h) are taken equal to the respective zones of influence in vertical and horizontal directions

(Cherubini 2000). Hence, L_v and L_h are taken equal to 2 m and 7 m respectively for a 1 m width of footing. Total eight profiles (CPT21, CPT23-29) are considered in the analysis, and it is assumed that all the eight cone tip resistance profiles considered in the analysis lie over a vertical plane surface, confined within the shear failure envelope.

Figure 6.1(a) shows the shear failure envelope below a loading footing resting on cohesionless soil deposit. In theoretical terms the average value of strength properties along the failure surface (not the average strength properties within the failure envelope) contributes to the resistance of the soil against the applied pressure of the footing. However, the shape and size of the failure envelope are functions of many parameters, viz., relative density, roughness of footing base, etc. Hence, it is highly difficult, albeit impossible, to arrive at the exact coordinates of every point on the failure surface. Hence, it has become customary to consider the strength of the soil properties within dashed lines shown in Figure 6.1(a) representing a rectangular area to evaluate the performance of the footing subjected to vertical applied pressures. Accordingly, the cone tip resistance (q_c) data from eight CPT soundings are considered within a vertical plane surface area of 7 m × 2 m below a vertically loaded footing of width 1 m, as shown in Figure 6.1(b).

The probabilistic characterization of the above cone tip resistance profiles is presented in Chapter 3. The averaged mean, standard deviation, and vertical autocorrelation distances for the above cone tip resistance profiles presented in Tables 6.1 are 5961 kPa, 2482 kPa, and 0.19 m, respectively.

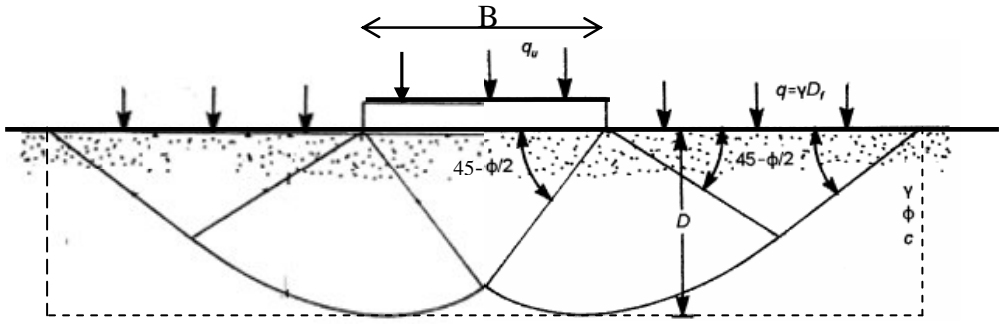

(a)

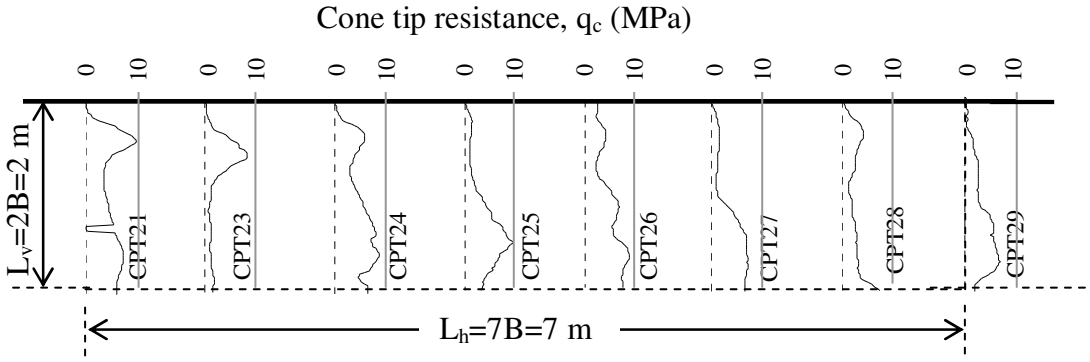

(b)

Figure 6.1(a). Shear failure envelope below a loaded footing; (b). Cone tip resistance (q_c) profiles considered within the shear failure envelope

Table 6.1. Statistical parameters of cone tip resistance (q_c) averaged over significant zone of influence for shear failure criterion (0-2 m below the footing base)

Sounding	Mean (kPa)	Standard deviation (kPa)	Coefficient of variation (CoV)	Vertical autocorrelation distance (m)	Vertical scale of fluctuation (m)
CPT21	7677	3418	45%	0.20	0.20
CPT23	6891	6188	90%	0.18	0.33
CPT24	7789	2066	27%	0.14	0.25
CPT25	5535	2619	47%	0.21	0.38
CPT26	7826	1544	20%	0.13	0.23
CPT27	5390	1567	29%	0.20	0.36
CPT28	2011	778	39%	0.19	0.19
CPT29	4569	1672	37%	0.23	0.23
Average values	**5961**	**2482**	**42%**	**0.19**	**0.27**

It is observed from the results of data analysis presented in Table 6.1 that a theoretical squared exponential function best fits the sample autocorrelation data for almost all the eight cone tip resistance data sets. However, due to lack of sufficient data for evaluation of autocorrelation structure for Riverside sand site in horizontal direction, autocorrelation distance ranging from 3-80 m is assumed in the horizontal direction.

6.3 Analysis of variance reduction factor in 2-D space

6.3.1 Isotropic behaviour of correlation structure in horizontal and vertical directions

In majority of the cases due to lack of closely spaced data of the site in horizontal direction, the autocorrelation distance in the horizontal and vertical directions are assumed equal to a finite value, leading to an isotropic correlation structure in the 2-D space. Hence, in this case, a reduced horizontal scale of fluctuation is used than the actual one. The resultant variance reduction factor for the data in 2-D space is computed as the product of individual variance reduction factors obtained for the 1-D data in vertical and horizontal space using Equation 2.35.

For isotropic assumption of correlation structure of cone tip resistance in horizontal and vertical directions, the following data are used for the evaluation of variance reduction factor.

Vertical autocorrelation distance of cone tip resistance (d_h) computed using the data obtained from CPT21, CPT23-29 profiles=0.19 m;

Horizontal autocorrelation distance of cone tip resistance (d_v)=0.19 m;

Spatial averaging length in vertical direction, L_v=2m, and

Spatial average length in the horizontal direction, L_h=7m.

For the above data, L_v/d_v is equal to 10.53 (=2/0.19), and L_h/d_h equals to 36.85 (=7/0.19). The variance reduction factors in vertical and horizontal directions are computed using Equation 2.35, as

$$\Gamma_v^2 = \left(\frac{0.19}{2}\right)^2 \left(\sqrt{\pi} \frac{2}{0.19} E\left(\frac{2}{0.19}\right) + \exp\left(-\left(\frac{2}{0.19}\right)^2\right) - 1 \right) = 0.159$$

$$\Gamma_h^2 = \left(\frac{0.19}{7}\right)^2 \left(\sqrt{\pi} \frac{7}{0.19} E\left(\frac{7}{0.19}\right) + \exp\left(-\left(\frac{7}{0.19}\right)^2\right) - 1 \right) = 0.047$$

Using Equation 2.44, the resultant variance reduction factor for the 2-D random field is computed from the above obtained variance reduction factors for 1-D space, as

$$\Gamma_A^2 = \Gamma_v^2 \times \Gamma_h^2 = 0.159 \times 0.047 = 0.0075$$

6.3.2 Anisotropic behaviour of correlation structure in horizontal and vertical directions

If the realistic values of autocorrelation distances, as reported by Phoon and Kulhawy (1999a) are replaced in the above calculations, the resultant variance reduction factor in 2-D field is obtained as given below.

Keeping all other parameters constant (vertical correlation distance, d_v=0.19 m, spatial averaging distance in vertical direction, L_v=2 m, and spatial averaging distance in horizontal direction, L_h=7 m), for a horizontal autocorrelation distance (d_h) of 3 m, the variance reduction factor for 2-D space is obtained as

$$\Gamma_v^2 = \left(\frac{0.19}{2}\right)^2 \left(\sqrt{\pi} \frac{2}{0.19} E\left(\frac{2}{0.19}\right) + \exp\left(-\left(\frac{2}{0.19}\right)^2\right) - 1 \right) = 0.159$$

$$\Gamma_h^2 = \left(\frac{3}{7}\right)^2 \left(\sqrt{\pi} \frac{7}{3} E\left(\frac{7}{3}\right) + \exp\left(-\left(\frac{7}{3}\right)^2\right) - 1 \right) = 0.576$$

$$\Gamma_A^2 = \Gamma_v^2 \times \Gamma_h^2 = 0.159 \times 0.576 = 0.0918$$

and, for a horizontal correlation distance of 80 m, the variance reduction factor for a 2-D space is obtained as given below.

$$\Gamma_v^2 = \left(\frac{0.19}{2}\right)^2 \left(\sqrt{\pi} \frac{2}{0.19} E\left(\frac{2}{0.19}\right) + \exp\left(-\left(\frac{2}{0.19}\right)^2\right) - 1 \right) = 0.159$$

$$\Gamma_h^2 = \left(\frac{80}{7}\right)^2 \left(\sqrt{\pi} \frac{7}{80} E\left(\frac{7}{80}\right) + \exp\left(-\left(\frac{7}{80}\right)^2\right) - 1 \right) = 0.9987$$

$$\Gamma_A^2 = \Gamma_v^2 \times \Gamma_h^2 = 0.159 \times 0.9987 = 0.1588$$

From the above calculations, it may be seen that when compared to the variance reduction factors obtained for realistic scales of fluctuation (i.e., $d_v/d_h<1$), the isotropic assumption (i.e., $d_h=d_v$) results in lower variance reduction factors. The lower variance reduction factors when multiplied with variance of point properties produce lower uncertainty of inherent variability of spatial average property, and subsequently underestimate the probability of failure. The results obtained from the above calculations are shown in Table 6.2 against $d_v=0.19$ m (2nd, 3rd, and 4th columns of 2nd row). The other results presented in Table 6.2 are discussed in the following sections.

Table 6.2. Variance reduction factors in 2-D space for cone tip resistance with L_v=2 m & L_h=7 m

Autocorrelation distance of cone tip resistance in vertical direction, d_v	d_h=0.19 m	d_h=3 m	d_h=80 m	d_h=∞
0.19 m	0.0075	0.0918	0.1588	0.159
∞				1

6.3.3 Perfect correlation of soil properties in horizontal direction

In cases where information on horizontal correlation structure is not available, the correlation distance is assumed to be perfectly (infinitely) correlated in the horizontal direction and the variance reduction in 2-D space is done considering the vertical correlation characteristics. For vertical correlation distance of 0.19 m, and spatial averaging distances in horizontal and vertical direction equal to 2 m and 7 m, the variance reduction factor for 2-D space is evaluated as given below.

$$\Gamma_v^2 = \left(\frac{0.19}{2}\right)^2 \left(\sqrt{\pi}\, \frac{2}{0.19} E\left(\frac{2}{0.19}\right) + \exp\left(-\left(\frac{2}{0.19}\right)^2 \right) - 1 \right) = 0.159$$

$$\Gamma_h^2 = \left(\frac{d_h}{7}\right)^2 \left(\sqrt{\pi}\, \frac{7}{d_h} E\left(\frac{7}{d_h}\right) + \exp\left(-\left(\frac{7}{d_h}\right)^2 \right) - 1 \right) = 1 \quad as\ d_h \to \infty$$

$$\Gamma_A^2 = \Gamma_v^2 \times \Gamma_h^2 = 0.159 \times 1 = 0.159$$

The above calculations show that the assumption of infinite autocorrelation distance in horizontal direction results in variance reduction factor of unity in that particular direction, and in this case, using Equation 2.44 the resultant variance reduction factor in 2-D space is equal to the variance reduction factor obtained for 1-D data in vertical direction.

It may be seen from the above calculations that the variance reduction factor in 2-D space with assumed perfect correlation in horizontal direction is more than that shown in section 3.6.2 for realistic autocorrelation distances. Hence, the assumption of infinite (or perfect) correlation length of soil strength properties in horizontal direction results in higher uncertainty and produces higher probability of failure than the actual estimate with realistic autocorrelation distances. This result with infinite

correlation length in horizontal direction is shown in Table 6.2 against $d_h=\infty$ and d_v=0.19 m. From Table 6.2 it can be seen that for d_v equals to 0.19 m, the variance reduction factor in 2-D space increases from 0.0075 to 0.159 as d_h increases from 0.19 m to ∞.

6.3.4 Perfect correlation of soil properties in horizontal and vertical directions

In conventional probabilistic analysis, the effect of spatial correlation of soil properties is totally ignored and soil properties are considered to be perfectly (or infinitely) correlated in space. But it is observed by many researchers that the soil properties are correlated only to a limited spatial extent, represented by autocorrelation distance.

$$\Gamma_v^2 = \left(\frac{d_v}{2}\right)^2 \left(\sqrt{\pi}\,\frac{2}{d_v} E\left(\frac{2}{d_v}\right) + \exp\left(-\left(\frac{2}{d_v}\right)^2\right) - 1 \right) = 1 \quad as\ d_v \to \infty$$

$$\Gamma_h^2 = \left(\frac{d_h}{7}\right)^2 \left(\sqrt{\pi}\,\frac{7}{d_h} E\left(\frac{7}{d_h}\right) + \exp\left(-\left(\frac{7}{d_h}\right)^2\right) - 1 \right) = 1 \quad as\ d_h \to \infty$$

$$\Gamma_A^2 = \Gamma_v^2 \times \Gamma_h^2 = 1 \times 1 = 1$$

The above calculations show that the assumption of infinite correlation distances of soil strength properties in both horizontal and vertical directions leads to higher variance reduction factor and thereby higher uncertainty than that obtained with realistic autocorrelation distances. This in turn produces conservative values of probability of failure.

6.4 Reliability analysis of bearing capacity

Reliability analysis is carried out to assess the influence of spatial correlation structure on the bearing capacity of shallow foundations. As mentioned in section 6.2, the width of foundation is 1 m and the footing is placed on the ground surface. The mean, standard deviation, coefficient of variation, and vertical autocorrelation distance of cone tip resistance of all the eight 'q_c' profiles within 0-2 m from ground surface are given in Table 6.1. The average of the values is given in the last row of the same table. For the reliability analysis, the horizontal autocorrelation distances of 0.19 m, 3 m, 80 m and infinity are assumed for cone tip resistance.

As explained in section 4.2, a two-step procedure (or indirect approach) is adopted to evaluate the mean and standard deviation of bearing capacity from the mean, standard deviation, autocorrelation distance of cone tip resistance, measurement uncertainty, and transformation model (Equation 4.1) uncertainty. In the first step, the point and spatial average statistical parameters (viz., mean and standard deviation) of the friction angle are evaluated from the mean, standard deviation, autocorrelation distance of cone tip resistance using the second-moment probabilistic techniques (Phoon and Kulhawy 1999b). In the second step, the statistical parameters of bearing capacity (q_u) are evaluated using the values of friction angle obtained in the first step.

Total four cases are analyzed in this section. In the first case, the analysis is done only for the effect of inherent variability of cone tip resistance on the reliability of shallow strip footing. In the second case both the inherent variability and measurement uncertainty of cone tip resistance are considered. Inherent variability and the uncertainty associated with transformation model given in Equation 4.1 are

considered in the third case. The last case considers the effect of all the three sources of uncertainty on the probabilistic evaluation of bearing capacity.

The coefficient of variation of transformation model given in Equation 4.1 is reported as 2.8˚. The coefficient of variation of measurement uncertainty of q_c (CoV_{eqc}) using an electric cone penetrometers is obtained as 8% (Phoon and Kulhawy 1999a). In the present analysis the variability of bearing capacity is assumed to be characterized by a lognormal distribution, and the variations in the load parameter are neglected. The reliability index corresponding to one third of the deterministic bearing capacity is assessed using Equation 2.57. Table 6.3 shows the coefficients of variation of bearing capacity (CoV_{qu}) for various combinations of autocorrelation distance in horizontal direction and CoV_{wqc}, CoV_{eqc}, and CoV_{ε}. The terms w, e, and ε refer to inherent variability, measurement uncertainty, and transformation model uncertainty components. The CoV_{qu} are also presented for different combinations of CoV_{wqc}, CoV_{eqc}, and CoV_{ε} and assuming perfect correlation of cone tip resistance in both directions.

The results show that the CoV_{qu} increases with increase of horizontal autocorrelation distance. Higher CoV_{qu} are obtained when the horizontal autocorrelation distance is perfectly correlated. Though the CoV_{qu} is 42% when considering inherent variability alone and perfect autocorrelation of cone tip resistance in both directions, its value significantly reduced for the remaining three combinations as given in Table 6.3. A least value of CoV_{qu} is obtained when inherent variability and measurement uncertainty are considered, neglecting the transformation uncertainty.

Table 6.3. Coefficients of variation of bearing capacity for different combinations of sources of uncertainty and horizontal correlation distance of cone tip resistance (autocorrelation distance in vertical direction, d_v=0.19 m)

Combinations of different sources of uncertainty	Coefficient of variation of bearing capacity (CoV_{qu})				
	Autocorrelation distance of q_c in horizontal direction				Perfect correlation in both directions
	0.19 m	3 m	80 m	∞	
w	4%	13%	17%	17%	42%
w+e	1%	2%	3%	3%	5%
w+ε	7%	7%	8%	8%	9%
w+e+ε	7%	7%	8%	8%	9%

Table 6.4. Variation of reliability index for different combinations of sources of uncertainty and horizontal correlation distance of cone tip resistance (autocorrelation distance in vertical direction, d_v=0.19 m)

Combinations of different sources of uncertainty	Reliability index (β)				
	Autocorrelation distance of q_c in horizontal direction				Perfect correlation in both directions
	0.19 m	3 m	80 m	∞	
w	30	9	7	7	3
w+e	108	63	51	51	22
w+ε	16	16	15	15	13
w+e+ε	16	16	15	15	13

Table 6.4 shows the variation of reliability index with different values of horizontal autocorrelation distance. When only the effect of inherent variability is considered, the reliability index varies quite widely from 30 to 7 with increase of horizontal scale of fluctuation from 0.19 m to ∞. Hence, it may be seen that assumption of isotropic correlation structure of q_c (d_v=d_h=0.19 m) produces higher reliability indices than that produced for cases with d_v/d_h<1. The remaining three cases also show significant variations of reliability index with horizontal scales of fluctuation. When the analysis

is based on the coefficients of variation obtained from all the three uncertainties (inherent, measurement, transformation uncertainties) the reliability index does not show significant decrease with horizontal autocorrelation distance. Here the transformation model is identified as the primary factor influencing the degree of variability of design parameter.

6.5 Conclusions

The assumption of isotropic correlation structure based on vertical autocorrelation distance underestimates the variability of design parameter in a 2-D space, than that obtained with realistic autocorrelation distances in horizontal and vertical directions (i.e., for the case with $d_v/d_h<1$).

Assumption of perfect correlation both in horizontal or vertical, or both directions, overestimates the variability of design parameters, and produces conservative estimates of bearing capacity.

In general, horizontal scale of fluctuation is difficult to measure as more sampling points are necessary in horizontal direction when compared to that in vertical direction. Hence in the absence of such data, it is recommended to assume perfect correlation in the horizontal direction, rather than isotropic behaviour based on vertical autocorrelation distance. The analysis based on this assumption produces conservative estimates of bearing capacity.

In the case of absence of data on scales of fluctuation in either direction for a particular site, it is suggested to use an upper bound value from the range of observed values from the records of past experience with the similar sites.

When inherent variability alone is considered, the assumption of perfect correlation of cone tip resistance in both horizontal and vertical directions, produce higher coefficient of variation of bearing capacity and hence, lower reliability index for ultimate limit state in shear criterion. The transformation model is identified as the crucial factor influencing the degree of estimated uncertainty in the design.

However, when both inherent and measurement uncertainty are considered, even the assumption of perfect correlation of cone tip resistance in horizontal and vertical directions, reduced the CoV_{qc} drastically, and as a result the analysis predicted higher reliability index. In this case, the design uncertainty (CoV_{qc}) is lower than the individual component uncertainties, viz., CoV_w=42% and CoV_e=8%.

The results of the study show that the transformation model undermines the effect of inherent variability on the design property variability.

In conclusion, the need for a proper evaluation methodology for calculation of correlation lengths of soil properties and their influence in foundation design is highlighted in this chapter.

CHAPTER 7

LOAD RESISTANCE FACTORED DESIGN OF SHALLOW FOUNDATIONS

7.1 Introduction

It is useful to calibrate engineering codes on regional basis, as similar ranges of parameter variations are encountered within a particular region, due to similar geologic processes involved with the deposition and formation of soil, the stress history to which the underlying soil is subjected, similar testing procedures, transformation functions developed based on local data, and socio-economical factors. These codes are calibrated to achieve a target reliability level in the designs, and recommend the load and resistance factors for direct use in design. In India efforts are being made in the evaluation of load resistance factors for foundation design codes and the contents of the present chapter focus in this direction. The objective of the present study is to evaluate the resistance factors for shallow foundations in ultimate limit state (ULS) by calibration through Working Stress Design (WSD) and Reliability Based Design (RBD). A comparison of foundation designs based on the above two approaches is also made.

7.2 Calibration of resistance factors

The critical load combinations given in Table 7.1 (Becker 1996b) for WSD are observed to be functions of two important ratios of loads, such as ratio of dead load and live load (D/L) and ratio of wind load and live load (W/L). These load combinations have been classified in four groups based on a range of W/L ratios.

.
They are 0-0.43, 0.43-1, 1-2.33, and >2.33. However, in case of Limit State Design (LSD), the load combinations are stated as functions of W/L alone (Becker 1996b). The effect of wind load is negligible, if it is within 43% of live load. Hence, under these circumstances, it does not produce a critical load combination.

The load combinations given in Table 7.1, are used in the present analysis for obtaining the resistance factors for design of shallow foundations in ultimate limit state (ULS), using calibrations based on WSD and RBD approach.

Table 7.1. Maximum load combinations for code calibration with Working Stress Design for ultimate limit state

Loading case	Wind/live load ratio (W/L)	Maximum load combinations	
		LSD ($\sum\alpha_i S_{ni}$)	WSD ($\sum S_{ni}$)
1	0-0.43	1.25D+1.5L	If D/L<3W/L-1 $\sum S_{ni}=0.75(D+L+W)$
			If D/L≥3W/L-1 $\sum S_{ni}=D+L$
2	0.43-1	1.25D+1.05(L+W)	If D/L<3W/L-1 $\sum S_{ni}=0.75(D+L+W)$
			If D/L≥3W/L-1 $\sum S_{ni}=D+L$
3	1-2.33	1.25D+1.05(L+W)	If D/L<3-W/L $\sum S_{ni}=0.75(D+L+W)$
			If D/L≥3-W/L $\sum S_{ni}=D+W$
4	>2.33	1.25D+1.5W	If D/L<3-W/L $\sum S_{ni}=0.75(D+L+W)$
			If D/L≥3-W/L $\sum S_{ni}=D+W$

7.2.1 By fitting with Working Stress Design (WSD)

In working stress design, the nominal or characteristic resistance (R_n) is expressed as the product of factor of safety and the sum of the nominal loads (S_{ni}) on the system (Becker 1996a), given by Equation 7.1. The random nature of loads and resistances is implicitly taken into account while selecting the nominal values.

.

$$R_n = FS \times \Sigma S_{ni} \tag{7.1}$$

The LRFD format in this case is

$$\Phi R_n \geq \sum \alpha_i S_{ni} \tag{7.2}$$

The resistance factor Φ is evaluated as

$$\Phi = \frac{\Sigma \alpha_i S_{ni}}{FS \, \Sigma S_{ni}} \tag{7.3}$$

where, α and FS are the load factor and factor of safety respectively.

Table 7.2 shows the resistance factors, Φ, evaluated using Equation 7.3 and critical load combinations shown in Table 7.1 by calibration with WSD for different values of W/L, L/D, and FS. The resistance factor at each of the combinations of W/L and FS is shown for L/D ratios ranging from 0.2 to 10. It is seen from the results that as W/L ratio increases, there is a slight increase of Φ value. It is also observed that the resistance factor decreases with increase of FS. This is obvious as higher factors of safety correspond to higher degree of uncertainty, and hence lower resistance factors should be used in the analysis to satisfy the designs based on Equation 7.2.

The resistance factors evaluated for all the ratios of W/L are averaged out and shown in Table 7.2. A range of Φ evaluated from all the possible W/L ratios for FS= 2.5 and 3.0 are shown as 0.52-0.61 and 0.43-0.51 respectively. The corresponding mid-values are 0.57 and 0.47. The last row of the Table 7.2 shows the suggested Φ values with respect to different FS.

Normally, a factor of safety of 2.5 to 3 is used in deterministic procedures to implicitly account for all the sources of uncertainty in the evaluation of onshore foundation design capacity (Meyerhof 1982). Hence, a Φ value of 0.5, which when

.
multiplied with the nominal resistance, produces identical designs having a factor of safety between 2.5 and 3.0.

Table 7.2. Summary of resistance factors, Φ, for bearing resistance from code calibration with working stress design (WSD)

W/L ratio	Range of Φ values for 0.2<=L/D<=10 and for various FS					
	FS=1.5	FS=2.0	FS=2.5	FS=3.0	FS=3.5	FS=4.0
0	0.86-0.98	0.65-0.74	0.52-0.59	0.43-0.49	0.37-0.42	0.32-0.37
0.4	0.86-0.97	0.65-0.73	0.52-0.58	0.43-0.49	0.37-0.41	0.32-0.36
0.5	0.87-0.98	0.65-0.73	0.52-0.59	0.43-0.49	0.37-0.42	0.33-0.36
1	0.93-1.02	0.70-0.77	0.56-0.61	0.46-0.51	0.40-0.44	0.35-0.38
2	0.90-0.98	0.67-0.73	0.54-0.59	0.45-0.49	0.38-0.42	0.34-0.37
3	0.90-0.99	0.67-0.75	0.54-0.60	0.45-0.50	0.38-0.43	0.34-0.37
5	0.92-1.00	0.69-0.75	0.55-0.60	0.46-0.50	0.39-0.43	0.34-0.37
10	0.94-1.00	0.71-0.75	0.57-0.60	0.47-0.50	0.40-0.43	0.35-0.37
Entire Φ range	0.86-1.02	0.65-0.77	0.52-0.61	0.43-0.51	0.37-0.44	0.32-0.38
Φ Mid-value	0.94	0.71	0.57	0.47	0.41	0.35
Suggested Φ value	0.95	0.70	0.55	0.45	0.40	0.35

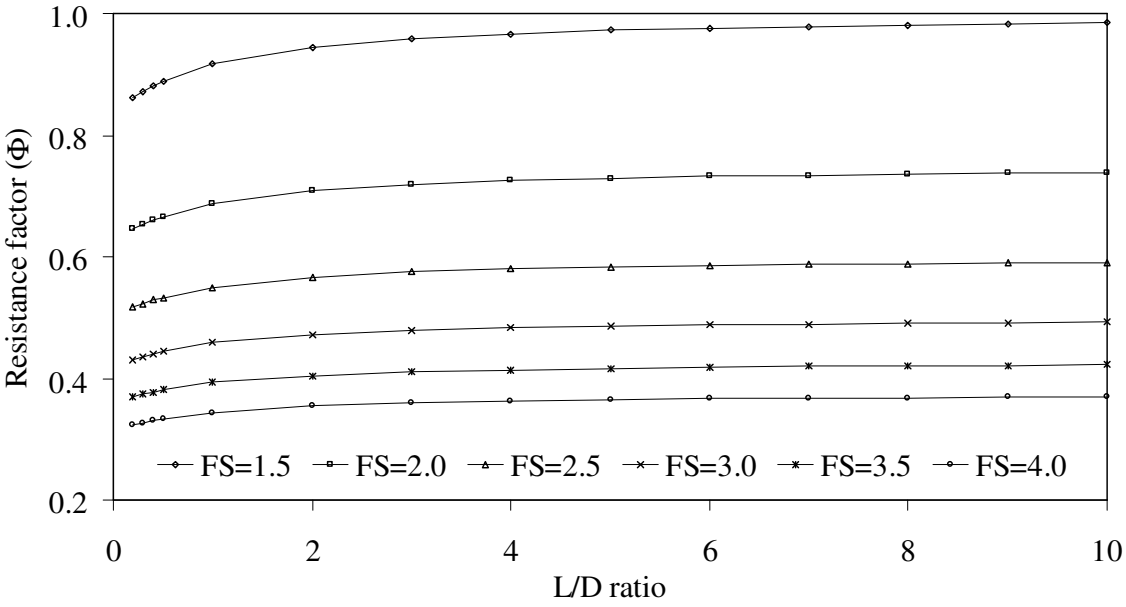

Figure 7.1. Code calibration with Working Stress Design for bearing capacity of shallow foundation in ultimate limit state using Q/L=0

.

The variation of resistance factors (Φ) for different values of L/D ratio, as a function of FS, for W/L ratios of 0, 0.4, and 2 are also shown in Figures 7.1 to 7.3.

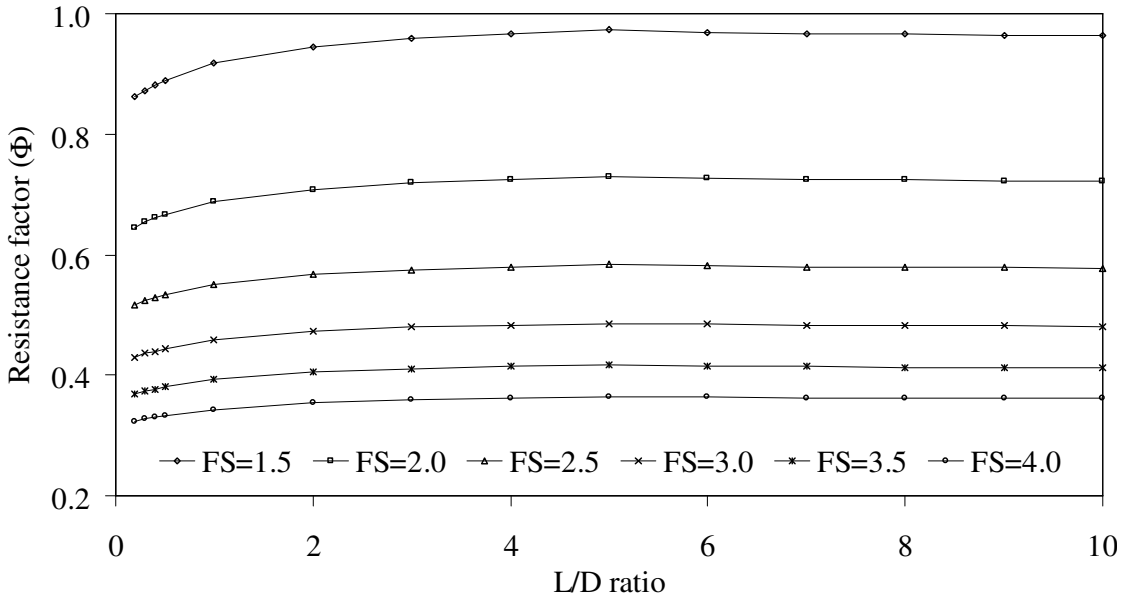

Figure 7.2. Code calibration with Working Stress Design for bearing capacity of shallow foundation in ultimate limit state using W/L=0.4

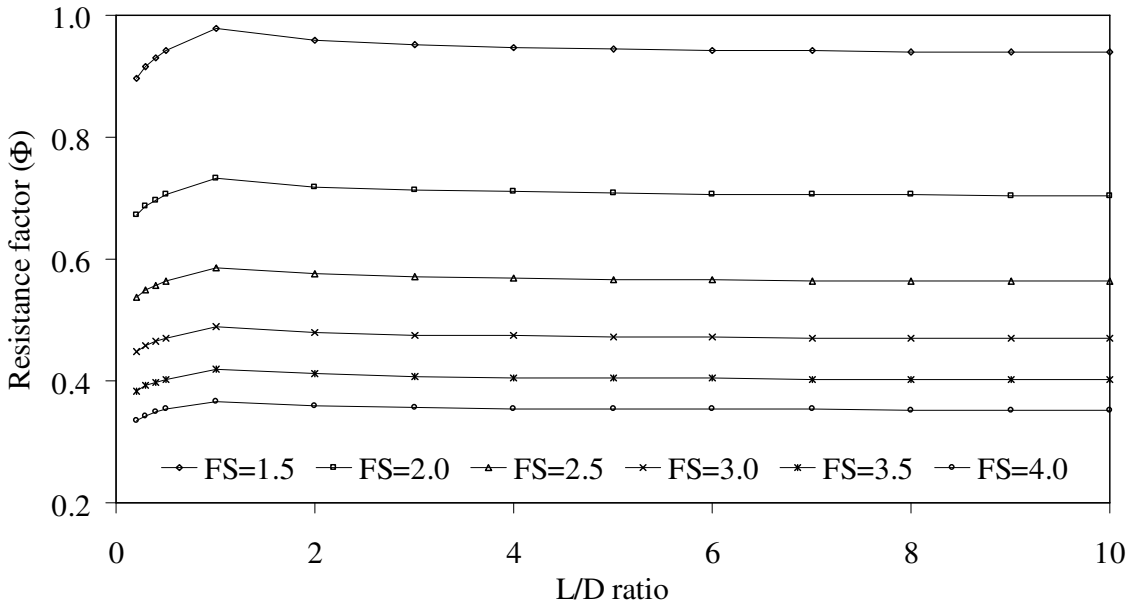

Figure 7.3. Code calibration with Working Stress Design for bearing capacity of shallow foundation in ultimate limit state using W/L=2

.

7.2.2 By fitting with Reliability Based Design (RBD)

The LRFD format in ultimate limit state (Becker 1996a) is given in Equation 7.4.

$$\Phi R_n \geq \alpha S_n \tag{7.4}$$

where Φ and α are evaluated as

$$\Phi = k_R \exp(-\beta\theta V_R) \tag{7.5}$$

$$\alpha = k_S \exp(\beta\theta V_S) \tag{7.6}$$

Where k_R and k_s are defined as $\frac{\overline{R}}{R_n}$ and $\frac{\overline{S}}{S_n}$, $\overline{R}$ and $\overline{S}$ are mean values of resistance and load parameters, and R_n and S_n are nominal values of resistance and load parameters, β is the target reliability index to be achieved in the designs, and V_R and V_S are coefficients of variation of resistance and load, 'θ' is termed as separation coefficient. For independent R and S variables following lognormal distribution, 'θ' is defined as given in Equation 7.7. Figure 7.4 shows the variation of separation coefficient with the ratio of V_R and V_S.

$$\theta = \frac{\sqrt{1+\left(\frac{V_R}{V_S}\right)^2}}{1+\frac{V_R}{V_S}} \tag{7.7}$$

Table 7.3 shows typical resistance factors for ultimate limit state (bearing resistance) calibrated using reliability based design based on Equation 7.5. These factors are calibrated for a coefficient of variation of resistance (V_R) of 0.3, and mean resistance to characteristic resistance, k_R=1.1. The ranges of Φ values tabulated against each FS and W/L ratio are obtained for L/D ratios ranging from 0.2 to 10. As seen from the Table 7.3, reliability index (β), and resistance factor (Φ) increase significantly with

.
factors of safety (FS) for a unique ratio of W/L. The β value ranges from a lower value of 0.49 to an upper value of 5.45 for variation of FS from 1.5 to 4.0.

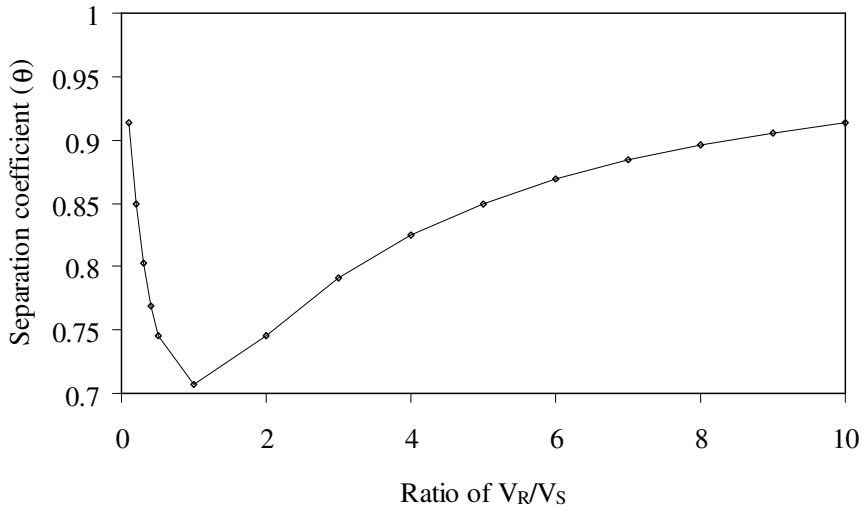

Figure 7.4. Variation separation coefficient with ratio of coefficients of variation of resistance (V_R) and load (V_S)

It is observed from the results of the analysis that β decreases with W/L ratio. Entire range of evaluated reliability indices (β), corresponding to each FS is also shown in the Table 7.3, along with the corresponding mid values. The resistance factors, which produce identical designs to that based on RBD approach, are evaluated from Equation 7.5 corresponding to different mid-values of reliability indices. From the results shown in Table 7.3, it can be seen that a FS of 2.5 corresponds to an average value of β equals to 3. For this case, a resistance factor, Φ, equals to 0.45 produces an identical design. Similarly, Φ values of 0.35 and 0.29 correspond to β of 3.8 and 4.5 respectively.

Similar to Figures 7.1-7.3, Figures 7.5-7.7 show the variation of reliability index with L/D ratio and FS using RBD approach of code calibration. The reliability indices are almost unaffected in the region, between L/D ratio of 3 and 10. However, a slight decrease of reliability indices is observed between L/D=0.2 and L/D=3. As seen in the previous section, the reliability indices decrease with increase of FS, and β of 3,

.
which is an acceptable target reliability level generally required to achieve in normal designs, could be achieved with a factor of safety of 3. From Table 7.3 and Figures 7.5-7.7, it can be said that the reliability indices are almost constant with increased W/L ratio. It may be noted from the Figure 7.7 that the reliability indices initially reduce with L/D ratio till L/D ratio of unity, and then increases slightly with further increase in L/D ratio.

Table 7.3. Summary of reliability index, β, and resistance factor, Φ, for bearing resistance from code calibration with Reliability Based Design (RBD) using coefficient of variation of resistance, V_R=0.3, ratio of mean resistance to characteristic resistance, k_R =1.1

	Range of β values for 0.2<=L/D<=10 and for various FS					
W/L ratio	FS=1.5	FS=2.0	FS=2.5	FS=3.0	FS=3.5	FS=4.0
0	0.49-1.09	1.77-2.37	2.76-3.36	3.57-4.17	4.26-4.85	4.85-5.45
0.4	0.55-1.09	1.83-2.37	2.82-3.36	3.63-4.17	4.31-4.85	4.91-5.45
0.5	0.52-1.05	1.80-2.32	2.79-3.32	3.60-4.13	4.29-4.81	4.88-5.40
1	0.33-0.76	1.60-2.04	2.60-3.03	3.41-3.84	4.09-4.52	4.69-5.12
2	0.52-0.92	1.80-2.19	2.79-3.19	3.60-4.00	4.29-4.68	4.88-5.27
3	0.45-0.91	1.73-2.19	2.72-3.18	3.53-3.99	4.21-4.68	4.81-5.27
5	0.44-0.81	1.72-2.09	2.71-3.08	3.52-3.89	4.20-4.58	4.80-5.17
10	0.43-0.68	1.71-1.96	2.70-2.95	3.51-3.76	4.20-4.44	4.79-5.04
Entire range of β	0.33-1.09	1.60-2.37	2.60-3.36	3.41-4.17	4.09-4.85	4.69-5.45
Mid-value of β	≈0.7	≈2.0	≈3.0	≈3.8	≈4.5	≈5.0
Suggested Φ value	0.89	0.61	0.45	0.35	0.29	0.24

Figure 7.8 shows the variation of factor of safety and reliability index with resistance factor. Higher safety indices in both the approaches of design, viz., WSD and RBD, correspond to lower resistance factors. Figures 7.9 and 7.10 show the variation of resistance factors with reliability index for various coefficients of variation of resistance.

.

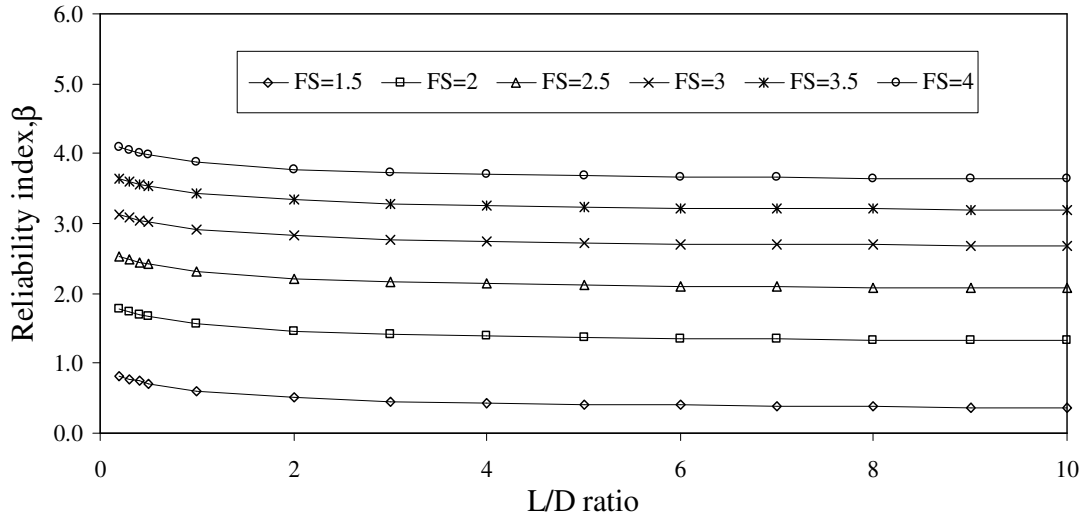

Figure 7.5. Code calibration with Reliability Based Design (RBD) for bearing capacity of shallow foundation in ultimate limit state using W/L=0

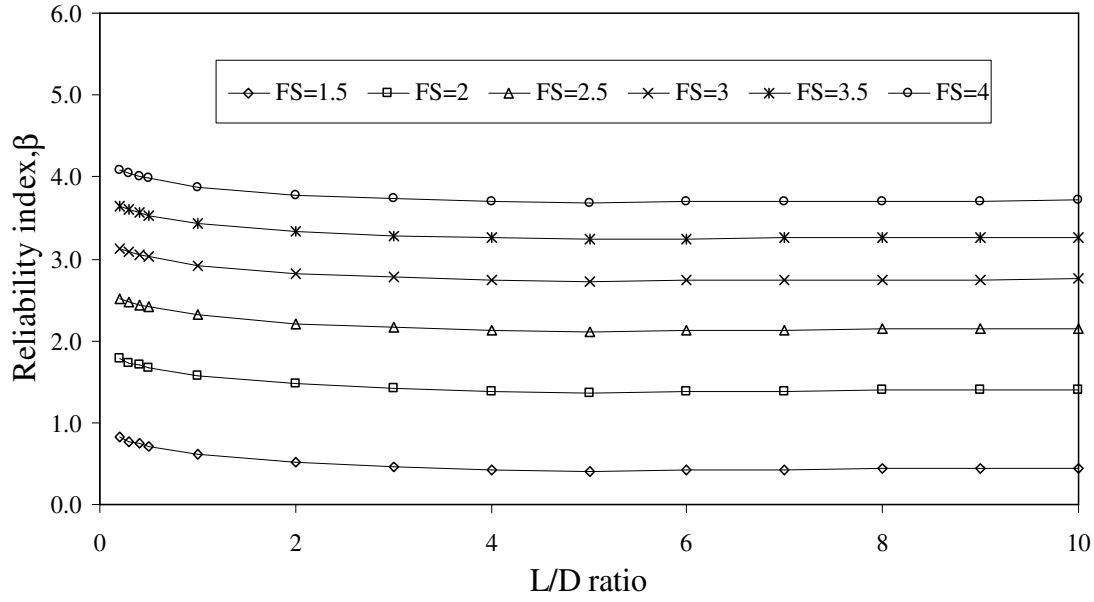

Figure 7.6. Code calibration with Reliability Based Design (RBD) for bearing capacity of shallow foundation in ultimate limit state using W/L=0.4

Higher variations in resistance give rise to lower resistance factors, corresponding to any particular target reliability level achieved in the design, and also for a unique coefficient of variation of resistance, as the target reliability index increases the resistance factor decreases. For example, if V_R is 0.3, the resistance factor reduces approximately from 0.7 to 0.4 for β increasing from 2 to 5.

.

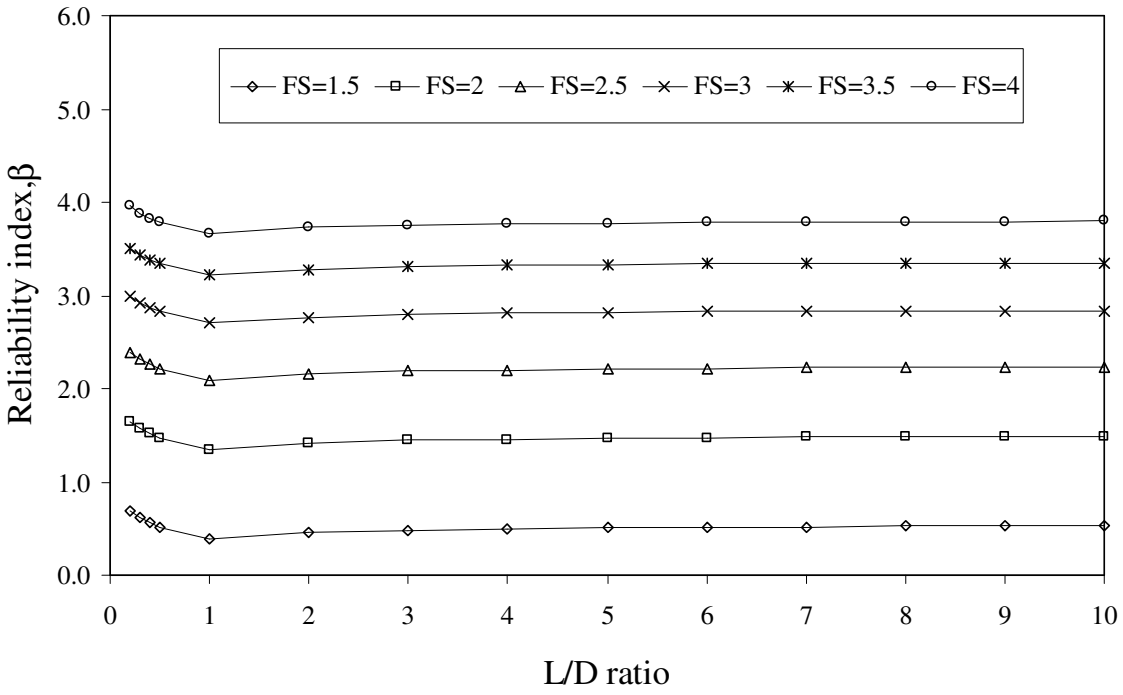

Figure 7.7. Code calibration with Reliability Based Design (RBD) for bearing capacity of shallow foundation in ultimate limit state using W/L=2

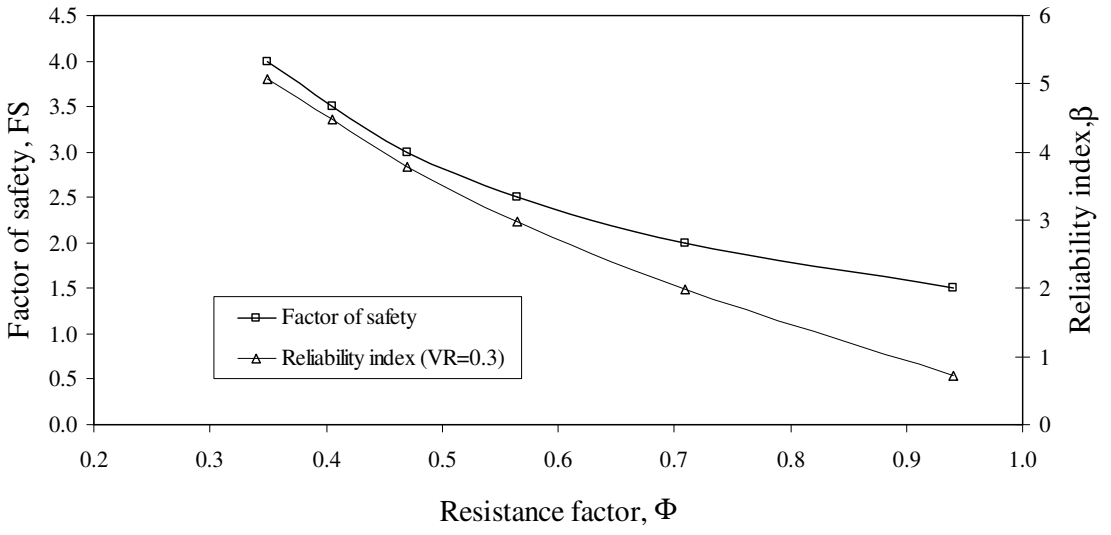

Figure 7.8. Variation of factor of safety, FS, and reliability index, β, with resistance factor, Φ

.

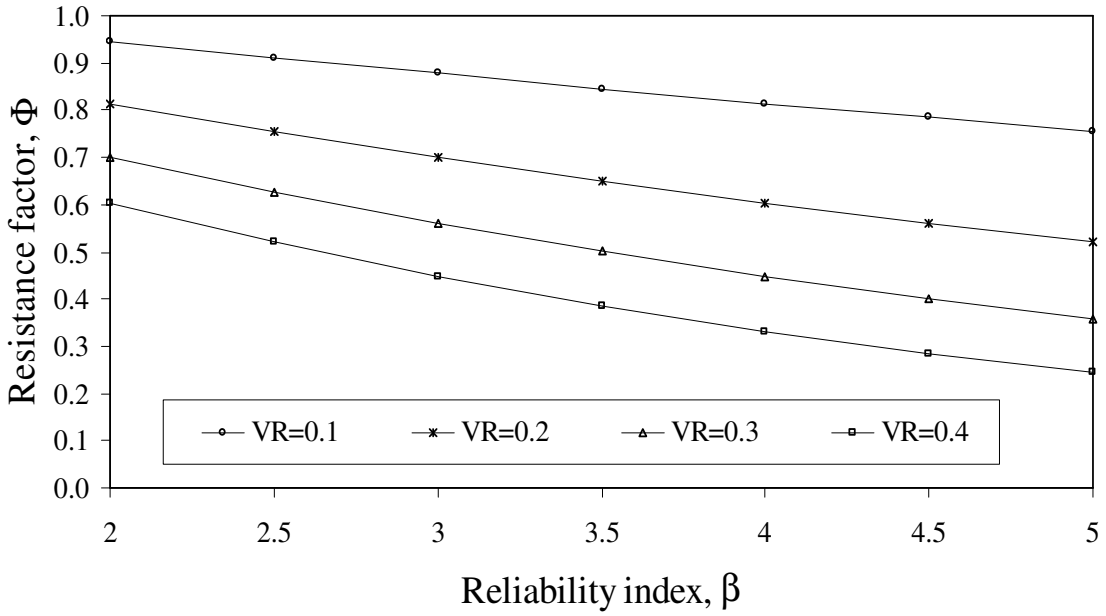

Figure 7.9. Variation of resistance factor, Φ, with coefficients of variation of resistance, V_R, for ratio of mean resistance to characteristic resistance, k_R=1.1

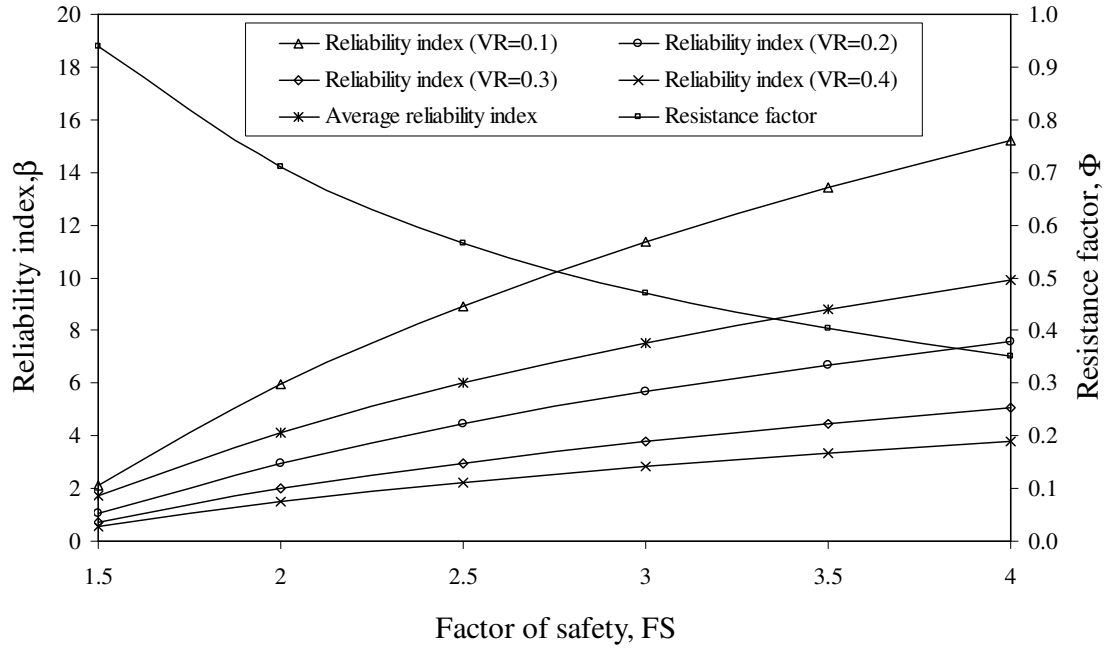

Figure 7.10. Variation of resistance factor, Φ, and reliability index, β, with factor of safety, FS, for α_D=1.2 and α_L=1.5

.

7.3 Design of foundations based on LRFD approach

7.3.1 Analysis for width of foundation

The above obtained resistance factors calibrated from both the WSD and RBD approaches are used to design two footings resting on surface of ground, one in cohesive soil and the other in cohesionless soil. In the first case, i.e., footing resting on surface of clayey soil, the size of the square footing is designed for a nominal applied load of 400 kPa using both the working stress design and limit state design based on resistance factors. Three values of undrained cohesion are used in the analysis. Factor of safety of 3 and resistance factor of 0.5 are adopted in the design, with load factors of 1.2 and 1.5 for dead and live loads respectively at critical combination of loads in ultimate limit state. Figure 7.11 shows the size of the footing obtained from WSD and LRFD approaches. The footing width decreases with increase of undrained cohesion. The footing width is unaffected with L/D ratio in the case of WSD, and it increases slightly approximately up to L/D ratio of 2 and thereupon constant in case of LRFD approach. This difference in variations of footing width with L/D ratio in WSD and LRFD is attributed to different load factors for dead and live loads used in LRFD approach. In WSD approach, no distinction is made on dead and live load factors to be used in critical load combinations. However, in LSD approach a higher load factor is applied on live load than that on the dead load, because of higher variations observed in the former case.

Figure 7.12 presents the ratio of footing widths obtained in both the approaches for different cohesion values, factors of safety, and L/D ratio. In all the cases, the ratio is unaffected by strength of soil in terms of cohesion.

.

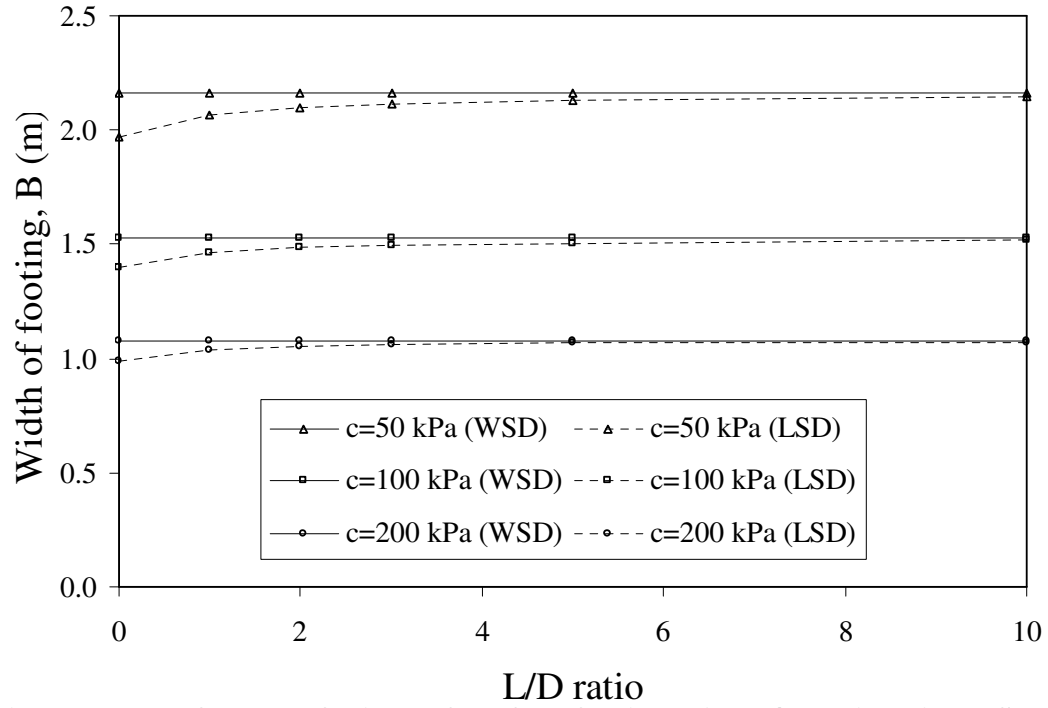

Figure 7.11. Influence of width of surface footing with L/D ratio using LSD and WSD, for S_n=400 kPa, γ=18 kN/m3, Φ=0.5, α_D=1.2, α_L=1.5, and FS=3

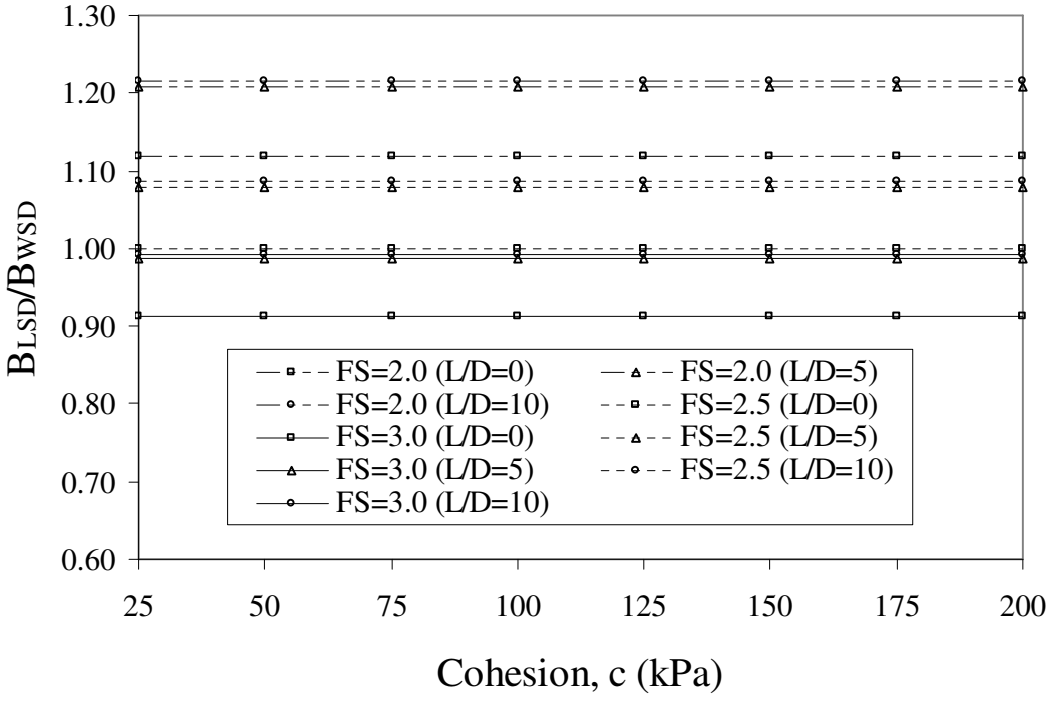

Figure 7.12. Relative comparison of widths of surface footing in cohesive soils using LSD and WSD, for S_n=400 kPa, γ=18 kN/m3, Φ=0.5, α_D=1.2 and α_L=1.5

Results from all these combinations shows that irrespective of factors of safety, L/D=0 always results in lower ratio of B_{LSD}/B_{WSD}, and this ratio is increases with

.
increase of L/D ratio, even though there is no much difference between the corresponding ratios obtained for L/D=5 and L/D=10. The ratio of B_{LSD}/B_{WSD} decreases with increase of factor of safety. In the case of FS=2.0 and 2.5, the width of footing obtained from LSD is higher than that obtained from WSD, with an exception to L/D=0 with FS=2.5. The case with FS=2.5 and L/D=0 results in B_{LSD}/B_{WSD} ratio of unity irrespective of cohesion of soil. Hence, if a conventional factor of safety of 2.5 is used one could say that a resistance factor of 0.5 is sufficient to produce a consistent design.

7.3.2 Evaluation of bearing capacity

The second case pertains to evaluation of nominal bearing capacity of 2 m × 2 m shallow foundation resting on cohesionless soil deposit. The results of analysis based on both approaches are shown in Figure 7.13.

Unit weight of soil, γ, Resistance factor, Φ, dead load factor (α_D) and live load factor (α_L) are taken from the previous example. From Table 7.3, it is evident that the resistance factor of 0.5 used in the analysis corresponds to coefficient of variation of resistance, V_R, of 0.3 and reliability index, β, of 3.5. The ratios of nominal loads obtained from LRFD approach and WSD approach are plotted against angle of internal friction (ϕ) for all the 6 combinations of L/D and FS, as described in the previous example. In this case, the results obtained from L/D=0 and FS=3.0 are invariant with respect to design approach, viz., WSD or LRFD.

The ratios of S_{nLSD}/S_{nWSD} less than unity implies that the WSD approach results in higher allowable bearing pressure, and the allowable pressure obtained by WSD approach using FS=2.0, corresponds to reliability index lower than the target value

.

of 3.5. Hence, it is concluded that a factor of safety of 2.0 on ultimate bearing pressure does not account for a coefficient of variation of resistance (V_R) of 30%, and the designs produced from this factor of safety overestimates the bearing capacity.

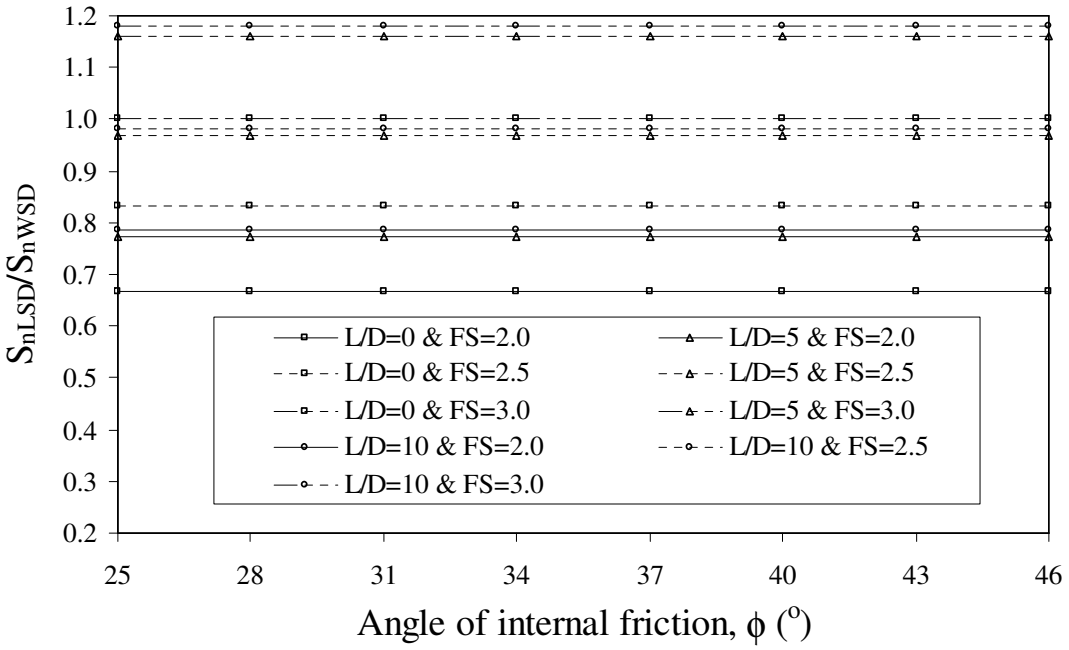

Figure 7.13. Relative comparison of nominal load on surface footings in cohesionless soils using LSD (factored resistance approach) and WSD, for B= 2m, γ=18 kN/m3, Φ=0.5, α_D=1.2 and α_L=1.5

To produce consistent designs based on WSD approach it is required to use higher factors of safety. Figure 7.14 shows the results of ratios of S_{nLSD}/S_{nWSD} obtained using factored strength approach for the surface footing resting on cohesionless deposit as described in the previous section, wherein a factored resistance approach has been adopted. The partial factor is applied on the angle of internal friction (ϕ) rather than on the bearing capacity. A partial factor ($f_{tan\phi}$) of 1.25 is used in the present analysis. Unlike in the previous case, the ratio of S_{nLSD}/S_{nWSD} is not constant, but, decreases with increase of angle of internal friction (ϕ). The variation is significantly high in the case of FS=3.0. Moreover, the S_{nLSD}/S_{nWSD} ratio is not invariant with respect to angle of internal friction.

.

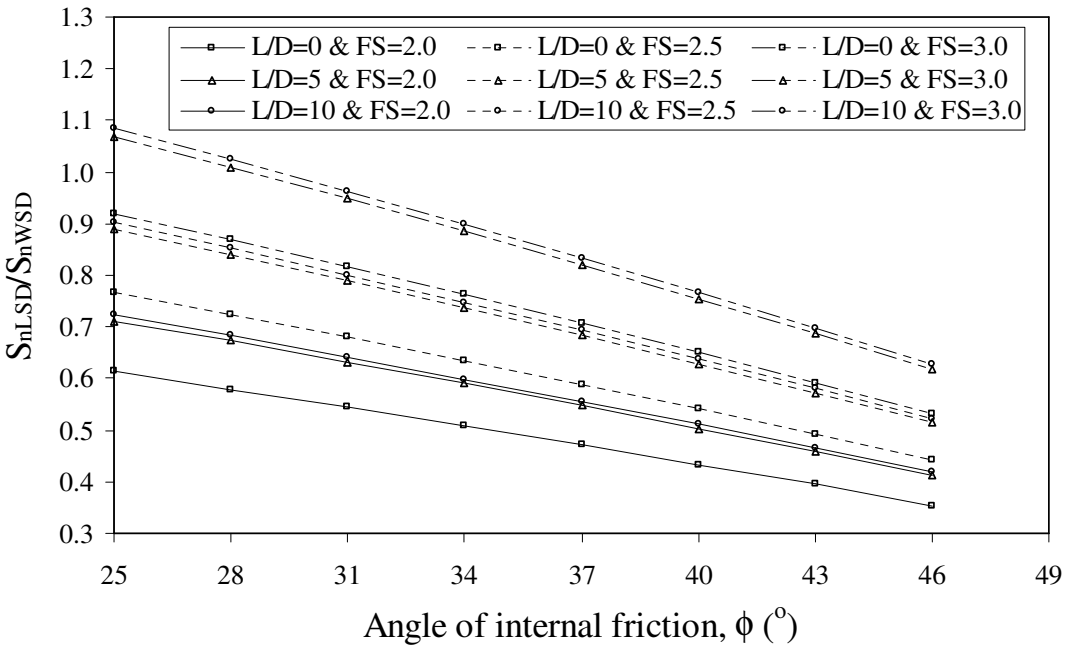

Figure 7.14. Relative comparison of nominal load on surface footings in cohesionless soils using LSD (factored strength approach) and WSD, for B=2 m, γ=18 kN/m3, $f_{tan\phi}$=1.5

7.4 Conclusions

Limit state design approaches facilitate the engineers to design the structures considering implicitly the prevailing uncertainty in design parameters arising out of various sources.

The limit state design based on load resistance factored design produces consistent designs with uniform safety levels than that using Working Stress Design approach.

The results from the code calibration using working stress design approach show that resistance factors of 0.45 and 0.55 correspond to conventional factors of safety of 3.0 and 2.5 respectively.

The resistance factors calibrated based on working stress design decreases with increase of required factors of safety in the design. Similarly, the computed resistance factors reduce with target reliability levels to be achieved in a design.

.

The results from the code calibration using reliability based approach show that for a coefficient of variation of resistance of 30%, and a target reliability index of 3.0, a resistance factor of 0.45 is obtained to produce consistent designs. The corresponding resistance factor for a reliability index 3.5 is approximately equal to 0.4.

The calibrated resistance factors depend on the degree of variations in ground conditions, confidence in the measured soil strength parameters, and computed design parameters, sensitivity of the project in terms of failure consequences, etc. Higher uncertainty in the design parameters and high failure consequences result in lower calibrated factors.

Since, it is not appropriate to recommend a single resistance factor for entire range of possible coefficient of variation, it is useful to divide the whole range of coefficients of variation (CoV) of strength parameters encountered in a region into number of intervals and calibrate the resistance factors for each of these classes.

The essential benefit derived from the load resistance factors or load strength factors is that the designs are consistent, in the sense that they produce uniform safety levels in the design.

The load resistance factored design or load strength factored design approaches give intermediate solutions when compared to solutions in terms of results obtained from traditional Working Stress Design (WSD) and complete Reliability Based Design (RBD) approaches.

Chapter 8

RELIABILITY ANALYSIS OF SOIL SLOPES

8.1 Introduction

As discussed in earlier chapters, the uncertainty is pervasive in nature, and analyses of stability of slopes based on deterministic approaches, explicitly accounting for the various sources of uncertainty, such as, natural variability of slope material, variability associated with the determination of mean soil properties, geometry of the slope, mechanistic stability model, etc., need analysis in terms of reliability and risk design considerations as well. Reliability based approaches have been found to present consistent results in these situations, as they appropriately consider all the possible sources of variability and their influence on the design process and decisions (Chowdhury 1987; Chowdhury et al. 1997; Griffiths and Fenton 2000, 2004; Chong et al. 2000; Tung and Chan 2003; Zhang et al. 2005).

In this chapter, the stability of slopes has been studied under two major sections. The first section deals with the stability of unsaturated soil slopes in the great Himalayan region of Indian sub-continent, and the second section deals with the stability of soil slopes in seismically active zones. The objectives of the study are (a) to recognize the importance of variability associated with the evaluation of soil parameters and the suction characteristics, and evaluation of performance of a typical slope against landslide; (b) to derive the optimum slope angles against static and pseudo-static loading, considering the affect of various sources of parameter uncertainty, their associated failures, and cost of failure consequences appropriately.

8.2 Analysis of unsaturated soil slopes

Many soil slopes are unsaturated in their initial state, and suction contributes to initial stability. Stability of these slopes decreases as suction decreases with time due to rainfall infiltration and water redistribution. Many of the parameters in the assessment of stability of soil slopes are highly variable. In this study, sensitivity/reliability analysis of design variables for a typical unsaturated soil slope is conducted. The objective of the study is to demonstrate the use of reliability analysis for a typical unsaturated soil slope in a slide area.

8.2.1 Method of analysis

Instability of unsaturated soil slopes after rainfall is common in many countries, and these failures are generally shallow and are usually parallel to the slope surface. The stability of these slopes can be analyzed by a simple infinite slope analysis (Cho and Lee 2002).

Rao et al. (1995) presented a few typical cases of landslides in the Sutlej valley of Himachal Pradesh, India and presented data pertaining to a landslide called Powari landslide, which is used in the present study. In the slide area under study, the unsaturated soil slopes tend to fail in shear along planar surfaces parallel to the ground surface. The observed depth of failure plane is in the range of 0.8 to 2.0 m and the length is in the range of 30 to 40 m, and hence the failure can be analysed as an infinite slope.

Fredlund and Rahardjo (1993) demonstrated that the shear strength of unsaturated soil can be expressed as

$$\tau = c' + (u_a - u_w)\tan\phi^b + (\sigma_n - u_a)\tan\phi' \tag{8.1}$$

where c' is effective cohesion, (u_a-u_w) is matric suction, u_a is pore-air pressure, u_w is pore water pressure, ϕ^b is the angle indicating the rate of increase in shear strength relative to the increase in matric suction, σ_n is the total stress normal to the sloping surface, and ϕ' is effective friction angle. Cho and Lee (2002) expressed the factor of safety (F) as a function of modified Mohr-Coulomb failure criterion using limit equilibrium method (Fredlund et al. 1978) for an infinite slope as

$$F = \frac{c'+(u_a - u_w)\tan\phi^b + \gamma z\cos^2\beta\tan\phi'}{\gamma z\sin\beta\cos\beta} \tag{8.2}$$

where β is slope angle, γ is unit weight of soil, and z is depth of failure plane.

The results of this study comprise three parts. First, a sensitivity analysis of parameters in the above equation (c', ϕ', ϕ^b, γ, and (u_a-u_w)) is performed. In the second part, reliability analysis of a typical unsaturated slope is performed. In the last part, the influence of variation of hydraulic conductivity of the slope material on the reliability index is studied. A one-dimensional finite difference code developed by Döll (1996, 1997) is used to compute suction values at different depths corresponding to different elapsed times. The elapsed time or time period is defined as the time since the application of the prescribed suctions at the top and bottom boundaries and cessation of rainfall. The code solves the non-linear equations of coupled heat and moisture flow under unsaturated conditions. The initial conditions (soil properties, water content profile, soil water characteristic curve, temperature gradient) used in the model were obtained for a typical slope profile presented in Rao et al. (1995). Figure 8.1 shows the matric suction profile with respect to depth of slope for different elapsed times (t) after the cessation of a single rain spell. The initial suction variations shown in Figure 8.1 corresponding to t=0 were obtained from soil water characteristic curve (Rao et al. 1995).

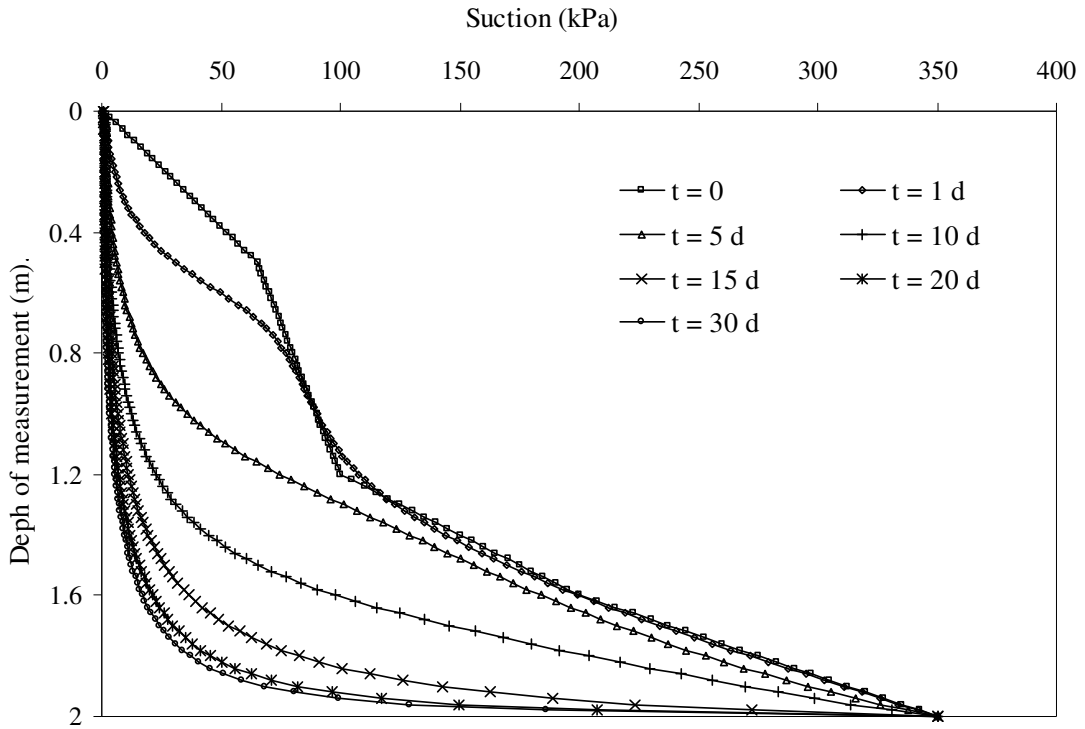

Figure 8.1. Variation of suction corresponding to different elapsed times

8.2.2 Sensitivity analysis

An analysis to determine the sensitivity of the reliability index (β) to variations in parameters is widely used in structural engineering (Nowak and Carr 1985) and can also be applied in geotechnical engineering. The influence of each of the five variables (c', ϕ', ϕ^b, γ, and (u_a-u_w)) on the limit state function G(X), defined in terms of Equation 8.2, is investigated for the probability of factor of safety F, being more than unity. The limit state function is evaluated with respect to design point. In non-linear limit state functions, an iterative procedure is used. In the present study, the direction cosines and the reliability index given by Equation 8.3 are evaluated using the Rackwitz and Fiessler (1978) algorithm.

$$\alpha_i = \frac{-\left.\frac{\partial F}{\partial Z_i}\right|_{\text{evaluated at design point}}}{\sqrt{\sum_{i=1}^{4}\left(\left.\frac{\partial F}{\partial Z_k}\right|_{\text{evaluated at design point}}\right)^2}} \qquad (8.3a)$$

$$\frac{\partial F}{\partial Z_i} = \frac{\partial F}{\partial X_i}\frac{\partial X_i}{\partial Z_i} = \frac{\partial F}{\partial X_i}\sigma_{X_i} \tag{8.3b}$$

$$z_i^* = \beta\alpha_i \tag{8.3c}$$

where z_i^* is a reduced variate corresponding to the design point, β is reliability index, and α_i is direction cosine.

The variation of reliability index (β) corresponding to the variations in each input parameter is determined and is shown in Figure 8.2 in terms of percent deviation from the mean value. The mean values of cohesion, friction angle, matric suction values and saturated hydraulic conductivity given in Table 8.1 are representative of a slide material, and the data are taken from Rao et al. (1995). The determination of the parameter ϕ^b involves use of special testing techniques that are applicable to unsaturated soils, and reported values range from 7° to 26° for silt like materials (Fredlund and Rahardjo 1993). Hence, a mean value of 20° is used for ϕ^b. Literature suggests that a correlation between cohesion and friction angle exists and the correlation coefficients are in the range of -0.25 to -0.75 (Cherubini 2000). Hence, calculations are performed using a correlation coefficient of -0.50. The parameters c', ϕ', (u_a-u_w), γ, and ϕ^b are taken as random variables following a normal distribution.

Table 8.1. Values of parameters used in the analysis of unsaturated slopes

Parameter	Mean value	Coefficient of variation
Effective cohesion (c')	5 kPa	10%
Effective angle of internal friction (ϕ')	28°	10%
Angle indicating the rate of increase of shear strength relative to increase matric suction (ϕ^b)	20°	10%
Matric suction (u_a-u_w)	1.48 - 312.5 kPa	10%-50%
Unit weight of soil (γ)	18 kN/m^3	5%-10%
Slope angle (β)	50°	--
Depth of failure plane (z)	0.1 m - 1.9 m	--

Lumb (1966) and Matyas (1977) showed that the inherent variations of soil properties such as friction angle, cohesion and unit weight of the soil can be characterized by a normal distribution. Sensitivity analysis is performed for various combinations of the coefficient of variation (CoV) of design parameters shown in Table 8.1 to demonstrate its use in unsaturated slope reliability analysis.

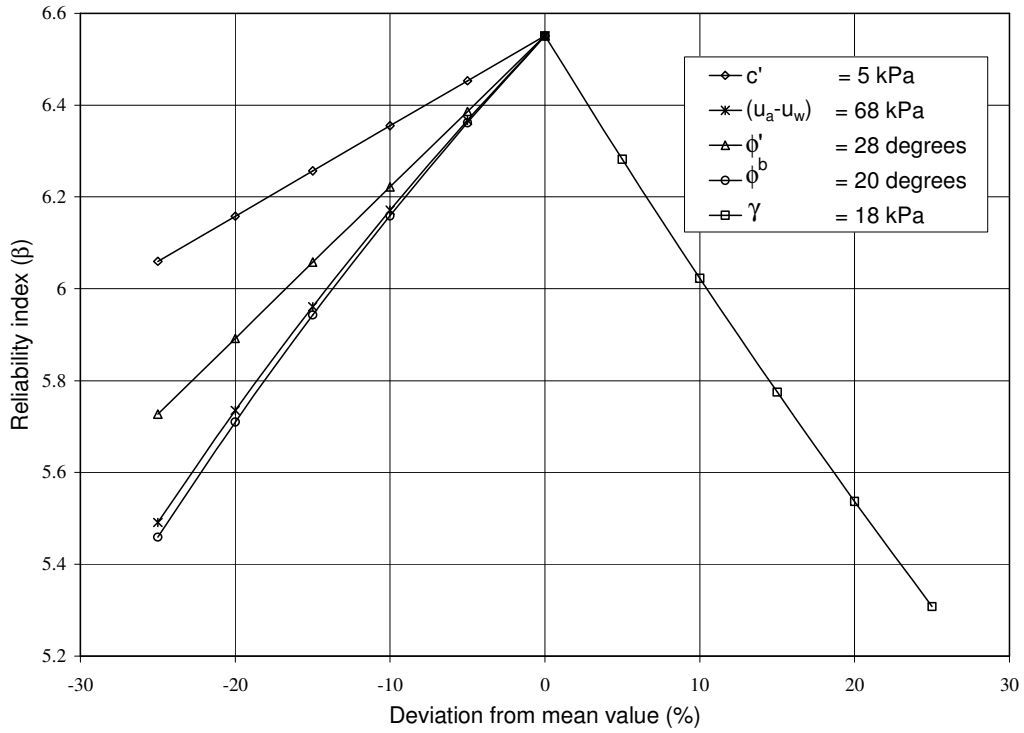

Figure 8.2. Results of sensitivity analysis for z=1.9 m and 30 days of elapsed time since application of prescribed suction boundary condition

The analysis is conducted for a slope inclination of 50°, a failure plane depth of 1.9 m, 30 days of elapsed time since application of prescribed boundary condition, and with the mean properties presented in Table 8.1.

The results presented in Figure 8.2 are obtained with an assigned value of coefficient of variation of 10% for each uncertain parameter. The effect of mean value variations on reliability index is evident from Figure 8.2. The corresponding factor of safety for the same slope stability case using the mean values and Equation 8.2 is 2.21. The reliability index using mean values is 6.55, shown as ordinate in Figure 8.2.

The slopes of the lines in Figure 8.2 represent the degree of sensitivity of reliability index to the parameters. Steeper lines correspond to more sensitive parameters. Hence, in this case, the reliability index is more sensitive to the parameters (u_a-u_w) and ϕ^b than c' and ϕ'. For example, if the mean friction angle is 21° instead of 28°, the corresponding factor of safety and reliability index are 2.09 and 5.73 respectively. That is, for a 25% variation in mean value of friction angle, there is 12.5% change in reliability index. Along similar lines, if suction is 51 kPa instead of 68 kPa (25% decrease), the corresponding factor of safety and reliability index are 1.84 and 5.49, respectively. In this case, the decrease in reliability index is of the order of 16.18%. Similar studies have been carried out for various other combinations of the coefficients of variation of the design parameters. In almost all the cases, it was observed that the matric suction (u_a-u_w) is a sensitive parameter affecting the stability of slope. Moreover, in view of the large possible variations in evaluating the empirical value of matric suction (u_a-u_w), a more detailed study is conducted to evaluate the effect of variation of suction values in the slide area in terms of reliability index and reported in the following sections.

8.2.3 Influence of suction variation on slope reliability

Many slope failures occur as suction decreases with time. Under constant suction conditions at top and bottom boundaries, suction within a soil profile is a function of initial suction level, soil-water characteristics as well as the hydraulic conductivity of the soil. A numerical program developed by Döll (1996, 1997) is used to calculate suction variations with time using initial water content/suction levels and the saturated hydraulic conductivity of the soil. The program solves two coupled partial differential equations of moisture and heat transport. The numerical program performs a

simulation run by discretizing a one-dimensional modeling domain and assigning initial and boundary conditions (suctions or water contents) and the soil parameters. The depth (vertical column) of the infinite slope is discretized into a number of nodes with a constant nodal distance of 2 cm. The initial conditions are the initial suction, length of the model domain, and the initial temperature (30^{o}C) at the beginning (t=0). Boundary conditions include prescribed suctions at the top and bottom, physical properties of the soil, properties of soil-water characteristics defined by van Genuchten parameters, saturated hydraulic conductivity and other factors. Though the program also handles suction variations due to changes in temperature, in the present study, a constant temperature (30^{o}C) is used. More details are available in Döll (1996, 1997). Simulations are conducted for different elapsed times, and suction variations are obtained. The variation of suction with water content is represented by van Genuchten relationship (van Genuchten 1980) as follows:

$$\Theta = \frac{(\theta - \theta r)}{(\theta s - \theta r)} = \left\{ \frac{1}{\left[1 + \left((\alpha \psi)^{n} \right) \right]} \right\}^{m} \tag{8.4}$$

where Θ is the effective saturation, θ, θ_r and θ_s are the volumetric water contents, residual volumetric water content and saturated volumetric water content, respectively, and α, n and m are the fitting parameters for the relationship. The term m is related to n as m = (1- 1/n). If $\theta_r = 0$, Θ is equal to the degree of saturation. The soil-water characteristic data are analyzed and fitted to obtain parameters, α, n and θ_s using a program for describing the hydraulic properties of unsaturated soils (van Genuchten et al. 1991). The properties used in the suction analysis are porosity (n_p), saturated water content (θ_s), residual water content (θ_r), van Genuchten

parameters (α, n, l), and saturated hydraulic conductivity (K_{sat}). The representative values of the variables are 0.385 m^3/ m^3, 0.37 m^3/ m^3, 0 m^3/ m^3, 0.003 1/ cm, 1.4, -1.5, and 1.5×10^{-7} m/s, respectively. Though it is recognized that these values also form another set of random variables, to keep the analysis simple, only variations in the parameters c', ϕ', (u_a-u_w), γ, and ϕ^b are taken as random variables following normal distributions. Factors of safety and reliability indices are computed for different elapsed times, and variations are shown in Figures 8.3 and 8.4.

Figure 8.3 shows the variation of factor of safety, computed from Equation 8.2. Conventional factors of safety, ignoring the suction contribution, are also plotted for comparison purposes. It can be observed that these values decrease with increase in depth of failure plane. If suction contribution is considered, the factors of safety are initially high, approximately 12 and 7 at failure surface depths of 0.1 m and 1.9 m, and gradually decrease with time as suction reduces, owing to the moisture redistribution with time, leading to factors of safety greater than unity. However, ignoring the suction contribution results in factors of safety less than unity at depths greater than 1 m. It is established that a calculated factor of safety of more than unity alone does not ensure safety (Alonso 1976). Hence, reliability analysis is performed to assess the risk involved in the project. Similar to earlier calculations, the coefficient of variation of the variables is taken as 10%, and reliability indices corresponding to different depths and time periods from cessation of rainfall are calculated.

The variation of reliability index with depth is shown in Figure 8.4. It is noted that reliability index decreases with increase in the elapsed time and falls below 3 for depths ranging from 0.8 to 1.4 m after 15 days. Based on the above consideration and

the suggested recommendations of expected levels of performance from USACE given in chapter 2, this zone can be considered susceptible to failure.

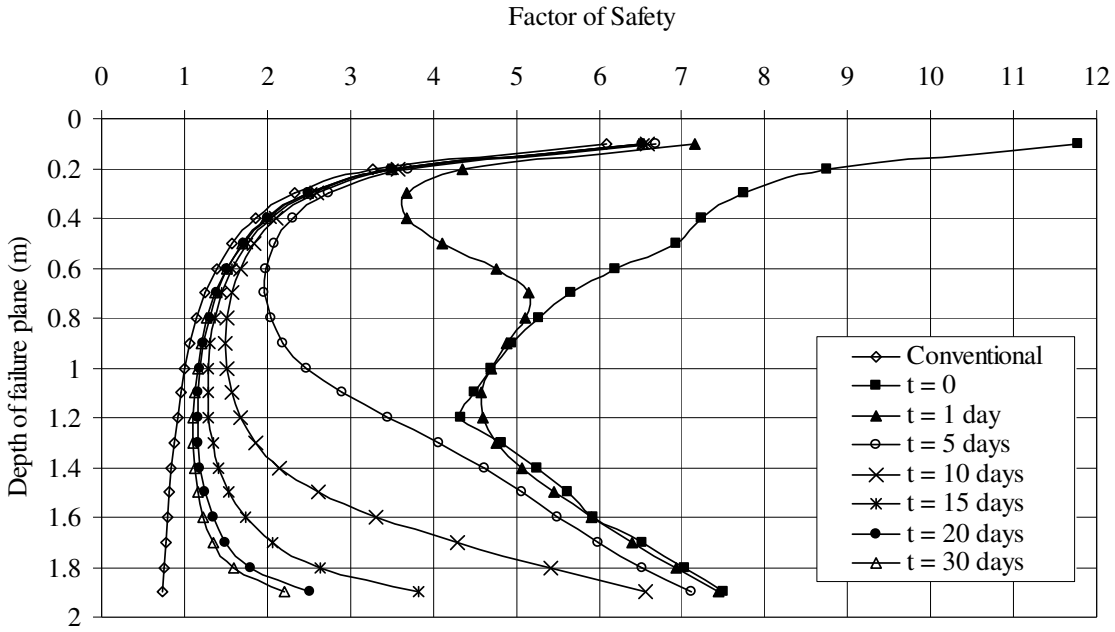

Figure 8.3. Variation of factor of safety with depth corresponding to different elapsed times

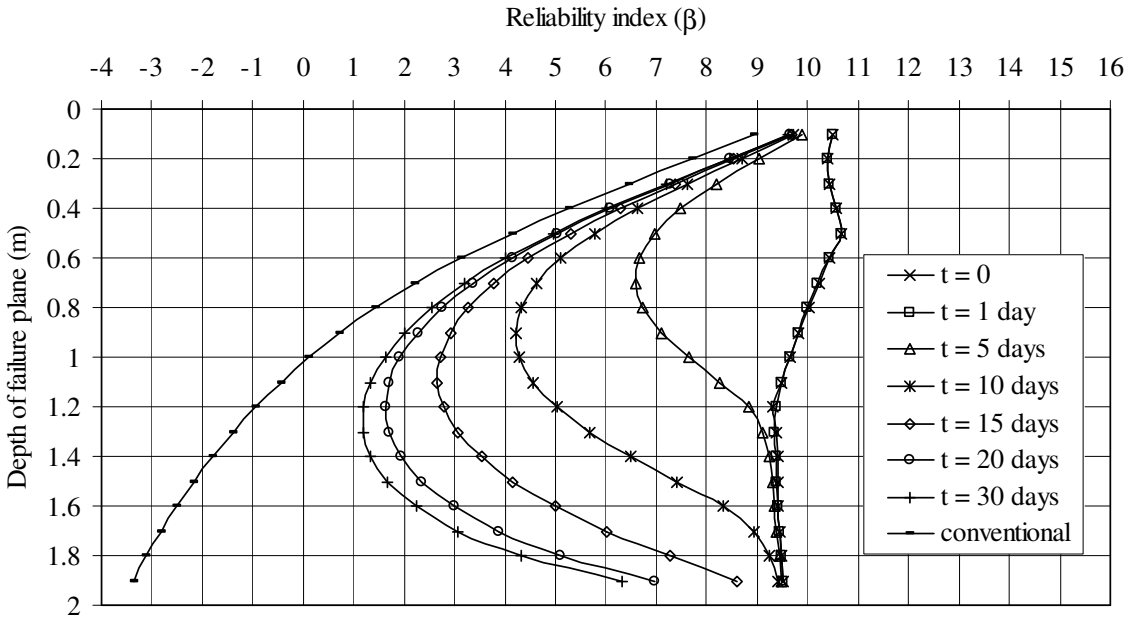

Figure 8.4. Variation of reliability index with depth corresponding to different elapsed times

Figure 8.4 also shows the reliability indices ignoring the suction contribution (conventional analysis). The values are lower compared to those obtained considering suction and decrease with depth. Excluding the effect of suction, critical failure surfaces are relatively deep. Especially, in the case of slopes whose depths of failure plane are between 0.8-1.9 m, the driving forces considerably increase with depth when compared to that of soil resisting forces. Thus, consideration of effect of suction and the variations in soil parameters in terms of reliability index is useful in the assessment of stability of unsaturated soil slopes.

8.2.4 Influence of hydraulic conductivity of soil

The rate of infiltration into the ground is high in the beginning and is a function of initial moisture content (and hence suction), rainfall intensity and hydraulic conductivity of the soil. The rate of infiltration reduces with time approaching a constant value equal to the saturated hydraulic conductivity (Cho and Lee 2002). Hence, the effect of variation of infiltration rate is studied in terms of variations in saturated hydraulic conductivity, and slope reliability is studied by assuming that the variation in hydraulic conductivity is represented by lognormal distribution. The coefficient of variation (CoV) is varied from 50% to 90% in accordance with the range of values reported by Duncan (2000). The influence of CoV of K_s on reliability index is examined and the results are presented in Figures 8.5(a), (b), (c), and (d), for elapsed times of 5 days, 10 days, 15 days, and 30 days after the cessation of rainfall. Although the reliability indices are calculated for depths of failure plane ranging from 0.1 m to 1.9 m, for purpose of brevity, values greater than 8 are not shown. The results shown in Figures 8.5(a), (b), (c), and (d) demonstrate that an increase in the coefficient of variation of hydraulic conductivity reduces the reliability index.

Considering an elapsed time of 5 days and a CoV of K_s equal to 90% (Figure 8.5(a)), the reliability indices are low (< 3) for depths of failure plane ranging from 0.3 m to 1.2 m. Figure 8.5(d) shows a different trend for 30 days of elapsed time, wherein the reliability indices are low for deeper depths of failure plane and high for shallower depths of failure plane. For 90% CoV of K_s, the failure zone can be considered to be limited to 0.3 m to 1.2 m and, in Figure 8.5(d), the failure zone varies from 0.5 m to 1.9 m. This difference is due to the moisture redistribution in the regime with time. The low values of reliability indices indicate that the slopes are in a failure state especially with higher coefficients of variation of K_s.

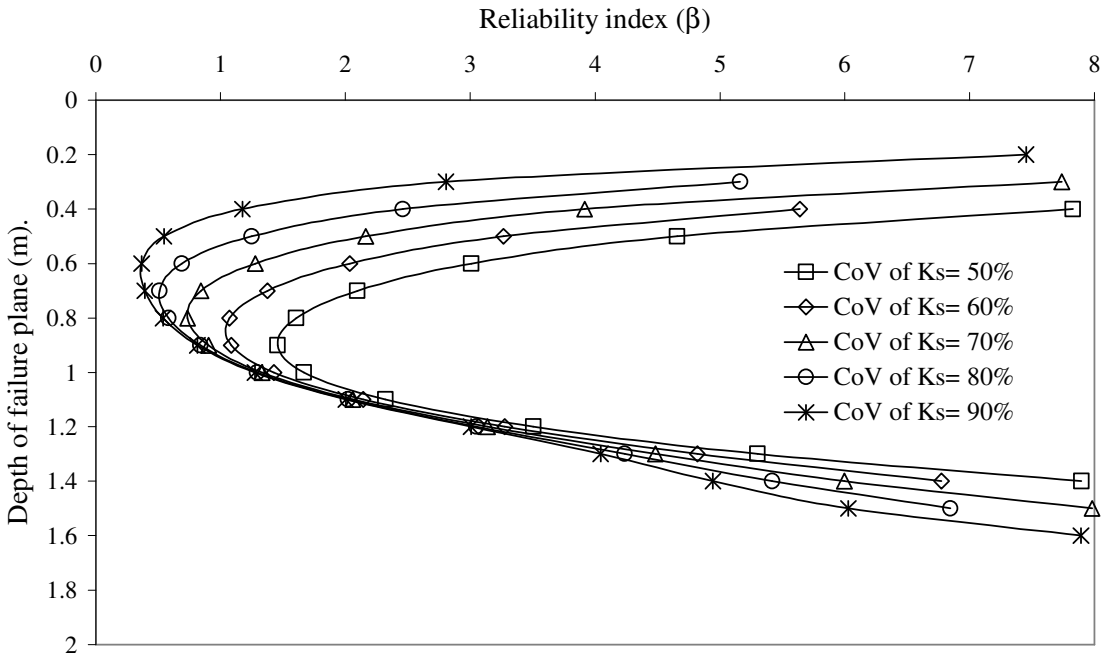

Figure 8.5(a). Variation of reliability index with depth corresponding to 5 days of elapsed time

The analysis is limited by the assumptions of an infinite slope model for stability and a one-dimensional analysis for evaluation of suction variations, and by the separate analysis of the effect of hydraulic conductivity. However, the results from a coupled two-dimensional numerical analysis are beneficial for better understanding of the behaviour of unsaturated soil slopes. Nevertheless, the results presented serve to point

out the importance of reliability analysis of unsaturated soil slopes within a simple framework.

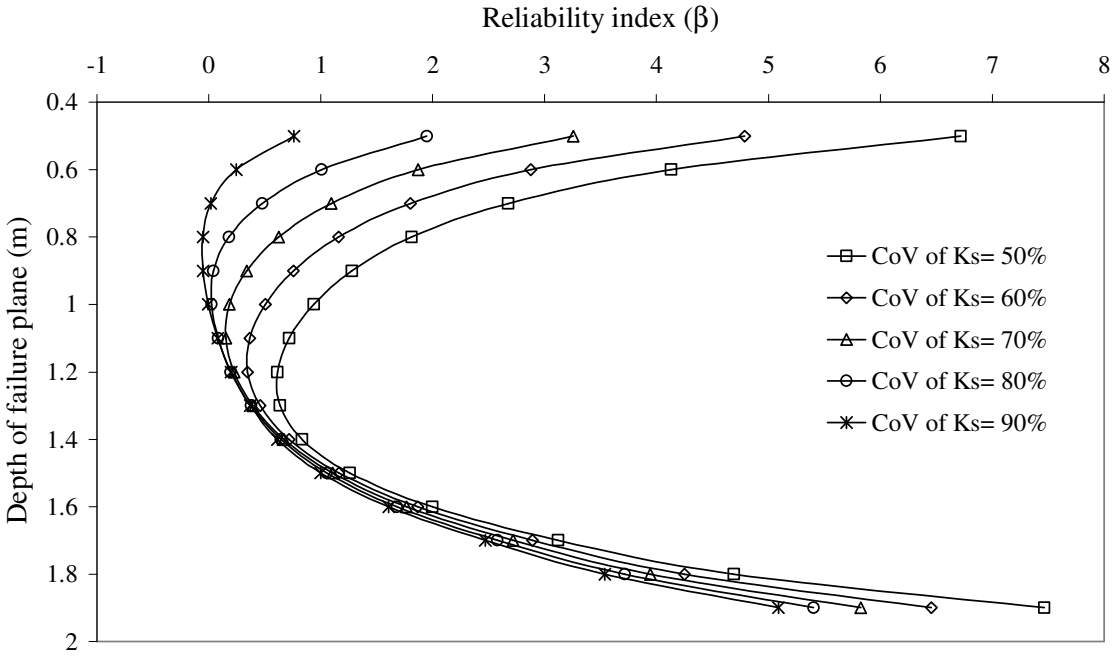

Figure 8.5(b). Variation of reliability index with depth corresponding to 10 days of elapsed time

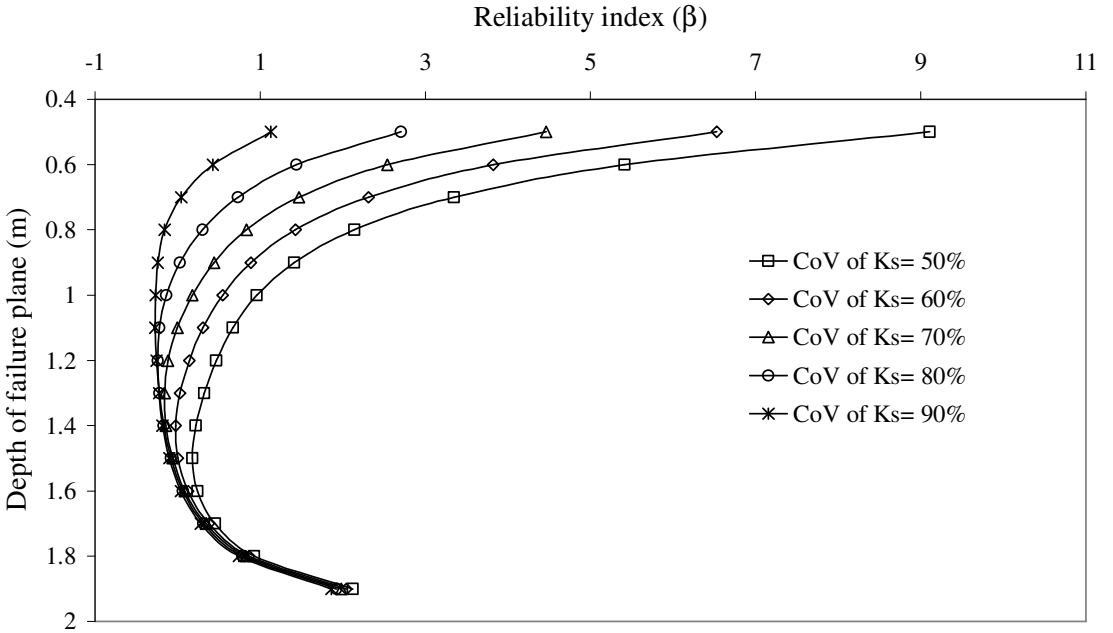

Figure 8.5(c). Variation of reliability index with depth corresponding to 15 days of elapsed time

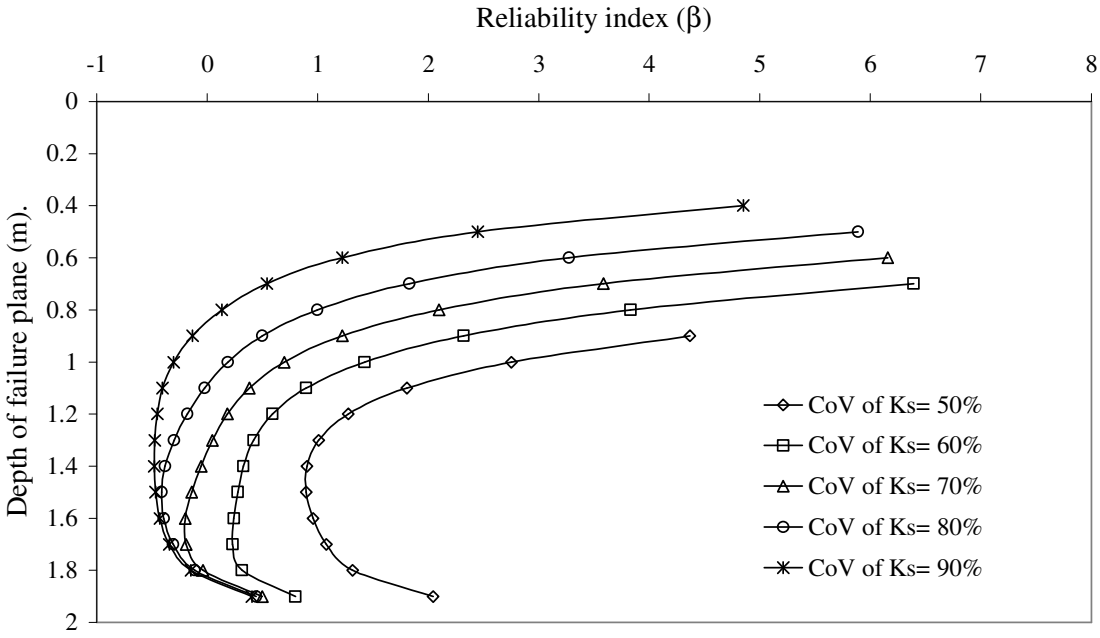

Figure 8.5(d). Variation of reliability index with depth corresponding to 30 days of elapsed time

8.3 Seismic stability analysis of soil slopes

In this section, a probabilistic stability analysis is carried out for slopes in seismically active zones, taking into consideration inherent uncertainties associated with the soil parameters. The effect of correlation between the strength parameters on the stability is studied. Safety in terms of reliability index, defining satisfactory performance is evaluated for various combinations of input parameters. The total expected cost of slope is evaluated for each set of data taking into account the initial cost, consequence cost and associated probability of failure. The likelihood, or the probability of an adverse event, is usually expressed in terms of the number of such events expected to occur during a defined duration. The consequence of an adverse event, sometimes called damage, is often expressed in monetary terms. The risk rating, as the combination of likelihood and consequence is evaluated for each project separately. Potentially catastrophic events, though unlikely, are considered carefully in the long

term planning of the project. The risk may appear insignificant, yet disaster can happen. If the consequences are unacceptable, then the risk must be avoided or at least mitigated (El-Ramly et al. 2002).

This section examines seismic slope stability in terms of reliability and consequence costs proposed in the context of the above guidelines. The objectives of the study conducted in this section are;

i) to show that the reliability index is a better measure of safety than the conventional factor of safety, and

ii) to show that it is possible to balance costs considering consequence costs, soil parameters, their variations and correlation, considering horizontal seismic coefficient and slope geometry. The following sections describe the mechanistic model adopted, calculation procedures and the results obtained.

8.3.1 Reliability analysis

The method of analysis described in this section of study is a simplified approach for predicting the optimum slope angle for a given slope height and the soil properties. The influence of variability of soil strength parameters, cohesion (c), angle of internal friction (ϕ), and correlation coefficient between cohesion and friction angle ($\rho_{c,\phi}$) is examined to provide a probabilistic assessment of stability of slopes. Statistical analysis of actual data by many researchers (Lumb 1966; Alonso 1976; Harr 1987; Christian et al. 1992; Duncan 2000) has revealed that cohesion and friction angle follow normal or log-normal distribution, and that there exists a negative correlation between the above mentioned strength parameters. Studies also show that the use of log-normal or normal distribution is not significant if the coefficient of variation of parameters is less than 30% (Ang and Tang 1975; Whitman 1984). The

effect of an earthquake on the soil mass comprising a slope is introduced as an increase in the inertia of the mass and is expressed in terms of the maximum acceleration experienced at the site of the slope.

8.3.2 Mechanistic model

In the present analysis, the stability of soil slopes is analysed by assuming a wedge type failure surface. The slope geometry along with the planar failure surface is shown in figure 8.6. The static factor of safety corresponding to the assumed failure surface (Christian and Urzua 1998) is

$$F = \frac{c + \frac{1}{2}\gamma H \frac{\sin(\psi - \theta)}{\sin\psi}\cos\theta\tan\phi}{\frac{1}{2}\gamma H \frac{\sin(\psi - \theta)}{\sin\psi}\sin\theta} \tag{8.5}$$

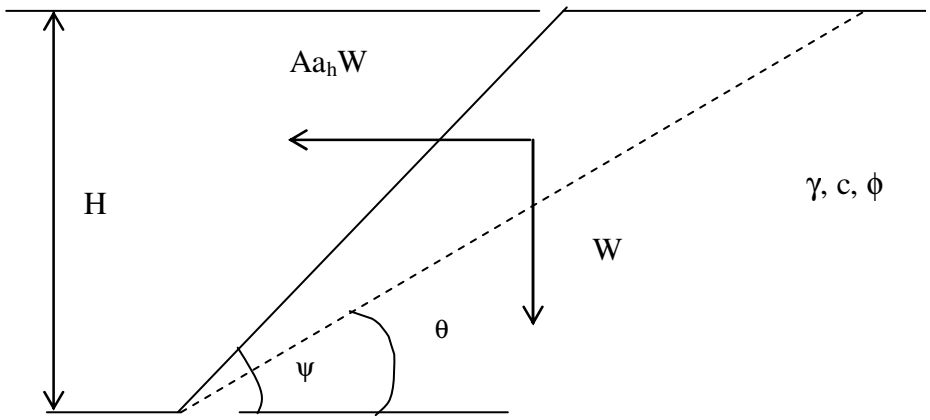

Figure 8.6. Slope Geometry along with planar failure surface

Of the vertical and horizontal peak earthquake accelerations, the latter component is more often used in the current geotechnical practice, to approximately model the system response to earthquakes, and hence the same is used in the present analysis.

If the ground acceleration is a_h and the amplification factor in the slope is A, the dynamic factor of safety (Christian and Urzua 1998) becomes

$$F^* = \frac{c + \frac{1}{2}\gamma H \frac{sin(\psi - \theta)}{sin\psi}\left[cos\theta tan\phi - Aa_h sin\theta tan\phi\right]}{\frac{1}{2}\gamma H \frac{sin(\psi - \theta)}{sin\psi}\left[sin\theta + Aa_h cos\theta\right]} \tag{8.6}$$

where c is cohesion, γ is unit weight of soil, H is height of slope, ψ is slope angle, θ is slope of failure wedge in degrees, and ϕ is friction angle, A is amplification factor in the slope, and a_h is the peak horizontal acceleration.

The slope is considered in the seismically active region and the seismic loading is expressed in terms of the maximum horizontal ground acceleration, a_h, to be experienced by the slope during an earthquake. This is introduced into the analysis through a range of values (deterministic) equal to 10-20% of the acceleration due to gravity, g (i.e., a_h in the range of 0.10g to 0.20g) in which, g= 9.81 m/s^2. The assumed horizontal ground acceleration should have a lower probability of exceedence during the design life of the slope.

The results of reliability analysis are expressed in terms of reliability index (β), which is expressed in terms of Hasofer and Lind formulation (Madsen et al. 1986). It has been observed that the coefficients of variation of c and ϕ are in the range of 10-40% and 7-26% respectively (Harr 1987; Becker 1996b; Duncan 2000). The strength parameters, viz., cohesion, c, and angle of internal friction, ϕ, are taken as normally distributed random variables. The unit weight of soil is considered as deterministic parameter as its variation does not normally exceed 3-7% (Duncan 2000). The values of the parameters used in the analysis are shown in Table 8.2.

Table 8.2. Values of parameters used in the analysis of seismic stability of soil slopes

Parameter	**value**
Mean value of cohesion (c)	10 kPa
Mean value of angle of internal friction (ϕ)	30°
Unit weight of soil (γ)	19 kN/m^3
Height of slope (H)	6m
Slope angle (ψ)	44° - 60°
Failure angle (θ)	40°
Amplification factor (A)	1
Peak horizontal acceleration (a_h)	0 - 0.2
Correlation coefficient ($\rho_{c,\phi}$)	-0.75 - 0

The normalized cost of the slope is calculated for different sets of data and the optimum slope angle is obtained. The optimum design is the design, which minimizes the expected cost without compromising on the expected performance of the system. The cost of failure, C, reflects the damage caused by the failure plus loss of utility as a result of failure. Hence, the expected cost (E), initial cost (I), cost of failure (C), and the probability of failure (p_f) of any system can be expressed as

$$E = I + C \times p_f \tag{8.7}$$

Wu and Kraft (1970) demonstrated the advantage of arriving at the relative cost rather than actual cost of the system in getting the optimum section for a slope, by considering the cost of construction of 1:1 slope (I_o) as basis. Hence, Equation 8.7 can be written as

$$E^* = I^* + C^* \times p_f \tag{8.8}$$

Where $E^* = E/I_o$, $I^* = I/I_o$, $C^* = C/I_o$, and $I = 0.5 * H^2 * \cot(\psi)$. Hence, initial cost of construction is proportional to the volume of earthwork involved. So, height of slope being constant, steeper is the slope, less is the earthwork involved and hence less is

the initial cost. However, as the slope angle increases, probability of failure and therefore the total consequence cost increases.

The following sections discuss the application of the above methodology to arrive at the balanced section considering uncertainties in parameters, safety in terms of reliability index and economy.

8.3.3 Results and discussion

8.3.3.1 Reliability index (β) versus expected factor of safety {E(FS)}

Figure 8.7 shows the variations of reliability index and expected factor of safety, for various possible combinations of horizontal earthquake coefficients (Aa_h) and correlation coefficients ($\rho_{c,\phi}$). Analyses are done for various slope angles in the range of 44^o-60^o using Aa_h of 0, 0.1 and 0.2 with coefficients of variation of cohesion and friction angle being 10%. It can be noted that the variation of factor of safety with horizontal earthquake coefficient (Aa_h) is very less when compared to that of reliability index. For $\rho_{c,\phi}$ of -0.75 between c and ϕ, β varies from 6.84 at Aa_h equals to 0 (i.e., static case) to 0.52 at Aa_h equals to 0.2, whereas the expected factors of safety for the above data are 1.38 & 1.02 respectively. It is observed that the reliability index decreases with increase in earthquake coefficient. Lower the $\rho_{c,\phi}$, higher is the reliability index. The horizontal earthquake coefficient, Aa_h, being a destabilizing parameter shows an adverse effect on the performance of structure. At higher values it even undermines the effect of $\rho_{c,\phi}$ on the stability. The effect of $\rho_{c,\phi}$ on β is well pronounced at low values of Aa_h than at higher values. In conventional analysis, the slope is considered unsafe (as the values are less than the recommended value of 1.5), whereas the slope can be considered as safe in the case of Aa_h equals to zero with any $\rho_{c,\phi}$ and also in case of Aa_h equals to 0.1 and $\rho_{c,\phi}$ equals to -0.75, in terms of the

reliability index values suggested by USACE (1997) and JCSS (2000). The results clearly show that factor of safety alone cannot adequately indicate status of safety in seismic conditions. The results also show that if one has the data with regard to coefficients of variation of cohesion and friction and $\rho_{c,\phi}$, one can arrive at the reliability index (β) for a given slope geometry and seismic coefficient.

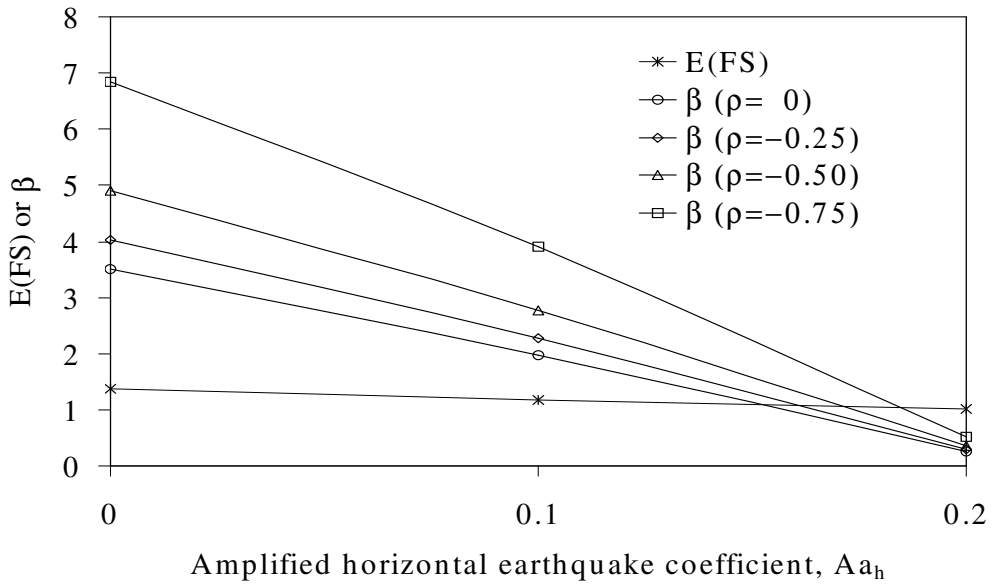

Figure 8.7. Variation of expected factor of safety (E(FS)) and reliability index (β) as function of Aa_h for cv_c & cv_ϕ = 10%

8.3.3.2 Influence of coefficients of variation of soil strength parameters on normalized costs

Figure 8.8(a) through 8.8(d) show the variation of normalized expected cost for various combinations of $\rho_{c,\phi}$, ψ, cv_c and cv_ϕ, for a typical case with Aa_h equals to 0.2. The normalized total cost is plotted on ordinate and the slope angle on abscissa. The normalized total cost corresponding to a slope angle is obtained by dividing the total cost (i.e., sum of initial cost and total consequence cost) for that particular slope with initial cost of a 45^o slope. All the variables and their variations are considered in arriving at the probability of failure, which is one of the two multiplicands in the calculation of total consequence cost. Normalized total cost of unity for any given

slope means that the total cost of that slope (i.e., Initial cost + probability of failure × consequence cost) is equal to initial cost of 1:1 slope. From the above figures it is evident that as uncertainty of basic parameters in terms of coefficients of variation increases, normalized total cost increases and optimum slope angle decreases. This is because as uncertainty in strength parameter increases the probability of failure or unsatisfactory performance of the system increases. This in turn increases the total consequence cost and so the normalized expected cost. For any particular data set, if $\rho_{c,\phi}$ increases, there will be a substantial decrease in normalized cost and a corresponding increase in optimum slope angle. For example considering Figure 8.8(a), up to a slope angle of 56^o, $\rho_{c,\phi}$ does not have any appreciable effect on normalized total cost. It means that if one chooses the slope angle within 56^o, it implicitly accounts for any value of $\rho_{c,,\phi}$ under study (between 0 and -0.75). The reliability index values corresponding to these points for various combinations of $\rho_{c,\phi}$, cv_c & cv_ϕ are presented in Table 8.3.

Table 8.3. Evaluation of reliability indices for slopes subjected to earthquake-induced loading with $Aa_h = 0.2$

Coefficient of variation of c and ϕ (cv_c & cv_ϕ)	Slope angle (ψ^o)	Reliability index values for different values of ($\rho_{c,\phi}$)			
		0	-0.25	-0.50	-0.75
5%	56	2.889	3.328	4.057	5.658
10%	52	2.962	3.378	4.039	5.349
15%	48	3.271	3.643	4.180	5.055
20%	46	3.029	3.309	3.685	4.227

If $\rho_{c,\phi}$ is known, higher reliability index can be assigned. It can also be noted that as cv_c and cv_ϕ increase, the optimum slope angle decreases. The variation of E^* is more pronounced at higher values of $\rho_{c,\phi}$ and also at steeper slope angles.

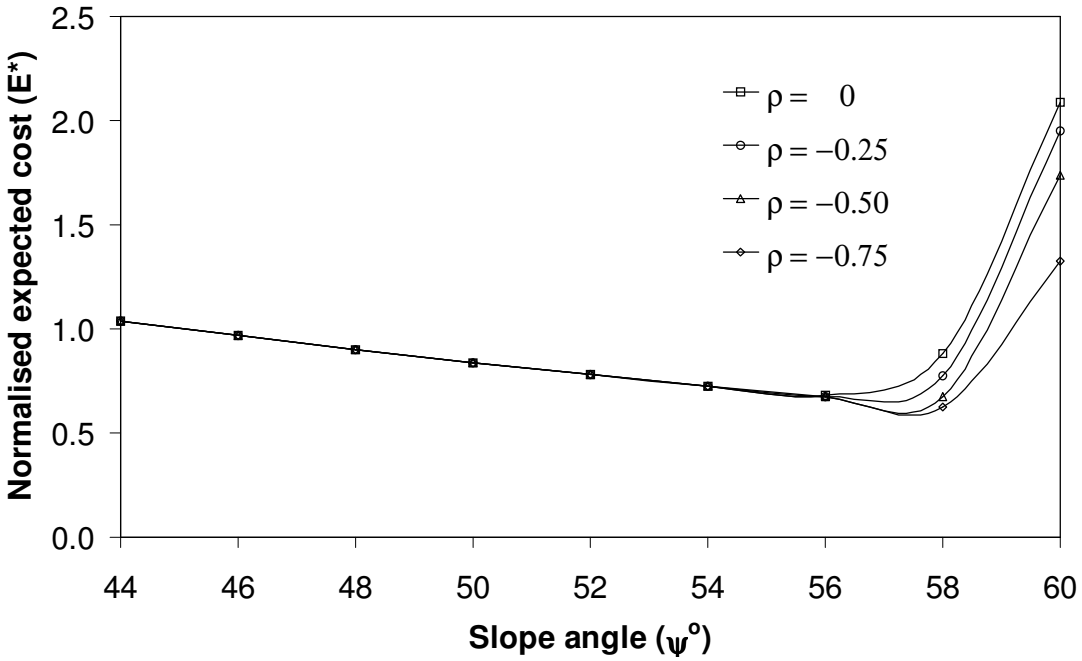

Figure 8.8(a). Normalized expected cost vs. slope angle for Aa_h = 0.2, C^*=5, cv_c & cv_ϕ = 5%

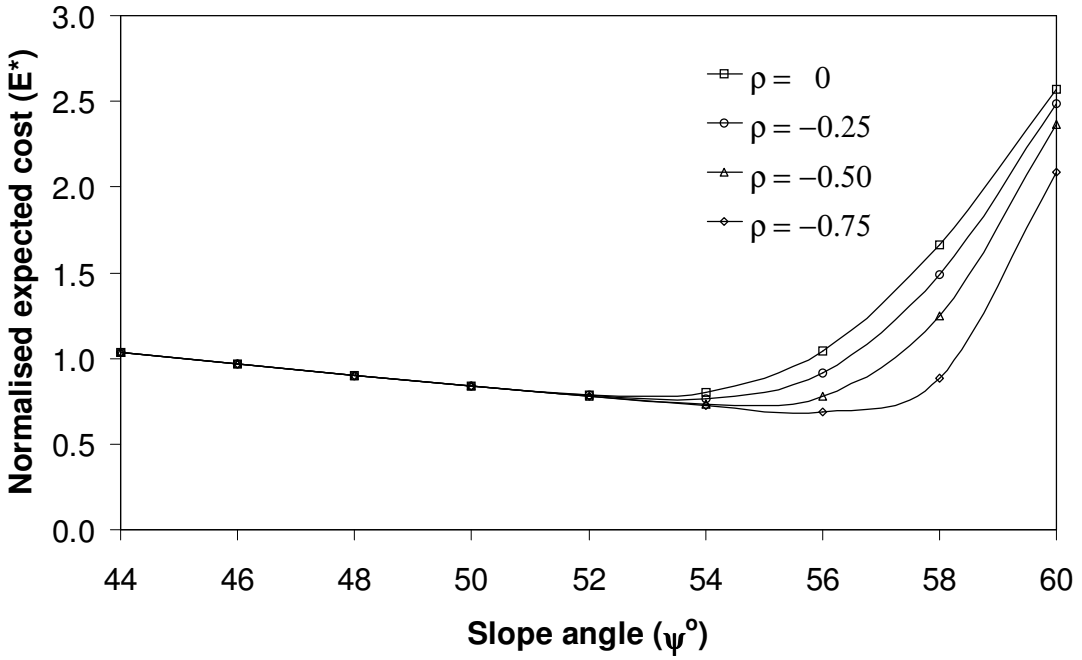

Figure 8.8(b). Normalized expected cost vs. slope angle for Aa_h = 0.2, C^*=5, cv_c & cv_ϕ = 10%

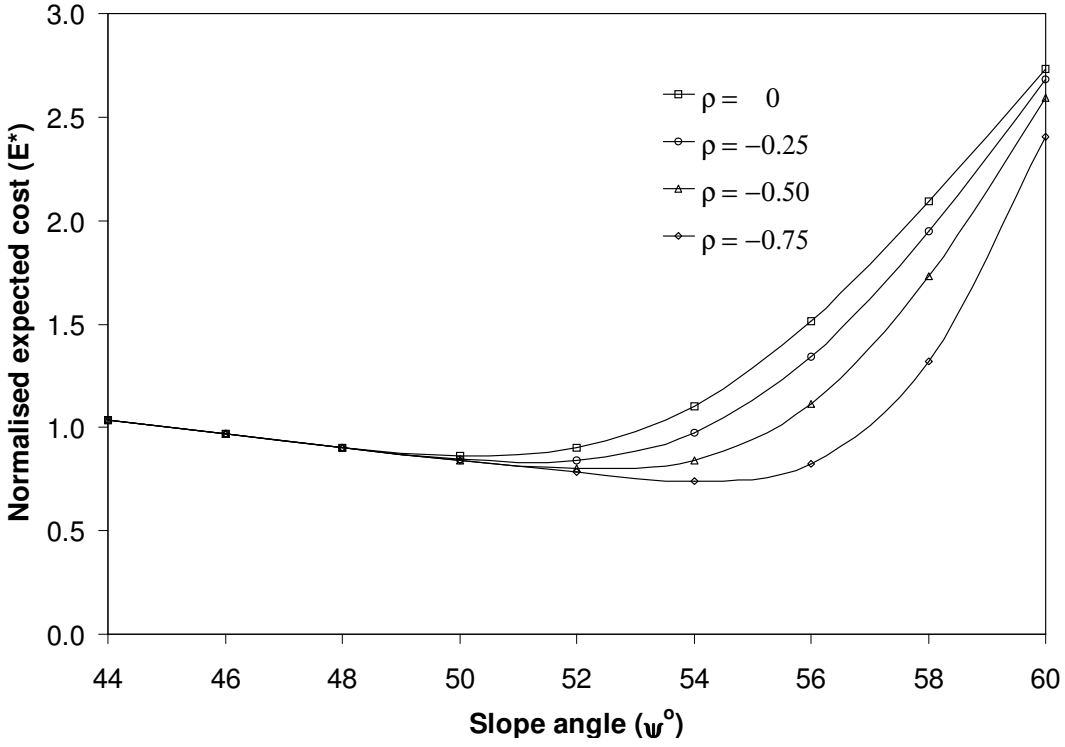

Figure 8.8(c). Normalized expected cost vs. slope angle for Aa_h = 0.2, C^*=5, cv_c & cv_ϕ = 15%

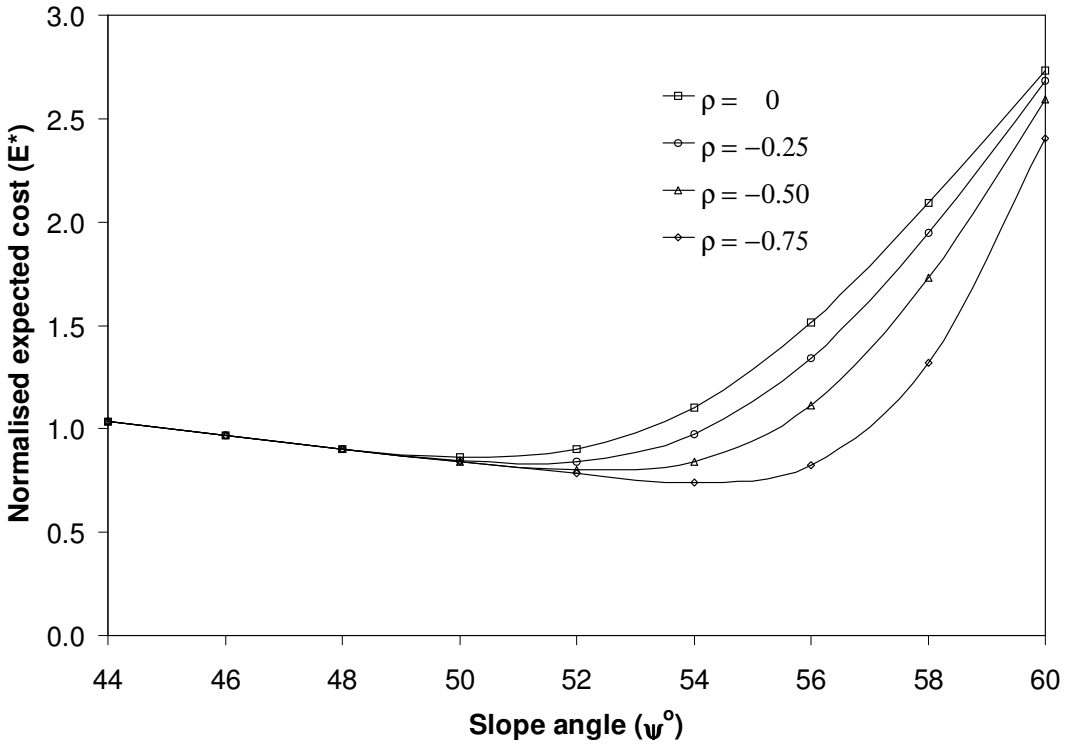

Figure 8.8(d). Normalized expected cost vs. slope angle for Aah = 0.2, C^*=5, cv_c & cv_ϕ = 20%

8.3.3.3 Influence of seismic coefficient (Aa_h) on normalized costs

Figure 8.9 shows the variation of normalized costs (E^*) as function of slope angle (ψ°) for different values of Aa_h. From the figure it can be noted that normalized cost decreases with increase of slope angle and reaches a minimum value close to a particular slope angle called optimum slope angle, beyond which it starts increasing. For Aa_h equals to 0.1 and 0.2, (with $\rho_{c,\phi}$ = 0, and C^* = 5), the optimum angles obtained from the analyses are 58° and 53° respectively. For Aa_h equals to zero, i.e., for the static condition, the optimum angle is not found within the domain of study [44°-60°] and beyond 60°, the slopes are no more admissible for the given set of data. The figure clearly shows that as Aa_h increases, the optimum slope angle reduces. There is no variation in E^* with respect to Aa_h for slope angles up to 52°.

8.3.3.4 Role of normalized consequence cost (C^*)

Figure 8.10 shows a typical result of effect of consequence costs due to failure of slope on expected cost for Aa_h and $\rho_{c,\phi}$ equal to 0.2 and -0.25 respectively. It can be noted that the normalized cost increases with the increase in consequence cost. The optimum slope angle also changes with the consequence cost. Lower consequence cost results in lower overall cost of the slope. For a given consequence cost, the increase in normalized cost is rather steep for slope angles higher than the optimum angle. It can also be noted that for slope angles lesser than 54º there are no variations and corresponding slope gives a balanced design independent of consequence costs.

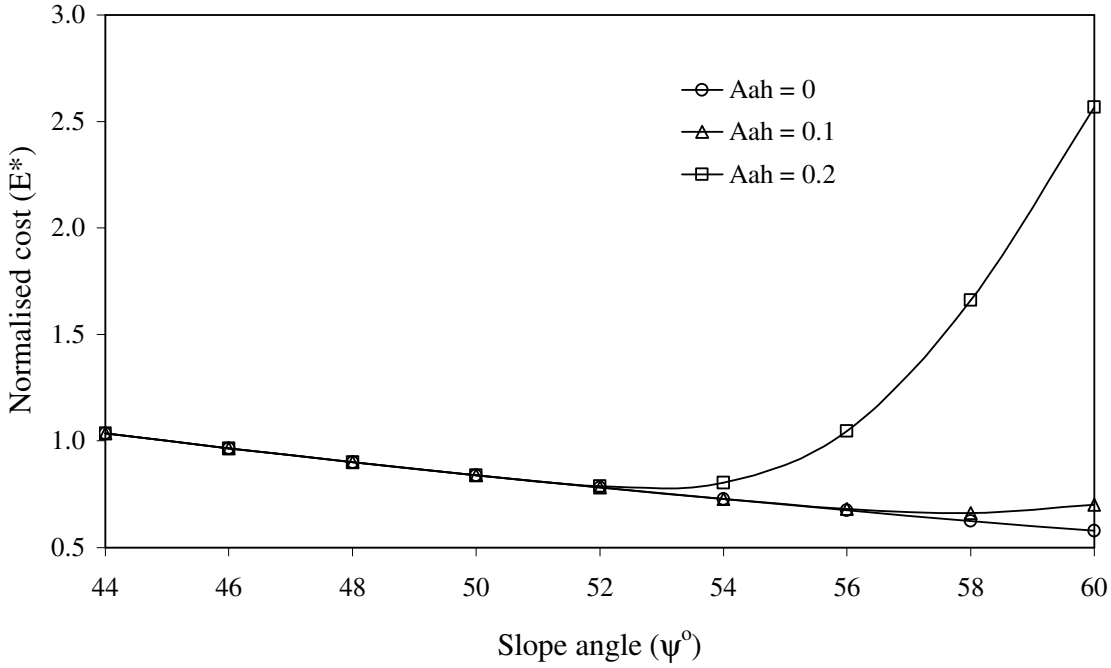

Figure 8.9. Normalized cost as function of slope angle for $\rho_{c,\phi}$=0 & C^*=5, cv_c & cv_ϕ = 10%

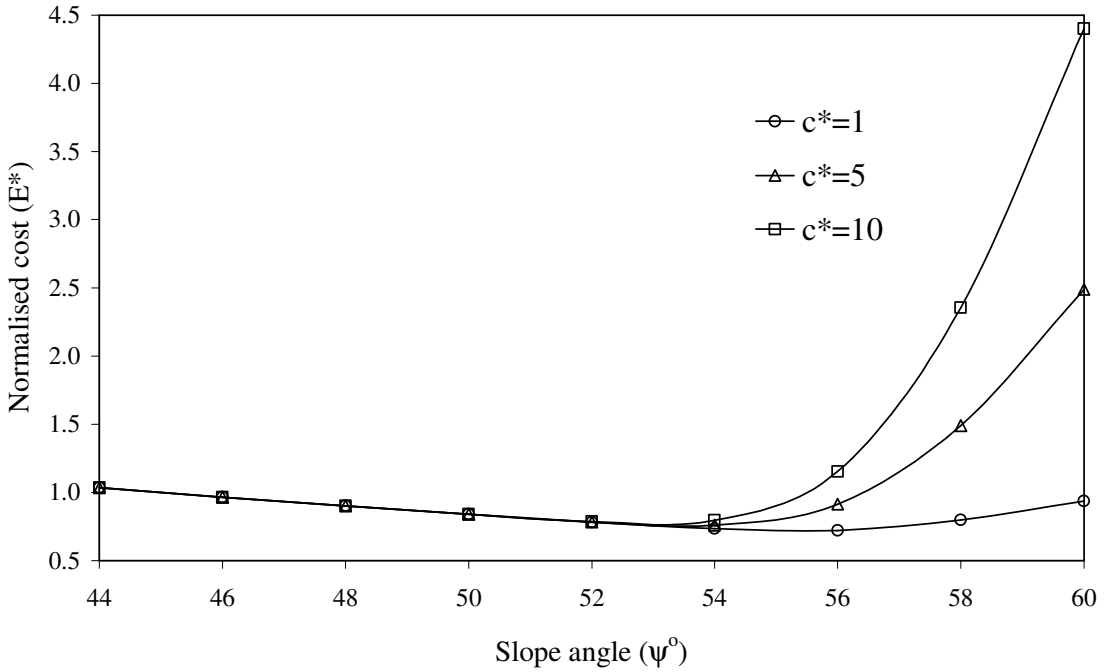

Figure 8.10. Normalized cost as function of slope angle for Aa_h=0.2, $\rho_{c,\phi}$= -0.25, cv_c & cv_ϕ = 10%

8.4 Conclusions

The results presented in this chapter indicate that the reliability theory can be used as a means of evaluating the effects of uncertainties in the parameters involved in unsaturated slope stability calculations. The results demonstrate that slope stability evaluation using reliability considerations is a rational way complementary to the conventional factor of safety approach.

The results of the study shows that for the case considered, the suction (u_a-u_w) and the angle indicating the rate of increase of shear strength relative to matric suction (ϕ^b) are critical random variables and incorporation of appropriate variations of these parameters in the analysis is important in slope reliability assessment.

The results show that failure zones are better captured by the reliability index than the conventional factor of safety.

The coefficient of variation of saturated hydraulic conductivity significantly affects the slope reliability.

The reliability analysis rather than conventional factor of safety approach proved praiseworthy to capture a significantly decreasing trend of safety of slopes with increased horizontal earthquake coefficient.

It can be noted that the variation of factor of safety with horizontal earthquake coefficient (Aa_h) is very less when compared to that of reliability index.

For a set of values of horizontal earthquake coefficient, correlation coefficient, and coefficients of variation of strength properties, the minimum slope angle beyond

which the normalized cost of the slope starts deviating with respect to different consequence costs gives a balanced design.

The optimum slope angle decreases with increase in horizontal earthquake coefficient. For slopes subjected to 1-g loading (static case), the normalized cost continues to decrease even for slope angle as high as 60˚. The normalized cost of the slope shows same decreasing trend till 52˚ irrespective of level of horizontal earthquake loading considered in the analysis.

The stability of slopes in terms of reliability index increases with decrease of correlation between cohesion and angle of internal friction ($\rho_{c,\phi}$).

The optimum slope angle decreases with increase of coefficients of variation of strength parameters.

Keeping all other parameters constant, at any value of consequence cost, the increase of normalized cost is rather steep for slope angles higher than the optimum angle. For the data considered, it is noted that for slope angles lesser than 54º the normalized cost is almost independent of consequence cost.

It is possible to arrive at the balanced or optimum angle for a given geometry of slope and the soil properties taking into account risk, seismic effects using a horizontal seismic coefficient, variability of soil properties, consequence costs for a given horizontal seismic coefficient in a probabilistic frame work.

While results are valid for the conditions used in the problem, the same methodology can be applied to any problem of geotechnical interest.

Chapter 9

CONCLUDING REMARKS

9.1 General

In view of the uncertainties at various stages of geotechnical design process, the deterministic methods of design based on factors of safety without due consideration to the effects of various sources uncertainty are subjective. Geotechnical engineers have recognized the importance of uncertainties in geotechnical engineering and the dominant role which they play in the foundation design, and researchers and engineers have been working rigorously for introducing reliability concepts in current practice as well as in codes.

For different engineering problems the acceptable reliability index or design reliability would vary depending on the significance of the project and loss associated with failure, and other societal factors. A good engineering design should always be based on a trade-off among safety, serviceability and economy. Deciding upon a trade-off is a complicated and subjective task, which requires a collective judgment keeping in mind the importance of the structure, the environmental regulations of the region, and the available resources allocated to the project. Hence, a comprehensive risk management plan should be prepared for every important civil engineering project during the planning stage itself, for optimum utilization of allocated resources.

General agreement among the geotechnical engineering community should be encouraged to introduce the probabilistic approaches in routine designs of many practical problems.

The following sections present specific conclusions based on results obtained in the present study.

9.2 Site characterization

The mean value of soil property may be obtained as statistical mean of soil point property, which is same as the mean of the trend in the data.

In the evaluation of autocovariance function, the sum of the product of residuals off the trend separated by a lag should be averaged over the number of pairs of data at the respective lags.

The data of stationary and non-stationary layers should be dealt separately for the evaluation of point variance of the soil property.

The choice of trend function is still a subjective judgment of the engineer and care should be taken to choose the same for the data analysis.

The results obtained from the Kendall's τ statistic shows that this method worked well in identifying the trend in the data, and in almost all cases, a quadratic detrending produces stationary data set.

The demarcation of the total soil profile into stationary and non-stationary layers by the Bartlett statistic approach is a promising method. However, this method does not suggest any guidelines on the cut-off values of Bartlett statistic, which distinguishes stationary and non-stationary layers within a soil profile.

The modified Bartlett statistic produces satisfactory results, as it is an improvement over the Bartlett approach. However, the results are sensitive to many parameters, such as window length, scale of fluctuation, etc.

The dual-window based method is simple and straightforward for the identification of statistical homogeneous layers within a soil profile. However, there is no explicit limit on the extreme values of 'BC' distance, the value above which a soil profile can be treated as statistically heterogeneous layer. The same 'BC' profile lead to two dissimilar results of statistical homogeneity depending on the scale to which the 'BC' profile is drawn. In the present study, it is suggested that the boundaries may be identified quantitatively at locations where the 'BC' distance crosses the mean±1.65×standard deviation of 'BC' distance fluctuations within the same profile.

Differencing technique of trend removal is not appropriate for geotechnical applications, as even first differencing produces results equivalent to that of removal of very high degree polynomial from the measured data, and results in lower scales of fluctuation than the true values.

9.3 Design of shallow foundations on sands

Scale of fluctuation, δ, and spatial averaging length, L, influence the inherent variability of soil property, CoV_w. The combined effect of spatial variability and spatial averaging reduces the inherent variability. The relative values of autocorrelation distance and spatial average length rather than the absolute values decide on the scale of reduction applied to inherent variability.

All the three sources of uncertainty, viz., inherent variability, measurement uncertainty, and the transformation model uncertainty play a dominant role on the coefficients of variation of design and spatial average uncertainty.

Transformation model has been identified as a crucial factor influencing the degree of variability of design parameter. Depending on the transformation model chosen the combined effect of all the three individual components of uncertainty (inherent

variability, measurement and transformation uncertainty) may either be more or less than their individual values of uncertainty.

For the data considered in the analysis, the deterministic procedures give higher allowable pressures than that obtained by probabilistic approaches at all the three settlement levels considered in the analysis, for a generally accepted target reliability index of 3.

It is observed that the mean and reduced standard deviations of spatial averaging soil property provide rational estimates of reliability of allowable bearing pressure of shallow foundations.

9.4 Design of shallow foundations in cohesive soil

For the Adelaide clay site, considering all the sources of uncertainty effecting the design parameter and effect of spatial averaging, the net ultimate bearing pressure reduced by 1.43 produces a target reliability index of 3.

The CoV of design q_u and spatial average q_u obtained for power plant site are 36% and 34% respectively. The higher variability of q_u for design of footings in the power plant site is mainly attributed to higher values of assumed CoV for transformation model based on Kulhawy (1992). In this case, the net ultimate bearing pressure needs to be reduced using a factor of 2.7 to produces a target reliability index of 3.

The reduction factor used on net ultimate bearing pressure for satisfying the safety requirements in the case footings on power plant site (i.e., FS=2.7) is almost double the value that obtained for Adelaide university site (i.e., FS=1.43). This difference is attributed to higher CoV_{qua} in the latter case.

9.5 Effect of anisotropic spatial correlation structure

The assumption of isotropic correlation structure based on vertical autocorrelation distance underestimates the variability of design parameter in a 2-D space, than that obtained with realistic autocorrelation distances in horizontal and vertical directions (i.e., for the case with $d_v/d_h<1$).

Assumption of perfect correlation both in horizontal or vertical, or both directions, overestimates the variability of design parameters, and produces conservative estimates of bearing capacity.

In general, horizontal scale of fluctuation is difficult to measure when compared to that in vertical direction, and hence in the absence of such data, it is recommended to assume perfect correlation in the horizontal direction, rather than isotropic behaviour based on vertical autocorrelation distance.

In the case of absence of data on scales of fluctuation in either direction for a particular site, it is suggested to use an upper bound value from the range of observed values from the records of past experience within the similar sites.

When inherent variability alone is considered, the assumption of perfect correlation of cone tip resistance in both horizontal and vertical directions, produce higher coefficient of variation of bearing capacity and hence, lower reliability index for ultimate limit state in shear criterion.

In conclusion, the need for a proper evaluation methodology for calculation of correlation lengths of soil properties and their influence in foundation design is highlighted.

9.6 Load resistance factored design

Limit state design approaches based on load resistance factored design facilitate the engineers to design the structures considering implicitly the prevailing uncertainty in design parameters arising out of various sources, without the need to get the enormous pool of soil data and complex and time consuming calculations.

The limit state design based on load resistance factored design produces consistent designs with uniform safety levels than that using Working Stress Design approach, as the variability in the load and resistance parameters is given appropriate treatment in the former case.

The results from the code calibration using working stress design approach show that resistance factors of 0.45 and 0.55 correspond to Conventional factors of safety of 3.0 and 2.5 respectively.

The resistance factors calibrated based on working stress design decreases with increase of required factors of safety in the design. Similarly, the computed resistance factors reduce with target reliability levels to be achieved in a design.

The results from the code calibration using reliability based approach show that for a coefficient of variation of resistance of 30%, and a target reliability index of 3.0, a resistance factor of 0.45 is obtained to produce consistent designs. The corresponding resistance factor for a reliability index 3.5 is approximately equal to 0.4.

Since, it is not suggested to recommend a single resistance factor for entire range of possible coefficient of variation, it is normally practiced to divide the whole range of coefficients of variation (CoV) of strength parameters encountered in a region into number of intervals and calibrate the resistance factors for each of these classes.

The load resistance factored design or load strength factored design approaches give intermediate solutions when compared to the solutions obtained from traditional Working Stress Design (WSD) and complete Reliability Based Design (RBD) approaches.

9.7 Design of soil slopes

The reliability theory is used as a means of evaluating the effects of uncertainties in the parameters involved in unsaturated slope stability calculations. The following are the specific conclusions made from the results of analysis.

The suction (u_a-u_w) and the angle indicating the rate of increase of shear strength relative to matric suction (ϕ^b) are critical random variables and incorporation of appropriate variations of these parameters in the analysis is important in slope reliability assessment.

Suction contributes significantly to the stability of unsaturated soil slopes. Hence, the evaluation of statistical parameters of suction with respect to both time and space is identified as a key factor in the prediction of potential zones of failure within a soil mass.

The failure zones are better captured by the reliability index than the conventional factor of safety.

The coefficient of variation of saturated hydraulic conductivity significantly affects the slope reliability.

With regard to reliability analysis of slopes subjected to earthquake-induced loading, the following conclusions are drawn.

The reliability analysis rather than conventional factor of safety approach proved praiseworthy to capture a significantly decreasing trend of safety of slopes with increased horizontal earthquake coefficient.

It can be noted that the variation of factor of safety with horizontal earthquake coefficient (Aa_h) is very less when compared to that of reliability index.

For a set of values of horizontal earthquake coefficient, correlation coefficient, and coefficients of variation of strength properties, the minimum slope angle beyond which the normalized cost of the slope starts deviating with respect to different consequence costs gives a balanced design.

The optimum slope angle decreases with increase in horizontal earthquake coefficient. For slopes subjected to 1-g loading (static case), the normalized cost continues to decrease even for slope angle as high as 60˚. The normalized cost of the slope shows same decreasing trend till 52˚ irrespective of level of horizontal earthquake loading considered in the analysis.

The stability of slopes in terms of reliability index increases with decrease of correlation between cohesion and angle of internal friction ($\rho_{c,\phi}$).

The optimum slope angle decreases with increase of coefficients of variation of strength parameters.

Keeping all other parameters constant, at any value of consequence cost, the increase of normalized cost is rather steep for slope angles higher than the optimum angle. For the data considered, it is noted that for slope angles lesser than 54º the normalized cost is almost independent of consequence cost.

It is possible to arrive at the balanced or optimum angle for a given geometry of slope and the soil properties taking into account risk, seismic effects using a horizontal

seismic coefficient, variability of soil properties, consequence costs for a given horizontal seismic coefficient in a probabilistic frame work.

While the results presented and comments made in this thesis are based on specific data and conditions mentioned, the same probabilistic methodology followed in this thesis can still be applied to any problem of geotechnical interest.

It is hoped that the efforts made and results presented in this thesis will draw the attention of engineers and practitioners working in Geotechnical Engineering towards understanding the need for proper site characterization methodologies and an early switchover to the reliability based approaches.

REFERENCES

A-Grivas, D. and Harr, M. E. (1979). Reliability approach to the design of soil slopes, *Proceedings of the European Conference on Soil Mechanics and Foundation Engineering*, Vol. 1, pp. 95-99.

A-Grivas, D. and Asaoka, A. (1982). Slope stability prediction under static and seismic loads, *Journal of the Geotechnical Engineering Division, ASCE,* Vol. 108, No. GT5, pp.713-729.

Akkaya, A. and Vanmarcke, E.H. (2003). Estimation of Spatial correlation of Soil Parameters Based on Data from the Texas A&M University National Geotechnical Experimentation Site (NGES), *In Probabilistic Site Characterization at the NGES,* GSP No. 121, ASCE, pp. 29-40.

Alonso, E. E. and Krizek, R. J. (1975). Stochastic Formulation of Soil Properties, In *Proc.2nd Int. Conf. on Applications of Statistics and Probability in Soil and Struct. Engg.,* Auchen, pp. 9-32.

Alonso, E.E. (1976). Risk analysis of soil slopes and its application to slopes in Canadian sensitive clays, *Geotechnique,* Vol. 26, No. 3, pp. 453-472.

Anderson, M.G. and Howes, S. (1985). Development and application of a combined soil water-slope stability model, *Quarterly Journal of Engineering Geology,* Vol. 18, pp. 225-236.

Ang, A.H.-S. and Tang, W.H. (1975). Probability Concepts in Engineering Planning and Design, Vol. 1, Basic Principles, *John Wiley,* New York.

Ang, A.H.-S. and Tang, W.H. (1984). Probability concepts in engineering planning and design. Volume II – decision, risk and reliability, *John Wiley & Sons, Inc.,* New York.

Awkati, Z. (1970). Ultimate bearing pressure of shallow footings in sands and clays, *unpublished work.*

Baecher, G.B. (1982). Simplified Geotechnical Data Analysis, *Proc. of the NATO Advanced Study Institute on Reliability Theory and its application in Structural and Soil Mechanics,* Bornholm, Denmark, Martinus Nijhoff, pp. 257-277.

Baecher, G. B. (1987). Statistical analysis of geotechnical data. *Report No. GL-87-1, U.S. Army Engineer Waterways Experiment Station,* Vicksburg, VA.

Baecher, G.B. and Christian, J.T. (2003). Reliability and Statistics in Geotechnical Engineering, *John Wiley and Sons,* London and New York.

Baikie, L.D. (1998). Comparison of limits states design methods for bearing capacity of shallow foundations, *Canadian Geotechnical Journal,* Vol. 35, pp. 175-182.

Bauer, J. and Pula, W. (2000). Reliability with respect to settlement limit-states of shallow foundations on linearly-deformable subsoil. *Computers and Geotechnics,* Vol. 26, pp. 281-308.

Becker, D.E. (1996a). Eighteenth Canadian Geotechnical Colloquium: Limit states Design for foundations, Part I. An overview of the foundation design process, *Canadian Geotechnical Journal,* Vol. 33, pp.956-983.

Becker, D.E. (1996b). Eighteenth Canadian Geotechnical Colloquium: Limit States Design for Foundations. Part II. Development for the National Building Code of Canada, *Canadian Geotechnical Journal,* Vol. 33, pp. 984-1007.

Bendat, J.S. and Piersol, A.G. (1986). Random Data: Analysis and Measurement Procedures, 2nd Edition, *John Wiley & Sons, Inc.*

Benjamin, J. R. and Cornell, C. A. (1970). Probability, Statistics, and Decision for Civil Engineers. *McGraw-HillBook Co.,* New York.

Berardi, R., Jamiolkowski, M., and Lancellotta, R. (1991). Settlement of shallow foundations in sands: Selection of stiffness on the basis of penetration resistance, *Proceedings of Geotechnical Engineering Congress, ASCE,* Boulder, Co., pp. 185-200.

Bergado, D.T. and Anderson, L.R. (1985). Stochastic analysis of pore pressure uncertainty for the probabilistic assessment of the safety of earth slopes, *Soils and Foundations,* Vol. 25, No. 2, pp. 87-105.

Bishop, A.W. and Blight, G.E. (1967). Effective stress evaluation for unsaturated soils, *Journal of Soil Mechanics and Foundation Engineering Division, ASCE,* Vol. 93, No. SM2, pp. 125-148.

Boden, B. (1981). Limit State Principles in Geotechnics, *Ground Engineering,* Vol. 14, No.6, pp. 2 - 7.

Bowerman, B. and O'Connell, R. (1983). Forecasting and Time Series: An Applied Approach, *Duxbury Press.*

Box, G.E.P. and Jenkins, G.M. (1970). Time series analysis – Forecasting and control, *Holden Day,* San Francisco.

Brand, E.W. (1982). Analysis and design in residual soils, *ASCE Sp. Conf. on Engineering and construction in tropical soils,* Honolulu, pp. 89-143.

Brand, E.W. (1984). Relationship between rainfall and landslides in Hong Kong, *Proceedings of the 4th International Symposium on Landslides,* Toronto, Canada, Vol.1, pp. 377-384.

Brinch Hansen, J. (1953). Earth Pressure Calculation. Dr. Tech. Thesis. *The Danish Geotechnical Press,* Copenhagen.

Brockwell, P. J. and Davis, R. A. (1987). Time Series: Theory and Methods, *Springer Verlag,* New York, 519 p.

Brzakala, W., El-Meligy, M., and Pula, W. (1995). Settlement analysis by non-linear finite element reliability method. *In Proceedings 7th International Conference on Applications of Statistics and Probability (ICASP-7),* Paris, Vol.1, pp. 55-63.

Burland, J. B. and Burbidge, M. C. (1985). Settlement of foundations on sand and gravel, *Proceedings of the Institution of Civil Engineers,* Part I, Vol. 78, No. 6, pp. 1325–1381.

Cafaro, F. and Cherubini, C. (2002). Large sample spacing in evaluation of vertical strength variability of clayey soil, *Journal of Geotechnical and Geoenvironmental Engineering, ASCE,* Vol. 128, No. 7, pp. 558-568.

Campanella, R.G., Wickremesinghe, D.S., and Robertson, P.K. (1987). Statistical treatment of cone penetrometers test data, *In Proceedings of 5th International Conference on Applications of Statistics and Probability in Soil and Structural Engineering,* Vancouver, pp. 1011-1019.

Casagrande, A. (1965). Role of the calculated risk in Earthwork and Foundation Engineering, *Journal of the Soil Mechanics and Foundations Division, Proceedings of ASCE,* Vol. 91, No. SM4, pp. 1-40.

Catalan, J.M. and Cornell, C.A. (1976). Earth slope reliability by a level crossing method, *Journal of Geotechnical Engineering Division, ASCE,* Vol. 102, No. GT6, pp. 591-604.

Cherubini, C. (1990). A closed-form probabilistic solution for evaluating the bearing capacity of shallow foundations, *Canadian Geotechnical Journal,* Vol. 27, pp. 526-529.

Cherubini, C., Giasi, C.I., and Rethati, L. (1993). The coefficients of variation of some geotechnical parameters, *In Probabilistic Methods in Geotechnical Engineering,* Rotterdam, pp. 179-184.

Cherubini, C. (2000). Reliability evaluation of shallow foundation bearing capacity on c′, ϕ′ soils, *Canadian Geotechnical Journal,* No. 37, pp. 264-269.

Cho, S. E. and Lee, S. R. (2002). Evaluation of surficial stability for homogeneous slopes considering rainfall characteristics, *Journal of Geotechnical and Geoenvironmental Engineering, ASCE,* Vol.128, No.9, pp. 756-763.

Chong, P. C., Phoon, K. K., and Tan, T. S. (2000). Probabilistic analysis of unsaturated residual soil slopes, *Applications of Statistics and Probability (ICASP 7),* Rotterdam: Balkema, pp. 375–382.

Chowdhury, R. N. and A-Grivas, D. (1982). Probabilistic Models of Progressive Failure of Slopes. *Journal of Geotechnical Engineering. Division, ASCE,* Vol. 108, No. 6, pp. 803-819.

Chowdhury, R. N. (1984). Recent developments in landslide studies: probabilistic methods. State of the Art Session, *VII International Symposium on Landslides,* Toronto, pp. 209-228.

Chowdhury, R.N. (1987). Analysis methods for assessing landslide risk – recent developments, *In Proceedings of 5th International Symposium on Landslides,* Lansanne, VI, pp.515-524.

Chowdhury, R.N., Tang, W.H., and Sidi, I. (1987). Reliability model of progressive slope failure, *Geotechnique,* Vol. 37, No. 4, pp. 467-481.

Chowdhury, R. N. and Xu, D. W. (1995). Geotechnical system reliability of slopes, *Reliability Engineering and System Safety,* Vol. 47, No. 3, pp. 141-151.

Chowdhury, R.N. (1996). Aspects of risk assessment for landslides, *Landslides,* Senneset (ed.), Balkema, Rotterdam, pp.183-188.

Christian, J.T., Ladd, C.C., and Baecher, G.B. (1992). Reliability and probability in stability analysis, *In Proceedings of Stability and Performance of Slopes and Embankments, ASCE,* GSP No.31, Vol. 2, pp. 1071-1111.

Christian, J. T., Ladd, C. C., and Baecher, G. B. (1994). Reliability applied to slope stability analysis. *Journal of Geotechnical Engineering, ASCE,* Vol. 120, No. 12, pp. 2180-2207.

Christian, J.T. and Urzua, A. (1998). Probabilistic evaluation of earthquake-induced slope failure, *Journal of Geotechnical and Geoenvironmental Engineering, ASCE,* Vol. 124, No.11, pp.1140-1143.

Christian, J.T. (2004). Geotechnical Engineering Reliability: How well do we know what we are doing?, *Geotechnical and Geoenvironmental Engineering, ASCE,* Vol. 130, No.10, pp. 985-1003.

CIRIA (2001). RiskCom: Software tool for managing and communicating risks, *Construction Industry Research and Information Association*, London.

Cornell, C. A. (1971). First order uncertainty analysis of soil deformation and stability. *In Proceedings of the 1st International Conference on Applications of Statistics in Soil and Structural Engineering (ICASP1),* Hong Kong, pp. 129-144.

Cornell, C.A. (1969). A probability-based structural code, *ACI Journal,* Vol. 66, No. 12, pp.974-985.

Cressie, N.A.C. (1993). Statistics for spatial data, Revised Edition, *Wiley,* New York.

D'Andrea, R.A. and Sangrey, D.A. (1982). Safety factors for probabilistic slope design, *Journal of Geotechnical Engineering Division, ASCE,* Vol. 108, No. GT9, pp. 1101-1118.

Daniel, W.W. (1990). Applied nonparametric statistics, 2nd edition, Boston: *PWS-Kent.*

Das, B.M. (1995). Principles of Foundation Engineering, 3rd Edition, *PWS Publishing Company,* Boston.

Day, R.A. (1998). Limit states design in geotechnical engineering–consistency, confidence or confusion? Department of Civil Engineering, The University of Queensland, *unpublished work.*

De Mello, V.F.B. (1977). Reflections on design decisions of practical significance to embankment dams, *Geotechnique,* Vol. 27, No. 3, pp. 279-355.

DeGroot, D.J. and Baecher, G.B. (1993). Estimating autocovariance of in-situ soil properties, *Journal of Geotechnical Engineering, ASCE,* Vol. 119, No. 1, pp.147-166.

DeGroot, D.J. (1996). Analyzing spatial variability of in-situ soil properties, *Uncertainty in Geologic Environment - From Theory to Practice,* Geotechnical Special Publication (GSP 58), ASCE, pp. 210-238.

Deutscher, M.S., Gasmo, J.M., Rahardjo, H., and Leong, E.C. (2000). Field measurements of pore-water pressure profiles in residual soil slopes of the Bukit Timah Granite Formation, Singapore, *Unsaturated Soils for Asia,* Rahardjo, Toll & Leong (eds.), Balkema, Rotterdam, pp. 777-782.

Diaz Padilla, J. and Vanmarcke, E. H. (1974). Settlement of structures on shallow foundations. *Research report R74-9,* Department of Civil Engineering, MIT, Cambridge, 167 p.

Dodagoudar, G.R. and Venkatachalam, G. (2000). Reliability analysis of slopes using Fuzzy sets theory, *Computers and Geotechnics,* Vol. 27, pp. 101-115.

Döll, P. (1996). Modeling of moisture movement under the influence of temperature gradients: Desiccation of mineral liners below landfills, Ph.D. thesis, *Technical University of Berlin,* Germany.

Döll, P. (1997). Desiccation of mineral liners below landfills with heat generation, *Journal of Geotechnical and Geoenvironmental Engineering, ASCE,* Vol. 123, No.11, pp. 1001-1009.

Duncan, J.M. (2000). Factors of safety and reliability in geotechnical engineering, *Journal of Geotechnical and Geoenvironmental Engineering, ASCE,* Vol.126, No.4, pp. 307-316.

Easa, S.M. (1992). Exact probabilistic solution of two-parameter bearing capacity for shallow foundations, *Canadian Geotechnical Journal,* Vol. 29, pp. 867-870.

Elkateb, T., Chalaturnyk, R., and Robertson, P.K. (2002). Implications of sand spatial variability on the behaviour of shallow foundation, *In Proceedings of the 55th Canadian Geotechnical Conference,* Ontario, Canada, pp. 1037-1044.

El-Ramly, H., Morgenstern, N.R., and Cruden, D.M. (2002). Probabilistic slope stability analysis for practice, *Canadian Geotechnical Journal,* Vol.39, pp.665-683.

EN 1997-1:2004. Eurocode 7: Geotechnical design - Part 1: General rules, *European codes of practice.*

Fell, R., Chapman, T.G., and Maguire, P.K. (1991). A model for prediction of piezometric levels in landslides, *Slope Stability Engineering, Thomas Telford,* London, pp. 37-42.

Fell, R. and Hartford, D. (1997). Landslide risk management, *Landslide risk assessment, Balkema,* Cruden and Fell (eds.), Rotterdam, pp.51-109.

Fenton, G.A. and Vanmarcke, E.H. (1998). Spatial variation in liquefaction risk, *Geotechnique,* Vol. 48, No.6, pp.819-831.

Fenton, G.A. (1999a). Estimation for Stochastic Soil Models, *Journal of Geotechnical and Geoenvironmental Engineering, ASCE,* Vol. 125, No.6, pp. 470-485.

Fenton, G.A. (1999b). Random Field Modeling of CPT Data, *Journal of Geotechnical and Geoenvironmental Engineering, ASCE,* Vol. 125, No.6, pp. 486-498.

Fenton, G.A. and Griffiths, D.V. (2000). Bearing capacity of spatially random soils, *In Proceedings of 8th ASCE Specialty Conference on Probabilistic Mechanics and Structural Reliability,* Notre Dame, Indiana.

Fenton, G.A. and Griffiths, D.V. (2002). Probabilistic foundation settlement on spatially random soil, *Journal of Geotechnical and Geoenvironmental Engineering, ASCE,* Vol. 128, No. 5, pp. 381-390.

Fenton, G.A. and Griffiths, D.V. (2003). Bearing capacity prediction of spatially random c - φ soils, *Canadian Geotechnical Journal,* Vol. 40, No.1, pp. 54-65.

Fenton, G.A. and Griffiths, D.V. (2005). Three-dimensional probabilistic foundation settlement, *Journal of Geotechnical and Geoenvironmental Engineering, ASCE,* Vol. 131, No.2, pp. 232-239.

Fredlund, D.G. and Morgenstern, N.R. (1977). Stress state variables for unsaturated soils, *Journal of the Geotechnical Engineering Division, ASCE,* Vol. 103, No. GT5, pp. 447-466.

Fredlund, D. G., Morgenstern, N. R., and Widger, R. A. (1978). The shear strength of unsaturated soils, *Canadian Geotechnical Journal,* Vol. 15, pp. 313–321.

Fredlund, D.G., Krahn, J., and Pufahl, D.E. (1981). The relationship between limit equilibrium slope stability methods, *In Proceedings of 10th International Conference on Soil Mechanics and Foundations Engineering,* Stockholm, Vol. 3, pp. 409-416.

Fredlund, D.G. (1987). Slope stability analysis incorporating the effect of soil suction, *Slope Stability, John Wiley & Sons,* Anderson, M.G. and Richards, K.S. (eds.), pp. 113-144.

Fredlund, D. G. and Rahardjo, H. (1993). Soil Mechanics for unsaturated soils, *John Wiley & Sons, Inc.* New York.

French, S.E. (1999). Design of shallow foundations, *ASCE Press,* USA, 374 pages.

Griffiths, D.V. and Fenton, G.A. (1997). Three-dimensional seepage through spatially random soil, *Journal of Geotechnical and Geoenvironmental Engineering, ASCE,* Vol. 123, No.2, pp. 153-160.

Griffiths, D.V. and Fenton, G.A. (2000). Influence of soil strength spatial variability on the stability of an undrained clay slope by finite elements, *In Slope Stability 2000, ASCE,* GSP No.101.

Griffiths, D.V. and Fenton, G.A. (2001). Bearing capacity of spatially random soil: the undrained clay Prandtl problem revisited, *Geotechnique,* Vol. 51, No. 4, pp. 351- 359.

Griffiths, D.V., Fenton, G.A., and Manoharan, N. (2002). Bearing capacity of rough rigid strip footing on cohesive soil: probabilistic study, *Journal of Geotechnical and Geoenvironmental Engineering, ASCE,* Vol. 128, No. 9, pp. 743-755.

Griffiths, D.V. and Fenton, G.A. (2004). Probabilistic slope stability by finite elements, *Journal of Geotechnical and Geoenvironmental Engineering, ASCE,* Vol. 130 No.5, pp. 507-518.

Gui, S., Zhang, R., Turner, J.P., and Xue, X. (2000). Probabilistic slope stability analysis with stochastic soil hydraulic conductivity, *Journal of Geotechnical and Geoenvironmental Engineering,* Vol. 126, No.1, pp. 1-9.

Haldar, A. and Mahadevan, S. (2000). Probability, Reliability and Statistical Methods in Engineering Design, *John Wiley & Sons,* 304 p.

Harr, M.E. (1987). Reliability based Design in Civil Engineering, *McGraw-Hill Publishers,* New York.

Hasofer, A.M. and Lind, N.C. (1974). Exact and invariant second moment code format, *Journal of Engineering Mechanics, ASCE,* Vol. 100, pp. 111-121.

Hegazy, Y.A., Mayne, P.W., and Rouhani, S. (1996). Geostatiscal assessment of spatial variability in piezocone tests, *In Proceedings of Conference on Uncertainty in the Geologic Environment—Form Theory to Practice (GSP 58),* C.D. Shackelford, P.P.Nelson and M.J.S. Roth, (eds.) ASCE, New York, pp. 254–268.

Hong Kong Government Planning Department (1994). Potentially hazardous installations, *Hong Kong planning standards and guidelines,* Chapter 11.

Honjo, Y., Suzuki, M., and Matsuo, M. (2000). Reliability analysis of shallow foundations in reference to design codes development, *Computers and Geotechnics,* Vol. 26, pp. 331-346.

Honjo, Y., Amatya, S., and Ohnishi, Y. (2003). Determination of Partial Factors for Shallow Foundations Based on Reliability Analysis, *LSD2003: International Workshop on Limit State Design in Geotechnical Engineering Practice,* Phoon, Honjo & Gilbert (eds.), World Scientific Publishing Company.

IS 456: 2000. Indian Standard plain and reinforced concrete - Code of practice (Fourth revision).

Jaksa, M.B. (1995). The influence of spatial variability on the geotechnical design properties of a stiff, overconsolidated clay. Ph.D. dissertation, *University of Adelaide.*

Jaksa, M.B., Brooker, P.I., and Kaggwa, W.S. (1997). Inaccuracies associated with estimating Random Measurement errors, *Journal of Geotechnical and Geoenvironmental Engineering, ASCE,* Vol. 123, No. 5, pp. 393-401.

Jaksa, M. B., Kaggwa, W. S., and Brooker, P. I. (1999). Experimental Evaluation of the Scale of Fluctuation of a Stiff Clay. **In Proceedings of 8th International Conference on the Application of Statistics and Probability,** R. E. Melchers and M. G. Stewart (eds.), Sydney, A. A. Balkema, Rotterdam, (Publ. 2000), Vol. 1, pp. 415-422.

Jaksa, M. B. (2000). Geotechnical risk and inadequate site investigations: A case study. **Australian Geomechanics,** Vol. 35, No. 2, pp. 39-46.

Jaksa, M.B., Yeong, K.S., Wong, K.T., and Lee, S.L. (2004). Horizontal Spatial Variability of Elastic Modulus in Sand from the Dilatometer, *In Proceeding of 9th Australia New Zealand Conference on Geomechanics,* Auckland, pp. 289-294.

JCSS (2000). Probabilistic model code, part 1: basis of design, 12th draft, Joint Committee on Structural Safety.

JCSS (2002). Probabilistic model code, Section 3.7: Soil properties, 5th (Final) version, Rackwitz, R., Denver, H., and Calle, E. (eds.).

Juang, C. H., Jhi, Y-Y., and Lee, D. H. (1998). Stability analysis of existing slopes considering uncertainty, *Engineering Geology,* Vol. 49, pp. 111-122.

Kanji, G. K. (1993). 100 statistical tests, *SAGE Ltd,* London.

Kay, J. N. and Krizek, R. J. (1971). Analysis of uncertainty in settlement predictions. *Geotechnical Engineering, A.I.T.,* Bangkok, pp. 119-129.

Kay, J. N. (1993). Probabilistic design of foundations and earth structures, *Probabilistic Methods in Geotechnical Engineering,* Li & Lo (eds), Balkema, Rotterdam, pp. 49-62.

Keaveny, J.M., Nadim, F., and Lacasse, S. (1989). Autocorrelation functions for offshore geotechnical data, *In Proceedings of International Conference on Structural Safety and Reliability (ICOSSAR 89),* pp. 263-270.

Kimmerling, R.E. (2002). Geotechnical Engineering Circular No.6, Shallow Foundations, *FHWA Technical Report No. FHWA-SA-02-054.*

Kottegoda, N.T. and Rosso, R. (1998). Statistics, Probability, and Reliability for Civil and Environmental Engineers. *McGraw-Hill,* New York, USA.

Krahn, J., Fredlund, D.G., and Klassen, M.J. (1989). Effect of soil suction on slope stability at Notch Hill, *Canadian Geotechnical Journal,* Vol. 26, pp.269-278.

Krizek, R.J. (1965). Approximation for Terzaghi's bearing capacity factors, *Journal of Soil Mechanics Division, ASCE,* Vol. 91, No. SM2, pp. 1-3.

Krizek, R.J., Corotis, R.B., and El-Moursi, H.H. (1977). Probabilistic analysis of predicted and measured settlements, *Canadian Geotechnical Journal,* Vol.14, pp. 17-33.

Kulatilake, P.H.S.W. and Miller, K.M. (1987). A scheme for estimating the spatial variation of soil properties in three dimensions, *In Proceedings of Fifth International Conference on Applications of Statistics and Probability in Soil and Structural Engineering,* Vancouver, British Columbia, Canada, pp. 669–677.

Kulatilake, P.H.S.W. and Ghosh, A. (1988). An investigation into accuracy of spatial variation estimation using static cone penetrometer data, *In Proceedings of First International Symposium on Penetration Testing,* Orlando, Fla., pp. 815–821.

Kulathilake, P.H.S.W. and Um, J.G. (2003). Spatial variation of cone tip resistance for the clay site at Texas A&M University, *Geotechnical and Geological Engineering,* Vol. 21, pp. 149–165.

Kulhawy, F.H. and Mayne, P. (1990). Manual on estimating soil properties on foundation design, *Report No. EL-6800, Electric Power Research Institute (EPRI),* Palo Alto, California, 327 pages.

Kulhawy, F. H. (1992). On the evaluation of soil properties. *Geotechnical Special Publication, ASCE,* No. 31, pp. 95-115.

Kulhawy, F.H., Birgisson, B., and Grigoriu, M.D. (1992). Reliability- based foundation design for transmission line structures: transformation models for in situ tests. *Report EL-5507(4), Electric Power Research Institute (EPRI),* Palo Alto, Calif.,

Lacasse, S. and Nadim, F. (1996). Uncertainties in characterising soil properties, Plenary paper for *ASCE Conference on Uncertainties,* Madison, Wisconsin, USA.

Lacasse, S. and Nadim, F. (1998). Risk and reliability in geotechnical engineering, *In Proceedings 4th International Conference on Case Histories in Geotechnical Engineering,* St. Louis, MO.

Lacasse, S. (2001). Terzaghi lecture, *unpublished.*

Lee, J. and Salgado, R. (2002). Estimation of footing settlement in sand, *International Journal of geomechanics,* Vol. 2, No. 1, pp. 1-28.

Li, K.S. and Lumb, P. (1987). Probabilistic design of slopes, *Canadian Geotechnical Journal,* Vol. 24, No.4, pp.520-535.

Li, K.S. and White, W. (1987). Reliability index of slopes, *In Proceedings of 5th International Conference on Applications of Statistics and probability in Soil and Structural Engineering,* Vol. 2, pp. 755-762.

Li, K. S., Lee, I. K., and Lo, S-C. R. (1993). Limit state design in geotechnics, *In Proceedings of the Conference on Probabilistic Methods in Geotechnical Engineering,* pp. 29-42.

Li, K.S. and Lim, J. (2001). Discussion on Factor of safety and Reliability in Geotechnical Engineering, by J.M. Duncan, *Journal of Geotechnical and Geoenvironmental Engineering, ASCE,* pp.714-715.

Lin, H.D. and Kung, J.H.S. (2000). Rainfall-induced slope failures in Taiwan, *Unsaturated Soils for Asia,* Rahardjo, Toll & Leong (eds.), Balkema, Rotterdam, pp. 801-806.

Lumb, P. (1966). The variability of natural soils, *Canadian Geotechnical Journal,* Vol. 3, No.2, pp. 74 – 97.

Lumb, P. (1967). Statistical methods in soil investigations. *In Proceedings of 5th Australian-New Zealand Conference on Soil Mechanics and Foundation Engineering,* Auckland, pp. 26-33.

Lumb, P. (1975a). Spatial Variability of Soil Properties. *In Proceedings of 2nd International Conference on Applications of Statistics and Probability in Soil and Structral Engineering,* Auchen, pp. 397-421.

Lumb, P. (1975b). Slope failures in Hong Kong, *Quarterly Journal of Engineering Geology,* Vol. 8, pp. 31-65.

MacGregor, J.G. (1976). Safety and limit states design for reinforced concrete, *Canadian Journal of Civil Engineering,* Vol. 3, pp. 484-513.

Madsen, H.O., Krenik, S., and Lind, N.C. (1986). Methods of Structural Safety, *Prentice-Hall, Inc.,* Englewood Cliffs, NJ.

Matyas, E.L. (1977). Discussion on Probabilistic analysis of predicted and measured settlements, by R.J. Krizek, R.B. Corotis, and H.H. El-Moursi, *Canadian Geotechnical Journal,* Vol. 14, pp. 159-163.

Meyerhof, G.G. (1951). The ultimate bearing capacity of foundations, *Geotechnique,* Vol.2, No.4, pp. 301-331.

Meyerhof, G.G. (1963). Some recent research on the bearing capacity of foundations, *Canadian Geotechnical Journal,* Vol. 1, pp. 16-26.

Meyerhof, G.G. (1970). Safety factors in soil mechanics, *Canadian Geotechnical Journal,* Vol. 7, pp. 349-355.

Meyerhof, G. G. (1976). Concepts of safety in foundation engineering ashore and offshore. *In Proceedings of 1st International Conference on Behavior of Offshore Structures,* Trondheim, Norway, Vol.1, pp. 900-911.

Meyerhof, G.G. (1982). Limit states design in geotechnical engineering, *Structural Safety,* Vol. 1, pp. 67-71.

Meyerhof, G.G. (1995). Development of geotechnical limit state design. *Canadian Geotechnical Journal,* Vol. 32, pp. 128-136.

Morgenstern, N.R. (1997). Towards landslide risk assessment in practice, *Landslide risk assessment* (Eds. Cruden and Fell), Balkema, Rotterdam, pp. 15-24.

Mostyn, G.R. and Soo, S. (1992). The effect of auto-correlation on the probability of failure of slopes, *In Proceedings of 6th Australian-New Zealand Conference on Geomechanics,* pp.542-546.

Nguyen, V.N. (1985). Reliability index in geotechnics, *Computers and Geotechnics,* Vol. 1, pp. 117-138.

Nobahar, A. and Popescu, R. (2001). Some effects of soil heterogeneity on bearing capacity of shallow foundations, *In Proceedings of ASCE Specialty Conference 2001: A Geo-Odyssey,* Blacksburg, pp. 1-11.

Nobahar, A. and Popescu, R. (2002). Bearing capacity of shallow foundations on heterogeneous soils, *In Proceedings of 2nd Canadian Speciality Conference on Computer Applications in Geotechnique,* Winnipeg, M.A.

Nowak, A.S. and Carr, R.I. (1985). Sensitivity analysis for structural errors. *Journal of Structural Engineering, ASCE,* Vol. 111, No.8, pp. 1734-1746.

Oka, Y. and Wu, T. H. (1990). System reliability of slope stability. *Journal of Geotechnical Engineering, ASCE,* Vol. 116, No. 8, pp. 1185-1189.

Paikowsky, S.G. (2002). Load and resistance factor design (LRFD) for deep foundations, *In Proceedings of Foundation design codes and soil investigation in view of International Harmonization and Performance based design,* IWS Kamakura, Tokyo, Japan, pp.59-94.

Phoon, K. K., Quek, S. T., Chow, Y. K., and Lee, S. L. (1990). Reliability analysis of pile Settlement. *Journal of Geotechnical Engineering, ASCE,* Vol. 116, No. 11, pp. 1717–1735.

Phoon, K.K. and Kulhawy, F.H. (1999a). Characterization of geotechnical variability, *Canadian Geotechnical Journal,* Vol. 36, pp. 612-624.

Phoon, K.K. and Kulhawy, F.H. (1999b). Evaluation of geotechnical property variability, *Canadian Geotechnical Journal,* Vol. 36, pp. 625-639.

Phoon, K.K. (2002). Potential application of reliability-based design to geotechnical engineering, *In Proceedings of 4th Colombian Geotechnical Seminar,* Medellin, pp. 1-22.

Phoon, K.K., Quek, S.T., and An, P. (2003a). Identification of Statistically Homogeneous Soil Layers using Modified Bartlett Statistics, *Journal of Geotechnical and Geoenvironmental Engineering, ASCE,* Vol. 129, No. 7, pp. 649-659.

Phoon, K.K., Becker, D.E., Kulhawy, F.H., Honjo, Y, Ovesen, N.K., and Lo, S.R. (2003b). Why Consider Reliability Analysis for Geotechnical Limit StateDesign?, *LSD2003: International Workshop on Limit State Design in Geotechnical Engineering Practice,* Phoon, Honjo & Gilbert (eds), World Scientific Publishing Company.

Phoon, K.K. and Kulhawy, F.H. (2003). Evaluation of model uncertainties for reliability-based foundation design, *In Proceedings of Applications of Statistics and Probability in Civil Engineering (ICASP 9),* pp.1351-1356.

Phoon, K.K., Quek, S.T., and An, P. (2004). Geostatistical analysis of cone penetration test (CPT) sounding using the modified Bartlett test, *Canandian Geotechnical Journal,* Vol. 41, pp. 356–365.

Popescu, R. Deodatis, G., and Nobahar, A. (2002). Bearing capacity of heterogeneous soils - a probabilistic approach, *In Proceedings of the 55th Canadian Geotechnical and 3rd Joint IAH-CNC and CGS Groundwater Specialty Conferences,* Niagara Falls, Ontario, pp. 1021-1027.

Przewlócki, J. (2000). Two-dimensional random field of mechanical soil properties, *Journal of Geotechnical and Geoenvironmental Engineering, ASCE,* Vol. 126, No. 4, pp. 373-377.

Pula, W. and Wyjadlowski, M. (1999). Effect of elastic parameters random variability on foundations settlements by finite layers method. *Studia Geotecnica et Mechanica,* pp. 3-4.

Rackwitz, R. and Fiessler, B. (1978). Structural reliability under combined random load sequences. *Computers and Structures,* Vol. 9, pp. 484-494.

Rao, P.J., Kishor kumar, Sivakumar Babu, G.L., Bhagwan, J., Panigrahi, R.K., Sharma, L., Shukla, A.D., Sahu, J.T., and Singh, D.N. (1995). CRRI Report on Investigation, Instrumentation and monitoring of landslide at Powari, Himachal Pradesh, India.

Reddy, L.N. and Wu, T.H. (1991). Probabilistic analysis of ground water levels in Hillside slopes, *Journal of Geotechnical Engineering, ASCE,* Vol. 117, pp. 872-890.

Robertson, P.K. and Campanella, R.G. (1989). Guidelines for Geotechnical Design Using the Cone Penetrometer Test and CPT with Pore Pressure Measurement, 4th ed., *Hogentogler & Co.,* Columbia, MD.

Satija, B.S. (1978). Shear behaviour of partly saturated soils, Ph.D. thesis, *Indian Institute of Technology, Delhi,* India.

Schmertmann, J.H. (1970). Static cone to compute static settlement over sand, *Journal of the Soil Mechanics and Foundation Division, ASCE,* Vol. 96, No. SM3, pp. 1011-1043.

Schmertmann, J.H., Hartmann, J.P., and Brown, P.R. (1978). Improved strain influence factor diagrams, *Journal of the Geotechnical Engineering Division, ASCE,* Vol. 104, No. GT8, pp. 1131-1135.

Schmertmann (2005). Personal communication.

Scott, B., Kim, B. J., and Salgado, R. (2003). Assessment of Current Load Factors for Use in Geotechnical Load and Resistance Factor Design, *Journal of Geotechnical and Geoenvironmental Engineering, ASCE,* Vol. 129, No. 4, pp. 287-295.

Shahin, M.A., Maier, H.R., and Jaksa, M.B. (2002). Predicting Settlement of Shallow Foundations using Neural Networks, *Journal of Geotechnical and Geoenvironmental Engineering, ASCE,* Vol. 128, No. 9, pp. 785-793.

Shao, L.T. and Wang, Zh.P. (2000). On the stability of unsaturated soil slopes, *Unsaturated Soils for Asia,* Rahardjo, Toll & Leong (eds.), Balkema, Rotterdam, pp. 825-829.

Sivakumar Babu, G. L. and Mukesh, M.D. (2004). Effect of soil variability on reliability of soil slopes, *Geotechnique,* Vol. 54, No. 5, pp. 335-337.

Skempton, A.W. (1951). The bearing capacity of clays, *Building Research Congress,* London, Vol. 1, pp. 180-189, reproduced in the "*Selected papers on Soil Mechanics, by A.W. Skempton, F.R.S.,"* Thomas Telford Limited, London, 1984.

Soulie, M., Montes, P., and Silvestri, V. (1990). Modelling spatial variability of soil parameters, *Canadian Geotechnical Journal,* Vol. 27, pp. 617-630.

SP 7(1):1983. Part III, Group I, The National Building Code of India, *Bureau of Indian Standards.*

Tang, W. H. (1984). Principles of Probabilistic Characterization of Soil Properties, *Probabilistic Characterization of Soil Properties: Bridge Between Theory and Practice, ASCE,* pp. 74-89.

Tang, W. H. (1993). Recent developments in geotechnical reliability. *In Probabilistic Methods in Geotechnical Engineering,* Rotterdam, pp. 3-27.

Tang, W.H., Stark, T.D., and Angulo, M. (1999). Reliability in back analysis of slope failures, *Soils and Foundations,* Japanese Geotechnical Society, Vol.39, No.5, pp. 73-80.

Taylor, D.W. (1948). Fundamentals of Soil Mechanics, *Asia Publishing House,* 700 pages.

Terzaghi, K. (1936). Stability of slopes of natural clay, *In Proceedings of First International Conference on Soil Mechanics and Foundation Engineering,* Harvard University, Vol. 1, pp. 161-165.

Terzaghi, K. (1943). Theoretical Soil Mechanics, *John Wiley and Sons,* NY.

Tsaparas, I., Rahardjo, H., Toll, D.G., and Leong, E.C. (2002). Controlling parameters for rainfall-induced landslides, *Computers and Geotechnics,* Vol. 29, pp. 1-27.

Tung, Y. K. and Chan, G. C. C. (2003). Stochastic analysis of slope stability considering uncertainties of soil-water retention characteristics. *In Proceedings of 9th International Conference on Applications of Statistics and Probability in Civil Engineering,* San Francisco, Vol. 2, pp. 1409–1414.

USACE (1990). Engineering and Design - Settlement Analysis, *EM 1110-1-1904, US Army Corps of Engineers,* Department of Army, Washington D. C.

USACE (1992). Engineering and Design – Bearing capacity of soils, *EM 1110-1-1905, US Army Corps of Engineers,* Department of Army, Washington D. C.

USACE (1997). Risk-based analysis in Geotechnical Engineering for Support of Planning Studies, Engineering and Design. *US Army Corps of Engineers,* Department of Army, Washington D. C., 20314-100.

Uzielli, M. (2004). Variability of Stress-Normalized CPT Measurements and Application to Seismic Liquefaction Initiation Assessment. Ph.D. dissertation, *University of Florence,* Italy.

Uzielli, M., Vannucchi, G., and Phoon, K.K. (2005). Normal field characterization of stress-normalised cone penetration testing parameters, *Geotechnique,* Vol. 55, No.1, pp. 3-20.

van Genuchten, M.Th. (1980). A closed-form equation for predicting the hydraulic conductivity of unsaturated soils, *Soil Science Society of American Journal,* Vol. 44, No. 5, pp. 892-898.

van Genuchten, M.Th., Leij, F., and Yates, S. (1991). The RETC code quantifying the hydraulic functions of unsaturated soils, *Rep. No. EPA/600/2-91/065, U.S. EPA,* Office of Research and Development, Washington, D.C.

Vanmarcke, E.H. (1977a). Probabilistic modeling of soil profiles, *Journal of the Geotechnical Engineering Division, ASCE,* Vol.103, No.GT11, pp.1227-1246.

Vanmarcke, E.H. (1977b). Reliability of Earth Slopes, *Journal of the Geotechnical Engineering Division, ASCE,* Vol. 103, No. GT11, pp. 1247-1265.

Vanmarcke, E. H. (1978). Probabilistic characterization of soil profiles, *In Proceedings of Specialty workshop on site characterization and exploration,* Northwestern University, Illinois, pp. 199-219.

Vanmarcke, E.H. (1983). Random fields: analysis and synthesis. *MIT Press,* Cambridge.

Vanmarcke, E.H. and Fenton, G.A. (2003). Probabilistic Site Characterization at the National Geotechnical Experimentation Sites, *Geotechnical Special Publication*, No. 121, Pub. ASCE.

Wang, Z., Gong, B.W., and Bao, C.G. (2000). The measurement of matric suctin in slopes of unsaturated soil, *Unsaturated Soils for Asia,* Rahardjo, Toll & Leong (eds.), Balkema, Rotterdam, pp. 843-846.

Wei, L., Tumay, M.T., and Abu-Farsakh, M.Y. (2005). Field testing of inclined cone penetration. *Geotechnical Testing Journal, ASTM,* pp. 31-41.

Whitman, R.V. (1984). Evaluating calculated risk in Geotechnical Engineering, The Seventeenth Terzaghi Lecture, *Journal of Geotechnical Engineering, ASCE,* Vol. 110, No. 2, pp. 145-188.

Whitman, R. V. (2000). Organizing and evaluating uncertainty in geotechnical engineering, *Journal of Geotechnical and Geoenvironmental Engineering, ASCE,* Vol. 126, No.7, pp. 583-593.

Wolff, T F. (1996). Probabilistic slope stability in theory and practice, *In Proceedings of the conference on Uncertainty in the Geologic Environment, Uncertainty 96,* Part 1, Madison, Wisconsin, pp. 419-433.

Wu, T.H. and Kraft, L.M. (1967). The probability of foundation safety, *Journal of Soil Mechanics and Foundation Engineering Division, Proceedings of ASCE,* Vol. 93, No. SM5, pp. 213-231.

Wu, T. H. and Kraft, L. M. (1970). Safety analysis of slopes, *Journal of Soil Mechanics and Foundation Engineering Division, ASCE,* Vol.96, No. SM2, pp.609-630.

Yagi, N., Yatabe, R., Yokota, K., and Bhandary, N.P. (2000). Suction measurement for the prediction of slope failure due to rainfall, *Unsaturated Soils for Asia,* Rahardjo, Toll & Leong (eds.), Balkema, Rotterdam, pp. 847-851.

Yamaguchi, H., Kimura, T., and Fujii, N. (1977). On the Scale Effect of Footings in Dense Sand. *In Proceedings of the 9th International Conference on Soil Mechanics and Foundation Engineering,* Vol. 1, pp. 795-798.

Yong, R. N., Alonso, E., and Tabba, M. M. (1977). Application of risk analysis to the prediction of slope stability, *Canadian Geotechnical Journal,* Vol.14, No.4, pp. 540–553.

Yucemen M.S., Tang W.H., and Ang A.H-S. (1973). A probabilistic study of safety and design of earth slopes, Civil Engineering Studies, *Structural Research Series 402. Urbana: University of Illinois.*

Zekkos, D.P., Bray, J.D., and Der Kiureghian, A. (2004). Reliability of shallow foundation design using the standard penetration test, *In Proceedings ISC-2 on Geotechnical and Geophysical Site Characterization,* Viana da Fonseca & Mayne (eds.), Millpress, Rotterdam, pp. 1575-1582.

Zhang, L., Tang, W.H., Zhang, L., and Zheng, J. (2004). Reducing uncertainty of prediction from empirical correlations, *Journal of Geotechnical and Geoenvironmental Engineering, ASCE,* Vol. 130, No. 5, pp. 526-534.

Zhang, L.L., Zhang, L.M., and Tang, W.H. (2005). Rainfall-induced slope failure considering variability of soil properties, *Geotechnique,* Vol. 55, No. 2, pp.183-188.